THE BUCKLING OF STRUCTURES

WITH PARTICULAR REFERENCE TO

STRUCTURES CONTAINING BOLTED ANGLE-SECTION MEMBERS

AND

LIGHTWEIGHT STRUCTURES

By M. Gregory

A Thesis submitted for the degree
of Doctor of Philosophy in the
Faculty of Engineering
of the
University of Tasmania.

Civil Engineering Department,
The University of Tasmania.

June, 1960.

- PREFACE -

The work described in this thesis has been carried out in the Civil Engineering Department of the University of Tasmania during the period July, 1956 to February, 1960. The research has been directed at obtaining some fundamental understanding of problems of instability of structures rather than the production of empirical information necessary for design purposes, though it is believed that the groundwork has been laid for the determination of valuable empirical data on certain types of problems. The treatment is restricted in the main to elastic buckling of non-redundant frames, though the problems met with in inelastic behaviour or with redundant frames are mentioned, and have been kept in mind throughout.

Chapter One begins with a detailed analysis of an unstable mechanism. This study forms an interesting introduction to problems of instability of structures without introducing the complication of the elastic beam equation. Various methods of analysis of structures have their counterpart, by analogy, in the treatment of the behaviour of this mechanism, and the treatment is rather detailed. The remainder of the chapter is devoted to standard methods of calculation of elastic critical loads. Because of the apparent confusion in some recent papers as to the meaning of various critical loads as determined by the moment distribution convergence criterion and other methods, the treatment is again rather full, and contains some very simple examples. More difficult problems are worked as illustrations and also because their results are used later.

Chapter Two is concerned with pin-ended struts and gives an introduction to the use of the Southwell Plot and the information that can be obtained from it. The Southwell Plot on deflections is first discussed. Particular emphasis is then laid on the power of the Southwell Plot on strain measurements. It is believed that the strain plot may have been used to ensure centrality of loading of a column for testing, but otherwise the treatment is new. It is intended that the discussion of single columns should furnish a basis for the arguments developed in Chapter Three.

In Chapter Three the Southwell Plot on strains is applied to a number of simple model frames and model or full-size structures. A design method for certain types of structures liable to instability is advanced, based on the equation of the Southwell Plot on measured strains. This work is new. The Southwell Plot on deflections has been used previously to confirm calculated values of critical loads of structures, but the equation of any Southwell Plot, and in particular the plot on strains, can be used to take account of imperfections and to relate the performance of the actual structure to the critical load of the perfect structure.

The investigation has followed the method of first establishing criteria analytically in the case of a number of simple frames, followed by experimental verification. More complicated frames were then treated.

Chapter Four draws attention to the buckling of bolted angle struts as the research project was initiated with this in view. While carrying out preliminary research on the behaviour of angle-section members under simple loading systems, a particularly interesting phenomenon, the bending effect of pure torque, was discovered. The effect has apparently not

been previously noticed. The behaviour is reported here, as there is probably a considerable effect on the torsion buckling of angle-section and similar members. (The general analysis of the bending and shortening effect of pure torque has since been carried out, but is not included in this thesis. See Aust. J. Appl. Science, Vol. 11, No. 3 (1960).) The remainder of the chapter contains the results of studies on model structures containing bolted angle members. A method of attack on the problem of obtaining design data is suggested.

It is thought that complementary energy methods will furnish the main means of tackling the problems of redundant frames. In view of the importance of energy methods in structural analysis, Chapter Five contains a brief outline of their application. The treatment is rather short and may be considered as a simple introduction to the problems of redundant frames. A pin-jointed redundant frame is solved by complementary energy, the crookedness of members being taken into account. However, any analysis of the behaviour of even the simplest rigid-jointed redundant frames is a problem of considerable complexity, and the determination of its strength is still more difficult. Nevertheless, it is the author's opinion that energy methods of analysis backed by the empirical information obtainable from Southwell Plots on strains will ultimately give a solution.

. . . . . .

Experimental work connected with this investigation has involved the testing of over twenty full-size girders and trusses, a model lattice girder, model Warren trusses, eleven triangulated model frames containing bolted angle members, and numerous triangular frames and single members. Since considerable information could often be obtained without causing permanent deformation, many of the frames or members tested were used over and over again.

The method followed in this research has been firstly to study simple problems such as single members or triangular frames, techniques and ideas being worked out analytically and experimentally on these problems as far as possible. Information gained in this way was then extended, often by analogy, to more difficult problems, then supported by experimental means and, where possible, analytically. The advantage of the prior study of simple problems for the clarification of ideas, the evaluation of the accuracy of any method, and for perfection of technique, is not always realised.

It is the intention of this thesis to propose the use of the Southwell Plot on strains or related plots as a basis for the determination of design formulae in problems of instability. It is considered that sufficient indication of the value of the method is given here to warrant the undertaking of research and testing on a large scale in order to determine the necessary empirical data for all types of structures. Attention should first be directed at non-redundant triangulated framed structures, but the author is convinced that, with the support of energy methods, it will eventually be possible to tackle other structures including redundant frames.

Acknowledgements:

The author has published a number of papers and communications dealing with this research, and a considerable quantity of this material is embodied in this thesis. A list is appended after Chapter Five, where acknowledgement is given to the periodicals and journals concerned. Where relevant, the author wishes to thank the editors for their permission to use material they have published.

Some of the argument and discussion in this thesis is drawn from various books and papers. References are given in the text, and an additional bibliography, with accompanying notes is given after each chapter. The author apologizes for any omissions. Where acknowledgement is not given in this way, the work is that of the author.

In conclusion the author wishes to thank the following persons:

Professor A. R. Oliver, the Professor of Civil Engineering in the University of Tasmania and supervisor of research;

Sir Richard Southwell, Trumpington, Cambridge, for his continued patience and kindness in giving helpful advice and encouragement by correspondence;

Professor dr. ir. C. B. Biezeno, Technische Hogeschool, Delft, Holland; Professor J. A. L. Matheson, formerly of the University of Manchester, now of Monash University, Melbourne, Victoria; and T. M. Charlton, University of Cambridge, for their comments and replies to questions on various aspects of the work.

- - - - oOo - - - -

THE BUCKLING OF STRUCTURES

C O N T E N T S

——— oOo ———

THEORY OF BUCKLING.

THE BUCKLING OF A SIMPLE MECHANISM, ELEMENTS OF STRUCTURES, AND PLANE TRIANGULATED FRAMES.

1. Introduction

In this chapter, the notion of unstable equilibrium of a structure is introduced by an analysis of the behaviour of a simple rod and spring mechanism. In this simple way, without the necessity of handling the equations of bending of a beam, the idea of a critical load at which the structure is in neutral equilibrium against static disturbances is presented. By this means it is possible to examine buckling divorced from the complication of the beam equation. The various energy and zero stiffness principles are worked out on this model, and also the related behaviour of the slightly imperfect structure.

The classical methods of calculation of buckling loads of single members and structures are then given, energy principles being very briefly reviewed. Various recent methods of handling the relevant equations for framed structures are illustrated with worked examples, the common mathematical foundation for all the methods being kept in mind throughout.

The way in which the behaviour of the practical structure under load may depart from the simple neutral equilibrium theory is briefly outlined.

2. Notation

The general notation used is as follows:

P	Compressive force.
T	Tensile force.
M	Bending moment.
θ	Rotation of end of member.
L, ℓ	Length of a member.
U	Energy.
F, W	Forces, loads.
u	Displacement, deflection.
E	Young's modulus.
EI	Flexural rigidity.

Other symbols are explained in the text.

3. The equilibrium of a compressed rigid bar, elastically restrained at one end.

The simple mechanism treated here is taken from an article by N. J. Hoff, "Dynamic Criteria of Buckling" - Research, Engineering Structures Supplement, (1949) p. 121 (Butterworth) in which the dynamic buckling is analysed, various types of damping being discussed. In this thesis, however, the mechanism is used to illustrate the principle of unstable equilibrium and methods of calculation of critical loads which are later used in relation to the buckling of structures. The analysis of the undampened vibration is taken from Hoff's paper, but the remainder is the work of the author.

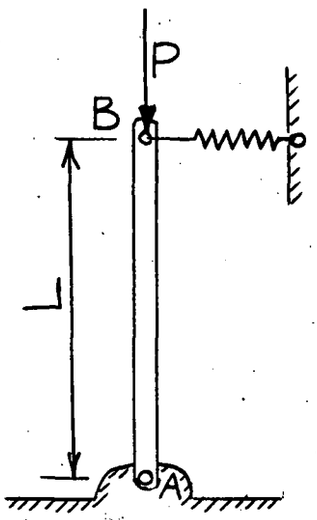

Fig. 1

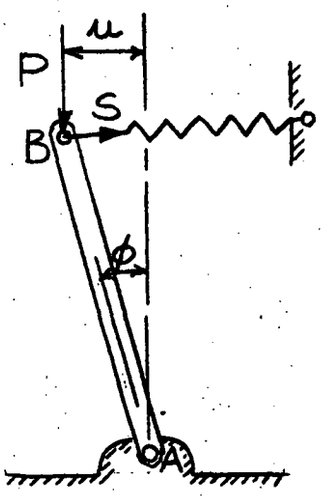

Fig. 2

Consider the rigid bar AB, pinned at A and acted on by a force P, as shown in Fig. 1. The end B of the bar is restrained against lateral movement in either direction by a weightless linear spring of stiffness K. It is evident that if the load P acts truly along the line AB the bar is in equilibrium for any magnitude of the load P. It is interesting to investigate the stability of the equilibrium.

4. Suppose the end B of the bar is displaced laterally by a small amount u, corresponding to an anticlockwise rotation ϕ about A, (Fig. 2), and the bar is brought to rest in this position. Then the force in the spring is given by

$$S = Ku = KL\phi$$

and the anticlockwise moment about the pin A of the forces acting on the bar, excluding the disturbing force, is

$$Pu - Ku\,L, \qquad \ldots\ \ldots \qquad (1)$$

if the moment of the weight of the bar is neglected. We notice that if P is less than KL, this moment is negative, and the bar tends to move in the clockwise direction. That is, on being released from its displaced position, the bar accelerates towards the central position, which is a position of stable equilibrium so far as small static disturbances are concerned.

However, if P equals KL, the resultant moment vanishes, and the bar is in neutral static equilibrium.

If P exceeds the value KL, the bar accelerates in a direction giving increased displacements, and the original position is one of unstable static equilibrium.

5. It can be seen that the stability of the equilibrium position depends on the relation between the magnitude of the acting force P and the stiffness of the restraining spring. If we consider the behaviour of the system as P is increased from zero, small static disturbances of the type described being given from time to time, then for values of P less than KL the effect of a disturbance is to set up a small oscillation about the equilibrium position. If P equals KL, when the bar is displaced it does not return. A very slight increase in load is then sufficient to cause large deflections after a slight disturbance. It is interesting to note that the argument, and in particular the value of the critical load at which instability occurs, is independent of the magnitude of the displacement provided the displacement is small, since the condition for instability is

$$|Pu - KuL| > 0 \qquad \ldots \qquad \ldots \qquad (2)$$

which yields

$$P > KL, \quad \text{whatever the magnitude of } u.$$

6. The effect of a dynamic disturbance can also be investigated. If the mass moment of inertia of the bar about the hinge A is I, and at some instant the bar is in the position shown in Fig. 2, then the equation of motion is

$$I\, d^2\phi/dt^2 + KL^2\phi - PL\phi = 0$$

This gives

$$d^2\phi/dt^2 + \phi L(KL - P)/I = 0 \qquad \ldots \qquad \ldots \qquad (3)$$

Putting $|(KL - P)L/I| = k^2$, the solution of this equation is

$$\left.\begin{array}{lll} \phi = A \sin (kt + B) & \text{provided } KL > P, & \text{Case 1.} \\ \text{or} \quad d\phi/dt = \text{constant} & \text{if } KL = P, & \text{Case 2.} \\ \text{or} \quad \phi = A \sinh (kt + B) & \text{if } KL < P, & \text{Case 3.} \end{array}\right\} \ldots \qquad (4)$$

A and B being arbitrary constants.

As a boundary condition, put

$$d\phi/dt = v/L \text{ when } t = o \text{ and } \phi = o.$$

That is, consider the motion when the end B of the bar is given an initial velocity v at the equilibrium position. Equations (4) then reduce to

$$\left.\begin{array}{lll} \phi = (v/kL) \sin kt & \text{if } P < KL, & \text{Case 1.} \\ \text{or} \quad \phi = vt/L & \text{if } P = KL, & \text{Case 2.} \\ \text{or} \quad \phi = v/kL \sinh kt & \text{if } P > KL, & \text{Case 3.} \end{array}\right\} \ldots \qquad (5)$$

If P is less than KL, Case 1 gives the equation of a vibration about the equilibrium position of amplitude $\phi = v/kL$ and frequency $k/2\pi$. If P equals KL, ϕ assumes values which increase steadily with time. If P is greater than KL, the acceleration away from the position of equilibrium is very rapid. The study of a dynamic disturbance leads to results which agree physically with the conclusions drawn from the analysis of a static disturbance. It should be remembered that the argument is restricted to small displacements.

7. In practice, many structures, structural elements, or parts of machinery show behaviour of this sort. Any structure fails by instability if and how most easily it can. A designer is concerned with avoiding unstable equilibrium, so that the equilibrium of a structure is not upset by disturbances of a magnitude which it is likely to encounter. The practical implications of instability will be discussed later, but certain principles can be introduced by the study of the simple rod and spring system under discussion.

8. Consider the energy changes involved in a small dynamic displacement of the bar from its equilibrium position, as shown in Fig. 2. At any instant, they may be listed as follows, the equilibrium position being considered as a datum.

U_1 = the work done by the load P

$= PL(1 - \cos\phi) = 2PL \sin^2(\phi/2) = PL\phi^2/2$ for small ϕ.

U_2 = the energy stored in the spring

$= \frac{1}{2} KL^2\phi^2$.

U_3 = the energy introduced into the system from outside, in order to cause the disturbance, called the perturbation energy.

U_4 = the kinetic energy of the rod

$= \frac{1}{2} I(d\phi/dt)^2$.

The spring is considered weightless. Then, we have

$$U_1 + U_3 = U_2 + U_4$$

assuming conservation of energy. It can be seen that when $P = KL$, $U_1 = U_2$. The effect of a perturbation, of energy U_3, may now be summarised.

(1) When $P < KL$, $U_1 < U_2$, and hence $U_3 > U_4$. Part of the perturbation energy is required to deform the spring, and the remainder is converted into kinetic energy.

(2) When $P = KL$, $U_1 = U_2$, and hence $U_3 = U_4$. The perturbation energy is converted into kinetic energy.

(3) When $P > KL$, $U_1 > U_2$, and hence $U_3 < U_4$. More kinetic energy is available than provided by the disturbance, as the work available from the load P exceeds the work required to deform the spring. Hence a vanishingly small perturbation energy is sufficient to upset the equilibrium. The system is dynamically unstable.

The argument is simplified by putting $U_3 = 0$, when the criterion for neutral or unstable equilibrium under static displacements becomes

$$U_1 \geqslant U_2 \qquad \ldots \qquad \ldots \quad (6)$$

This principle is very powerful in the determination of the critical loads of structures.

9. It has been shown (Equations (5), Case 1) that, on displacement and release, the rod executes harmonic vibrations about its equilibrium position if P is less than KL. We have

$$\phi = (v/kL) \sin kt.$$

Assume for the moment that the frequency of vibration (and hence k) is unknown, though the motion is known to be harmonic. Put

$$\phi = A \sin \omega t.$$

Then $d\phi/dt = A\omega \cos \omega t.$

The kinetic energy at $\phi = o$ is

$$I(d\phi/dt)^2/2 = IA^2\omega^2/2.$$

When ϕ reaches its maximum value, $\phi = A$, the kinetic energy is zero. Conservation of energy then gives that the kinetic energy at $\phi = 0$ plus the energy given up by the load in the motion out to $\phi = A$ equals the energy stored in the spring at $\phi = A$. Hence

$$IA^2\omega^2/2 + PL(1 - \cos\phi_{max}) = KL^2\phi^2_{max}/2.$$

Therefore $IA^2\omega^2 + PLA^2 = KL^2A^2$,

and $$\omega^2 = (KL - P)\,L/I,$$

and the result is independent of the amplitude A of the vibration, provided A is small. The value of ω is in agreement with the value of k obtained from equation (3). Use of the energy principle furnishes an easy means of obtaining the frequency of harmonic vibrations of a stable system about its equilibrium position. It should be noticed that as P approaches the value KL, ω tends to zero, and the frequency of the vibration tends to zero.

10. Consider the stiffness of the rod and spring system against a disturbing force F applied at B in the direction normal to P. (Fig. 3).

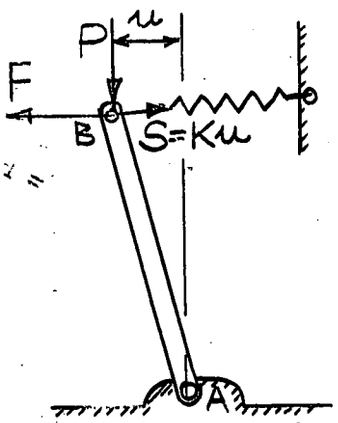

Fig. 3

Then for equilibrium, we have

$$Pu - KuL + FL = 0.$$

The stiffness of the system against the force F is F/u and equals (KL - P)/L. It is positive for $P < KL$ and becomes zero for $P = KL$ and negative for $P > KL$. If P is considered as increasing from zero, small disturbing forces being applied from time to time, then as P approaches the value KL, F/u tends to zero, and a vanishingly small disturbing force causes large displacements. This principle is of use in determining the loads at which instability occurs in structures.

It should also be noted that for a given value of P, F/u is constant, and the work done by the disturbing force is Fu/2 and equals $(KL - P)u^2/2L$, which is positive so long as $KL > P$.

It can also be seen that as P approaches the value KL large forces S = Ku are called into play in the spring to resist the action of the disturbing force F.

11. The practical implications of the liability of certain structures to instability are very wide. The rod and spring mechanism has served to illustrate certain concepts, but, in practice, many more complications are introduced. Problems which are relevant to the study of the rod and spring system, each of which has its counterpart in the study of the instability of structures, are the effect of a non-linear spring, the effect of damping or friction, the effect of large displacements, or the effect of a change in the load P as the system displaces. It may occur that P is not constant, but a function of the distance through which it acts, or a function of the rate of displacement. The relation between P and u may be affected by the inertia of the bar and of the loading apparatus, as this will affect the speed with which the load can "follow" the movement of the bar. The qualitative effects of such variations from the simple problem discussed may sometimes be evident, but the quantitive effects are also important in practice.

12. One modification of the simple system will be discussed here. Consider the effect of the rod being initially out of line with the direction of P. This may be considered as an imperfection in manufacture, resulting from the spring being made up of incorrect length by an amount u_o. That is, when P is zero, u has the value u_o. Then, for equilibrium under load P, we have

$$Pu - K(u - u_o)L = 0$$

$$\text{therefore} \quad u = Ku_oL/(KL - P) = u_o/(1 - P/KL) \qquad .. \qquad .. \quad (7)$$

The previous condition of stable equilibrium in the central position $u = 0$ up to a critical value of P equal to KL with a change to unstable equilibrium once this load is exceeded now no longer exists. Instead, displacements occur as soon as P is given a value, and the initial displacement u_o is magnified in the ratio $1/(1 - P/Pcr)$ where $Pcr = KL$, the critical load to cause instability where no imperfections exist. The graph of u/u_o against P/Pcr is shown in Fig. 4 [illegible] of u_o.

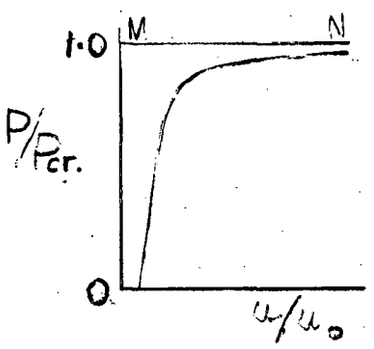

Fig. 4

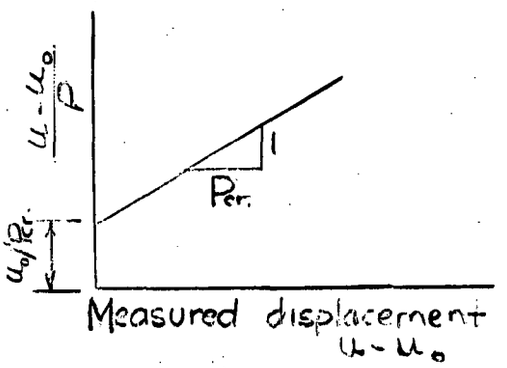

Fig. 5

It is interesting to note that the behaviour under load is a function of the imperfection u_o and the critical load when no imperfections are present. In the limiting case when u_o tends to zero, the graph of u against P/Pcr follows the path O M N, but for larger values of u_o, the knee in the curve becomes less pronounced. Equation (7) is the equation of the curve. This reduces to

$$(u - u_o)/P = (u - u_o)/Pcr + u_o/Pcr.$$

Thus if the displacement on loading, $u - u_o$, is measured, and $(u - u_o)/P$ is plotted against $u - u_o$, the graph is a straight line of slope $1/Pcr$. and intercept on the $(u - u_o)/P$ axis of u_o/Pcr. (See figure 5).

This plot forms a convenient means of relating the measured behaviour of an imperfect system to the magnitude of its imperfections and the critical load of the perfect system.

13. Under load, the behaviour of structures liable to instability is usually similar to that of the rod and spring model possessing imperfections, (Fig. 4), rather than the case where no imperfections are present. The latter behaviour is a limiting case of the former, and difficult to obtain in practice. Both types of behaviour are often referred to as buckling. There is a close relation between the two. In practice, buckling usually means the occurrence of large deformations with a small change in load (and there is often no true instability.) This occurs on the upper parts of the curves in Fig. 4. We are often interested in the load carrying capacity of structures, and where buckling occurs such problems can be tackled by a study of the behaviour of idealized structures, followed by analysis and empirical correlation of the effects of imperfections.

14. <u>The equilibrium of a compressed elastic bar of uniform flexural rigidity</u>:

Consider the single pin-ended column AB of length ℓ, acted on by a central axial force P. (Fig. 6)

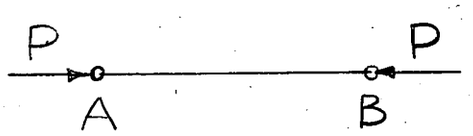

Fig. 6

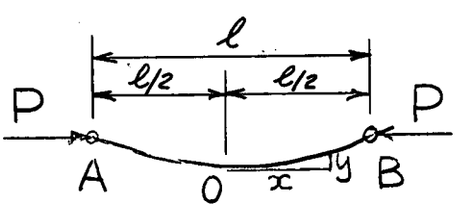

Fig. 7

The bar is in equilibrium, provided yield of the material does not occur, for any magnitude of the force P. The stability of the equilibrium will now be considered. Suppose the bar is displaced by some means from its equilibrium position to the position given by y(x) and brought to rest there. (Fig. 7). Then at point (x,y) on the displaced bar, the bending moment is

$$M = P(a - y)$$

$$= EI\ d^2y/dx^2$$

(where EI is the flexural rigidity of the bar), if the bar is in equilibrium in its displaced position.

Therefore $d^2y/dx^2 + k^2y = Pa/EI$

where $k = \sqrt{P/EI}$

Therefore $y = a + A \sin kx + B \cos kx$,

A and B being arbitrary constants.

If the displaced curve is symmetrical about the line $x = o$, the boundary conditions

$x = o,\ y = o,\ dy/dx = o$ give the solution

$$y = a(1 - \cos kx) \qquad .. \quad .. \quad (8)$$

Substituting the condition that $y = a$ when $x = \ell/2$ yields the equation

$$a = a - a \cos k\ell/2$$

This equation, which holds provided a is small, (otherwise the moment curvature relation is in error), is independent of the magnitude of a. It gives

$$k\ell/2 = \pi/2,\ 3\pi/2,\ 5\pi/2,\ ....$$

or $$P = \pi^2EI/\ell^2,\ 9\pi^2EI/\ell^2,\ 25\pi^2EI/\ell^2,\ ....$$

If the displaced form is assumed to be antisymmetrical about o, (when $x = o$, $y = o$ and $d^2y/dx^2 = o$ and hence $a = o$), we obtain

$$y = A \sin kx \qquad .. \quad .. \quad (9)$$

Substituting the condition that $y = o$ when $x = \ell/2$ yields

$$k\ell/2 = \pi,\ 2\pi,\ 3\pi,\ ....$$

or $$P = 4\pi^2EI/\ell^2,\ 16\pi^2EI/\ell^2,\ ....$$

and the solution is independent of the value of A. We have therefore, for equilibrium of the bar in the displaced state,

$$P = n^2\pi^2EI/\ell^2 \qquad .. \quad .. \quad (10)$$

where $n = 1, 2, 3, ...$

The bar is in equilibrium in the corresponding bent form as well as in the straight form when any of these loads are acting, and the magnitude of the displacement is unimportant, provided it is small. The shape of the displacement curve is determined by equation (8) or equation (9), whichever is relevant, and depends on the value of n. The bar is thus in neutral equilibrium when any load given by equation (10) acts on it, so far as static disturbances into the given shape are concerned. In fact, the moment curvature relationship used in this derivation is inexact, as the expression for the curvature is only approximate. There is no point of neutral equilibrium, but it can be shown that, once displaced, the deflection of the bar increases very rapidly for values of P greater than the lowest of equation (10), that is π^2EI/ℓ^2. This complete behaviour is discussed in the theory of the elastica (see R. V. Southwell "Theory of Elasticity" O.U.P. 1941, pp. 429 - 438) but the approximate treatment given here serves as a simple mathematical model of the behaviour of an idealized column, and the behaviour of an actual column can be referred to it.

15. Critical loads and characteristic modes of distortion of a column of uniform flexural rigidity:
(See R. V. Southwell "Theory of Elasticity p. 424).

Consider the initially straight pin-ended strut shown in Fig. 8.

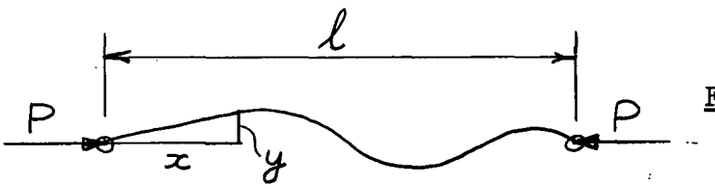

Fig. 8

The strut is assumed to be displaced into some curve $y(x)$. For equilibrium in this position, as well as in the initial straight configuration, the bending moment curvature relation yields

$$EI\, d^2y/dx^2 + Py = 0 \qquad .. \qquad .. \qquad (11)$$

This is satisfied by $y = A_n \sin n\pi x/\ell$, which gives, on substitution,

$$P_n = n^2 \pi^2 EI/\ell^2 \qquad .. \qquad .. \qquad (12)$$

P_n is the n^{th} critical load at which neutral static equilibrium exists, and the associated mode of distortion is $y = A_n \sin n\pi x/\ell$, where the value of A_n is unrestricted. This value of y defines the n^{th} characteristic mode of distortion. The smallest value of P_n is $P_1 = \pi^2 EI/\ell^2$, when the strut assumes the form $y = A_1 \sin \pi x/\ell$. This value of P is called the first Euler load of the strut. At values of P_n higher than P_1, the strut is in neutral equilibrium when displaced into its corresponding mode, but it is in unstable equilibrium when displaced into any other shape. Hence to achieve values of P higher than P_1, restraint of some form is necessary.

16. The uniform strut from the standpoint of energy.

As in the case of the rod and spring mechanism previously discussed, energy methods can be used to determine the critical loads of the uniform strut.

We have, (equation 11),

$$EI\, d^2y/dx^2 + Py = 0.$$

Multiply each side of the equation by $\frac{1}{2}\, d^2y/dx^2$, and integrate from o to ℓ.

Hence
$$\tfrac{1}{2}\int_0^\ell EI(d^2y/dx^2)^2\, dx = -\tfrac{1}{2} P\int_0^\ell y\,(d^2y/dx^2)\, dx.$$
$$= \tfrac{1}{2} P\int_0^\ell (dy/dx)^2\, dx - \tfrac{1}{2} P\left[y\, dy/dx\right]_0^\ell$$

on integrating by parts. So long as either y or dy/dx vanish at o and ℓ, we have

$$\tfrac{1}{2}\int_0^\ell EI(d^2y/dx^2)^2\, dx = \tfrac{1}{2} P\int_0^\ell (dy/dx)^2\, dx \qquad .. \qquad (13)$$

The term on the left is recognizable as the strain energy of bending, and that on the right as the work done by the load when the bar assumes the bent position $y(x)$.

Hence $$P = \frac{\int_o^\ell \frac{1}{2}EI(d^2y/dx^2)^2\,dx}{\int_o^\ell \frac{1}{2}(dy/dx)^2\,dx} \qquad .. \qquad .. \qquad (14)$$

where y represents the characteristic mode of distortion. In practice, closely approximate values of P can be found by assuming values of y which fit the given boundary conditions, and the energy method becomes a powerful means of obtaining approximate values of the critical load. The above is known as Rayleigh's method.

If equation (11) is multiplied through by $(y/EI)\,dx$ and integrated we obtain

$$\int_o^\ell y(d^2y/dx^2)\,dx = -P\int_o^\ell y^2\,dx/EI$$

therefore $$P = \frac{-\int_o^\ell y(d^2y/dx^2)\,dx}{\int_o^\ell y^2\,dx/EI} \qquad .. \qquad .. \qquad (15)$$

This equation can be given a complementary energy interpretation. It is derived by Westergaard using the methods of complementary energy, and he shows that it is also valuable in determining approximate critical loads using assumed forms for y(x).

Since $d^2y/dx^2 = -Py/EI$, equation (13) can be rewritten as

$$\tfrac{1}{2}\int_o^\ell EI\,(Py/EI)^2\,dx = \tfrac{1}{2}P\int_o^\ell (dy/dx)^2\,dx$$

or $$P = \frac{\int_o^\ell (dy/dx)^2\,dx}{\int_o^\ell y^2\,dx/EI} \qquad .. \qquad .. \qquad (16)$$

For approximate calculations this is better to handle than equation (14). Equation (16) can be reduced to equation (15) on integration by parts, provided either y or dy/dx vanish at o and ℓ.

When using such approximate methods for the evaluation of critical loads, it is best to consider those having relevance in terms of strain or complementary energy as particular cases of a family of methods which can be obtained by manipulation of equation (11).

For a treatment of Rayleigh's principle, see R. V. Southwell "Theory of Elasticity" pp. 442 - 455. In Southwell's book Rayleigh's method of calculation of critical loads or vibration frequencies is presented without prior reference to the principle of conservation of energy. The mathematics of the member behaviour is carried out first, and then given an energy interpretation provided certain boundary conditions hold; and these conditions fit the energy picture. The method is due to Lord Rayleigh (Theory of Sound Vol. I) and is clearly presented in Temple G. and Bickley W.G. "Rayleigh's Principle" O.U.P. (1933). Here again the principle of conservation of energy is not used. In the case of a harmonic vibration it is shown that the average kinetic energy equals the average potential energy, whereas conservation of energy equates the corresponding maximum values. The final equations are, of course, the same. The energy discussion in Art. 8 is drawn from this book.

The complementary energy approximate method of calculation of critical loads given above, is drawn from H. M. Westergaard "On the Method of Complementary Energy", Proc. A.S.C.E. Vol. 67, No. 2, p.199, Feb. 1941. The same equation is derived by Westergaard using complementary energy conceptions, but in this thesis it is derived mathematically from the column equation, and can be given Westergaard's complementary energy interpretation if desired. It should be noted that equation (16) is reducible to equation (15) only if the given boundary conditions hold. These are not mentioned in Westergaard's paper, and this omission may cause confusion. In certain cases Westergaard has shown that equation (15) gives a closer approximation to the critical load than equations (16) or (14).

Other useful approximate methods are given in S. Timoshenko "Theory of Elastic Stability" (1935) McGraw Hill p.81, but Rayleigh's method has been widely used: an interesting example is the calculation of the critical load of an unbraced arch rib when buckling out of its plane occurs: "The Lateral Buckling of Tied Arches", W. G. Godden, Proc. I.C.E., Aug. 1954, Vol. 3, No. 2, p. 496. The power of Rayleigh's method is also illustrated in a discussion by the author on a paper by R. Frisch Fay "The Buckling of Struts of Varying Cross-Sections" Journal I.E. Aust. Vol. 31 No. 3 Mar. 1959 p. 81. In the original paper Bessel functions are used to solve the problems, but the author has shown that the approximate solution obtained very simply by Rayleigh's method is very close. This gives a guide to the accuracy of Rayleigh's method where no standard solution is available for comparison. See M. Gregory, discussion on the above paper, Journal I.E. Aust. Vol. 32, No. 9, Sept. 1959, p.231.

17. <u>The vibrations of a compressed bar</u>:

Assume the bar is of mass ρ per unit length and vibrates in the form

$$y = a \sin(\pi x/\ell) \sin \omega t.$$ (See Fig. 9)

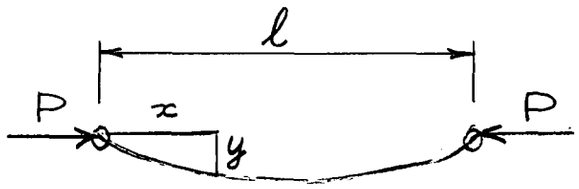

Fig. 9

Then, applying the same method as was used in the case of the rod and spring mechanism, the value of ω can be calculated. The total kinetic energy when y = o is

$$\tfrac{1}{2}\int_0^{\ell} \rho \, dx \, \omega^2 a^2 \sin^2(\pi x/\ell)$$
$$= \tfrac{1}{4}\omega^2 \rho \ell a^2.$$

When y reaches its extremum, the energy given up by the load is

$$P \int_0^{\ell} \tfrac{1}{2}(\partial y/\partial x)^2 \, dx$$
$$= P\pi^2 a^2/4\ell,$$

and the strain energy of bending is

$$\tfrac{1}{2} \int_0^{\ell} EI \, (\partial^2 y/\partial x^2)^2 \, dx$$
$$= EI \, \pi^4 a^2/4\ell^3$$

From conservation of energy,

$$P\pi^2a^2/4\ell + \omega^2 \rho \ell \, a^2/4 = EI\pi^4a^2/4\ell^3$$

and therefore $\omega^2 = \pi^2 P(1 + Q/P)/\rho\ell^2$ .. .. (17)

where $Q = \pi^2 EI/\ell^2$, the first Euler load of the strut. It is interesting to note that the result is independent of the amplitude of vibration a, though the analysis is restricted to small values of a. The value of ω is real for P less than Q, and becomes zero when P is equal to Q. The results of the analysis of the static disturbance of the strut and of the vibration analysis are physically consistent.

The above discussion is drawn in principle from Temple and Bickley's "Rayleigh's Principle", but the equations are derived here using the principle of conservation of energy.

18. <u>The behaviour of an initially crooked uniform elastic strut</u>: (See R. V. Southwell "On the Analysis of Experimental Observations in Problems of Elastic Stability". Proc. Roy. Soc. London, Series A Vol. 135 p. 601 and R. V. Southwell "Theory of Elasticity" p. 428.)

Suppose AB is an axially loaded pin-ended strut of length ℓ, having initial crookedness given by $y_o(x)$. (See Fig. 10).

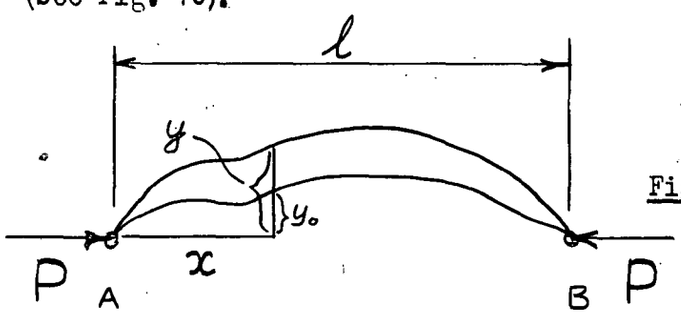

Fig. 10

If the centre line of the strut under load P is given by y(x), the bending moment at x is

$$M = Py$$

and we have $Py = -EI\, d^2(y-y_o)/dx^2 = -EI\, d^2y/dx^2 + EI\, d^2y_o/dx^2$

therefore $d^2y/dx^2 + (P/EI)y = d^2y_o/dx^2$ .. .. (18)

The form of y(x) is thus dependent on the form of $y_o(x)$.

Put $y_o = \sum_{n=1}^{\infty} a_n \sin n\pi x/\ell$,

assuming y_o to have any form between A and B and provided y_o and d^2y_o/dx^2 both vanish at $x = o, \ell$.

Equation (18) is satisfied by

$$y = \sum_{1}^{\infty} b_n \sin n\pi x/\ell$$

and substitution gives

$$\sum_{1}^{\infty} \left[-n^2\pi^2 b_n/\ell^2 + k^2 b_n \right] \sin n\pi x/\ell$$

$$= \sum_{1}^{\infty} -n^2\pi^2 a_n/\ell^2 \sin n\pi x/\ell ,$$

where $k = \sqrt{P/EI}$

This applies for all x.

Therefore $(b_n - a_n)\ n^2\pi^2/\ell^2 = k^2 b_n$

and $b_n = a_n/(1 - k^2\ell^2/n^2\pi^2)$ .. .. (19)

Now $\pi^2 EI/\ell^2 = Q$, the first Euler load of the strut

and therefore $b_n/a_n = (1 - P/n^2Q)^{-1}$, giving the ratio in which the the initial shape

$a_n \sin n\pi x/\ell$ is magnified by the end thrust. Now as P approaches Q, $b_1/a_1 = (1 - P/Q)^{-1}$ .. .. (20)

and a_1 is greatly magnified, since

$$\lim_{P = Q} (1 - P/Q)^{-1} = \infty .$$

Also $b_2/a_2 = (1 - \frac{1}{4})^{-1} = 4/3$, when $P = Q$,

$b_3/a_3 = (1 - 1/9)^{-1} = 9/8$ when $P = Q$.

The central deflection of the strut is

$$b = b_1 - b_3 + b_5 - b_7 + \ldots$$

and as P approaches Q, the terms after b_1 can be neglected.

Hence $b = b_1 = a_1/(1 - P/Q)$

provided equation (18) is applicable, that is the curvature is small and yield does not occur. The behaviour is thus similar to that of the initially out of line rod and spring mechanism. Deflection of the strut occurs as soon as P has a value, and becomes very large as P approaches first critical load $Q = \pi^2 EI/\ell^2$.

19. The measured central deflection is

δ = b - (the central value of y_o)

$= b - a_1$

$= a_1/(1 - P/Q) - a_1$

This reduces to $\delta/P = \delta/Q + a_1/Q$ .. .. (21)

Now a_1/Q is constant for a given strut, so the graph δ/P against δ is a straight line of slope $1/Q$ and intercept on the δ/P axis of a_1/Q. (Fig. 11)

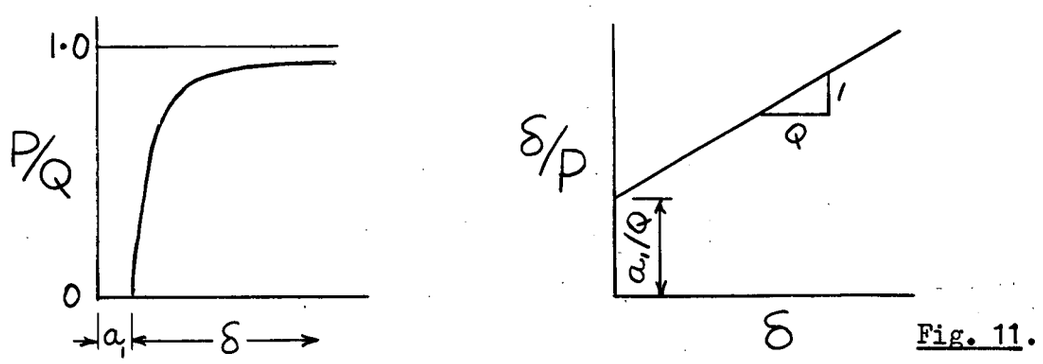

Fig. 11.

The behaviour of the initially crooked strut is thus a function of its initial crookedness and of the critical load of the perfectly straight member. The linear plot, (equation 21 and Fig. 11) is a valuable means of empirically relating the behaviour of the member possessing practical imperfections to that of the perfect member, and is due to Southwell. The plot is often called the Southwell Plot on deflections. It was introduced in the first place as a means of inferring the first Euler load of a strut from measurements of deflections taken during loading, but the implications are much more far reaching.

20. <u>The behaviour of a column subject to compression P and bending moments at its ends</u>:

Columns in structures are never pinned at their ends, but fixed in some way to other members of the structure. Often the joints are quite rigid. Rotation of the end of a column is therefore restrained by the other members framing into the joint, and any rotation calls into play end moments. To discuss the buckling of frames consisting of an assemblage of members, it is convenient to analyse first the behaviour of a single column subject to end moments.

21. Consider the initially straight bar AB acted on by an axial load P and end moments M_A and M_B, anticlockwise moments and slopes being considered positive. (Fig. 12).

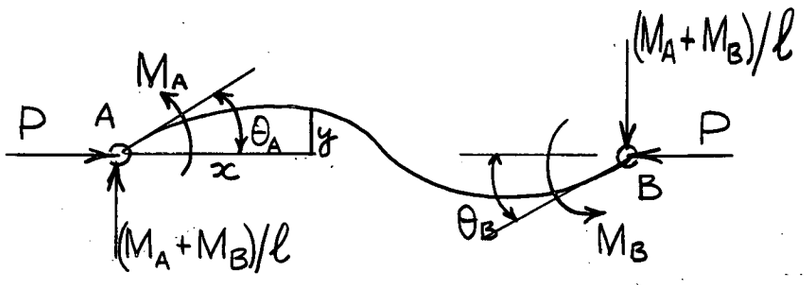

Fig. 12

At the point x, the bending moment is

$$M = M_A - (M_A + M_B)x/\ell + Py = -EI\, d^2y/dx^2,$$

which gives the differential equation

$$d^2y/dx^2 + Py/EI = -M_A(1 - x/\ell)/P + M_B\, x/EI\,\ell$$

Putting $P/EI = k^2$, the solution can be written

$$y = A \sin kx + B \cos kx - M_A(1 - x/\ell)/EI + M_B\, x/P\ell$$

Substituting the boundary conditions

$x = o$, $y = o$ and $x = \ell$, $y = o$,

we have $B = M_A/P$ and $A = -(M_A/P)\cot k\ell - (M_B/P)\ \mathrm{cosec}\ k\ell$

Now $dy/dx = Ak \cos kx - Bk \sin kx + (M_A + M_B)/P\ell$.

Putting $x = o$, the slope at A is given by

$$EI\theta_A = M_A \ell\beta/3 - M_B \ell\alpha/6 \quad .. \quad .. \quad (22)$$

where $\alpha = (6/k^2\ell^2)(k\ell \operatorname{cosec} k\ell - 1)$)
)
and $\beta = (3/k^2\ell^2)(1 - k\ell \cot k\ell)$) .. .. (23)

and $k = \sqrt{P/EI}$.

The treatment given here is similar to that given in Niles and Newell "Airplane Structures" Vol. 2 (Wiley) but is believed to be simpler. In this book the α and β functions are derived in connection with the three moment equation for two adjacent struts. Equation (22) is simpler.

22. Bending of a bar subject to tension T and bending moments applied at its ends.

In this case we have

$$EI\,\theta_A = M_A \ell\beta_1/3 - M_B \ell\alpha_1/6 \quad .. \quad .. \quad (24)$$

where $\alpha_1 = (6/k_1^2\ell^2)(1 - k_1\ell \operatorname{cosech} k_1\ell)$)
)
and $\beta_1 = (3/k_1^2\ell^2)(k_1\ell \coth k_1\ell - 1)$) .. .. (25)

and $k_1 = \sqrt{T/EI}$.

The functions α and β for axial compression and α_1 and β_1 for axial tension are tabulated on pages 72 and 107 of Niles and Newell "Airplane Structures" Vol. II, 3rd ed., 1948, (Wiley).

23. The behaviour of a column fixed at one end.

Consider the column AB which is fixed at A and pinned at B (Fig. 13).

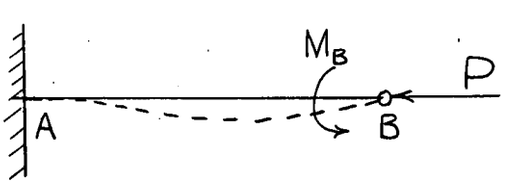

Fig. 13

Suppose a bending moment M_B is applied at B. This causes a deflection of the column as shown in the figure, and a bending moment M_A at A arises. Then we have

$$EI\,\theta_A = M_A \ell\beta/3 - M_B \ell\alpha/6,$$

and $$EI\,\theta_B = M_B \ell\beta/3 - M_A \ell\alpha/6.$$

Now since $\theta_A = o$, we have

$$M_A = (\alpha/2\beta)\ M_B.$$

and therefore $M_B/\theta_B = 4\beta EI/\ell(4\beta^2 - \alpha^2)$ .. .. (26)

M_B/θ_B represents the stiffness of the end B against an applied moment. The graph of M_B/θ_B against $k\ell$ is shown in Fig. 14. It is positive for values of $k\ell$ up to 4.495, becoming zero at this value, which corresponds to

$$P = k^2EI = 20.2\ EI/\ell^2.$$

When M_B/θ_B becomes zero, a vanishingly small applied moment causes a large rotation, and this gives the buckling load of the member.

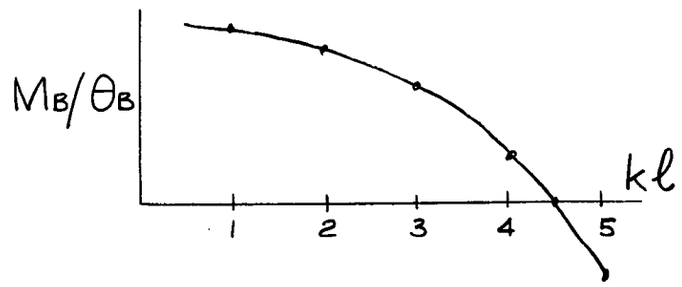

Fig. 14

24. The procedure can be given an energy interpretation. The work done by the applied moment is $\frac{1}{2} M_B \theta_B$ since M_B and θ_B are linearly related for any given values of P (Equation 26). The strut has not become unstable provided positive energy is required to deform it. The condition for stability is thus $\frac{1}{2} M_B \theta_B$ is positive. At neutral equilibrium $\frac{1}{2} M_B \theta_B$ is zero, and the expression becomes negative when the equilibrium is unstable. These criteria are consistent with those for stiffness given above, as they reduce to M_B/θ_B positive zero or negative.

25. <u>The buckling of a simple frame</u>.

Consider the simple plane frame shown in Fig. 15. The joint B is assumed to be rigid and the members have the same length and flexural rigidity.

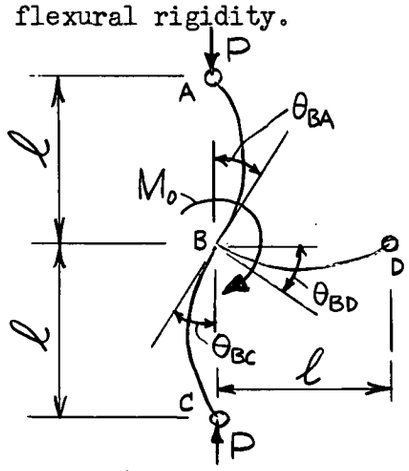

Fig. 15

To find the load P to cause buckling in the plane of the frame, a distorted form such as that shown is assumed. To cause the distortion, a small moment M_o is applied at the joint B. Clockwise moments and rotations are considered positive. The rotation at B is then given by

$$EI\theta_B = EI\theta_{BA} = M_{BA}\ell\beta/3$$
$$= EI\theta_{BD} = M_{BD}\ell/3$$
$$= EI\theta_{BC} = M_{BC}\ell\beta/3$$

Also $M_{BA} + M_{BD} + M_{BC} = M_o$, where M_{BA} is the moment that arises at B in the member BA, etc.

Therefore $(3EI/\ell)\left[\theta_{BA}/\beta + \theta_{BD} + \theta_{BC}/\beta\right] = M_o$

which gives $M_o\ell/EI\theta_B = 3(2/\beta + 1)$.

The stiffness is therefore zero when $\beta = -2$, and this occurs at $k = 3.5$ or $P = 12.3\ EI/\ell^2$.

26. Principles useful in the calculation of the buckling loads of more complicated frames can be illustrated by reference to the frame shown in Fig. 16.

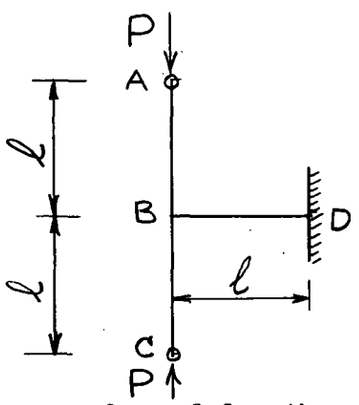

Fig. 16

The members are of equal length and flexural rigidity and the end D is fixed.

We have $EI\theta_B = EI\theta_{BA} = M_{BA}\ell\beta/3$,
$= EI\theta_{BD} = M_{BD}\ell/3 - M_{DB}\ell/6$,
$= EI\theta_{BC} = M_{BC}\ell\beta/3$

Also $EI\theta_{DB} = M_{DB}\ell/3 - M_{BD}\ell/6 = 0$ .. .. (28)

and $M_{BA} + M_{BD} + M_{BC} = M_o$ .. .. (29)

if an external moment M_o is applied at the joint B. Clockwise moments and rotations are considered positive.

Equation (28) gives

$$M_{DB} = \tfrac{1}{2} M_{BD}.$$

Hence equations (27) and (29) give

$$(3EI\theta_B/\ell)(1/\beta + 4/3 + 1/\beta) = M_o.$$

The stiffness of the joint is zero when $M_o/\theta_B = 0$,

or $\beta = -3/2$. This is the buckling condition, and yields

$k = 3.6$, or $P = 13.0\ EI/\ell^2$.

27. Alternatively, we may treat the behaviour as an eigenvalue problem. We have, putting M_o equal to zero,

$$M_{BA} + M_{BD} + M_{BC} = 0$$

$$M_{BA} - M_{BC} = 0$$

$$\beta M_{BA} - 3M_{BD}/4 = 0 .$$

These three equations, being linear and homogeneous in the three unknowns M_{BA}, M_{BD} and M_{BC}, have in general only the zero solutions $M_{BA} = M_{BD} = M_{BC} = 0$ (in which case all the end rotations are zero and the structure has not altered shape), unless the determinant of the coefficients is zero. In this case the equations are not independent and there is insufficient information to solve for the unknowns, which are therefore undefined.

Putting
$$\begin{vmatrix} 1 & 1 & 1 \\ 1 & 0 & -1 \\ \beta & -\frac{3}{4} & 0 \end{vmatrix} = 0$$

we obtain $\beta = -6/4$

which is the same condition as given above. The interpretation is that when the moments are undefined, then the linearly related end slopes are undefined and the system has buckled.

For a discussion of eigenvalue problems see Biezeno and Grammel "Engineering Dynamics" Vol. 1 (Blackie) p. 183, also Courant and Hilbert "Methods of Mathematical Physics" Vol. 1 (Interscience Publishers).

28. It will also be shown that at the buckling load the ratio of some internal bending moment to an externally applied disturbing moment M_o becomes infinite.

We have $M_{BA} + M_{BD} + M_{BC} = M_o$.

$$M_{BA} - M_{BC} = 0 .$$

$$\beta M_{BA} - 3M_{BD}/4 = 0 .$$

These give $2M_{BA} + M_{BD} = M_o$

Therefore $(6/4\beta + 1)\ M_{BD} = M_o$,

and $M_{BD}/M_o = (6/4\beta + 1)^{-1}$

The ratio becomes infinite when

$\beta = -3/2$, which is the same condition as previously.

29. We have therefore three conditions or methods for obtaining the buckling load of the frame in the mode considered. They are

(i) the stiffness of a joint to an applied disturbing moment becomes zero (or the energy required to rotate the joint becomes zero.)

(ii) the determinant of the coefficients in the equations in the bending moments is zero. (Similar equations in the deformations of the system, e.g. the end slopes of the members, can be handled in the same way.)

(iii) an applied disturbing moment causes an infinite internal moment in some member of the frame.

It is to be noted that the methods are mathematically equivalent once the desired buckling mode has been decided on. Various techniques are available for solving the equations, which become numerous and lengthy where a frame contains more than a few members even if these all lie in one plane. These techniques will be illustrated by referring to the buckling of a triangular frame.

30. <u>The Buckling of an Equilateral Triangular Frame in its Plane</u>.

One of the simplest frames is a triangle, and the buckling of an equilateral triangular frame having initially straight equal members will be considered. It is assumed that the frame is made up without any internal stresses being set up. Buckling in the plane of the frame without tension of the members can be ensured by placing the minor axis of inertia of the cross-section of the members so that it lies in the direction perpendicular to the plane of the frame.

Suppose the frame ABC is loaded in its plane as in Fig. 17, the applied forces passing through the intersections of the central axes of the members, so that no external moments are applied to the joints.

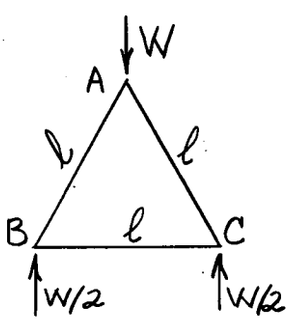

Fig. 17

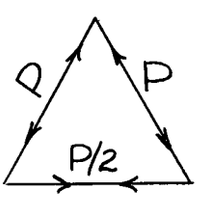

Fig. 18

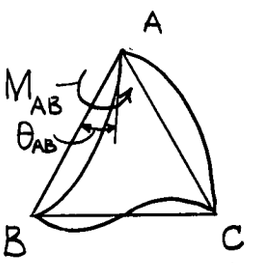

Fig. 19

Then the axial forces in the members AB, AC and BC can be written as P, P and $-\frac{1}{2}P$, (Fig. 18) where $P = W/\sqrt{3}$ and compression is considered positive.

Suppose the equilibrium of the structure is now disturbed in some way, giving rise to moments and slopes at the ends of the members as indicated in Fig. 19. Anticlockwise moments and slopes are considered positive.

Then we have

$$\left.\begin{aligned} EI\,\theta_{AB} &= M_{AB}\,\ell\beta/3 - M_{BA}\,\ell\alpha/6 \\ EI\,\theta_{BA} &= M_{BA}\,\ell\beta/3 - M_{AB}\,\ell\alpha/6 \\ EI\,\theta_{BC} &= M_{BC}\,\ell\beta'/3 - M_{CB}\,\ell\alpha'/6 \\ EI\,\theta_{CB} &= M_{CB}\,\ell\beta'/3 - M_{BC}\,\ell\alpha'/6 \\ EI\,\theta_{CA} &= M_{CA}\,\ell\beta/3 - M_{AC}\,\ell\alpha/6 \\ \text{and} \quad EI\,\theta_{AC} &= M_{AC}\,\ell\beta/3 - M_{CA}\,\ell\alpha/6 \end{aligned}\right\} \quad .. \quad .. \quad (30)$$

where α and β refer to members of length ℓ having axial compressive load P, and α' and β' refer to a member of length ℓ having axial tension P/2. For continuity at the corners,

$$\theta_{AB} = \theta_{AC},\ \theta_{BA} = \theta_{BC},\ \text{and}\ \theta_{CB} = \theta_{CA}.$$

Also, since there are no external moments at the joints

$$M_{AB} + M_{AC} = 0,\ M_{BA} + M_{BC} = 0,\ M_{CB} + M_{CA} = 0.$$

Hence, putting

$$M_{AB} = M_A = -M_{AC}$$

$$M_{BC} = M_B = -M_{BA}$$

$$M_{CA} = M_C = -M_{CB},$$

we have

$$4\beta M_A + \alpha M_B + \alpha M_C = 0$$

$$\alpha M_A + 2(\beta + \beta')\,M_B + \alpha' M_C = 0$$

$$\alpha M_A + \alpha' M_B + 2(\beta + \beta')\,M_C = 0$$

At the buckling load, M_A, M_B, and M_C are undefined.

Therefore

$$\begin{vmatrix} 4\beta & \alpha & \alpha \\ \alpha & 2(\beta+\beta') & \alpha' \\ \alpha & \alpha' & 2(\beta+\beta') \end{vmatrix} = 0.$$

This determinant, on expanding and factorising, gives

$$(2\beta + 2\beta' - \alpha')\left[2\beta(2\beta + 2\beta' + \alpha') - \alpha^2\right] = 0 \quad .. \quad .. \quad (31)$$

There are two modes of buckling. The symmetrical mode, (Fig. 20a) is obtained by putting the second factor equal to zero, and gives

$$k\ell = 5.0 \quad \text{or} \quad P = 25\ EI/\ell^2.$$

The unsymmetrical mode, (Fig. 20b), which occurs at a lower load is obtained by putting the first factor equal to zero, and gives

$$k\ell = 4.0 \text{ or } P = 16\ EI/\ell^2.$$

(It should be remembered that if $k = \sqrt{P/EI}$, then $\sqrt{P/2EI}$ equals $k/\sqrt{2}$. α and β are thus functions of $k\ell$, for axial compression while α' and β' are functions of $k\ell/\sqrt{2}$ for axial tension).

(a) (b)

Fig. 20

In the above analysis for the triangular frame, all the equations have been written down. From considerations of symmetry or antisymmetry, this is in this case (and usually) unnecessary. The full treatment is given here because in certain cases, notably when dealing with problems of buckling out of the plane, the simplifications available from symmetry considerations are often rather difficult to handle.

31. It is interesting to note that the solution for the unsymmetrical mode of buckling can be obtained by applying a small external moment at one of the joints. Consider the triangle ABC loaded as in Fig. 21. A small moment M_o is applied to the joint A so as to bend the frame into the shape shown.

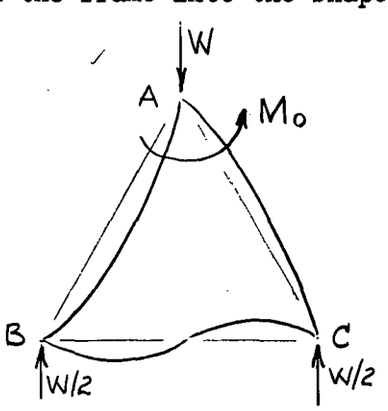

Fig. 21

Suppose the moments set up at the ends of the members are M_{AB}, etc., and the corresponding end slopes θ_{AB}, etc. Then equations (30) still hold. However, in this case

$$M_{AB} + M_{AC} = M_o.$$

$$M_{BA} + M_{BC} = 0.$$

and $$M_{CB} + M_{CA} = 0.$$

Also, from the antisymmetry of the distorted shape,

$$\theta_{BA} = \theta_{BC} = \theta_{CB} = \theta_{CA}, \text{ and } \theta_{AB} = \theta_{AC}.$$

Inspection of equations (30) then gives

$$M_{BA} = M_{CA} = -M_{BC} = -M_{CB}$$

and $$M_{AB} = M_{AC} = \tfrac{1}{2} M_o. \qquad .. \quad .. \quad (32)$$

$\theta_{BA} = \theta_{BC}$ and the second and fourth equations of (30) then give

$$M_{BA}/M_o = (\alpha/2)/(2\beta + 2\beta' - \alpha') \qquad .. \quad .. \quad (33)$$

The frame buckles when a small applied moment M_o produces an internal moment which tends to infinity, or M_{BA}/M_o tends to infinity. Hence, at the buckling load,

$$2\beta + 2\beta' - \alpha' = 0$$

which is the same condition as we obtained previously.

The solution is unaltered by putting M_o equal to zero in the equations (32).

This gives $M_{AB} = M_{AC} = 0$

We then have, from

$$\theta_{BA} = \theta_{BC},$$

$$M_{BA}\,(2\beta + 2\beta^1 - \alpha^1) = 0.$$

If $$2\beta + 2\beta^1 - \alpha^1 = 0,$$

M_{BA} is undefined, and a vanishingly small disturbance has resulted in buckling.

32. The unsymmetrical buckling mode can also be solved by using the moment distribution convergence criterion. This method is valuable in determining the critical loads of more complicated frames. The solution of this problem is carried out here as an illustration. The method is merely the solution of equation (33) by moment distribution. So long as the process converges, M_{BA}/M_o is finite. At or above the buckling load, M_{BA}/M_o is infinite and the process of moment distribution diverges.

For a discussion of the moment distribution convergence criterion, see N. J. Hoff "The Analysis of Structures" (Wiley) pp. 294 - 318. The unified treatment given in this thesis of the calculation of critical loads by all methods is, however, believed to be original.

33. Consider first the frame ABC with no external forces acting, so that the axial forces in the members are zero. A small moment of 100 units is applied at A. In this case, all carry over and distribution factors are equal to 0.5 and the moment distribution is as follows .

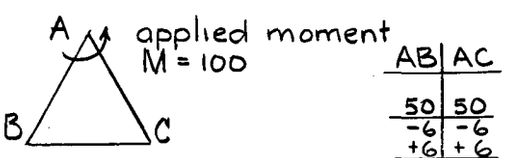

BA	BC
25	
-12	-13
	-6
+3	+3
+3	+1
-2	-2
+16	-17

AB	AC
50	50
-6	-6
+6	+6
+1	+1
-1	-1
50	50

CB	CA
-17	+16

Fig. 22.

The final bending moment diagram is

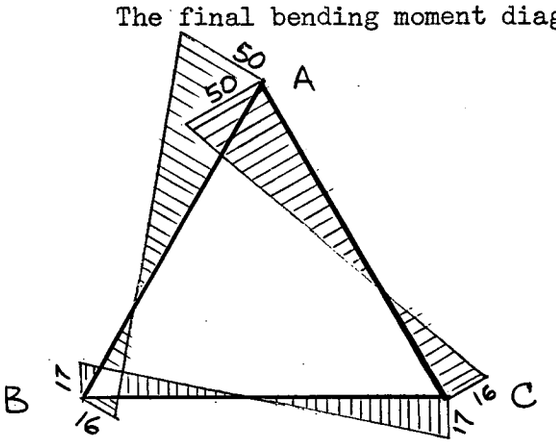

Fig. 23

This can be checked, since

$$EI\,\theta_{BA} = M_{BA}\,\ell/3 - M_{AB}\,\ell/6$$
$$= EI\,\theta_{BC} = M_{BC}\,\ell/3 - M_{CB}\,\ell/6 .$$

But $M_{BA} + M_{BC} = 0$ and $M_{BC} = M_{CB}$

Therefore $M_{BA} = M_{AB}/3$

If $M_{AB} = 50$, $M_{BA} = 16.7$.

Where there is an axial force in a member, the carry over and distribution factors must be adjusted accordingly. Consider a bar AB subject to axial force P and bending moments M_A and M_B.

Then $$\theta_A = M_A\,\ell\beta/3EI - M_B\,\ell\alpha/6EI$$

and $$\theta_B = M_B\,\ell\beta/3EI - M_A\,\ell\alpha/6EI.$$

If rotation is not allowed at B, $\theta_B = 0$

and $$M_B = M_A\alpha/2\beta$$

For an applied moment M_A at A, the carry over to B, if rotation is not allowed there, is $\alpha M_A/2\beta$. The rotation at A is given by

$$EI\,\theta_A = M_A\,\ell\beta/3 - M_A\,\alpha^2/12\beta$$
$$= M_A\,(\ell/3)(\beta - \alpha^2/4\beta)$$
$$= M_A\,(\ell/4)\,(4\beta^2 - \alpha^2)/3\beta .$$

Consider a number of members 1, 2, 3, etc., meeting at a joint, (Fig. 24), their far ends being prevented from rotating. Suppose a moment M applied to the joint causes rotation θ. If the moments induced in the individual members are M_1, etc., then

$$M_1 = (4EI_1/\ell_1)(3\beta_1\theta)/(4\beta_1^2 - \alpha_1^2$$

But $$M = \Sigma M_1 = 4E\theta\,\Sigma\,(I/\ell)\left[3\beta/(4\beta^2 - \alpha^2)\right]$$

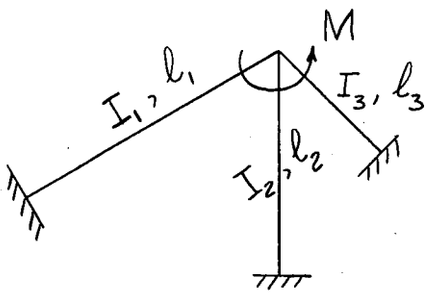

Fig. 24

Therefore $$\theta = \frac{M}{4E \Sigma (I/\ell)\ 3\beta/(4\beta^2 - \alpha^2)}$$

and $$M_1 = \frac{M\ (I_1/\ell_1)\left[\ 3\beta_1/(4\beta_1^2 - \alpha_1^2)\right.}{\Sigma\ (I/\ell)\ \ 3\beta\ /(4\beta^2\ \ -\alpha^2)}$$

These stiffnesses and carry-over factors are tabulated on pages 122 and 125 of Niles and Newell "Airplane Structures", Vol. ii, for both axial compression and axial tension.

The moment distribution for the triangle loaded as in Fig. 25 can now be proceeded with.

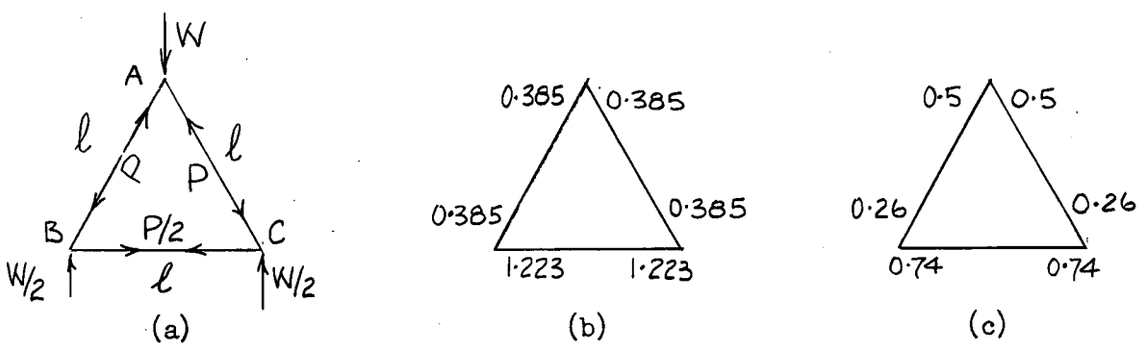

Fig. 25

Put $$(k\ell)_{AB} = 3.8; \quad \text{that is } P = (3.8)^2 EI/\ell^2$$

Then the α and β functions, and the carry over stiffness factors are as in the table:

Member	Thrust	$k\ell$	α	β	$\alpha/2\beta$	$\frac{3\beta}{4\beta^2 - \alpha^2}$
AB	P	3.8	-2.9961	-0.8128	1.843	0.3850
AC	P	3.8	-2.9961	-0.8128	1.843	0.3850
BC	-P/2	2.7	0.533	0.716	0.3685	1.223

Stiffness and distribution factors are shown in Figs. 25b and 25c. The distribution of an external moment of 100 units applied at joint A is carried out in Fig. 26. Only half the calculation is shown, as the distribution is symmetrical. Fig. 27 shows the resulting bending moment diagram. Comparison with Fig. 23 shows that large bending moments are induced in the frame as the buckling load is approached.

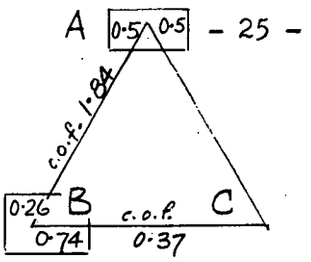

M_{BA} summed	BA	BC
	92	
68	-24	-68
	81	-29
146	-13	-39
	+44	-16
183	-7	-21
	+24	-9
203	-4	-11
	+13	-4
214	-2	-7
	+7	-3
220	-1	-3
	+3	-1
222	-1	-1
	+222	+222

AB	AC
100	
50	50
-44	
+44	
-24	
+24	
-13	
+13	
-7	
+7	
-4	
+4	
-2	
+2	
50	50

Fig. 26

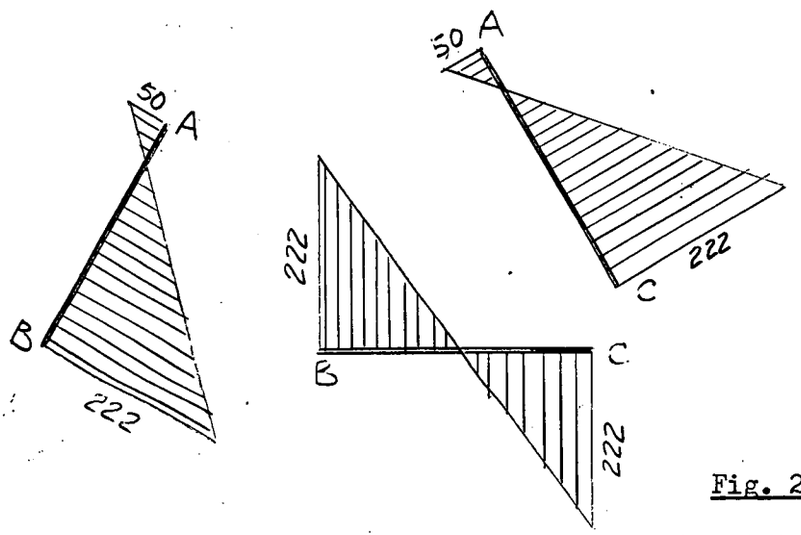

Fig. 27

The accuracy of the distribution may be checked by substitution in equation (33).

We have $M_{BA}/M_o = (\alpha/2)/(2\beta + 2\beta' - \alpha')$

$= 2.21$ for $k\ell = 3.8$

In this case $M_o = 100$

therefore $M_{BA} = 221$. This agrees with Fig. 26.

In this case, the distribution has converged, and the buckling condition is therefore $(k\ell)_{AB} > 3.8$. However, induced moments are large, and the buckling load is being approached.

Put $(k\ell)_{AB} = 4.0$

Then the carry-over and stiffness factors for the members are:

Member	$k\ell$	$\alpha/2\beta$	$\frac{3\beta}{4\beta^2 - \alpha^2}$
AB	4.0	2.56	0.293
AC	4.0	2.56	0.293
BC	2.81	0.362	1.238

Fig. 28 shows the distribution of an external moment of 100 units applied at joint A.

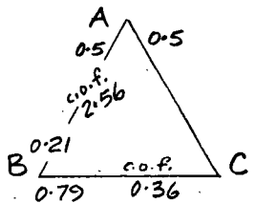

AB	AC
	100
50	50
-70	
+70	
-74	
+74	

BA	BC
+128	
-27	-101
+178	-42
-29	-107
+190	-45

Fig. 28

This distribution is diverging, so the buckling load has been reached (or passed) at $k\ell = 4.0$.

The two solutions to equation (31) for the two buckling modes were checked by experiments with a model made of flexible strip, and resulted in good agreement. It is also possible to calculate the higher critical load for the symmetrical buckling mode by the determinant method as in Art. 30 or by imposing the required distortion pattern as in Art. 31.

The application of suitable disturbing moments consisting of equal moments of opposite sign at B and C, also permits solution by the moment distribution convergence method. However, it appears that in the case of more complicated frames, unless some sort of symmetry or anti-symmetry can be preserved, considerable care is required in the calculation by the moment distribution method of higher critical loads for buckling modes other than the fundamental. Even if a suitable disturbance is given, slight errors in distribution might well cause divergence at the first critical load.

It should be noted that the calculation of higher critical loads is not always merely an academic problem. The pattern of imperfections throughout a structure may be such that at failure it deflects in a mode which does not correspond to the fundamental mode of the corresponding perfect structure.

34. When the moment distribution method is used to find the first critical load for more complicated frames, it often becomes difficult to ascertain whether the process is converging or diverging. The zero stiffness method proposed by H.G. Allen overcomes this difficulty in certain cases. Allen has contributed two valuable papers on the calculation of critical loads using the zero stiffness conception: "The Estimation of the Critical Load of a braced Framework" Proc. Roy. Soc. London Series A Vol. 231 (1955) p. 25, and "The Estimation of the Critical Loads of Certain Frameworks" The Struct. Engnr. Vol. 35, No. 4, April, 1957, p. 135. In his first paper Allen uses the conception of positive energy being required to displace a stable structure. In the second paper the emphasis is placed on stiffness, and it is also shown that his procedure of successive reduction of triangular frames to single members of equivalent stiffness is mathematically equivalent to reducing the determinant.

The principle of zero stiffness of a joint to an applied moment at the buckling load has been explained. Professor Allen's technique of solving the equations will be applied to the triangular frame.

Firstly, consider the strut AB, (Fig. 29),

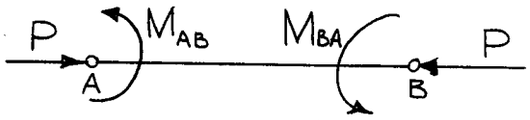

Fig. 29

Then, using the previous notation, we have

$$EI\,\theta_{AB} = M_{AB}\,\ell\beta/3 - M_{BA}\,\ell\alpha/6 \quad \text{(See equation 22)}$$

and $$EI\,\theta_{BA} = M_{BA}\,\ell\beta/3 - M_{AB}\,\ell\alpha/6,$$

α and β being defined by equations (23).

These equations may be rewritten in the form

$$\left.\begin{aligned} M_{AB} &= P\ell(\alpha\theta_{AB} + \beta\theta_{BA}) \\ M_{BA} &= P\ell(\alpha\theta_{BA} + \beta\theta_{AB}) \end{aligned}\right\} \quad \ldots\ \ldots (34)$$

where α and β are now defined by

$$\left.\begin{aligned} \alpha &= \frac{1}{2k\ell}\left[\frac{k\ell}{2 - k\ell\cot\frac{1}{2}k\ell} + \cot\tfrac{1}{2}k\ell\right] \\ \beta &= \frac{1}{2k\ell}\left[\frac{k\ell}{2 - k\ell\cot\frac{1}{2}k\ell} - \cot\tfrac{1}{2}k\ell\right] \end{aligned}\right\} \quad (35)$$

where $k = \sqrt{P/EI}$.

Values of α and β are tabulated against P/Q in "The Analysis of Engineering Structures" by Pippard and Baker, (1943). The notation used here is that of these authors, and care should be taken that equations (22) and (34) are not confused.
Equations (34) can be rewritten

$$\left.\begin{aligned} M_{AB} &= U_{AB}\,\theta_{AB} + V_{AB}\,\theta_{BA} \\ M_{BA} &= U_{BA}\,\theta_{BA} + V_{BA}\,\theta_{AB} \end{aligned}\right\} \quad \ldots\ \ldots (36)$$

where

$$\left.\begin{aligned} U_{AB} &= U_{BA} = P\ell\alpha \\ V_{AB} &= V_{BA} = P\ell\beta \end{aligned}\right\} \quad \ldots\ \ldots (37)$$

Consider the triangle ABC loaded in its plane (Fig. 30), where the members are subjected to axial loads.

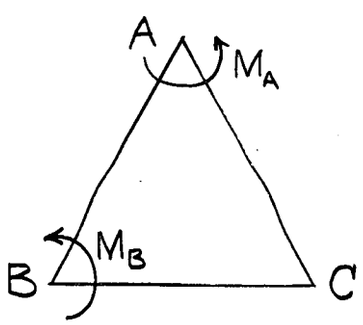

Fig. 30.

Now suppose disturbing moments M_A and M_B are applied at the joints A and B. We then have

$$M_A = M_{AB} + M_{AC}.$$

$$M_B = M_{BA} + M_{BC}.$$

$$M_{CA} + M_{CB} = 0.$$

Now $$M_{AB} = U_{AB}\,\theta_{AB} + V_{AB}\,\theta_{BA}$$

$$M_{AC} = U_{AC}\,\theta_{AC} + V_{AC}\,\theta_{CA}$$

and $$\theta_{AB} = \theta_{AC} = \theta_A.$$

Similar equations apply at the other joints. Elimination of θ_C throughout gives

$$\left.\begin{aligned} M_A &= U'_{AB}\,\theta_A + V'_{AB}\,\theta_B \\ \text{and}\quad M_B &= U'_{BA}\,\theta_B + V'_{BA}\,\theta_A \end{aligned}\right\} \quad .. \quad .. \quad (38)$$

where

$$\left.\begin{aligned} U'_{AB} &= U_{AB} + U_{AC} - V^2_{AC}/(U_{CA} + U_{CB}) \\ U'_{BA} &= U_{BA} + U_{BC} - V^2_{AC}/(U_{CA} + U_{CB}) \\ \text{and}\quad V'_{AB} &= V'_{BA} = V_{AB} - V_{AC}\,V_{CB}/(U_{CA} + U_{CB}) \end{aligned}\right\} \quad . \quad (39)$$

The modified slope deflection equations (38) give the relationships between the moments M_A and M_B applied to the triangle ABC and the rotations of the joints, θ_A and θ_B. The triangle ABC can therefore be replaced by a hypothetical member A'B' of equal stiffness with respect to disturbing moments. Neutral equilibrium exists when M_A/θ_A is zero for zero M_B. The condition for stability is that M_A/θ_A is positive. From equations (38), if M_B is zero, we have

$$M_A/\theta_A = (U'_{AB}\,U'_{BA} - V'_{AB}\,V'_{BA})/U'_{BA}$$

The criterion for stability is therefore

$$U'_{AB}\,U'_{BA} - V'_{AB}\,V'_{BA} > 0 \quad .. \quad .. \quad (40)$$

35. If the triangle ABC is loaded as shown in Fig. 31a, the values of U and V are as in the table, if P/Q for the struts AB and AC has the value 1.5.

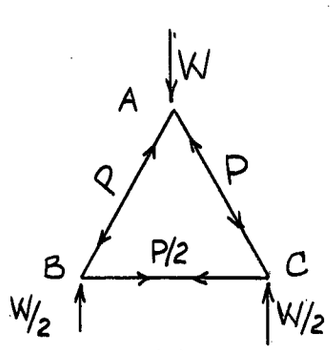

(a)

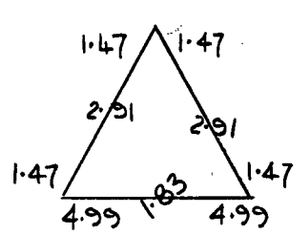

(b)

P/Q = 1·5

Fig. 31

Member	Type	Q	ℓ	P/Q	α	β	U=P$\ell\alpha$	V=P$\ell\beta$
AB	strut	1	10	1.5	.098	.194	1.47	2.91
AC	strut	1	10	1.5	.098	.194	1.47	2.91
BC	tie	1	10	0.75	.665	.244	4.99	1.83

The values of U and V for each member are shown in Fig. 31b, U values being written near the ends of the members and V values near the centres. The triangle ABC may now be replaced by a member A'B' of equal stiffness so far as disturbing moments are concerned. We have, using equations (39),

$$U'_{AB} = 1.47 + 1.47 - (2.91)^2/(1.47 + 4.99) \qquad = 1.62$$

$$U'_{BA} = 1.47 + 4.99 - (1.83)^2/(1.47 + 4.99) \qquad = 5.94$$

$$V'_{AB} = V'_{BA} = 2.91 - (2.91 + 1.83)/(1.47 + 4.99) = 2.09$$

The expression of the left of equation (40) has the value

$$(1.62 \times 5.94) - (2.09)^2 = 4.25.$$

This expression may be called the stability criterion. In this case it is positive, and the frame is stable.

When P/Q has the value 1.6, the calculation is as follows

Member	P/Q	α	β	U	V
AB	1.6	.078	.189	1.24	3.02
AC	1.6	.078	.189	1.24	3.02
BC	0.8	.628	.227	5.00	1.82

$$U'_{AB} = 1.24 + 1.24 - (3.02)^2/(1.24 + 5.00) = 1.02$$

$$U'_{BA} = 1.24 + 5.00 - (1.82)^2/(1.24 + 5.00) = 5.71$$

$$V'_{AB} = V'_{BA} = 3.02 - (3.02 \times 1.82)/(1.24 + 5.00) = 2.14$$

Stability criterion = $(1.02 \times 5.71) - (2.14)^2 = 0.24$. This is positive and the frame is stable.

For P/Q = 1.7, we have

Member	P/Q	α	β	U	V
AB = AC	1.7	.058	.184	0.99	3.13
BC	0.85	.599	.213	5.09	1.81

$$U'_{AB} = 0.99 + 0.99 - (3.13)^2/(0.99 + 5.09) = 0.37$$

$$U'_{BA} = 0.00 + 5.09 - (1.81)^2/(0.99 + 5.09) = 5.54$$

$$V'_{AB} = V'_{BA}\ \ 3.13 - (3.13\ \ 1.81)/(0.99 + 5.09) = 2.40$$

Stability criterion

$= (0.37 \times 5.54) - (2.40)^2 = -3.7$. This is negative and the critical load has been exceeded.

A graph of the stability criterion against P/Q is shown in Fig. 32. It becomes zero at P/Q = 1.61 which corresponds to $k\ell = \pi\sqrt{1.61} = 3.99$, or $P = 16\ EI/\ell^2$. This is in good agreement with the value obtained in Art. 30 as the solution of equation (31) which corresponds to the lowest critical load for the gravest buckling mode.

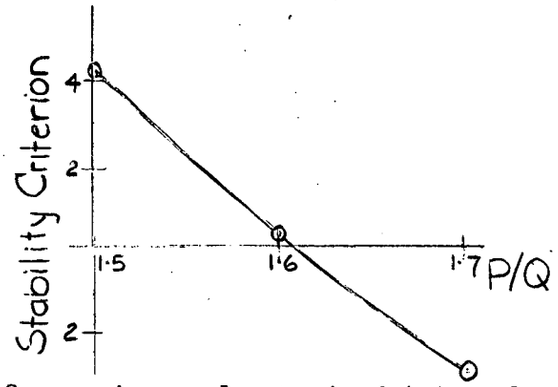

Fig. 32

36. Successive replacement of triangular frames by members of equal stiffness furnishes a method for the determination of the critical loads of plane triangulated rigid-jointed frames which are not redundant if the joints are considered pinned.

The value of Allen's method is that there is no question of having to determine the convergence or otherwise of a distribution process. The buckling load is given by the stability criterion becoming zero. Interpolation and the plotting of a curve of the stability criterion against load aids the calculation, whereas no such aid is available when using the moment distribution convergence criterion. The method as given is limited to plane triangulated non-redundant frames. It is of course extendable in principle to redundant frames (if the forces in the members can be estimated by some means), and to space frames, but the equations then become very difficult.

37. In the discussion of the buckling of the triangular frame, the mathematical equivalence of the classical methods of analysing the frame and the various special techniques for handling the equations, such as Allen's stability criterion or zero-stiffness method, or the moment distribution convergence criterion, can be clearly seen. The methods all depend on the properties of linear equations where the coefficients are functions of the applied loading.

Where there exists more than one buckling mode having different critical loads, the determinant method gives all the solutions. Other methods such as the application of a single disturbing moment (this includes Allen's method and the moment distribution convergence criterion) will in general give the lowest critical load associated with the gravest buckling mode though the author has found that this may not always be the case if a joint which does not rotate in the gravest buckling mode of deformation is chosen for the application of the disturbing moment. Some care is therefore necessary in the application of these methods.

38. It is worth mentioning that when considering any structure, we are concerned with the stability or instability of the structure as a whole. Though compression members or elements must be present for buckling to occur, the critical load and the associated mode are dependent on the properties of the whole of the frame and its loading. This is still the case for practical frames under load.

39. The buckling of a Warren truss in its plane.

As an example of the application of various methods of calculation of critical loads of plane triangulated frames, the buckling of a Warren truss will be considered. The classical method will first be used to determine the buckling mode.

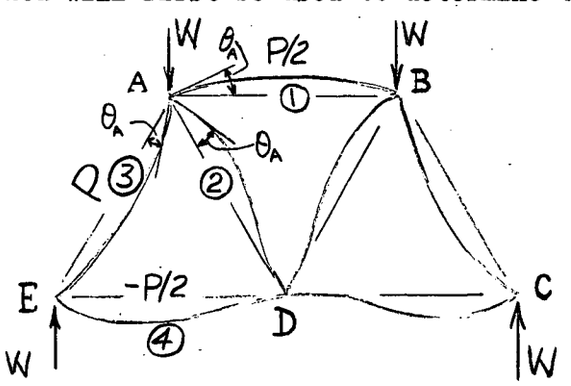

Fig. 33

The truss, when loaded as in Fig. 33, may buckle in various modes, but the critical load for the symmetrical mode shown will be calculated. The forces in the members are given in the figure, and all members have equal length and flexural rigidity. On applying a distortion of this form, we have

$$\theta_A = -\theta_B, \quad \theta_E = -\theta_C, \quad \theta_D = 0 .$$

Then $$\theta_A = \theta_{AB} = M_{AB}\beta_{AB}\ell/3EI - M_{BA}\alpha_{AB}\ell/6EI$$

and $$\theta_B = \theta_{BA} = M_{BA}\beta_{BA}\ell/3EI - M_{AB}\alpha_{AB}\ell/6EI .$$

Hence $$M_{BA} = -M_{AB}$$

The other equations of symmetry are easily written down. We then have, denoting the members by the numerals in the figure,

$$\left.\begin{aligned} 6EI\ \theta_{AB}/\ell &= M_{AB}(2\beta_1 + \alpha_1) \\ 6EI\ \theta_{AD}/\ell &= M_{AD}\cdot 2\beta_1 - M_{DA}\ \alpha_2 \\ 6EI\ \theta_{AE}/\ell &= M_{AE}\cdot 2\beta_3 - M_{EA}\ \alpha_3 \end{aligned}\right\} \quad .. \quad (40)$$

Also from $$\theta_{EA} = \theta_{ED},$$

$$M_{EA}\cdot 2\beta_3 - M_{AE}\alpha_3 = M_{ED}\cdot 2\beta_4 - M_{DE}\alpha_4 .. \quad (41)$$

and from $$\theta_{DE} = \theta_{DA} = 0,$$

$$M_{DE}\cdot 2\beta_4 - M_{ED}\alpha_4 = 0 = M_{DA}\cdot 2\beta_2 - M_{AD}\alpha_2$$

$$\left.\begin{aligned} \text{Hence } M_{DE}/M_{ED} &= (\alpha/2\beta)_4 \\ \text{and } \quad M_{DA}/M_{AD} &= (\alpha/2\beta)_2 \end{aligned}\right\} \qquad .. \quad .. \quad (42)$$

The subscript numerals apply to the members marked in Fig. 33. For no applied moments at the joints,

$$\left.\begin{aligned} M_{AB} + M_{AD} + M_{AE} &= 0 \\ M_{EA} + M_{ED} &= 0 \end{aligned}\right\} \qquad .. \quad .. \quad (43)$$

and $$M_{DE} + M_{DA} + M_{DB} + M_{DC} = 0.$$

The latter equation is satisfied by the equations of symmetry. Substitution of equations (42) in the second equation of (40) and in equation (41) results in five equations in the five unknowns M_{AB}, M_{AD}, M_{AE}, M_{EA}, M_{ED}. Setting the determinant equal to zero for the buckling condition gives

$$\begin{vmatrix} (2\beta_1 + \alpha_1) & -\left(\frac{4\beta^2 - \alpha^2}{2\beta}\right)_2 & 0 & 0 & 0 \\ (2\beta_1 + \alpha_1) & 0 & (-2\beta_3) & (+\alpha_3) & 0 \\ 0 & 0 & (-\alpha_3) & (+2\beta_3) & -\left(\frac{4\beta^2 - \alpha^2}{2\beta}\right)_4 \\ 1 & 1 & 1 & 0 & 0 \\ 0 & 0 & 0 & 1 & 1 \end{vmatrix} = 0$$

Because of the simplicity of its last two rows, this determinant is easily reduced to one of the third degree which on expansion and graphical solution gives

$$(k\ell)_{AE} = 4.68 \quad \text{or} \quad P = 22\ EI/\ell^2.$$

It is seen that there will be considerable difficulty in solving by this method frames of higher complexity than this.

40. The solution of this simple frame by the moment distribution convergence criterion is somewhat lengthy. The slow convergence or divergence of the process at loads near the critical load tends to make the determination of critical loads by this method rather tedious. The reason for this is evident, and has been clearly stated in a recent paper by Bolton: "Basically this difficulty arises because the testing distortion used is not the critical mode, but merely the rotation of one joint. If the critical mode were to be used as the testing distortion, one cycle would be sufficient to decide whether the calculations were converging or not." The reason for this is that it takes many distributions for the effect of a single disturbance at a single joint to be felt throughout the whole frame, and many more for the carry-over to reflect back to the originally disturbed joint. In many cases, even after several of these rather lengthy cycles, it is difficult to determine whether the process is converging or diverging.

41. Several methods have been advanced with a view to reducing the length of the calculation involved. A method due to the author is to apply disturbing moments at several joints rather than at one joint, particularly if the disturbances can be given the correct sign, which is often the case if the desired buckling mode can be pictured. If any disturbance is given an incorrect sign, the effect is then to hinder the quicker convergence or divergence being aimed at.

For the truss loaded as in Fig. 33, we have, if $(k\ell)$ for the member AE equals 4.8:

Member	Load	$k\ell$	Carry-over factor $\alpha/2\beta$	Stiffness $3\beta/(4\beta^2 - \alpha^2)$
AE = BC	P	4.8	-4.093	-0.257
AB	P/2	3.4	1.206	0.537
AD = BD	0	0	0.500	1.000
ED = DC	-P/2	-3.4	0.321	1.338

For disturbing moments as shown in Fig. 34, the distribution is carried out in Fig. 35.

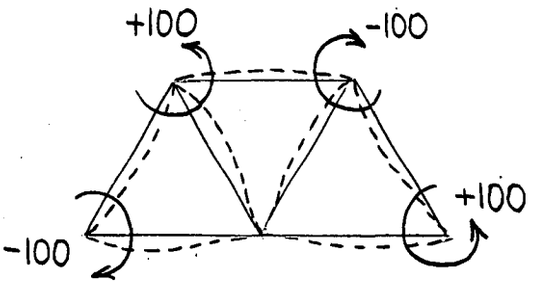

Fig. 34.

(+100)

AE	AD	AB
-20	+78	+42
-98	0	-51
-30	+117	+63
-82	0	-77
-32	+124	+67
-123	0	-33
-31	+121	+65
-127	0	-79
-41	+151	87
-131	0	-105

(-100)

BA	BD	BC
-42	-78	+20
+51	0	+98
-63	-117	+30
+77		

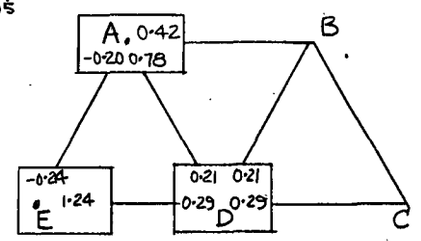

(-100)

EA	ED
24	-124
82	0
20	-102
123	0
30	-153
131	0
31	-163
127	0
32	-158
168	

DE	DA
0	0
-40	+39
0	0
-33	+58
0	0
-49	+60
0	0
-52	+60
0	0
-51	+75

DB	DC
0	0
-39	+40
0	0

(+100)

CD	CB
+124	-24
0	-82
+102	-20

Fig. 35

It is evident from inspection that the process is diverging. It is worthwhile keeping a running table of the moments distributed at each stage if block distribution is used. They are:-

Distribution No.	Moments distributed at A	B	C	D	E	Half Numerical sum of moments
1	+100	-100	+100	0	-100	200
2	+149	-149	+ 82	0	- 82	231
3	+159	-159	+123	0	-123	282
4	+156	-156	+131	0	-131	288
5	+206	-206	+127	0	-127	333
6	+236	-236	+168	0	-168	404

The variation of the numerical sum of the moments distributed at each stage appears to be a guide to the determination fo whether the process is converging or diverging.

Experiments made by the author with a carefully made flexible model indicate that the buckling mode solved here is the fundamental mode possessing the lowest critical load. Divergence of the distribution here for $(k\ell)_{AE} = 4.8$ is in agreement with the fact that the critical load is given by $(k\ell)_{AE} = 4.68$. (Art. 39). It can be shown that if a moment is applied at D, or if the signs of any of the other disturbing moments are changed, then the divergence is slower and it is more difficult to decide whether the distribution is in fact diverging. More distributions are required in order to be sure. Also, if any of the disturbing moments have incorrect signs, the keeping of running totals of the moments distributed at each stage (whether summed algebraically or numerically) appears to convey very little information.

In conclusion it may be stated that when using the moment distribution convergence criterion it is best to apply only one disturbing moment unless the buckling mode can be at least partly pictured. If this is so other disturbing moments can be added, but any given the wrong sign will hinder the rate of convergence or divergence.

The above discussion will be found to be in disagreement with a paper by A. Bolton "A Convergence Technique for Determining the Elastic Critical Loads of Rigidly Jointed Trusses" The Struct. Engnr. Vol. 37 No. 8 Aug. 1959 p. 233. In this paper, Bolton has worked some problems in which disturbing moments are applied at several joints of a frame. These moments are given any sign (the buckling mode is not pictured), and a guide to the determination of whether the moment distribution is converging or diverging appears to be available by attention to the algebraic sum of the moments distributed in each cycle. However, the method does not appear to be generally valid.

42. A further method of simplifying the moment distribution is to carry out the process for only part of the frame. The member with the lowest stiffness is chosen, a disturbing moment is applied at one end, and the moment distribution is carried out considering joints some distance away as either (i) fixed or (ii) pinned. The convergence divergence criterion is used to find the critical load in either case, and the critical load solutions to (i) and (ii) appear in some cases to sandwich the critical load of the structure as a whole. Though there is some supporting experimental evidence in these cases, it is by no means evident that the principle is generally valid.

(See A. Bolton "A Quick Approximation to the Critical Loads of Rigidly Jointed Trusses" The Struct. Engnr. Vol. 33 p. 9, Mar. 1955. The method was used by N. W. Murray, in "A Method of Determining an Approximate Value of the Critical Loads at which Lateral Buckling Occurs in a Rigidly Jointed Truss" Proc. I.C.E. June 1957 p. 387, with good experimental agreement).

43. It may be mentioned that some difficulty was encountered by the author in applying Professor Allen's method (Art. 34) to the Warren truss loaded as in Fig. 33. This truss contains unloaded members, but it can be shown that though the parameters α and β (equations 34 and 35 become infinite when P is zero, the parameters U and V (equations 36) take the finite values EI and $\frac{1}{2}$EI respectively. The application of the method to this problem seems to hinge a great deal on the accuracy with which U and V can be written down for all the members, and it was not found possible to achieve agreement with the foregoing calculations.

44. The buckling of space frames, or of plane structures out of their plane:

In principle, space frames can be handled by any of the methods previously discussed. It is necessary to write down the three components of the rotations of the ends of a member in terms of its torsional and flexural rigidities about each axis and the bending and twisting moments in the member. The equations of continuity and equilibrium of each joint then provide sufficient information to solve for the buckling load. The equations become, of course, very difficult to handle. As examples, Murray has applied the approximate technique given in Art. 42 to calculate the critical load at which a lattice girder buckles laterally when laterally restrained at the panel points. The author has also solved by the classical method the buckling of a plane triangular frame out of its plane, and this will be given later. Certain problems of buckling in space such as lateral buckling of beams are also amenable to solution by energy methods such as Rayleigh's principle.

45. The buckling of redundant frames.

Where the forces in a frame cannot be obtained simply from statics, the joints being considered pinned, strain or complementary energy methods are available for their estimation. Any of the foregoing techniques, except Professor Allen's method unless it is modified, are then applicable for the calculation of critical loads.

46. The load carrying capacity of practical frames.

Attention has up to this point been devoted mainly to the calculation of critical loads of elastic structures. The critical load for a given mode of deformation has been defined as the load at which the structure is in neutral equilibrium with respect to static displacements in that mode. The critical load is a property of the structure if it is initially perfect - that is, the members are initially straight, loads are centrally applied, and no eccentricities at joints are present. The structure is also assumed to remain elastic during the specified displacement. Flexible structures of sufficiently high yield strength, when carefully made and loaded, do reach approximately this load in practice, and then assume large deformations. But for most practical structures the critical load remains a mathematical property of the structure. The effects of crookedness of members, imperfections of alignment of members and loads at joints, and the limited deformations which are available before yielding of the material

occurs, cause the load carrying capacity to depart considerably from the critical load. All the imperfections listed, and particularly their pattern throughout the whole structure, may also influence the buckling mode at failure. In practice, the problem is usually to determine, not one of the critical loads of a structure, but its load carrying capacity. This is defined in some way to suit the purpose of the structure, such as the maximum load the structure can carry, or the load at which there occur deformations which cannot be tolerated. Once the load carrying capacity of the structure is known, safe or working loads can be estimated.

47. Some discussion as to the relation between the practical behaviour of a structure under load, its critical load, and its imperfections, has already been given for the case of a rod and spring mechanism and a pin-ended column. This approach will later be further elaborated.

48. The failure or even deformation of a structure (by instability or otherwise) is of course a dynamic problem. The loads placed on a structure are often moving. Even if the loads are stationary with respect to the structure, they act through distances as the structure deforms. In general, a load is therefore a function of its displacement and often its rate of displacement or, more simply, a function of distance and time. The rate at which a load can act, and the rate at which a strut can move or unload, the latter being affected by the inertia of the strut, obviously partly govern the failure of a structure. The dynamics of the whole system is very involved. In this thesis, only static problems will be considered, though, of course, the dynamic aspect must affect any experimental work. Any work discussed is given for slowly applied loads, where dynamic effects have been minimized to some extent, though in certain cases failure is quite rapid where a structure approaches close to its critical load and then fails quickly.

Though the correspondence between the neutral equilibrium of a system with respect to static disturbances and the vibrations of the system has been shown to some extent (Arts. 6 and 17), this is done only as a very preliminary move towards the analysis of dynamic effects, and has very little bearing on the practical problems of dynamic buckling under load.

For a discussion of the dynamic aspects of buckling, see N. J. Hoff "Dynamic Criteria of Stability" Research Engineering Structures Supplement (1949) p. 121 and N. J. Hoff "The Dynamics of the Buckling of Elastic Columns" Jnl. of App. Mechanics, Trans. A.S.M.E., Vol. 18 No. 1 March 1951. The latter article considers the dynamics of the buckling of a single column in a testing machine where the head of the machine is driven downwards at a constant rate. The inertia of the column is taken into account in the buckling action. This appears to be one of the few published articles where the dynamic effects are carefully investigated. See also N. J. Hoff "Buckling and Stability" Journal Roy. Aero. Soc. Jan. 1954, J.F. Davidson "Buckling of Struts under Dynamic Loading", Journal of Mechanics and Physics of Solids, Vol. 2, 1953, and J.F. Davidson "The Dynamic Lateral Instability of Beams", Proc. Royal Soc. London, Vol. 226, Series A, p.111, 1954.

49. Inelastic buckling.

The term inelastic buckling covers two important aspects of buckling theory. The first is the calculation of

critical loads of "initially perfect" compressed bars (and loaded structures) consisting of inelastic material. The main problem is that on displacing (by bending) a bar of such material which is under axial load, the stress strain relation on one side may be different from that on the other side depending on whether or not the strains begin to reverse on one side. It is now fairly well established that the Shanley tangent modulus relation gives a lower limit to the critical load in a test where the axial load is continuously increasing and strains at no stage reverse in any part of the material. The Karman reduced modulus relation may apply where the axial load remains constant during deformation.

50. It should not be thought, however, that the mere substitution of the tangent modulus instead of Young's modulus in all formulae for critical loads furnishes a solution to all inelastic buckling problems. The solution is still a critical load, a property of the perfect structure. Departure from linear elasticity in the stress strain relationship has also an important bearing on the behaviour of practical structures. A structure may deform elastically under load until the yield strain is reached at some point. The material then strains plastically, and plastic buckling may occur very quickly or take some time to develop. This effect will be considered later.

For treatment of inelastic buckling, see

F. Bleich "Buckling Strength of Metal Structures" pp. 8 - 21 (1952) McGraw Hill,

N. J. Hoff "The Analysis of Structures" pp. 318 - 328,

L. H. Larsson "Inelastic Column Buckling" Journal Aero Sciences Sept. 1956 p. 867,

S. Timoshenko "Theory of Elastic Stability" p. 54 and p. 156.

51. In this chapter, the overall stability of members and structures has been considered. An important subsidiary effect is that of local instability of portions of members, especially where thin sections are involved. This effect will also be considered later.

BIBLIOGRAPHY FOR CHAPTER ONE

For further articles on elastic stability and buckling see,

R. V. Southwell "On the General Theory of Elastic Stability" Phil. Trans. Roy. Soc. London (1914) Vol. 213 p. 187.

N. J. Hoff et al "The Buckling of Rigidly Jointed Plane Trusses". Proc. A.S.C.E. Vol. 76 separate No. 24.

Gough and Cox "Some Tests on the Stability of Thin Strip Material under Shearing Forces in the Plane of the Strip" Proc. Roy. Soc. London Series A Vol. 137 P. 145 (1932)

E. E. Lundquist "The Stability of Structural Members under Axial Load" N.A.C.A. tech. Note 617 (1937), and "A Method of Estimating the Critical Buckling Load for Axial Members". N.A.C.A. Tech. Note 717 (1939).

Lundquist and Fligg "A Theory for Primary Failure of Straight Centrally Loaded Columns" N.A.C.A. Report 582, (1937).

R. W. Hawken "Column Analysis and Design" published by the University of Queensland (1918).

E. H. Salmon "Columns" (Frowde, Hodder and Stoughton)(1921).

A. Burn "The Theory of Columns and Methods of Design" I.E. Aust. Paper No. 6, Vol. 3 (1922).

THE LOAD CARRYING CAPICITY OF PIN-ENDED STRUTS.

51. Introduction

This chapter discusses the behaviour of pin-ended columns in testing machines. The linear deflection plot used by Southwell is developed for a single pin-ended column, and it is shown how the Euler load can be determined from deflection readings taken during loading, and the effect of initial imperfections estimated. As loading progresses, the initial deformation is magnified in the ratio $1/(1 - P/Q)$ where P is the load on the column and Q its Euler load. The method is extended to take account of eccentric loading.

The Southwell Plot on strains, as developed in this thesis, is however, much more powerful. Strains are usually easily measured. Substitution of the yield strain (or some proof strain) in the equation of the linear strain plot is presented as a method of obtaining the collapse load of a column. Experimental work is included as an indication of the validity and also the limitations of the method.

The whole of the work should be regarded as introductory. The behaviour of struts built into structures or structures liable to instability will be studied in Chapter Three.

52. The interpretation of column tests in testing machines.

Though no column is initially straight homogeneous or perfectly elastic, the Euler buckling load remains a useful result. The conditions of testing a column in a machine may approximate fairly closely to those assumed when calculating the Euler load if we attempt to load the column as nearly concentrically as possible and minimize friction. Suppose we have an initially straight strut whose Euler load is Q centrally loaded with an axial load P. Then if P is less than Q, the straight form is stable, and the bent form is not. But if P equals Q, a state of neutral equilibrium exists. Suppose however the strut is initially bowed, having an initial crookedness δ_0 when P = 0. Then if the central deflection δ is measured as the applied load is increased, the load deflection curve is of the form shown in Fig. 36.

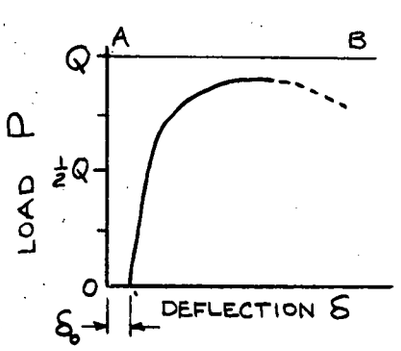

Fig. 36

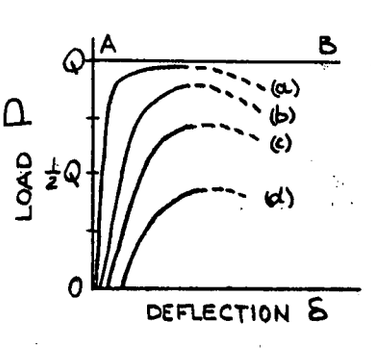

Fig. 37

If $\delta_0 = 0$ and the material does not yield, the load deflection curve follows the path OAB. But if δ_0 has a value, then the plot obtained is that of the curve in Fig. 36. If δ_0 is small, under good testing conditions we may obtain a curve such as curve (a), Fig. 37. For increasing values of δ_0, curves such as (b), (c), (d) are obtained. If yield occurs due to high bending stresses, the curves can show maxima, as indicated by the dotted lines of Fig. 37. These are the experimental crippling loads. Thus the loads measured experimentally even for a pin-ended centrally loaded member, may not reach anywhere near the Euler load Q, depending on the value of δ_0. Long struts loaded as concentrically as possible may give the crippling load P max. approximately equal to Q since considerable deflection is necessary to cause the column to yield. The smaller the value of δ_0, the closer do the curves approach the limiting path OAB, and the more pronounced is the knee in the curve. The curves also have a flatter peak. For simple struts up to the yield the curves approximate to rectangular hyperbolas. Friction at the ends of the column tested has the effect of raising the measured crippling load.

In loading a long column in a testing machine, the buckling load is often taken as the load at which the column seems to flick sideways, or exhibit sudden deflection. This will generally correspond to some point K beyond the knee of the curve in Fig. 38 and the "buckling" load reported will be P_1.

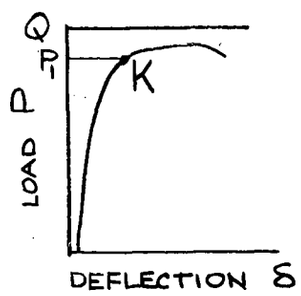

Fig. 38.

Or the buckling load for long struts where no sudden deflection occurs may be taken as the load for which there are two positions of stability, one each side of the central position, as in Fig. 39.

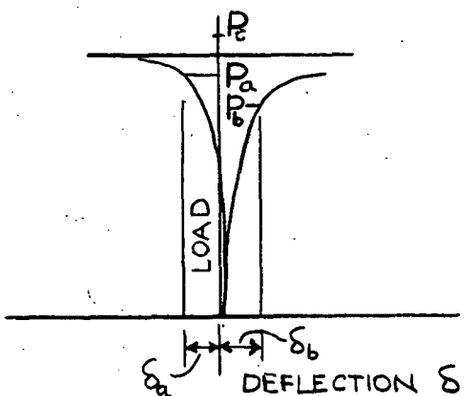

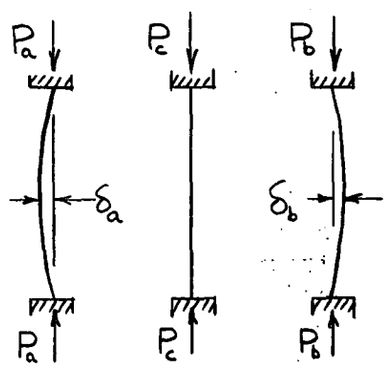

There are two positions of stability provided $P_a < P_c$ and $P_b < P_c$.

Fig. 39.

This load will be dependent on the testing machine used, and in particular on the stiffness of the head of the machine, which depends on the method used in the machine to measure the load. With a flexible load-measuring system it may be necessary to load to large deflections well beyond the knee in the curve of δ against P before two stable positions can be obtained. Loads obtained in testing machines may be almost as much a function of the machine and technique used as of the column tested even under conditions as close as possible to pin-ended. The term buckling has no meaning for an initially crooked or eccentrically loaded column.

But the smaller the eccentricity or initial curvature, the sharper is the knee in the load deflection curve, the instability of the column is more marked, and the measured critical load approaches the Euler value.

53. The estimation of the critical load from a load test on a column.

In his paper, "On the Experimental Analysis of Observations in Problems of Elastic Stability", (Proc. Royal Society, London, 135A, p.601), Southwell gives a method of estimating the Euler load of the corresponding perfect column, even though there is initial crookedness present in the column tested. This has been given in Art. 18. If deflections are measured normal to the minor axis of the section during a column loading test, this gives a method of analysing the experimental results, and ascertaining if they agree with the calculated Euler load.

54. Extension of Southwell's method to eccentric loading.

The above treatment due to Southwell has been extended by the author to the case of a pin-ended column having small eccentricity of loading as well as initial crookedness.

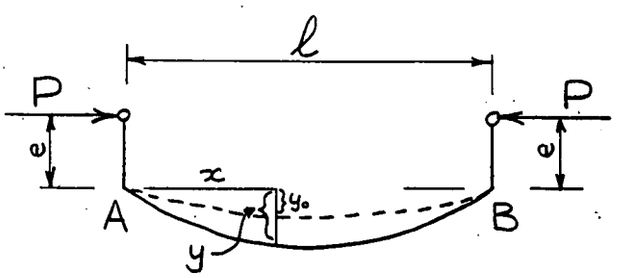

Fig. 40.

Suppose AB (Fig. 40) is a column of initial form

$$y_o(x) = \sum_{n=1}^{\infty} a_n \sin n\pi x/\ell$$

loaded with an axial load P at eccentricity e. Under load it takes up the shape y(x). Then the bending moment at x is

$$M_x = P(y + e) = -EI\, d^2(y - y_o)/dx^2.$$

and therefore $d^2y/dx^2 + Py/EI = d^2y_o/dx^2 - Pe/EI$

$$= -\sum (n^2\pi^2/\ell^2) a_n \sin n\pi x/\ell - Pe/EI \quad .. \quad (44)$$

where $k = \sqrt{P/EI}$.

Again the form of y is dependent on the initial shape y_o and also on the eccentricity of loading. Try a solution of the form

$$y = A \sin kx + B \cos kx - e + \sum_{1}^{\infty} b_n \sin n\pi x/\ell$$

.. (45)

Then $d^2y/dx^2 = -k^2A \sin kx - k^2B \cos kx - \Sigma (n^2\pi^2/\ell^2)\, b_n \sin n\pi x/\ell$.

Substitution in equation (44) gives

$$b_n = a_n/(1 - P/n^2Q) \text{ where } Q = \pi^2EI/\ell^2.$$

A and B may be obtained from the boundary conditions

$$y = o \text{ at } x = o, \ell .$$

This gives $B = e$ and $A = e(1 - \cos k\ell)/\sin k\ell$.

On substitution in equation (45), putting $x = X + \ell/2$,

we obtain $$y = e\left[\sec(k\ell/2) \cos kX - 1\right] + \Sigma \left[a_n/(1 - P/n^2Q)\right] \sin n\pi x/\ell. \quad .. \quad (46)$$

At the centre, $x = \ell/2$, $X = o$, and

$$Y = e(\sec k\ell/2 - 1) + \Sigma \frac{a_n}{1 - P/n^2Q} \sin n\pi/2. \quad (47)$$

The measured central deflection is

$$\delta = y - y_o = e(\sec k\ell/2 - 1) + \Sigma a_n \left\{\frac{1}{1 - P/n^2Q} - 1\right\} \sin n\pi/2.$$

As P approaches Q the n = 1 terms dominate, and using the approximation for the secant

$$\sec k\ell/2 = \sec(\pi/2)\sqrt{P/Q} = (1 + P/4Q)/(1 - P/Q)$$

we have $$\delta = (P/Q)(a_1 + 5e/4)/(1 - P/Q),$$

and therefore $$\delta/P = \delta/Q + (a_1 + 5e/4)/Q \quad .. \quad .. \quad (48)$$

The graph of δ/P against δ is again a straight line of slope $1/Q$ and intercept on the δ/P axis of $(a_1 + 5/4\ e)$.

55. This expression holds for eccentricities which are of the same order as the initial crookedness. At large eccentricities the error in the approximation for the secant must be investigated. Then neglecting y_o/e, that is, supposing a_n/e is small, we have

$$y = e \sec (k\ell/2) \cos kX - e.$$

If we put $Y = y + e$, then

$$Y = e \sec (k\ell/2) \cos kX.$$

The strut is bent in a cosine curve (see Fig. 41) of which the half wave length L may be obtained by putting

$$Y = o \text{ at } X = L/2.$$

This gives $\cos kL/2 = o$.

therefore $kL/2 = \sqrt{P/EI}\ L/2 = \pi/2.$

therefore $L = \pi\sqrt{EI/P}\ .$ .. .. (49)

This length L varies with the load. As P increases L is reduced, as shown in Fig. 42.

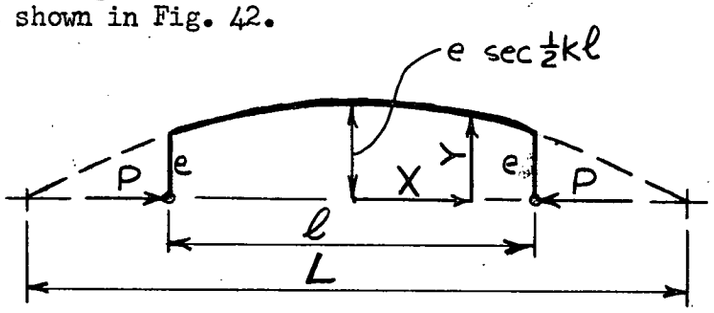

Fig. 41

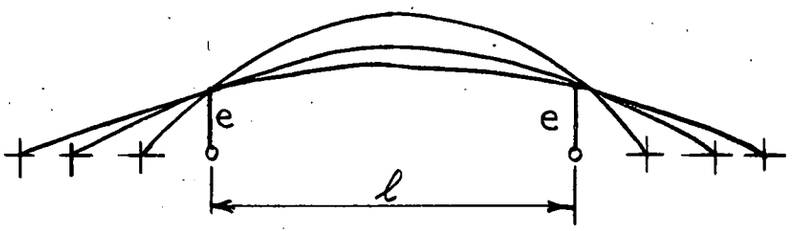

Fig. 42

The measured central deflection is

$$\delta = e\left[\sec\ (\pi/2)\ \sqrt{P/Q}\ - 1\right] .$$

Values of $(\delta/e)\cdot(Q/P)$ are plotted against δ/e in Fig. 43. The graph proves to be very close to a straight line of slope 45°, whose equation is

$$\delta Q/eP = 1.2\ + \delta/e.$$

This reduces to

$$\delta/P = \delta/Q + 1.2e/Q.$$

Thus the plot of δ/P against δ again gives a straight line of slope 1/Q, if e is constant. Eccentric loading has had no effect on the linearity of the plot. Southwell's original article suggests that in the case of eccentric loading the slope of the plot will be a measure of the critical load of the equivalent concentrically loaded column L (equation 49). As this varies continually, a straight line plot is not expected. This argument is, however, incorrect.

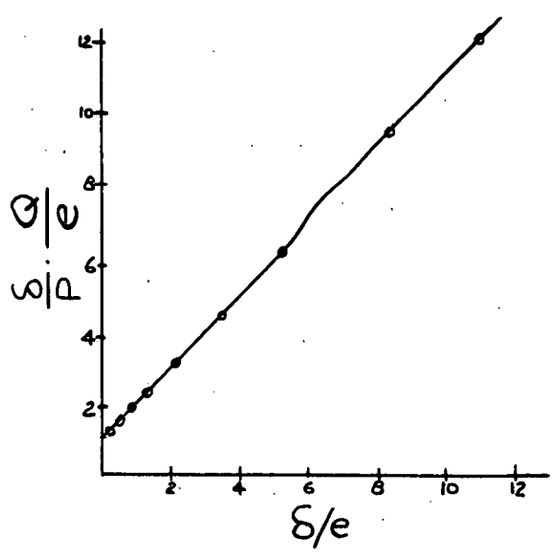

Fig. 43.

56. The Southwell Plot on Measured Strains

It is often more convenient to measure strains instead of the deflection of the column during loading. In his paper "On the Analysis of Experimental Observations in Problems of Elastic Stability", Southwell restricted the analysis to deflections, but, from the title, the generality can be inferred. Now the obvious deformation parameter to measure for columns is strain, but this has apparently not previously been done, though Rayleigh has stated that the assumption that any distorted configuration in any eigenvalue problem can be expressed as a synthesis of normal modes exaggerated by the loading is defensible from a physical standpoint for any elastic system, though it may require much elaborate analysis to justify it from the standpoint of a mathematician. However, it is hardly sufficient to extend Southwell's method to the analysis of strain measurements merely by analogy, and some analytical basis is required. In this chapter the strain plot for a single column is examined both analytically and experimentally. In chapter three an analysis and the consequent justification of the method where strain is the deformation measured is given for some simple structures.

For the initially crooked column under eccentric load, equation (47) gives the deflection. The central bending moment is then

$$M = P(y + e)$$

$$= Pe \sec (k\ell/2) + P \sum_{1}^{\infty} a_n/(1-P/n^2Q) \quad \sin n\pi/2 .$$

If v is the co-ordinate of a point in the cross-section, measured normal to the axis of bending, and $I = Ar^2$ is the moment of inertia of the section about this axis, then at this point the compressive stress is given by

$$f = P/A + Mv/I = (P/A)(1 + Mv/Pr^2)$$

and the corresponding strain is, if the n = 1 terms dominate,

$$\epsilon = \frac{f}{E} = \frac{P}{EA}\left[1 + \frac{ev}{r^2}\sec\frac{k\ell}{2} + \frac{a_1 v}{r^2}\cdot\frac{1}{1 - P/Q}\right] .$$

This reduces to $$\epsilon - \frac{P}{EA} = \frac{P}{EA}\cdot\frac{v}{r^2}\left[e\cdot\frac{1 + P/4Q}{1 - P/Q} + \frac{a_1}{1 - P/Q}\right] \quad .. (50)$$

which gives $$\frac{\epsilon}{P} = \frac{\epsilon}{Q} + \frac{v}{EI}(e + a_1 + Pe/4Q) + \frac{1 - P/Q}{EA} .$$

The plot of ϵ/P against ϵ rises above a straight line of slope $1/Q$ by an amount equal to

$$\frac{v}{4EI}\cdot\frac{Pe}{Q} - \frac{P}{QEA} .$$

When strains are measured on the compression side, these terms tend to cancel. In many cases, especially for small e, they can be neglected.

PLATE 1

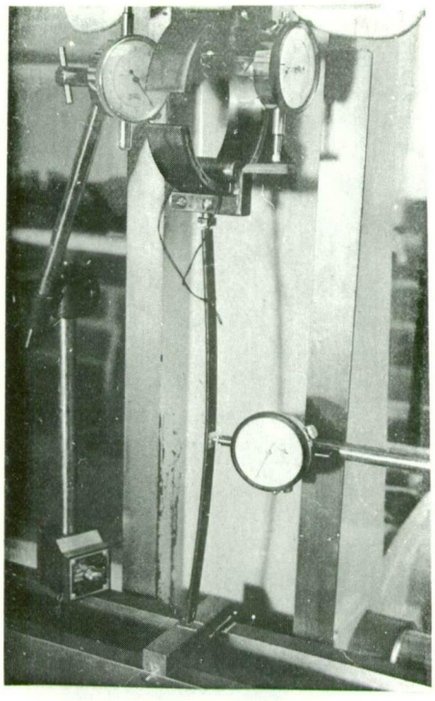

Measurement of deflection of rectangular section steel column. Load measured with a proving C.

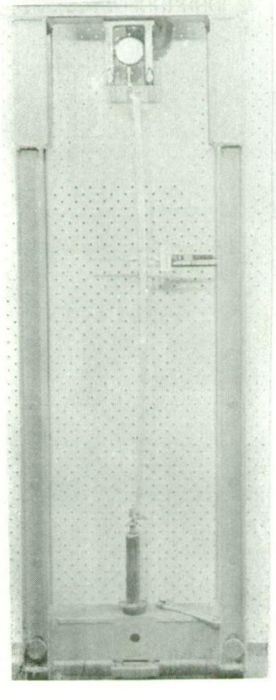

Measurements of longitudinal strains in an aluminium angle-section column.

PLATE 2

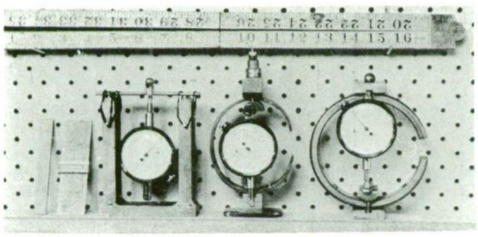

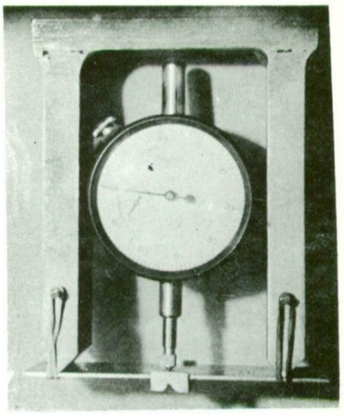

Small calibrated load measuring devices.

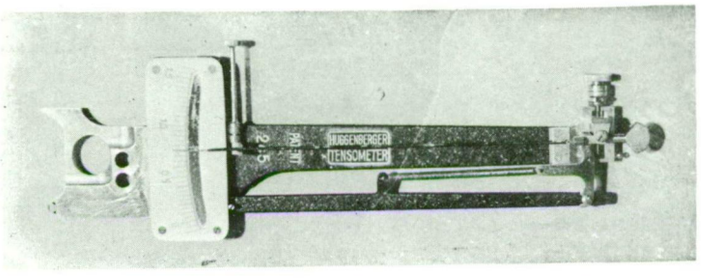

Huggenberger mechanical strain gauge.

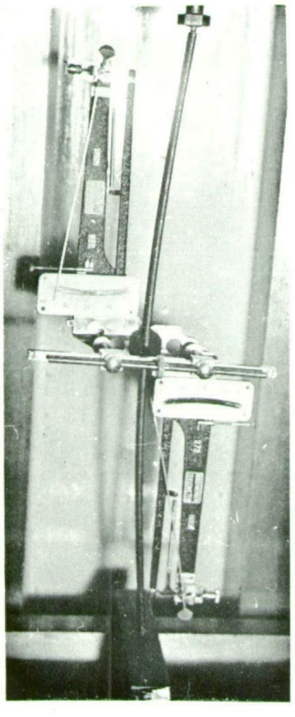

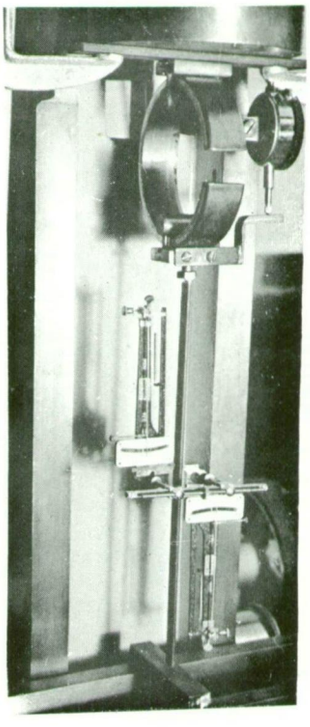

Measurement of strains in rectangular section steel column.

PLATE 3

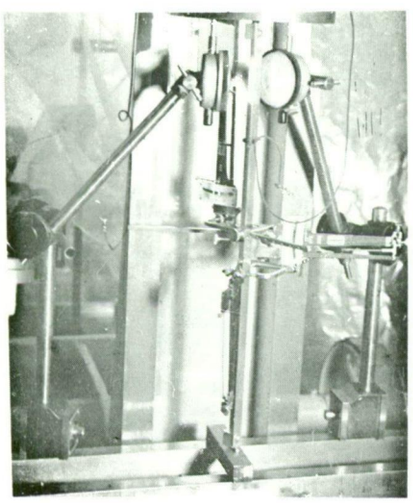

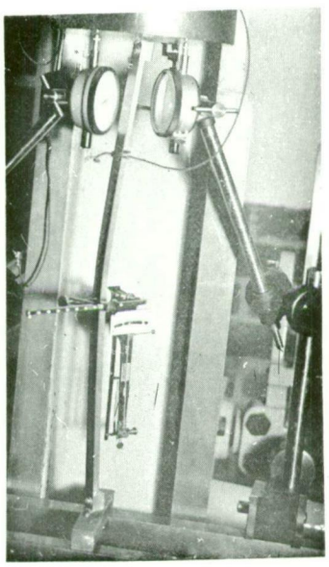

Measurement of longitudinal strains in angle-section members loaded as columns. The shortening of the member is being measured simultaneously.

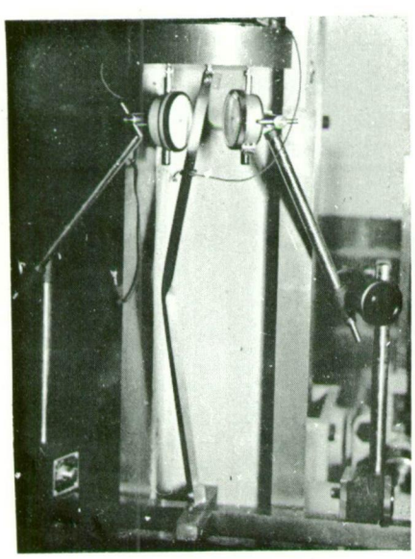

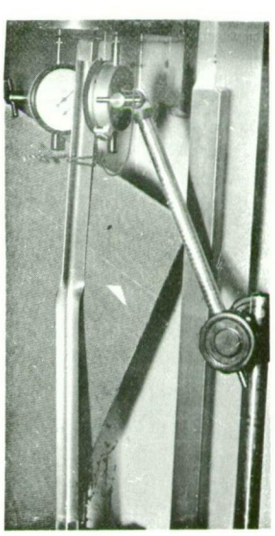

Local buckling of angle-section strut.

However, equation (50) can be reduced to the form

$$\frac{\varepsilon - P/EA}{P} = \frac{\varepsilon - P/EA}{Q} + \frac{V}{EI}(e + a_1 + Pe/4Q) \quad .. \quad (51)$$

The significance of the terms may be noted:

ε is the total measured longitudinal strain.

P/EA is the longitudinal strain if no buckling occurs, and is independent of any instability effects.

$(\varepsilon - P/EA)$ is a measure of instability effects.

The Southwell Plot on $(\varepsilon - P/EA)$ as given by equation (60) is very close to a straight line. Since $(\varepsilon - P/EA)$ is a measure of the bending, this is the part of the strain that one would expect to run away as the Euler load is approached.

57. Experimental work. The Southwell Plot on Deflections.

A rectangular section steel member measuring 0.501" x 0.132" x 11.6" long was loaded as a beam and its flexural rigidity determined as EI = 2530 lb. in.^{2} The member was then loaded as a column as concentrically as possible between $\frac{1}{8}$" dia. balls set in countersunk holes in its ends. During loading, deflections δ perpendicular to the minor axis were measured at the centre of the column. They are shown plotted in Fig. 44. The curve appears to be approximately a rectangular hyperbola.

The corresponding Southwell Plot of δ/P against δ is shown in Fig. 45. It is linear, and its equation is

$$\delta/P = \delta/183 + (0.15 \times 10^{-3}) \quad .. \quad .. \quad (52)$$

This may be compared with equation (48) derived in Art. 54, which is $\delta/P = \delta/Q + (a_1 + 5e/4)/Q$ .. .. (48)

The calculated Euler load of the strut is

$$Q = \pi^2 EI/\ell^2 = 188 \text{ lb.}$$

The value given by the Southwell Plot is 183 lb. which is in good agreement. The initial crookedness of the strut measured by using feeler gauges and a straight edge was about 0.018 in. The above equations give

$$a_1 + 5e/4 = 188 \times 0.15 \times 10^{-3} = 0.027 \text{ in.}$$

This indicates reasonable agreement as there might well have been eccentricity of loading of the order of the 0.006 in. required to give perfect agreement.

58. Experimental Work. The Southwell Plot on Strains.

An aluminium angle section member measuring 0.59 in. x 0.59 in. x 0.036 in. and 32.5 in. long was fitted with brass end pieces in which were cut grooves parallel to the minor axis at various eccentricities. It was loaded as a column in a frame using a screw jack and calibrated load gauge, consisting of a dial gauge in a frame. (See Fig. 46)

Strains at the corners of the angle at its mid-height were measured with light Huggenberger mechanical strain-gauges during loading. The Youngs' modulus of the material was first measured, and found to be 9,000,000 p.s.i. For the stress-strain curve see Fig. 150. The properties of the member were:

Cross-sectional area = 0.038 sq. in.

Moment of inertia about minor axis $I = 56.4 \times 10^{-5}$ in.^{4}

Flexural rigidity $EI = 5100$ lb. in.^{2}

This value was in good agreement with the value obtained when a similar member was loaded as a beam.

The calculated Euler load for buckling about the minor axis of inertia is then

$$Q = \pi^2 EI/\ell^2 = 48 \text{ lb.}$$

The graphs of measured strain ϵ against load P for eccentricities of 0, 0.3 in. and 0.4 in. are shown in Figs. 47 and 48. They are of the same form as those for deflection against load previously discussed. For zero eccentricity they exhibit fairly sharp knees as the calculated Euler load is approached. The Euler load is not reached and could not be inferred from the loading test directly. With pronounced eccentricity of the load, no sharp knee occurs but the curves have a gradual sweep. Large strains are attained at loads much less than the Euler load. Figures 49 and 50 show the Southwell Plots for these strain measurements. With zero eccentricity, the slopes of the graphs, which prove to be straight lines are 1/44 lb.$^{-1}$ and 1/46 lb.$^{-1}$ These agree well with the calculated Euler load of 48 lb. With eccentricity present, there is a little deviation from the straight line, and the graphs are steeper, as predicted, with inverse slopes of 38 lb. or less. Another angle was taken and loaded in a similar way using a proving C to measure the load, as in Fig. 51. Typical graphs of ϵ against P, and ϵ/P against ϵ are shown in Figs. 52 and 53. They are of the same form as before. The critical loads, or inverse slopes of the ϵ/P against ϵ graphs are however less than before and there is a discrepancy between the inverse slopes of the e = o graphs and the Euler load. It is thought that this is due to the rotation of the top of the proving C as it deflects. Because of this rotation the effective length of the column is more than its actual length. When a symmetrical load gauge was used as previously, allowing no rotation, there was no discrepancy.

These graphs are included here chiefly in order to show the way in which the curves in Fig. 52 can all be turned into the straight lines of Fig. 53. As a check on the experimental work, equation (50) can be taken and used to predict the strains. We have

$$\epsilon = P/EA + \frac{Pv}{EI} \cdot \frac{1}{1 - P/Q} \left[a_1 + (1 + P/4Q)e \right]$$

The measured value of the initial crookedness of the column used was less than 0.001 in., so a_1 can be neglected. Values of the strain ϵ can be calculated using the following values:

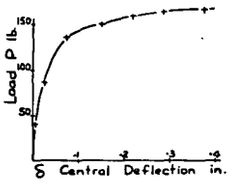

Fig. 44.

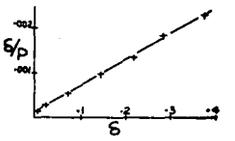

Fig. 45.

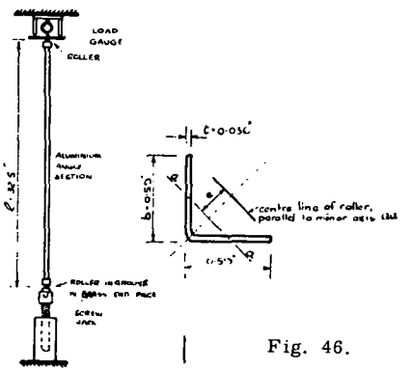

Fig. 46.

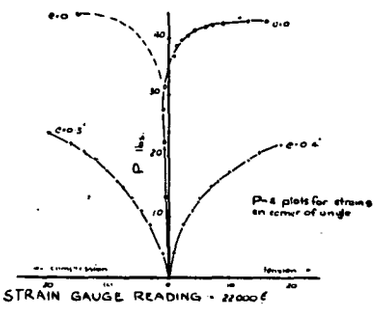

Fig. 47.

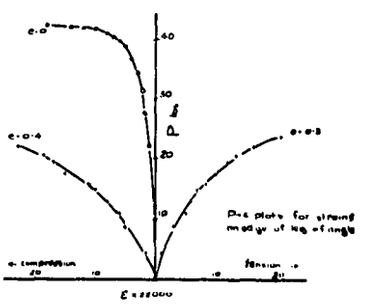

Fig. 48.

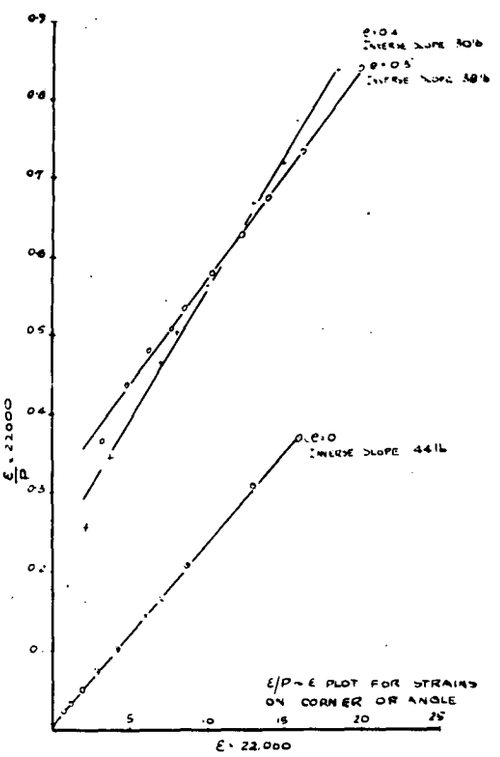

Fig. 49.

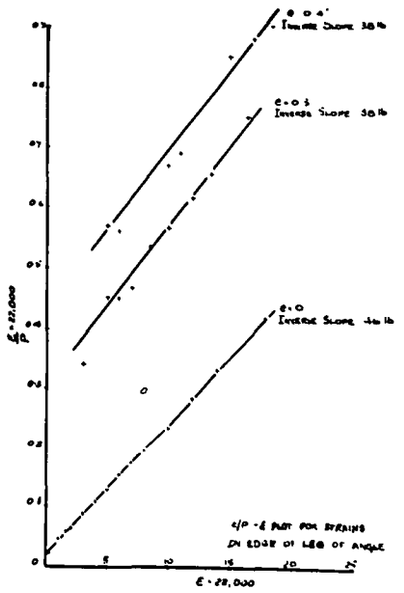

Fig. 50.

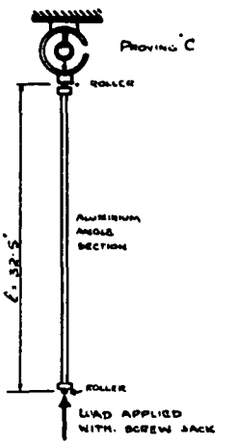

Fig. 51.

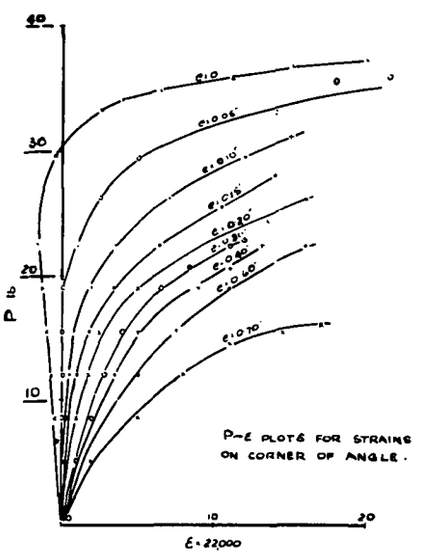

Fig. 52.

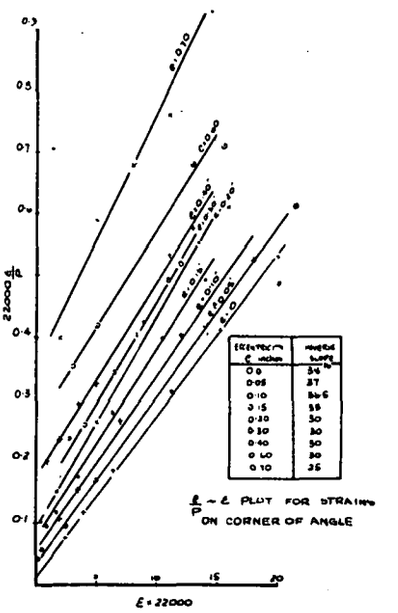

Fig. 53.

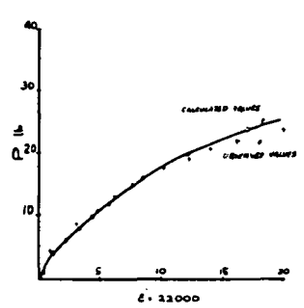

Fig. 54.

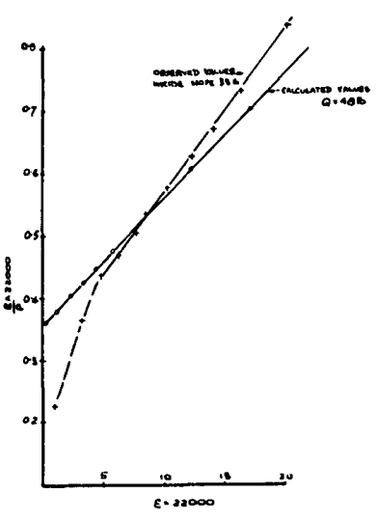

Fig. 55.

$Q = 48$ lb., $v = 0.224$ in., $I = 56.4 \times 10^{-5}$ in^4.,
$E = 9 \times 10^6$ lb. in^{-2}, $A = 0.038$ in^2, $a_1 = o$, $e = 0.3$ in.,
$P = o$ to 25 lb. Calculated and observed strains are plotted in Fig. 54. The agreement is marked, the measured strains at higher loads being rather more than those calculated. The difference is sufficient to alter the slope of the Southwell Plot of ϵ/P against ϵ from 1/48 lb^{-1} (Euler load = 48 lb.) to 1/38.5 lb.$^{-1}$. See Fig. 55. The explanation probably lies in the fact that at the higher loads the aluminium is stressed up to 9000 lb./sq. in. and its Young's modulus at this stress is less than that assumed.

59. Further experimental work on the Southwell Plot on Strains.

The preceding work has shown the linearity of the Southwell Plot on strains. The following experimental work indicates the order of accuracy of information obtained from the plot. A method of estimating the load carrying capacity of a strut is then presented.

The member used in the work described in Art. 57 was loaded again as a strut and longitudinal strains ϵ at its mid height were measured. The strain load plots are shown in Fig. 56. Graph 1 shows the measurements taken on the convex side of the member where the strains were tensile, and graph 2 those of the concave side where the strains were compressive. On the same graph, the line $\epsilon = P/EA$ is plotted. This is the calculated axial strain if no buckling occurs. Graphs 1 and 2 are symmetrical about this line. Values of $(\epsilon - P/EA)$ - See equation 51, Art. 56 - are easily obtained from this graph. Fig. 57 shows the corresponding Southwell Plot on strains. $(\epsilon - P/EA)/P$ is plotted against $(\epsilon - P/EA)$. It proves to be a straight line whose equation is

$$(\epsilon - P/EA)/P = (\epsilon - P/EA)/185 + (0.7 \times 10^{-6}) \quad .. \quad (53)$$

This may be compared with equation (51) which is

$$(\epsilon - P/EA)/P = (\epsilon - P/EA)/Q + v/EI(e + a_1 + Pe/4Q \quad .. \quad (51)$$

From Art. 57 we have $Q = 188$ lb. so the value of 185 lb. obtained from equation (53) is in good agreement. Also, since $(e + a_1 + Pe/4Q)$ is approximately equal to $(a_1 + 5e/4)$ as P approaches Q, we have

$$(a_1 + 5e/4) = (EI/v)\ (0.7 \times 10^{-6}) = 0.027 \text{ in.}$$

if $EI = 2530$ lb. in^2 and $v = 0.066$ in. This is in exact agreement with the value obtained in Art. 57 from the deflection plot on the same member.

In Figs. 58 and 59 are shown the measured strains and the Southwell Plot on strains for a rectangular section steel member 0.738 in. x 0.132 in. x 15.1 in. long, for which $EA = 26.4 \times 10^5$ lb., and $EI = 3820$ lb. in^2, and hence the Euler load is $Q = 166$ lb. The measured initial central crookedness was 0.020 in.

The equation of the Southwell Plot on strains is

$$(\varepsilon - P/EA)/P = (\varepsilon - P/EA)/170 + (0.3 \times 10^{-6}) .$$

Hence Q = 170 lb., and $(a_1 + 5e/4) = 3820 \times 0.3 \times 10^{-6}/.066 = 0.018$ in. These are in reasonable agreement with the values given above.

60. An aluminium angle-section member was then taken. It had the following properties: leg width b = 0.575 in., leg thickness t = 0.036 in., length ℓ = 16.2 in., cross-sectional area A = 0.040 in^2, Young's modulus in tension E = 9×10^6 lb. $in.^{-2}$ up to a strain of 0.0013; hence EA = 3.6×10^5 lb., EI = 4640 lb. in^2, and the Euler load Q = 160 lb. The member was fitted with brass end pieces and loaded as a column between $\frac{1}{8}$ in. dia. balls. Strains were measured on each of the corners of the member at its mid-height as indicated in Fig. 60, where the graphs of load against strain are also shown. Strains were measured beyond the stage where maximum load was reached, and until considerable plastic straining of the material had occurred. The elastic range of strains is shown in Fig. 60. Within the elastic range, the average strain is also plotted. All the points lie very close to the line $\varepsilon = P/EA$. This gives an indication of the accuracy of the strain measurements. Graphs of $|\varepsilon - P/EA| /P$ against $|\varepsilon - P/EA|$ are also shown in Fig. 60 for each of the three sets of strain measurements. They prove to be parallel straight lines which lie very close together and have slope 1/147 $lb.^{-1}$. This is in fairly close agreement with the calculated Euler load of 160 lb. and is probably more accurate as the value of EI was obtained by calculation from the measurement of the section, not from stiffness measurements.

61. Some angle section members were bent from mild-steel sheet. The tensile stress strain curve for this material is shown in Fig. 61. The material is elastic up to a strain of 0.001 and the Young's modulus is 30×10^6 lb. in^{-2}. Beyond the yield strain and up to a strain of 0.003 the stress may be taken as having the constant value of 28,500 lb. per sq. in. The angle section members had the dimensions: leg width 0.595 in., leg thickness 0.037 in., length 16.2 in. The angle had somewhat rounded corners and the stiffness could not be calculated easily. The flexural rigidity was therefore measured in a test as a simple beam (see Fig. 62) and had the value EI = 1.24×10^4 lb. $in.^2$. The members were loaded as struts between $\frac{1}{8}$ in. dia. hard brass rods placed in grooves in their ends so as to induce simple buckling about their minor axes.

Measured strains are plotted in Fig. 63. Readings were taken well beyond maximum load until the load had fallen off to a small value. Local buckling finally occurred when the compressive stresses in the outstanding leg of the member were high enough to cause it to fail in this manner. The elastic range of strains is indicated. The Southwell Plot on strains in the elastic range is shown in Fig. 64. It is linear, and of slope 1/470 lb^{-1} whereas the calculated Euler load is $Q = \pi^2 EI/\ell^2 = 467$ lb. The plot is however less definite than previously, as the direct strain P/EA is of a magnitude comparable with the "buckling" strain $(\varepsilon - P/EA)$.

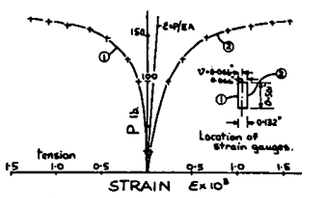

Fig. 56.

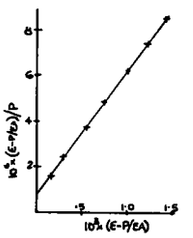

Fig. 57.

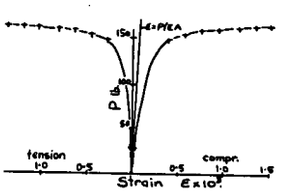

Fig. 58.

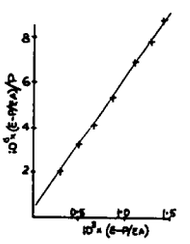

Fig. 59.

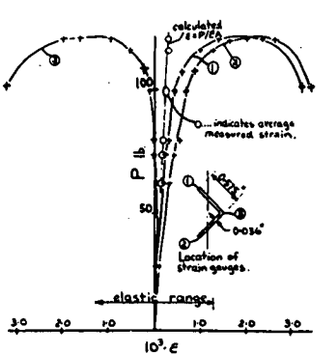

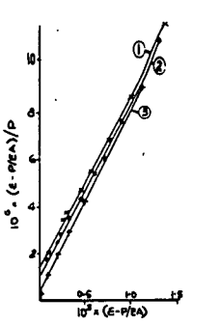

Fig. 60.

62. A similar member was loaded as a strut, its central deflections being measured. The plot of load against deflection is shown in Fig. 65, and the corresponding Southwell Plot on deflections in the elastic range is shown in Fig. 66. The slope of the plot is $(1/440)\ \text{lb}^{-1}$ whereas the Euler load of the strut is 467 lb.

It is interesting to investigate analytically the behaviour of this member in the plastic range. Assuming all the material of the member on the cross-section at its mid height has yielded, a stress diagram such as shown in Fig. 67 can be drawn. Then the load on the column is

$$P = 2\,(g - h)\,t\,f_y = 2\,a\,t\,f_y \quad \text{with } (g - h) = a$$

where f_y is the yield stress of the material, in this case 28500 lb. per sq. in. The bending moment is

$$M = 2 \cdot \frac{b - a}{2} \cdot t\,f_y \cdot \frac{b + a}{2\sqrt{2}} = (b^2 - a^2)\frac{t}{2\sqrt{2}}\,f_y .$$

Putting $a/b = k$, we have

$$P = 2\,b\,t\,f_y\,k$$

and $$M = b^2\,t\,f_y\,(1 - k^2)/2\sqrt{2} = P.\delta .$$

Therefore $$\delta = M/P = b(1 - k^2)/4\sqrt{2}\ k$$

If $2\,b\,t\,f_y = P_y$, we have

$$\left.\begin{aligned} P/P_y &= k \\ \text{and} \quad \delta/b &= (1 - k^2)/4\sqrt{2}\ k, \end{aligned}\right\} \qquad \ldots\ \ldots\ (54)$$

The relation between P/P_y and δ/b given by equations (54) is plotted in Fig. 68. It is labelled "Fully Developed Plastic Action". The deflections measured previously and shown in Fig. 65 are now plotted non-dimensionally in Fig. 68. For the member concerned, we have $P_y = 2\,b\,t\,f_y = 1160$ lb. and hence $Q/P_y = 440/1160 = 0.38$. This is indicated in Fig. 68. If the material remained perfectly elastic, we would expect the deflection readings to become asymptotic to this line. The deflection readings can be extrapolated on this basis, using the equation of the Southwell Plot from Fig. 66, which is

$$\delta/P = \delta/440 + (0.35 \times 10^{-4})$$

This has also been carried out in Fig. 68. It can be seen that the actual deflection readings beyond the point where yield occurs lie below the line given by fully developed plastic action, but tend towards this line as the deflections increase. This is due to the fact that the material near the central axis of the member has not yet yielded, and hence equation (54) results from a considerable overestimate of P but a less serious overestimate of M. When local buckling occurs, the load to cause a certain deflection drops off again, as is to be expected.

The stage at which yielding first occurs is indicated in Fig. 68. It is estimated by analogy from Fig. 63, as strains were not measured. It is seen that the ratio of maximum load attained to load to cause first yield is very little greater than unity. The reserve of strength beyond first yield is not considerable, and is of the order of only a few per cent.

63. The load carrying capacity of a pin-ended strut

Though it might appear reasonable to relate the load carrying capacity of the strut to an analysis of its fully developed plastic action, it appears that the plastic analysis can be avoided, and its failure defined in terms of elastic behaviour only. All that is necessary is to substitute the condition

$$\varepsilon = \text{strain to cause yielding} = f_y/E$$

in the equation of the Southwell Plot on strains, and to solve for the load to cause first yield. This is close to the failure load and for practical purposes the reserve of strength beyond first yield can be treated as a slight additional factor of safety.

We have, as the equation of the Southwell Plot on strains obtained experimentally,

$$(\varepsilon - P/EA)/P = (\varepsilon - P/EA)/Q_1 + C_1 \quad .. \quad .. \quad (55)$$

where Q_1 is the reciprocal of the slope of the plot, equal to the Euler load Q of the column, and C_1 the intercept of the plot on the $(\varepsilon - P/EA)/P$ axis. Equation (53), obtained from fig. 57 is typical. Equation (55) reduces to

$$\frac{E\varepsilon - P/A}{P/A} = \frac{E\varepsilon - P/A}{Q/A} + EA\,C_1$$

Putting $E\varepsilon = f$, and $EA\,C_1 = \eta_1$

we have $$f = P/A\left(1 + \frac{\eta_1}{1 - P/Q}\right) \quad .. \quad .. \quad (56)$$

When ε equals the yield strain, then f equals the yield stress f_y. Hence, putting $f = f_y$, it is possible to solve for the load P to cause first yield, and this is close enough for practical purposes to the load carrying capacity of the strut.

Equation (56) is familiar as it is similar to the equation used in the derivation of the Perry Robertson formula for pin-ended struts. Consider a pin-ended strut having initial crookedness given by a_1 and concentrically loaded. Then the central deflection, from equation (47), is

$$y = a_1/(1 - P/Q)$$

and the maximum stress is, from equation (50)

$$f_{max} = (P/A)\left[1 + a_1 v/r^2(1 - P/Q)\right]. \quad .. \quad .. \quad (57)$$

The Perry Robertson formula is obtained by putting

$$a_1 v/r^2 = \eta$$

and giving η the "empirical" value $0.003\,\ell/r$ necessary to make the failure loads of struts in certain tests equal to the value for P calculated from equation (57) when f_{max} was put equal to the yield stress. To summarize, the formula attempts to predict the load carrying capacity of a practical pin-ended strut in the following manner. Due to lack of knowledge of the behaviour of the strut in the plastic range, the safe assumption was made that the collapse load equals the load to cause first yield. The load to cause first yield of an initially crooked column was calculated (Equation 57).

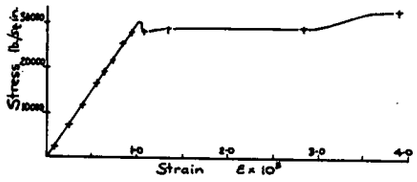

Fig. 61.

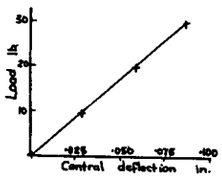

Fig. 62.

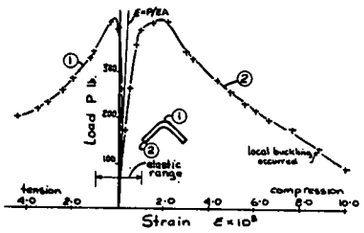

Fig. 63.

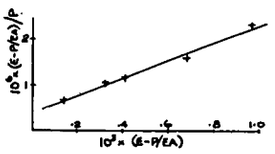

Fig. 64.

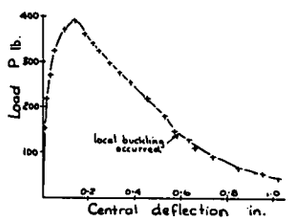

Fig. 65.

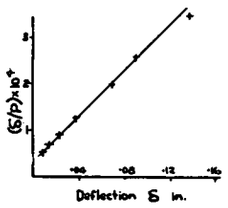

Fig. 66.

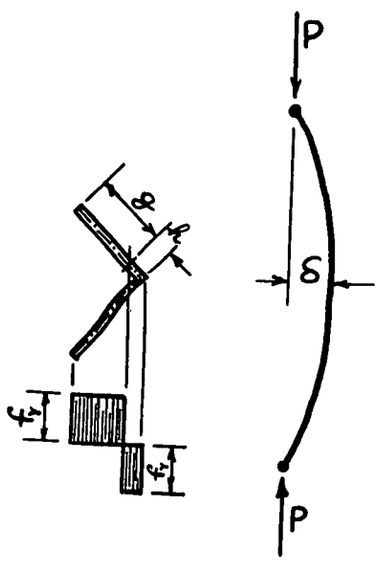

Fig. 67

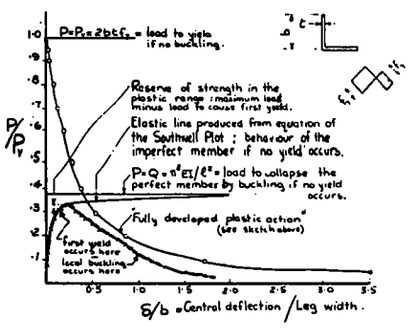

BEHAVIOUR OF A PIN-ENDED ANGLE STRUT
buckling about its minor axis
x.... indicates measured deflections.

Fig. 68.

It contained the parameter a_1, and an empirical value was set for a_1, intended to include the effects of all imperfections besides initial crookedness such as the effect of small unavoidable eccentricity of loading. This was done by comparison with a certain set of tests on columns. Equation (56), of course, forms a similar but better basis for obtaining the load carrying capacity of a pin-ended strut, as empirical values of η_1 are obtained directly from the Southwell Plot on strains.

It is intended here only to emphasize the similarity between Equation (56) and the Perry Robertson formula. It is sufficient to state that the solution of the equation (56), when considered as a design formula, is familiar to engineers so long as empirical values of η_1, expressed in some suitable form, are available.

The load carrying capacity of struts as built into structures is the problem required to be solved in practice, and this will be discussed in chapter three.

----oOo----

BIBLIOGRAPHY and NOTES for CHAPTER TWO

The numerals refer to the articles in the text.

53. In 1938, E. E. Lundquist published a paper entitled "Generalized Analysis of Experimental Observations in Problems of Elastic Stability". N.A.C.A. Tech. Note No. 658 (1938). In this generalization, it was shown that if deflections of a pin-ended column are measured beginning at some load $P = P_1$, thus avoiding the use of deflection readings taken at low load in case they are inaccurate, then a linear plot is still obtained. To obtain the Euler load, P_1 is added again to the reciprocal of the slope of the linear plot. This generalisation is fairly obvious from the fact that the plot is merely a method of finding the asymptote of a rectangular hyperbola. The origin of co-ordinates is immaterial. For this reason the lengthy mathematics presented by Lundquist is considered rather unnecessary and not really an extension or generalization of Southwell's earlier article.

54 & 55. In his original article Southwell restricted the method to columns having small eccentricity of loading. This restriction is, however, unnecessary.

The accuracy of the given approximation for the secant may not be generally realized. It holds quite well up to $P/Q = 1$, and is within 1% up to $P/Q = 0.8$.

62. Though the linear plot on strains gives a simple method of predicting the load at which a column first yields, the behaviour of the column once yield occurs can be studied in a simple manner from the deflection aspect. The method given here is suggested by analogy from a paper by N.W. Murray "The determination of the collapse loads of rigidly jointed frameworks in which the axial forces are large", Proc. I.C.E. London Vol. 5 No. 1 April 1956 p.213. It should be noted that, because the assumption of fully plastic action is not fulfilled until very large deflections occur, the "fully developed plastic action" line in Fig. 68 has less relevance at the collapse load than might at first be imagined. It does however give an increasingly accurate idea of the subsequent behaviour of a ductile column as large deflections are attained, and this is often important with regard to the energy absorbed by a structure during failure.

63. For the origin of the Perry Robertson formula, see "First Report of the Steel Structures Research Committee" H.M.S.O. (1931), p.211, p.224 and p.228. The justification for the yield stress of 18 tons/sq. in., the crookedness eccentricity function $\eta = 0.003\, \ell/r$, and the load factor of 2.36 are very hard to find in this report. J. F. Baker's comments in this report, and also in "The Steel Skeleton" Vol. 1. (1954) are interesting. The general opinion seems to be that there is little reserve of strength in a pin-ended strut once yield of some portion occurs. This is borne out by the limited number of experiments carried out by the author, some of which are described in this thesis.

The problem of reserve of strength of a strut beyond the point of first yield is discussed in Bleich "Buckling strength of Metal Structures" (1952) McGraw Hill p. 27 - 54. Merchant also attempts to take into account this reserve of strength in "The Buckling of Pin-ended Struts under Axial Load". The Struct. Engnr. Sept. 1949 Vol. 27 p. 363.

----oOo----

CHAPTER III.

THE USE OF THE SOUTHWELL PLOT ON STRAINS TO ESTIMATE THE LOAD CARRYING CAPACITY OF STRUCTURES LIABLE TO INSTABILITY

64. Introduction.

A structure may be considered to be in a state of stable equilibrium, from the practical point of view, when slight changes in loading do not produce disproportionate distortions of the system. When discussing buckling problems we are concerned with avoiding potential unstable equilibrium. In the long run, this is controlled by the complex stress strain relationships of the material, the deformation of every part of the structure, and the action of every part on every other part.

Every elastic system under certain loading conditions may pass into an unstable state of equilibrium. But only when considerable elastic deformation can occur before the plastic region is reached will structural members become unstable in the elastic range. This is the case only when one or two dimensions of a member are small compared with the other dimension or dimensions. Slender columns or thin plates are examples. But, above the elastic limit, Young's modulus rapidly decreases, so many systems can become unstable. Every structure fails by instability if and how most easily it can.

65. This thesis is concerned mainly with the field of framework stability. Broadly speaking, there are two types of instability. This is shown diagrammatically in Fig. 69.

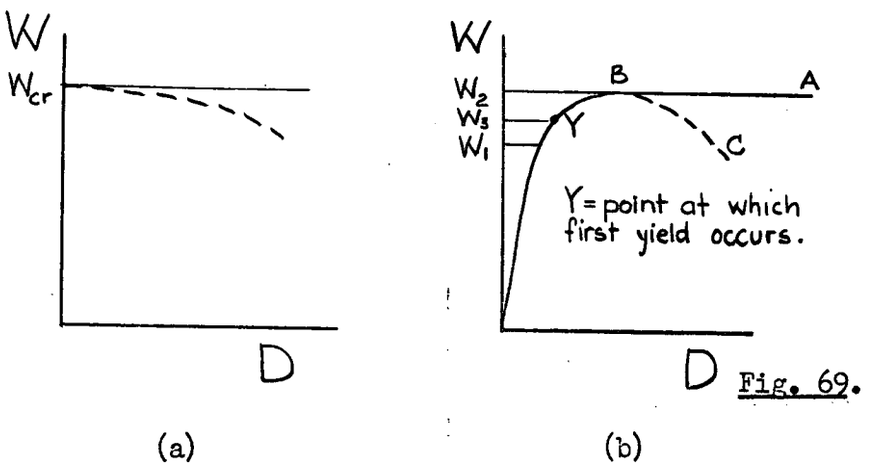

Fig. 69.

(a) (b)

In this figure, a load determining parameter W is plotted against a deformation parameter D. It is understood that D participates in the buckling mode on which our interest is centred and this is usually the mode in which failure of the structure occurs. Then in Fig. 69 (a) we have $D = 0$ for $W < Wcr$. At the value $W = Wcr$. there is a bifurcation of the load deformation diagram, which may continue to follow the path $D = 0$ to greater loads, or at constant or decreasing load D may assume large values.

This type of behaviour may describe a structure made of material having a linearly elastic stress-strain diagram. In this case Wcr. is the elastic critical load. Methods of calculation of Wcr, in certain cases have been given in Chapter One. The diagram may also describe a structure containing material having a non-linear stress strain diagram. In certain simple cases the substitution of the tangent modulus for the Young's modulus of the material in the elastic critical load formula will give a reasonable value for Wcr.

The type of behaviour shown in Fig. 69 (b) is, however more usual. The load deformation graph shows no bifurcation, and there is strictly speaking no instability. There is, however, a stage in the loading at which a slight increase in load produces a large increase in deformation, and this, for practical purposes, can be considered as a type of instability. The stage at which instability occurs and the margin by which it should be avoided in practice is a matter of practical definition. This will depend on the purpose for which the structure is designed and, in particular, the allowable deformations.

If in Fig. 69 (b) we consider W increasing from zero, then at the value $W = W_1$ the deformations begin to increase quite rapidly. As loading progresses W reaches its maximum value W_2 at the point B. If the structure is loaded with dead weights, W can not reduce, the diagram then follows the path BA, and the structure collapses. If the structure is being loaded by a straining device, it is possible to draw the remainder of the diagram where W reduces and D continues to increase along the path BC. The maximum load carrying capacity of the structure is W_2, and this equals the collapse load under conditions where the structure does not unload as it deforms. In practice we may be interested in the value W_2, or alternatively in the value of W for some value of D defined in some other way, such as a limiting strain or a limiting deflection.

In the case of a structure made of approximately linearly elastic material, suppose Y in Fig. 69 (b) denotes the point at which material at some point in the structure first yields, the corresponding load being W_3. Then it is possible in certain cases to obtain the value of W_3 by an elastic analysis, and subsequently to empirically relate W_2 to W_3. The purpose of this chapter is to indicate a method of carrying out the first step in this procedure.

The relation between the types of behaviour shown in Figs. 69 (a) and (b) has been discussed in Chapter One for the rod and spring mechanism and the pin-ended column. For these examples, the load deformation relation (b) within the elastic range has been shown to be a function of the elastic critical load Wcr. and the initial imperfections of the system.

66. Methods exist for determining the critical loadings for mathematically perfect structures for simple buckling modes. The critical load is analogous to the Euler load of an initially perfect pin-ended strut. However all structures have imperfections such as crooked members or eccentric joints. The behaviour of an actual structure possessing imperfections is a more difficult problem.

Some method of relating the behaviour of the practical structure to the critical loading for the perfect structure is required. Without some method of obtaining the effect of imperfections the designer is in the same position as one who would design a pin-ended column having at his command only the Euler formula for the perfect member.

The equation of the Southwell Plot on strains furnishes a method of estimating W_3, the load to cause first yield, for a practical structure. (See fig. 69(b)). For certain structures, namely those possessing fairly flexible members, W_3 may be close to the collapse load W_2, and it may not be worthwhile relating W_3 to W_2. The analysis of the structure in the plastic range is then entirely avoided. If the reserve of strength in the plastic range, W_3 to W_2, is considerable, then a plastic analysis, or empirical correlation of W_3 to W_2, is required. This effect becomes important for structures made of ductile material where the members involved are somewhat stiff.

67. The approach as outlined above will be elaborated in the succeeding pages. It overcomes to some extent two main objections to the use of elastic theory and the yield criterion in problems of instability. It is not stated that the carrying capacity of a structure is reached if in one of the members the maximum stress becomes equal to the yield stress. The solution of the stability problem does not require an exact stress analysis of the structure. What is stated is that it is possible to determine in certain cases the load to cause first yield at certain locations where first yield precedes collapse by buckling. Attention is paid to the strains which participate in the buckling mode. The reserve of strength in the plastic range is not neglected. It must be taken into account if the ratio of collapse load to load to cause first yield is considerable.

It is also sometimes stated that the yield criterion fails completely when the deflected equilibrium form to which the stress analysis is applied suddenly changes to a completely different configuration, as for example, in the lateral buckling of a beam. It will be shown that this type of problem is no exception. In fact the lateral buckling of a beam can be described by Fig. 69. It is, however, essential that the deformation D be a participant in the buckling mode that precedes failure.

68. The limitations of the method are:

(a) It is restricted to elastic theory. The reserve of strength in the plastic state must be taken care of by some other means, or, at least by a modification. Also, in practice, local buckling problems are not usually amenable to solution by this method.

(b) Where structures are statically indeterminate in certain ways, the buckling modes are not easily defined, and no parameter D may give a clear definition of failure.

(c) In many cases the whole behaviour of a structure is important, including the load deformation characteristic beyond maximum load.

It should also be noted that certain initial crookedness and imperfection patterns throughout a structure may cause it to buckle and fail in a configuration which does not correspond to the gravest buckling mode of the perfect structure. This does not affect the main argument presented, but this occurrence must not be neglected in practice.

69. Apart from refinements in methods of calculation of critical loads, a great deal of the work done on the instability of structures has followed the purely experimental approach. This may be necessary as an expedient in order to obtain certain information quickly. However, in the long run, because of the great number and wide range of the variables which characterize each individual problem, success can be hoped for only if close co-operation is achieved between theoretical and experimental research. That is, empirical methods must be soundly based theoretically. A summary of some of the work of various investigators follows.

In studying problems of elastic stability, the Southwell Plot on deflections has been found a valuable experimental tool. The linear deflection plot used by Southwell was developed for a single pin-ended column, and showed how the Euler load could be determined from deflection readings taken during loading. The plot also shows the effects of initial imperfections and furnishes a means of determining the magnitude of these effects. As loading progresses, the initial deformation of the column is magnified in the ratio $1/(1 - P/Q)$ where P is the applied load and Q the Euler load. The method is easily extendable to take account of eccentric loading.

In studying frames, W. Merchant has suggested that it be assumed that initial deflections are magnified in the ratio $1/(1 - W/Wcr)$, where W is the applied loading, and Wcr the critical load for the initially perfect frame. The following analogy is drawn. For the case of a pin-ended strut we can write

$$p_f = f\ (p_e\ ,\ p_y, \eta\ )$$

where p_f = the failure stress (the failure load divided by the area of the column), p_e = the Euler stress, p_y = the yield stress of the material, and η = an imperfections function. f indicates a functional relation. Then in the case of a framed structure, it should be possible to write

$$P_f = f\ (P_c, P_y, \eta\ )$$

where P_f = the failure load, P_c = the critical load, P_y = the collapse load if no instability occurs, and η = an imperfections function. The analogy is vaguely drawn, but the suggestion of applying the Southwell Plot on deflections to structures is a valuable one.

N. W. Murray has applied this suggestion and obtained good agreement between the reciprocal of the slope of the deflection plot and the calculated critical load in the case of the lateral buckling of a rigidly jointed truss held at the panel points. Murray and Nutt have also applied the method in reverse to braced frames in order to predict the deflections in the elastic range from crookedness and eccentricity measurements taken in the unloaded state. The Southwell Plot on the measurements taken during loading does not however appear from their published work to have been carried out by these investigators in these experiments.

In an interesting paper, W. G. Godden has described experiments on the lateral buckling of tied arches. Deflection measurements were analysed by using the Southwell Plot, and gave good agreement with the calculated critical load. This paper has been recently followed by an article by Chin Fung Kee in which the significance of the intercept of the plot has been noticed. This point seems to have eluded investigators up to the appearance of Mr. Kee's paper, in which he uses information obtained from the intercept of the plot in order to calculate the maximum stress in the arch rib.

70. Several important points emerge from this discussion. Firstly it appears that the application of Southwell's deflection plot to structures has not yet received analytical justification. Secondly, attention has been concentrated mainly on the slope of the plot and the agreement with calculated critical loads; important information available from the intercept of the plot with regard to the effect of imperfections has been largely neglected. Thirdly, most of the work reported would have been facilitated or at least broadened by measurement of strains.

71. <u>The Southwell Plot on Measured Strains applied to Problems of Instability of Framed Structures</u>.

Strains are usually easily measured, and stress can be directly inferred, hence the determination of a yield criterion is facilitated by the use of the strain plot. It has been shown previously that the Southwell Plot on longitudinal strains in a pin-ended strut is linear. The method may be extended to structures on the basis of a physical argument, but it is desirable to have some mathematical justification if this is possible.

The simplest frame is a triangle, and the Southwell Plot on strains at certain points in the members of a triangle will be examined both mathematically and experimentally. This preliminary justification of the use of the plot to obtain the critical load of a frame and the effect of imperfections on the load carrying capacity opens up the possibility of bridging the gap between the buckling of an initially perfect frame and the deformation and load carrying capacity of a practical frame.

72. <u>The Buckling of an Equilateral Triangular Frame in its Plane</u>.

The first buckling mode of a simple frame made up of three equal members rigidly connected at their ends to form a triangle has been treated in Art. 30.

By analogy with single column theory, the initially perfect frame, made up of initially straight members, was considered, and its buckling load determined mathematically. The behaviour of a similar frame made of initially crooked members will now be treated. It will be shown that Southwell Plots on strains which occur due to the buckling are linear, and can be used to determine the critical load of the initially perfect frame. Load tests on an experimental frame have resulted in good agreement. This analysis and its experimental verification forms a preliminary justification of the use of the Southwell Plot on strains to determine both the critical load of a structure and the effect of practical imperfections on the failure load.

73. <u>The Behaviour of a Triangular Frame whose Members are Initially Crooked</u>.

To discuss this problem it is convenient to first consider the behaviour of:

(a) An initially crooked compression member
(b) An initially crooked tension member
(c) An initially crooked compression member subject to bending moments applied at its ends.

(a) <u>An initially crooked compression member</u>.

Consider the initially crooked member AB shown in Fig. 70 having the unloaded shape

$$y_o = \sum_1^\infty a_n \sin n\pi x/\ell.$$

The limits of summation throughout are 1 to ∞, and ℓ is the length of the member.

Then $dy_o/dx = \Sigma (n\pi/\ell) a_n \cos n\pi x/\ell$

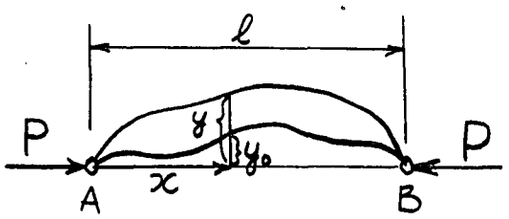

Fig. 70.

and the initial slope at x = o is given by

$$\theta_{A_o} = \Sigma (n\pi/\ell) a_n$$

The bending moment at x, under axial load P, is

$$M_x = Py = -EI\, d^2(y - y_o)/dx^2$$

Therefore

$$d^2y/dx^2 + Py/EI = d^2y_o/dx^2 = \Sigma -(n^2\pi^2/\ell^2) a_n \sin n\pi x/\ell.$$

As the solution, put

$$y = \Sigma b_n \sin n\pi x/\ell$$

Then, $$-n^2\pi^2 b_n/\ell^2 + P b_n/EI = -n^2\pi^2 a_n/\ell^2$$

which gives $$b_n = \frac{a_n}{1 - P\ell^2/n^2\pi^2 EI} = \frac{a_n}{1 - P/n^2Q}$$

where $$Q = \pi^2 EI/\ell^2 .$$

Each component a_n of the initial shape is "exaggerated" by the axial load in the ratio $1/(1-P/n^2Q)$.

Also we have $dy/dx = \Sigma\, (n\pi/\ell) b_n \cos n\pi x/\ell$.

At x = o, the slope is

$$\theta_A = \Sigma\, (n\pi/\ell) b_n = \Sigma\, (n\pi/\ell) a_n/(1 - P/n^2Q)$$

In the case of initial shape one half wave, we have

$$\theta_{A_o} = \pi a_1/\ell \quad \text{and} \quad \theta_A = (\pi a_1/\ell)/(1 - P/Q) \quad .. \quad (58)$$

(b) An initially crooked tension member. (See Fig. 71)

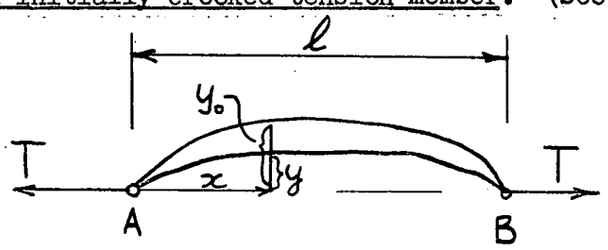

Fig. 71.

In this case $M_x = -T_y = -EI\, (d^2y/dx^2 - d^2y_o/dx^2)$

and we obtain $b_n = (n\pi/\ell) a_n/(1 + T/n^2Q)$

In the case of the initial shape

$$y_o = a_2 \sin 2\pi x/\ell$$

we have $$\theta_{A_o} = 2\pi a_2/\ell \quad \text{and} \quad \theta_A = (2\pi/\ell) a_2/(1 + T/4Q) \quad .. \quad (59)$$

(c) An initially crooked compression member subject to bending moments applied at its ends. (See Fig. 72)

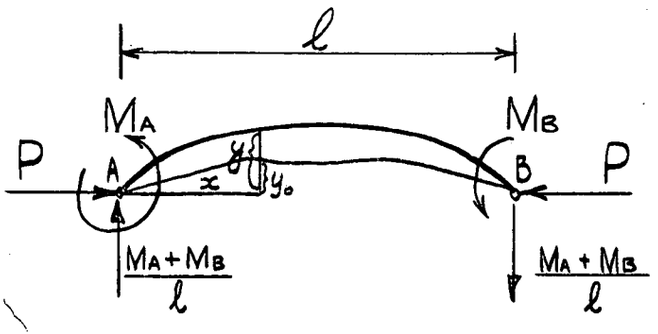

Fig. 72

Suppose the unloaded shape is

$$y = \sum_1^\infty a_n \sin n\pi x/\ell .$$

Then $$M_x = Py + M_A - (M_A + M_B)\, x/\ell$$

$$= -EI\, (d^2y/dx^2 + d^2y_o/dx^2)$$

Therefore $$d^2y/dx^2 + Py/EI = d^2y_o/dx^2 - M_A/EI + (M_A + M_B)x/EI\ell$$

Put $$y = A \sin kx + B \cos kx + \sum_{1}^{\infty} b_n \sin n\pi x/\ell - (M_A/P)(1 - x/\ell) + M_B x/P\ell .$$

This satisfies the differential equation and the boundary conditions at $x = o$ and $x = \ell$, if

$$b_n = a_n/(1 - P/n^2Q)$$

$$B = M_A/P$$

and $$A = - (M_A/P) \cot k\ell - (M_B/P) \operatorname{cosec} k\ell .$$

The solution is of course merely the sum of previously obtained solutions, as the differential equations are linear.

At the centre of the bar we have $x = \ell/2$ and the central deflection is

$$y = A \sin k\ell/2 + B \cos k\ell/2 + \Sigma b_n \sin n\pi/2 - M_A/2P + M_B/2P$$

which reduces to

$$y = (M_A - M_B)(\sec k\ell/2 - 1)/2P + \Sigma \left[a_n/(1 - P/n^2Q)\right] \sin n\pi/2 . \quad .. \quad (60)$$

For an eccentrically loaded column (see Fig. 73) we can put

$M_A = Pe_A$, $M_B = -Pe_B$, and the central deflection is then

$$y = (e_A/2 + e_B/2)(\sec k\ell/2 - 1) + \Sigma \left[a_n/(1 - P/n^2Q)\right] \sin n\pi/2 \quad .. \quad (61)$$

Fig. 73.

For the particular case of one end of the column pinned, we can put $M_B = 0$. If the initial shape is a simple half sine wave, then the deflection is

$$y = (M_A/2P)(\sec k\ell/2 - 1) + a_1/(1 - P/Q) \quad .. \quad (62)$$

These results will be used in the following analysis.

74. Consider an equilateral triangular frame whose initial shape is as shown in Fig. 74. This crookedness pattern is of the same form as the deflections for the gravest buckling mode. It is assumed that there are no initial stresses, and that the initial crookedness of the members is of simple form given by

$$y = a_1 \sin \pi x/\ell \quad \text{for AB and AC,}$$

and $$y = a_2 \sin 2\pi x/\ell \quad \text{for BC,}$$

where a_1/ℓ and a_2/ℓ are small.

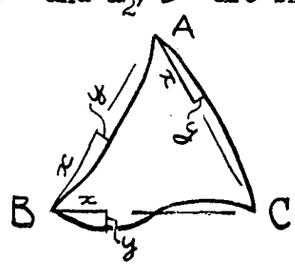

Fig. 74.

The initial angles that the ends of the members make with the straight lines joining their intersections are then

$$(-\pi a_1/\ell) \quad \text{for BA and CA,}$$

$$(+\pi a_1/\ell) \quad \text{for AB and AC,}$$

and $$(-2\pi a_2/\ell) \quad \text{for BC and CB.}$$

Anticlockwise rotations and moments are considered positive.

By putting $2a_2 = a_1$, all the included corner angles can be made equal to 60°.

Under load (see Fig. 75), if angles θ_{AB} etc. are measured anticlockwise from straight lines AB etc., we have, using equations (58) and (59)

$$\left.\begin{aligned} EI\,\theta_{AB} &= M_{AB}\,\ell\beta/3 - M_{BA}\,\ell\alpha/6 + \pi EIa_1/\ell\,(1 - P/Q) \\ \text{and} \quad EI\,\theta_{BC} &= M_{BC}\,\ell\beta'/3 - M_{CB}\,\ell\alpha'/6 - 2\pi EIa_2/\ell\,(1 + P/8Q) \\ \text{etc.} \end{aligned}\right\} \quad \ldots \quad (63)$$

where $Q = \pi^2 EI/\ell^2$, and the functions α, β, α', β' are defined in Arts. 21 and 22.

Now for equilibrium and continuity at the joints

$$M_{AB} + M_{AC} = 0$$

$$M_{BA} + M_{BC} = 0$$

$$M_{CA} + M_{CB} = 0$$

and $\theta_{AB} = \theta_{AC}$, $\theta_{BA} = \theta_{BC}$, $\theta_{CA} = \theta_{CB}$.

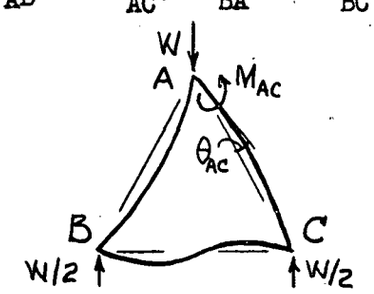

Fig. 75.

Also from the antisymmetry of the frame,

$$\theta_{BA} = \theta_{CA}.$$

Inspection of equations (63) then gives

$$M_{BA} = M_{CA}, \quad M_{AB} = M_{AC}, \text{ and } M_{BC} = M_{CB}.$$

Hence $M_{AB} = M_{AC} = 0.$

Substituting in the expressions for θ_{BA} and θ_{BC} (equations 63) we have

$$M_{BA}\ell\beta/3 - \pi EIa_1/\ell(1 - P/Q)$$
$$= M_{BC}\ell(\beta'/3 - \alpha'/6) - 2\pi EIa_2/\ell(1 + P/8Q).$$

Since $a_1 = 2a_2$, this reduces to

$$M_{BA}\ell^2/\pi EIa_1 = 27P/4Q(1 - P/Q)(1 + P/8Q)(2\beta + 2\beta' - \alpha') \quad .. \quad (64)$$

It is seen that M_{BA} tends to infinity when

$(2\beta + 2\beta' - \alpha') = 0$, i.e. when $k\ell = 4.0$. This is the buckling condition when the members are initially straight. It might be expected, from the fact that the term $(1 - P/Q)$ appears in the denominator on the right of equation (64), that M_{BA} also becomes infinite at $P/Q = 1$, but this is not so. It is evident that the buckling load must be higher than the Euler load of the pin-ended strut, and it can be shown that

$$\lim_{\substack{P = Q \\ k\ell = \pi}} M_{BA}\ell^2/\pi EIa_1 = 5.0.$$

In these expressions, $Q = \pi^2 EI/\ell^2$, $P = k^2 EI$, and hence $P/Q = (k\ell/\pi)^2$. M_{BA} can thus be obtained as a function of $k\ell$, using equation (64). Fig. 76 shows the resulting plot of

$$X = M_{BA}\ell^2/\pi EIa_1 \quad \text{against} \quad k\ell = \sqrt{P/EI}.\ell.$$

Fig. 77 shows a type of Southwell Plot on M_{BA}, where $X/(k\ell)^2$ is plotted against X. It proves to be a straight line of slope 1/16, and intercept on the $X/(k\ell)^2$ axis of 0.19, whose equation is

$$X/(k\ell)^2 = X/16 + 0.19.$$

This reduces to

$$M_{BA} = 0.19\ \pi\ a_1\ P/(1 - P/P_{cr}).$$

M_{BA} is thus a function of the load P, the crookedness parameter a_1, and the critical load of the frame, since P_{cr} is given by $k\ell = \sqrt{16} = 4.0$. That is $P_{cr} = 16EI/\ell^2$, the buckling load of the triangle having initially straight members. Thus the Southwell Plot on M_{BA} is a straight line. The reciprocal of the slope of the plot gives the buckling load for the initially perfect frame.

It is interesting to investigate the behaviour of the angle θ_{BA} as the load increases. It will be shown that the way in which θ_{BA} runs away as the critical load is approached is similar to the more well-known behaviour of deflections. The analysis is introduced here to strengthen the argument that the Southwell Plot can be applied to any distortion parameter which participates in the buckling mode concerned. We have, from the equations (63), since $M_{AB} = 0$,

$$\theta_{BA} = M_{BA}\, \ell\beta/3EI - \pi a_1/\ell\,(1 - P/Q)$$

$$= (\pi a_1/\ell)\left[\beta X/3 - 1/(1 - P/Q)\right].$$

The initial value of θ_{BA} is $(-\pi a_1/\ell)$. Therefore the rotation from the initial position is

$$\theta'_{BA} = \theta_{BA} + \pi a_1/\ell.$$

Fig. 78 shows the plot of the rotation under load θ'_{BA}, divided by the initial angle $(-\pi a_1/\ell)$, against $k\ell$.

It is interesting to plot the variation of M_{BA} with θ'_{BA}. This is carried out in Fig. 79, where $M_{BA}\,\ell/EI\;\theta'_{BA}$ is plotted against $k\ell$. We notice that the stiffness of the joint B, as far as the restraint it affords to the member BA is concerned, falls steadily to the value given by

$$M_{BA}\,\ell/EI\;\theta'_{BA} = 6.5. \qquad \ldots\ldots \quad (65)$$

As the axial force in AB increases, the stiffness of the joint reduces.

Consider the member AB in the frame ABC having initially straight members. Suppose $M_{AB} = 0$ as in the case of unsymmetrical buckling.

Put $M_{BA} = -\mu EI\;\theta_{BA}/\ell$

where μ is a variable factor relating the restraining moment to the rotation. Then we have

$$EI\theta_{BA} = M_{BA}\,\ell\beta/3 - M_{AB}\,\ell\alpha/6$$

$$= -\mu EI\beta\;\theta_{BA}/3 \quad \text{since } M_{AB} = 0.$$

Therefore

$$\mu = -3/\beta.$$

At the buckling load we have $k\ell = 4.0$, $\beta = -0.46$, and hence $\mu = 6.5$, thus confirming the value found from the plot in Fig. 79.

Fig. 80 shows the Southwell Plot on the rotation at B. The graph is a straight line whose equation is

$$\frac{\theta'BA/(-\pi a_1/\ell)}{(k\ell)^2} = \frac{\theta'BA/(-\pi a_1/\ell)}{16} + 0.025,$$

the slope of the plot being 1/16 and the intercept 0.025.

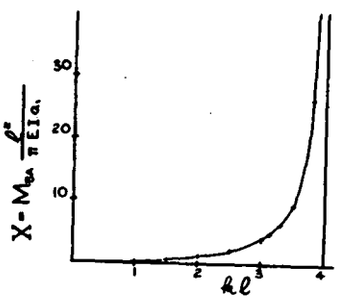

Fig. 76.

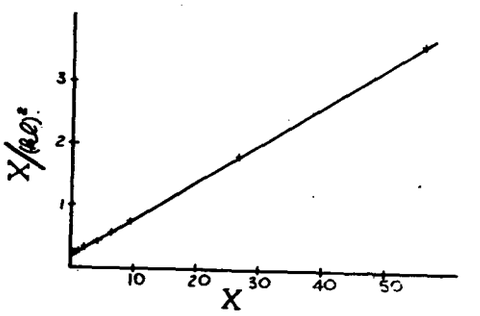

Fig. 77.

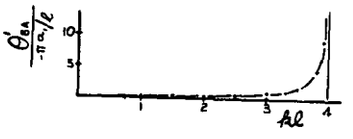

Fig. 78.

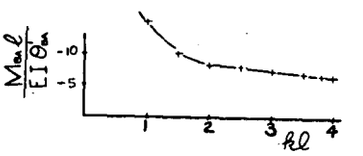

Fig. 79.

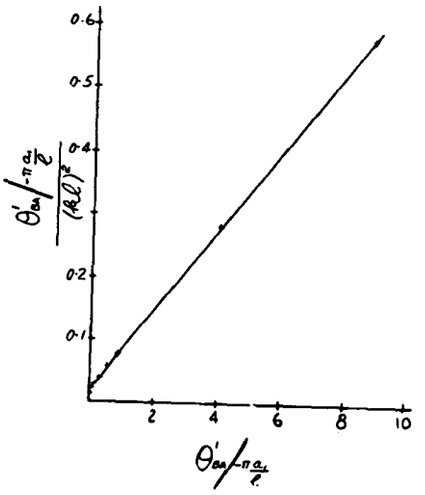

Fig. 80.

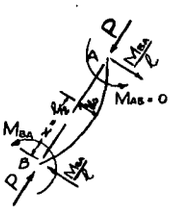

Fig. 81.

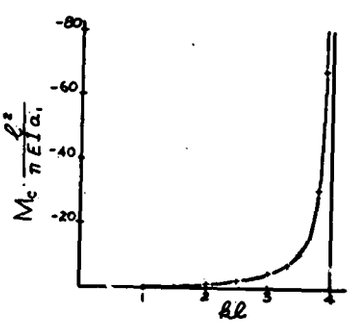

Fig. 82.

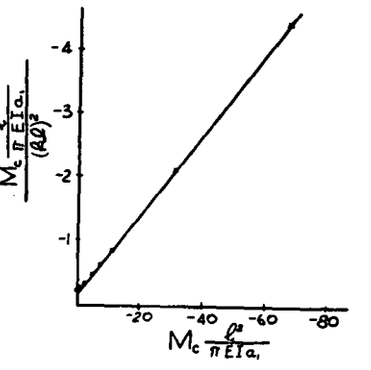

Fig. 83.

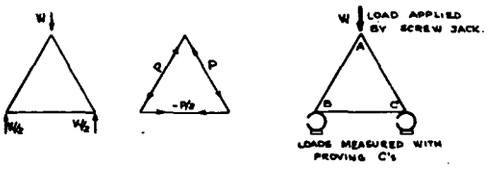

Fig. 84.

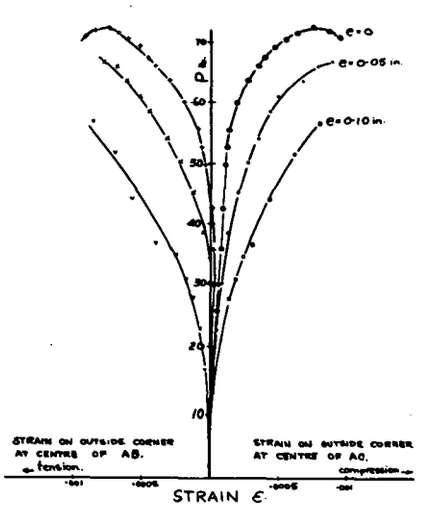

Fig. 85.

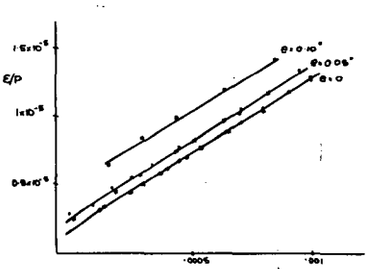

Fig. 86.

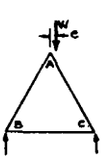

Fig. 87.

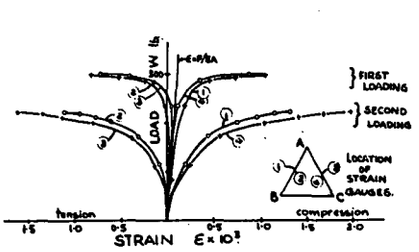

Fig. 88.

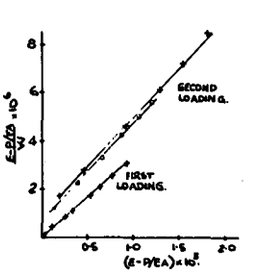

Fig. 89.

As in the case of M_{BA}, the Southwell Plot is a straight line of slope 1/16.

A parameter which is related to the first buckling mode, and which is conveniently measured, is the strain at the centre of one of the compression members. If the bending moment at the centre of AB is M_D, then the strain measured there is

$$\epsilon = P/EA \pm M_D \, v/I$$

where A is the cross-sectional area of the member, and v is the co-ordinate of the point where strain is measured. The term P/EA is linear with P, and independent of the buckling. M_D depends on the buckling alone, and runs away as the critical load is approached. Therefore, when strains are measured, the Southwell Plot should be carried out on $(\epsilon - P/EA)$ which equals $M_D \, v/I$. It is thus sufficient to investigate the behaviour of M_D as k increases. Consider the member AB. It has been shown that $M_{AB} = 0$,

therefore $M_D = Py_D - M_{BA}/2$

where y_D is the deflection at D. (See Fig. 81.)

Now $y_D = a_1/(1 - P/Q) - M_{BA} \, (\sec k\ell/2 - 1)/2P$ from equation (62).

We thus obtain

$$M_D \ell^2/\pi \, EI \, a_1 = (X/2) \sec k\ell/2 - (k\ell)^2/\pi \, (1 - P/Q).$$

This equation is plotted in Fig. 82, and the corresponding Southwell Plot in Fig. 83. A straight line of slope 1/16 is obtained.

This analysis shows that the Southwell Plot on M_D is linear. Hence if strains are measured at D, the Southwell Plot on $(\epsilon - P/EA)$ is linear and the reciprocal of the slope of the plot is the critical load of the frame. In the analysis presented, the standard classical approach has been given in full in order to show how the behaviour of the initially imperfect frame deviates from that of the perfect frame, and the method by which the two can be related using the Southwell Plot on strains.

75. Experimental Work on the Buckling of an Equilateral Triangular Frame in its Plane.

An equilateral triangular frame ABC was made up of $\frac{5}{8}$ in. x $\frac{5}{8}$ in. x 0.036 in. aluminium angle section members (ℓ = 31.75 in., EI = 5080 lb. in.^{2}) bolted to brass end pieces so that the major axes of the members lay in the plane of the frame. The frame was loaded as in Fig. 84. The expected buckling condition is

$$P_{cr} = 16EI/\ell^2 = 80 \text{ lb.}$$

The frame was loaded as in Fig. 84 and strains were measured on the corners of the angle members at the centres of members AB and AC using Huggenberger mechanical strain gauges.

In Fig. 85 the measured strains are plotted against load in the compression member, and graphs of strain/load against strain are shown in Fig. 86. The Southwell Plot on strains gives straight lines for both members, and the reciprocals of the slopes are 79 lb. in each case. This is in good agreement with the calculated critical load, but would not have been obtained from the loading test alone, as the maximum load reached was 72.3 lb. The frame was set up again as in Fig. 87, the load being applied with a slight eccentricity e at the apex. The strain against load plots and the strain/load against strain plots for two values of e are also shown in Figs. 85 and 86. Due to the eccentric loading, the strains increase more rapidly than for e zero, but Fig. 86 still shows straight lines, which have an inverse slope of 80 lb. in each case. This critical load could not have been inferred from loading tests. Very large deflections were obtained at much smaller loads than when e was zero.

Of course, the initial crookedness pattern in the experimental frame was not of the simple form assumed in the mathematical analysis. The experimental measurement has however justified the use of the linear strain plot in determining the critical load for the gravest buckling mode.

Another triangular frame was made up from 0.500" x 0.1325" steel strip (ℓ = 15.1", EI = 2530 lb.in.^{2}). The expected buckling condition is $P_{cr} = 16EI/\ell^2 = 176$ lb. or $W_{cr} = 305$ lb. (See Fig. 84.) Graphs of strain against load and the corresponding Southwell Plots on strain are shown in Figs. 88 and 89, and labelled "first loading". The equation of the Southwell Plot is

$$\frac{\varepsilon - P/EA}{W} = \frac{\varepsilon - P/EA}{304} + (0.08 \times 10^{-6})$$

The critical load of 304 lb. obtained from the plot is in good agreement with the calculated critical load of 305 lb.

The frame was then bent by hand and given the artificial initial crookedness pattern shown in Fig. 90. The resulting strain and Southwell Plots are also shown in Figs. 88 and 89.

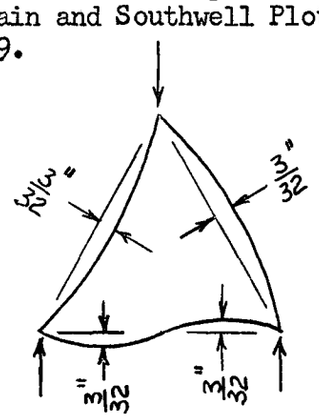

Fig. 90

The equation of the Southwell Plot is now

$$\frac{\varepsilon - P/EA}{W} = \frac{\varepsilon - P/EA}{270} + (0.7 \times 10^{-6}) \quad .. (66)$$

The intercept is larger than before, as is to be expected from the increased crookedness. Also the critical load obtained from the plot is lower. This tendency has been noted before in the case of single members where crookedness or eccentricity of loading was large. Because the deflections increase quickly with load, the method of obtaining the asymptote is less accurate. Yield of the material probably has an effect also, tending to lower the critical load.

It is interesting to compare the calculated strains with those measured. The equation of the calculated Southwell Plot (Fig. 83) is

$$\frac{M_D \ell^2/\pi EIa_1}{(k\ell)^2} = \frac{M_D \ell^2/\pi EIa_1}{16} - 0.20 \qquad .. \qquad (67)$$

where $M_D = (\varepsilon - P/EA)\ EI/v$ and $(k\ell)^2 = P\ell^2/EI$.

Comparison of equations (66) and (67) gives the value a_1 equals approximately 0.06 in. This is rather lower than the crookedness used, (Fig. 90), but is of the correct order. It is quite possible for a suitable initial stress pattern in the frame, due for example to one member being too long, to offset the initial crookedness and to make the intercept of the plot lower than the value calculated in much the same way as suitable eccentricity of loading of a pin-ended column can offset its initial crookedness.

76. It is to be noted that a simple initial crookedness pattern such that buckling of the compression members of the frame in single curvature results, has been chosen for the argument given in this paper. Tests made by the author on models and some full-size structures indicate that although a higher mode (double or triple curvature) often governs the initial deformations, unwrapping usually occurs fairly early, and single curvature becomes the gravest mode. The mode of buckling which governs failure of a structure is of course dependent on the slenderness of the members, their initial crookedness, joint eccentricities, and the yield stress of the members. If the form of the frame is such that a higher mode than single curvature exerts the main influence at failure, then the strain gauge can be suitably located to pick up this mode.

The above analysis and its experimental verification forms a preliminary justification of the use of the Southwell Plot on strains in problems of buckling of plane frames in their plane, without torsion of the members. In practice, however, many frames fail by combined torsional flexural buckling, and it is felt that some mathematical analysis of such a problem must be carried out before the method can be validly extended to such structures. The analysis of such a problem is carried out in Art. 78.

77. <u>The Buckling of a Warren Truss in its Plane</u>.

A Warren Truss was made from steel strip measuring 0.370 in. x 0.1265 in. The flexural rigidity of a sample of the strip was measured as $EI = 1770$ lb. in.^{2} The truss had equal members of length $\ell = 10.08$ in. welded together so that their minor axes pointed in the direction normal to the plane of the frame. Buckling in the plane of the frame without torsion of the members was thus ensured. The frame was loaded through $\frac{1}{8}$ in. diameter balls as shown in Fig. 91.

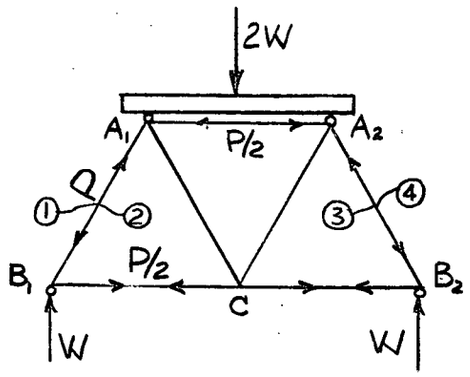

The numerals indicate the locations of the strain gauges.

Fig. 91

Strains were measured in the members $A_1 B_1$ and $A_2 B_2$ at the locations shown. They are plotted against the load 2W in Figs. 92 and 93, and the corresponding Southwell Plots are shown in Fig. 94. The points on the Southwell Plot lie very close to a single straight line of slope 1/620 lb.$^{-1}$. The calculated critical load is given by

$$P_{cr.} = (4.68)^2 EI/\ell^2 = 382 \text{ lb.} \quad \text{(see Art. 41)}$$

or $\quad 2W_{cr.} = 660$ lb.

There is a larger dicrepancy than usual here, amounting to 8%, between the calculated critical load and the value obtained from the Southwell Plot.

78. The Buckling of a Triangular Frame out of its Plane.

The simple flexural buckling of a triangular frame in its plane has been solved analytically and the Southwell Plot on longitudinal strains shown to be linear. The slope of the plot is related to the critical load of the frame, and the intercept is related to the initial imperfections. Tests resulted in good numerical agreement. However, many structures fail by instability where buckling of members in torsion and flexure is involved. The buckling of the members of a plane frame out of the plane of the frame is an example. It is assumed that in such cases inspection or a preliminary loading reveals the places where strain gauges should be put in order to measure strains which are governed by the gravest buckling mode, whether or not the gravest mode or the correct locations of the gauges are evident from theory. The question then arises: does the Southwell Plot on strains give the critical load for the mode concerned? Some analytical justification is required before the method can be used for such problems.

It has previously been stated that a structure fails by instability in the way in which it deforms most easily. If buckling occurs, a given structure subjected to a certain loading condition fails in a given mode dependent on the form of the structure, the stiffnesses of its members, and its initial imperfections (such as initial curvature of members or eccentricities at joints). This buckling mode possesses a critical load, or the theoretical load at which the initially perfect structure buckles into that mode (when restrained, if necessary, to prevent the occurrence of lower modes if these exist.)

Tests on several structures in which torsional-flexural buckling of members occurred have resulted in linear Southwell Plots on strain. These are reported in Chapter Four. It was evident by inspection or from a preliminary loading where to locate the strain gauges in order to pick up the gravest mode. Most of the structures were of a form which made calculation of the critical load for the buckling mode which occurred far too difficult for the operation to be carried out in order to check that the linear strain plot did in fact give this critical load.

However, it has been found possible to solve for the critical load of a plane triangular frame when it buckles out of the plane of the frame in either of two distinct modes. Torsion and flexure of all the members is involved, and the relative torsional and bending stiffnesses of the members markedly influences the critical load. Tests made by the author on small frames resulted in linear Southwell Plots on strains, and good numerical agreement with the calculated critical load was obtained. This experimental verification of the validity of the results of the Southwell Plot on longitudinal strains in the case of a simple frame is presented here, and forms a preliminary justification for the use of the method in more difficult problems of buckling of framed structures.

The experimental work emphasizes the fact that the pattern of initial imperfections may be a determining factor in the final buckling mode of a frame.

Notation:

W	external load on frame
P	compressive force in member
ϕ	joint rotation
θ	slope at the end of a member
ω	twist at the end of a member
M	bending moment
T	torque
γ_1	flexural rigidity
γ_2	torsional rigidity
E	Young's modulus
G	Shear modulus
ℓ	length of member
k	$= \sqrt{P/\gamma_1}$

Other symbols are defined in the text.

Consider the triangular frame ABC (Fig. 95) made of initially straight uniform members of length ℓ, loaded as shown. The minor axis of inertia of the members lies in the plane of the frame so that buckling in the plane of the frame does not occur.

Two distinct buckling modes designated Mode A and Mode B will be considered. Mode A occurs when the centres of AB and AC deflect in opposite senses relative to the plane ABC. Mode B occurs when the centres of AB and AC both deflect behind (or in front of) the plane ABC. It is evident that buckling in either of the forms described causes bending moments and torsion in the members of the frame. When considering any given mode, buckling in any other mode must, if necessary, be restrained.

Under load, the axial forces in the members are as shown in Fig. 96. Compression is considered positive.

Now $2P \cos 30^\circ = W$, hence $W = 1.73\ P$.

Assume that in the buckled condition the rotations of the joints A, B and C are given by the angles ϕ_{1A}, ϕ_{2A}, etc., as shown in Fig. 97. These rotations are treated as vectors, and the right-hand screw rule is used. As buckling in the plane of the frame is not being considered, no joint rotation vectors normal to the plane of the frame are introduced. Fig. 98 shows the slopes θ and twists ω at the ends of the individual members due to the joint rotations, and Fig. 99 shows the resulting bending moments and torques at the ends of the members. Moments, slopes, torques, and twists are also treated as vectors.

The end slopes θ and end twists ω can be found terms of the joint rotations ϕ as follows:

$$\left.\begin{aligned} \omega_{AB} &= \tfrac{1}{2}\sqrt{3}\phi_{1A} + \tfrac{1}{2}\phi_{2A} \\ \theta_{AB} &= -\tfrac{1}{2}\phi_{1A} + \tfrac{1}{2}\sqrt{3}\phi_{2A} \\ \omega_{AC} &= \tfrac{1}{2}\sqrt{3}\phi_{1A} - \tfrac{1}{2}\phi_{2A} \\ \theta_{AC} &= -\tfrac{1}{2}\phi_{1A} - \tfrac{1}{2}\sqrt{3}\phi_{2A} \end{aligned}\right\} \quad .. \quad (68)$$

$$\left.\begin{aligned} \omega_{BC} &= \tfrac{1}{2}\sqrt{3}\phi_{1B} + \tfrac{1}{2}\phi_{2B} \\ \theta_{BC} &= -\tfrac{1}{2}\phi_{1B} + \tfrac{1}{2}\sqrt{3}\phi_{2B} \\ \omega_{BA} &= \tfrac{1}{2}\sqrt{3}\phi_{1B} - \tfrac{1}{2}\phi_{2B} \\ \theta_{BA} &= -\tfrac{1}{2}\phi_{1B} - \tfrac{1}{2}\sqrt{3}\phi_{2B} \end{aligned}\right\} \quad .. \quad (69)$$

$$\left.\begin{aligned} \omega_{CA} &= \tfrac{1}{2}\sqrt{3}\phi_{1C} - \tfrac{1}{2}\phi_{2C} \\ \theta_{CA} &= -\tfrac{1}{2}\phi_{1C} + \tfrac{1}{2}\sqrt{3}\phi_{2C} \\ \omega_{CB} &= -\tfrac{1}{2}\sqrt{3}\phi_{1C} - \tfrac{1}{2}\phi_{2C} \\ \theta_{CB} &= -\tfrac{1}{2}\phi_{1C} - \tfrac{1}{2}\sqrt{3}\phi_{2C} \end{aligned}\right\} \quad .. \quad (70)$$

From equations (68) we obtain

$$\omega_{AB} + \omega_{AC} = -\sqrt{3}(\theta_{AB} + \theta_{AC}) \quad .. \quad (71)$$

and

$$\sqrt{3}(\omega_{AB} - \omega_{AC}) = \theta_{AB} - \theta_{AC} \quad .. \quad (72)$$

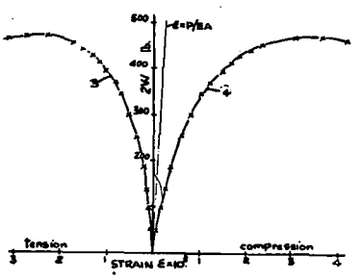

Fig. 92.

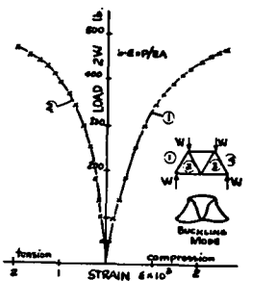

Fig. 93.

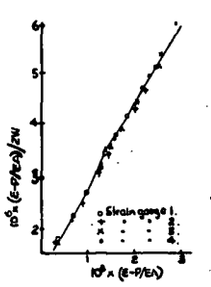

Fig. 94.

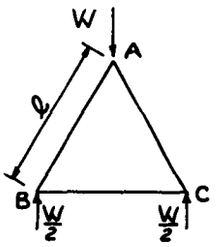

Fig. 95.

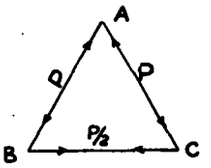

Fig. 96.

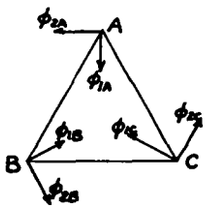

Fig. 97.

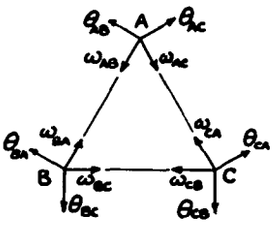

Fig. 98.

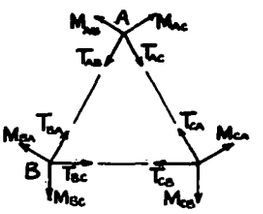

Fig. 99.

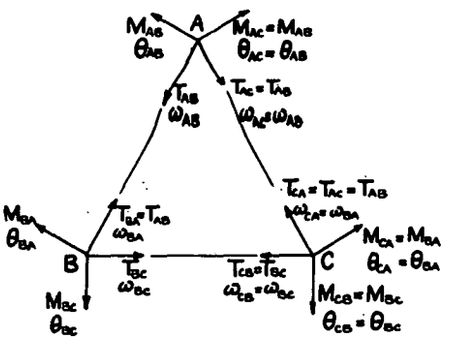

Fig. 100.

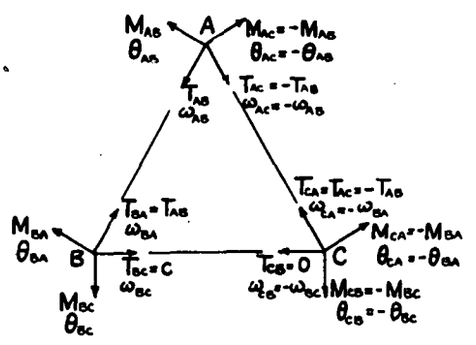

Fig. 101.

Similar expressions can be obtained at B and C by use of cyclical symmetry.

For equilibrium at joint A, we have

$$\tfrac{1}{2}\sqrt{3}\,(T_{AB} + T_{AC}) - \tfrac{1}{2}\,(M_{AB} + M_{AC}) = 0 \qquad .. \quad (73)$$

and $$\tfrac{1}{2}\sqrt{3}\,(M_{AB} - M_{AC}) + \tfrac{1}{2}\,(T_{AB} - T_{AC}) = 0 \qquad .. \quad (74)$$

Similar equations can be written down at B and C.

The equations relating the end moments and slopes for the member AB are

$$\theta_{AB} = M_{AB}\,\ell\beta/3\,\gamma_1 - M_{BA}\,\ell\alpha/6\,\gamma_1$$

and $$\theta_{BA} = M_{BA}\,\ell\beta/3\,\gamma_1 - M_{AB}\,\ell\alpha/6\,\gamma_1$$

where γ_1 is the flexural rigidity of the member and α and β are functions tabulated in Niles and Newell "Airplane Structures", p. 72. Similarly for the member BC,

$$\theta_{BC} = M_{BC}\,\ell\beta'/3\,\gamma_1 - M_{CB}\,\ell\alpha'/6\,\gamma_1$$

and $$\theta_{CB} = M_{CB}\,\ell\beta'/3\,\gamma_1 - M_{BC}\,\ell\alpha'/6\,\gamma_1$$

where α' and β' are functions tabulated in Niles and Newell "Airplane Structures" p. 107. Putting $P/\gamma_1 = k^2$, α and β are functions of $k\ell$, and α' and β' are functions of $(-k\ell/\sqrt{2})$

Also put

$$\ell\beta/3\gamma_1 = Y, \quad \ell\beta'/3\gamma_1 = Y'$$

$$\ell\alpha/6\gamma_1 = X, \quad \ell\alpha'/6\gamma_1 = X'$$

and $\ell/\gamma_2 = Z$, where γ_2 is the torsional rigidity of the member.

Then $$\theta_{AB} = M_{AB}\,Y - M_{BA}\,X, \qquad .. \quad .. \quad (75)$$

$$\theta_{BA} = M_{BA}\,Y - M_{AB}\,X. \qquad .. \quad .. \quad (76)$$

Also $$\theta_{AC} = M_{AC}\,Y - M_{CA}\,X \qquad .. \quad .. \quad (77)$$

$$\theta_{CA} = M_{CA}\,Y - M_{AC}\,X \qquad .. \quad .. \quad (78)$$

and $$\theta_{BC} = M_{BC}\,Y' - M_{CB}\,X' \qquad .. \quad .. \quad (79)$$

$$\theta_{CB} = M_{CB}\,y' - M_{BC}\,X' \qquad .. \quad .. \quad (80)$$

The equations relating torque and twist in the members are

$$T_{AB} = T_{BA} = \gamma_2(\omega_{AB} + \omega_{BA})/\ell$$

Therefore

$$\omega_{AB} + \omega_{BA} = Z\,T_{AB} = Z\,T_{BA} \qquad .. \quad .. \quad (81)$$

$$\omega_{AC} + \omega_{CA} = Z\,T_{AC} = Z\,T_{CA} \quad .. \quad .. \quad (82)$$

and $$\omega_{BC} + \omega_{CB} = Z\,T_{BC} = Z\,T_{CB} \quad .. \quad .. \quad (83)$$

Buckling modes A and B will now be considered separately.

Buckling Mode A.

This mode occurs when the centres of AB and AC deflect in opposite senses relative to the plane ABC. The buckled shape is antisymmetrical about the bisector of the angle at A

Hence $$\phi_{2A} = 0, \quad \phi_{1B} = \phi_{1C}, \text{ and } \phi_{2B} = -\phi_{2C} \quad .. \quad (84)$$

Equations (68) then give

$$\omega_{AB} = \omega_{AC}, \text{ and } \theta_{AB} = \theta_{AC}.$$

Hence equation (71) reduces to

$$\omega_{AB} = -\sqrt{3}\,\theta_{AB}. \quad .. \quad .. \quad (85)$$

Now equations (84), (69) and (70) give

$$\omega_{BA} = \omega_{CA}, \ \theta_{BA} = \theta_{CA}, \ \omega_{BC} = \omega_{CB}, \text{ and } \theta_{BC} = \theta_{CB}.$$

Hence, from equations (75) to (83)

$$M_{AB} = M_{AC}, \ M_{BA} = M_{CA}, \ M_{BC} = M_{CB}, \text{ and } T_{AB} = T_{AC}.$$

Therefore equation (73) reduces to

$$\sqrt{3}\,T_{AB} - M_{AB} = 0 \quad .. \quad .. \quad (86)$$

Writing down the equations at B similar to equations (71) and (72) at A, we have

$$\omega_{BA} + \omega_{BC} = -\sqrt{3}\,(\theta_{BA} + \theta_{BC}) \quad .. \quad .. \quad (87)$$

and $$\sqrt{3}(\omega_{BA} - \omega_{BC}) = \theta_{BA} - \theta_{BC} \quad .. \quad .. \quad (88)$$

Since $\theta_{BC} = \theta_{CB}$, equations (79) and (80) reduce to

$$\theta_{BC} = M_{BC}\,(Y' - X') \quad .. \quad .. \quad (89)$$

and since $\omega_{BC} = \omega_{CB}$ equation (83) reduces to

$$2\omega_{BC} = Z\,T_{BC} \quad .. \quad .. \quad (90)$$

For equilibrium at B, equations (73) and (74) become

$$(\sqrt{3}/2)(T_{BC} + T_{BA}) - (M_{BC} + M_{BA})/2 = 0 \quad .. \quad (91)$$

and $(\sqrt{3}/2)(M_{BC} - M_{BA}) + (T_{BC} - T_{BA})/2 = 0$ .. (92)

Equations (75), (76), (81) and (85) to (92) may now be considered as eleven equations in the eleven unknowns M_{AB}, θ_{AB}, T_{AB}, ω_{AB}, M_{BA}, θ_{BA}, ω_{BA}, M_{BC}, θ_{BC}, T_{BC} and ω_{BC}. These paremeters define the buckled condition of the frame, and are shown in Fig. 100. The buckling load can be obtained by setting the determinant of the coefficients in the eleven equations equal to zero, but it is more convenient to reduce the eleven equations to two equations in M_{AB} and M_{AC}.

Multiplying equation (87) by $\sqrt{3}$ and adding equation (88), we have

$$\omega_{BA} = -(2\theta_{BC} + \theta_{BA})/\sqrt{3} \quad .. \quad (93)$$

By subtracting, we have

$$\omega_{BC} = -(\theta_{BC} + 2\theta_{BA})/\sqrt{3} \quad .. \quad (94)$$

Equation (90) gives

$$2\omega_{BC} = Z\, T_{BC}.$$

Also equations (89) and (76) give expressions for θ_{BC} and θ_{BA}. Hence equation (94) gives

$$2\, M_{BC}\, (Y' - X') + 4\, M_{BA}\, Y - 4\, M_{AB}\, X + \sqrt{3}\, Z\, T_{BC} = 0. \quad (95)$$

Equations (81), (85), (93) and (86) give

$$-3\theta_{AB} - 2\theta_{BC} - \theta_{BA} = Z\, M_{AB}.$$

Substitution from equations (75), (89) and (76) gives

$$(3Y - X + Z)\, M_{AB} + (Y - 3X)\, M_{BA} + 2(Y' - X')\, M_{BC} = 0. \quad (96)$$

Noting that

$T_{AB} = T_{BA} = M_{AB}/\sqrt{3}$ from equations (86), equation (91) becomes

$$M_{BA} + M_{BC} = M_{AB} + \sqrt{3}\, T_{BC}, \quad .. \quad (97)$$

and equation (92) becomes

$$3M_{BA} - 3M_{BC} = -M_{AB} + \sqrt{3}\, T_{BC}.$$

Subtraction gives

$$M_{BA} - 2\, M_{BC} + M_{AB} = 0 \quad .. \quad (98)$$

Equations (95) and (97) give

$$(2Y' - 2X' + Z)\, M_{BC} - (4X + Z) M_{AB} + (4Y + Z)\, M_{BA} = 0 \quad (99)$$

Substituting $2M_{BC} = M_{BA} + M_{AB}$ from equation (98) in equations (96) and (99) we obtain two equations in M_{AB} and M_{BA}.

$$(Y' - X' + 3Y - X + Z)M_{AB} + (Y' - X' + Y - 3X)M_{BA} = 0$$

$$(Y' - X' - 4Y - \tfrac{1}{2}Z)\, M_{AB} + (Y' - X' + 4Y + 3Z/2)M_{BA} = 0 .$$

Putting the determinant of the coefficients equal to zero for the buckling load, factorizing, and substituting for X, Y and Z, gives

$$(\alpha + 2\beta)(\alpha' - 2\beta') + 2(\alpha + 2\beta)(\alpha - 2\beta)$$
$$+ (6\gamma_1/\gamma_2)(\alpha' - 2\beta' + \alpha - 6\beta)/2$$
$$- (6\gamma_1/\gamma_2)^2/4 = 0 \qquad .. \qquad .. \qquad (100)$$

Substitution of α, β, α', and β' as functions of $k\ell$ gives the buckling load. (α and β refer to axial compression given by k, while β' and α' refer to axial tension given by $(k/\sqrt{2})$.)

In the case of mild steel members of rectangular section of width b and thickness t, $\gamma_1 = E\, bt^3/12$ and $\gamma_2 = G\, bt^3/3$. Therefore

$$6\,\gamma_1/\gamma_2 = 3.75 \text{ if } E/G = 30/12.$$

Substitution of this value in equation (100) and graphical solution yields

$$k\ell = 4.5 \qquad .. \qquad .. \qquad (100a)$$

In the case of members of equal angle-section of leg width b and thickness t, $\gamma_1 = E\, b^3t/12$ and $\gamma_2 = 2G\, bt^3/3$.

A particular aluminium angle section has the values

b = 0.55 in., t = 0.036 in., E = 9,000,000 lb./sq. in, and G = 3,300,000 lb./sq. in.,
giving

$6\,\gamma_1/\gamma_2 = 440$. Substitution of this value in equation (100) and graphical solution yields

$$k\ell = 3.16 \qquad .. \qquad .. \qquad (100b)$$

Buckling Mode B

This mode occurs when the centres of AB and AC deflect in the same sense relative to the plane ABC. The buckled shape is symmetrical about the bisector of the angle at A.

Hence $\phi_{1A} = 0$, $\phi_{1B} = -\phi_{1C}$, and $\phi_{2B} = \phi_{2C}$ .. (101)

Equations (68) then give

$$\theta_{AB} = -\theta_{AC} = \sqrt{3}\,\omega_{AB} = -\sqrt{3}\,\omega_{AC} \qquad .. \qquad (102)$$

and equations (69) and (70) give

$$\omega_{BA} = -\omega_{CA},\ \theta_{BA} = -\theta_{CA},\ \omega_{BC} = -\omega_{CB},\ \text{and}\ \theta_{BC} = -\theta_{CB}.$$

Hence, from equations (75) to (83)

$$T_{AB} = - T_{AC} = T_{BA} = -T_{CA},\ T_{BC} = 0,\ M_{AB} = - M_{AC},$$

$M_{BA} = - M_{CA}$, and $M_{BC} = - M_{CB}$.

Equation (74) then becomes

$$\sqrt{3}\ M_{AB} + T_{AB} = 0 . \qquad .. \quad (103)$$

Since $M_{BC} = - M_{CB}$, equation (79) becomes

$$\theta_{BC} = M_{BC}\ (Y' + X') \qquad .. \quad (104)$$

For equilibrium at B, equations (73) and (74) become

$$\tfrac{1}{2}\sqrt{3}\ T_{BA} - \tfrac{1}{2}(M_{BC} + M_{BA}) = 0 \qquad .. \quad (105)$$

and

$$\tfrac{1}{2}\sqrt{3}(M_{BC} - M_{BA}) - \tfrac{1}{2}\ T_{BA} = 0 \qquad .. \quad (106)$$

Equations (97) and (98) still hold for this mode, and hence equations (75), (76), (81), (87), (88) and (102) to (107) may be considered as ten equations in the ten unknowns M_{AB}, θ_{AB}, T_{AB}, ω_{AB}, M_{BA}, θ_{BA}, ω_{BA}, M_{BC}, θ_{BC}, and ω_{BC} since $T_{BC} = 0$. These equations can be reduced to two equations in M_{AB} and M_{AC} as before.

Equations (93) and (94) still hold, and substituting in equation (81) for ω_{AB} from equation (102), ω_{BA} from equation (93), and T_{AB} from equation (103), we have

$$\theta_{AB}/\sqrt{3} - (2\theta_{BC} + \theta_{BA})/\sqrt{3} = - \sqrt{3}\ \mathbf{Z}\ M_{AB} .$$

Therefore $$\theta_{AB} - \theta_{BA} - 2\theta_{BC} + \sqrt{3}\ \mathbf{Z}\ M_{AB} = 0.$$

Equations (75), (76) and (104) when used in conjunction with this equation give

$$(Y + X + 3Z)M_{AB} - (X + Y)M_{BA} - 2(Y' + X')\ M_{BC} = 0 \qquad .. \quad (107)$$

Substitution of $T_{AB} = - \sqrt{3}\ M_{AB}$ from equation (103) in equations (105) and (106) gives

$$3\ M_{AB} + M_{BA} + M_{BC} = 0 \qquad .. \quad (108)$$

and

$$M_{AB} - M_{BA} + M_{BC} = 0$$

Hence

$$M_{BC} = - 2\ M_{AB}.$$

Substitution in (107) and (108) gives

$$(Y + X + 3Z + 4\ Y' + 4X')\ M_{AB} - (X + Y)\ M_{BA} = 0$$

and

$$M_{AB} + M_{BA} = 0.$$

At the buckling load,

$$Y + X + 3Z + 4Y' + 4X' = -(X + Y) .$$

Therefore

$$Y + X + 2Y' + 2X' + 3Z/2 = 0 .$$

Hence

$$(2\beta + \alpha) + 2(2\beta' + \alpha') + (3/2)(6\ \gamma_1/\gamma_2) = 0. \qquad (109)$$

(β and α refer to axial compression given by k, while β' and α' refer to axial tension given by $k\sqrt{2}$.)

For a mild steel rectangular section member, $6\gamma_1/\gamma_2 = 3.75$, and graphical solution yields

$$k\ell = 3.48 \qquad .. \qquad .. \qquad (109a)$$

For the angle section member previously discussed, $6\gamma_1/\gamma_2 = 440$, and graphical solution yields

$$k\ell = 3.15 \qquad .. \qquad .. \qquad (109b).$$

79. Experimental Work on the Buckling of a Triangular Frame out of its Plane:

Triangular frames made of members of rectangular or angle section have been tested by the author, and Southwell Plots on measured longitudinal strains drawn. The type of member and the buckling mode are indicated as headings in the following discussion.

Mode B. Rectangular strip member

A triangular frame ABC was made up from 0.503 in. x 0.132 in. steel rectangular section material. For these members, cross-sectional area A = 0.0665 sq. in., E = 27,000,000 lb./sq. in., and $\gamma_1 = 2{,}530$ lb. in.^{2}. (by calculation, checked by measurement of deflections when loaded as a simple beam, resulting in very good agreement). The minor axes of inertia of the members lay in the plane ABC. The frame was loaded as in Fig. 102. The initial crookedness of the members was very small. During loading, longitudinal strains were measured at the centres of the members AB and AC using Huggenberger mechanical strain gauges. In Fig. 103 the measured strains are plotted against the applied load W. The locations of the strain gauges are indicated. The strains on the front of AB and the front of AC are both tensile, and using the previous notation, the buckling is in Mode B. Fig. 104 shows the Southwell Plots on strains $(\epsilon - P/EA)/W$ being plotted against $(\epsilon - P/EA)$, where the symbols have the following meaning:

W = applied load at the apex of the triangle
P = axial load in members AB and AC, = W/1.73
ϵ = measured strain
E = Young's modulus
A = cross-sectional area of member.

Hence P/EA = axial strain if no buckling occurs. The Southwell Plots are parallel straight lines passing quite near the origin and the reciprocal of the slope of the plots is $W_{cr} = 253$ lb.

The members AB and AC were then bent about their minor axes by hand, to give initial crookedness for each in the same sense relative to the plane ABC. The frame was loaded again, and strains measured in a similar way to that described above. Fig. 105 shows the measured strains, which increase rather more rapidly with load than in Fig. 103 due to the greater initial crookedness of the members. Fig. 106 shows the corresponding Southwell Plots. Parallel straight lines are again obtained, and the reciprocal of the slope is $W_{cr} = 260$ lb.

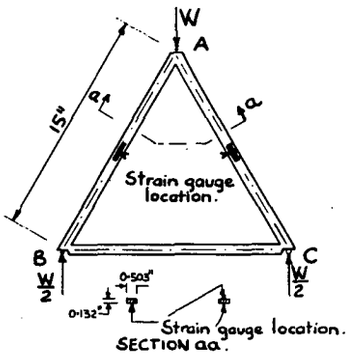

Fig. 102.

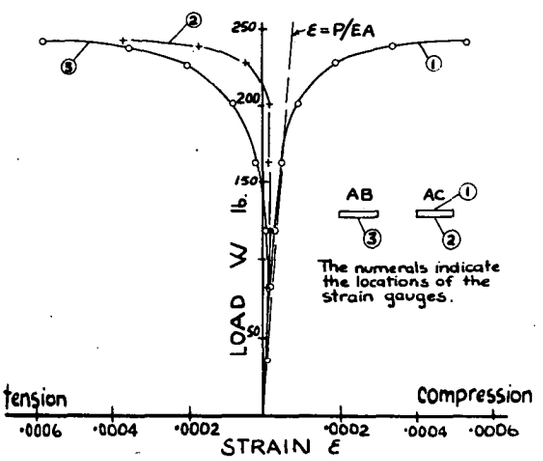

Fig. 103.

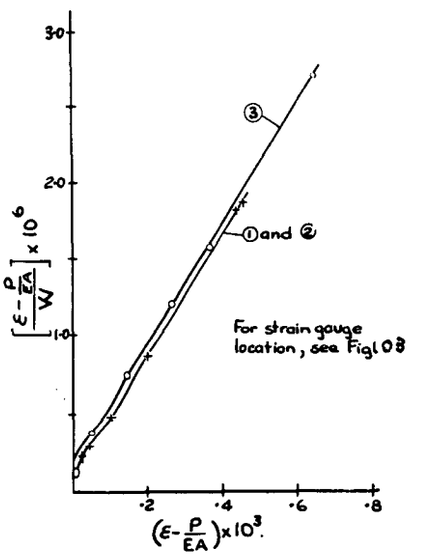

Fig. 104.

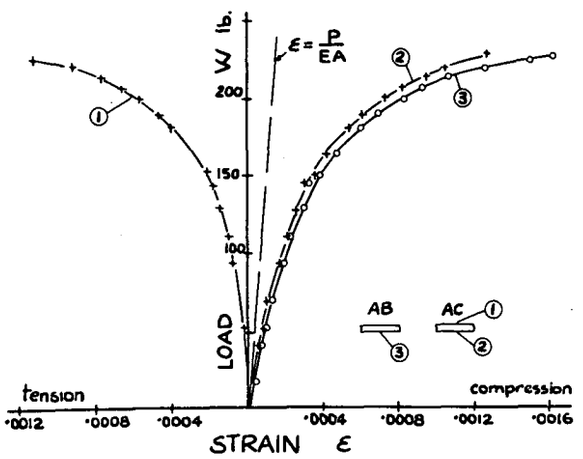

Fig. 105.

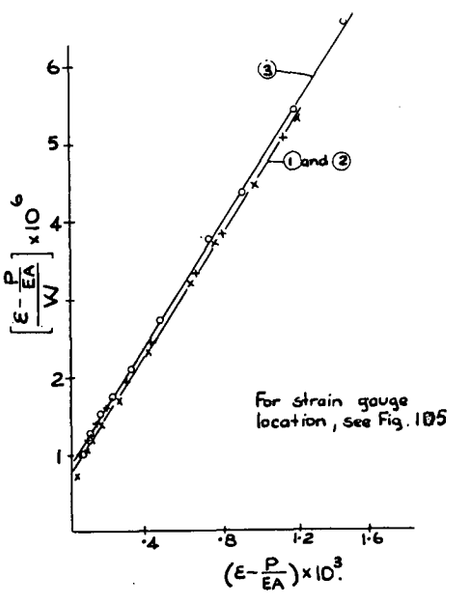

Fig. 106.

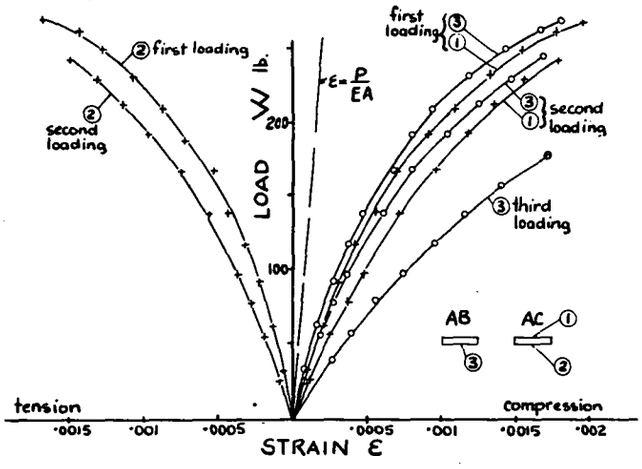

Fig. 107.

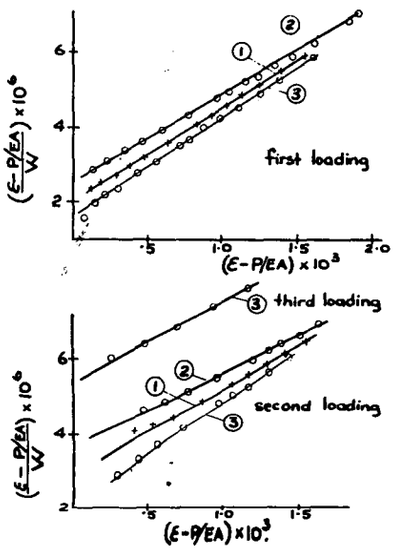

For strain gauge location see Fig. 107.

Fig. 108.

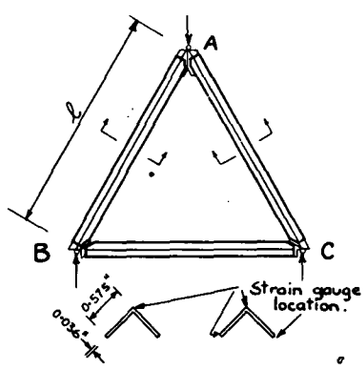

Fig. 109.

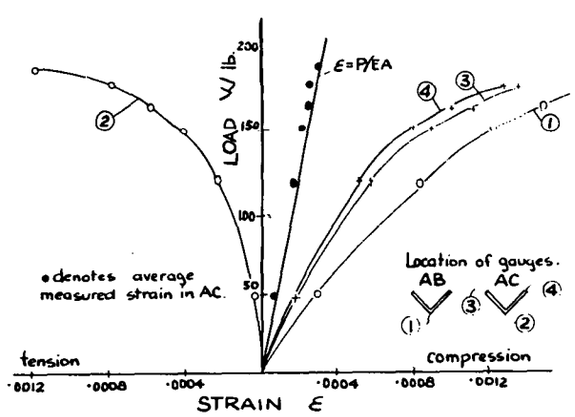

Fig. 110.

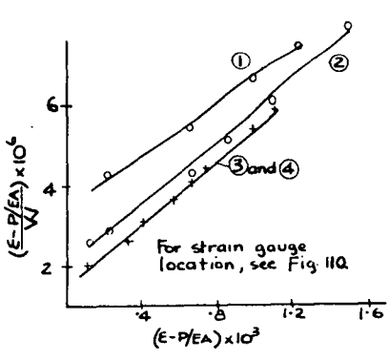

Fig. 111.

In this case the linear plots have a large positive intercept than previously. This is due to the increased initial crookedness.

The theoretical buckling condition as given by equation (109a) is

$$P_{cr} = k^2 \gamma_1$$
$$= (3.48)^2 \gamma_1 / \ell^2$$

where γ_1 is the flexural rigidity of the member about its minor axis. In this case

$$\gamma_1 = 2{,}530 \text{ lb. in.}^2 \text{ and } \ell = 15.0 \text{ in.}$$

Therefore

$$P_{cr} = 146 \text{ lb.}$$

and $W_{cr} = \sqrt{3}\, P_{cr} = 252$ lb.

The experimental values of 253 lb. and 260 lb. are in good agreement with the value of 252 lb. obtained analytically.

Mode A. Rectangular Strip Members

The members AB and AC were then bent by hand about their minor axes to give initial crookedness in opposite senses relative to the plane ABC, in order to induce buckling in Mode A. Strain measurements were taken during loading, and are shown in Fig. 107 (designated "first loading"). The Southwell Plots are shown in Fig. 108.

The initial crookedness values were again successively increased in two increments and the frame reloaded each time. The measured strains are also shown in Fig. 107 (designated second and third loading) and the corresponding Southwell Plots on strains are given in Fig. 108. The Southwell Plots are approximately parallel straight lines of average slope $1/395$ lb.$^{-1}$. The theoretical buckling condition as given by equation (100a) is

$$P_{cr} = (4.5)^2 \gamma_1 / \ell^2 = 228 \text{ lb.}$$

and $W_{cr} = 394$ lb.

The value obtained from the Southwell Plot on strains is again in good agreement with the theoretical value of the critical load.

It has therefore been possible to induce buckling in two different modes having critical loads differing by about 50% by altering the initial crookedness of the members of the frame, but when buckling occurs in either mode, the Southwell Plot has given a close estimate of the critical load.

Mode A. Angle-section members

A triangular frame ABC was made up from aluminium angle-section members having the minor axis of the section in the plane of the frame. (See Fig. 109). The members had the following properties: cross-sectional area A = 0.0402 sq. in., E = 9,000,000 lb./sq. in., mid-line breadth of leg b = 0.557 in., and flexural rigidity γ_1 = 4,640 lb. in.^{2} (checked by measurement of deflections when loaded as a simple beam.)

The frame was loaded as in Fig. 109, longitudinal strains being measured at the centres of AB and AC at various points around the cross-section. For member length ℓ = 16.75 in., measured strains are plotted in Fig. 110. The accuracy of the strain measurements is worth noting. This is demonstrated in Fig. 110 where the measured strains around the cross-section at the centre of AC are plotted. The average strain is also plotted, and though the calculation of the average strain involves only the small differences between the actual strains measured, close agreement is achieved with the calculated value $\epsilon = P/EA$. The corresponding Southwell Plots are shown in Fig. 111. They are parallel straight lines of slope (1/280) lb.$^{-1}$ The theoretical buckling condition as given by equation (100b) is

$$P_{cr} = (3.16)^2 \gamma_1/\ell^2 = (3.16)^2 \times 4640/(16.75)^2 = 165 \text{ lb.}$$

or $$W_{cr} = \sqrt{3}\, P_{cr} = 286 \text{ lb.}$$

The agreement is very close.

The experiment was repeated using member length ℓ = 32.7 in. Measured strains are plotted in Fig. 112, the average strain over the cross-section of AC again agreeing well with the calculated value $\epsilon = P/EA$. The Southwell Plots are shown in Fig. 113. Every point calculated from each of the four sets of strain measurements lies on a single straight line of slope (1/72) lb.$^{-1}$.

The crookedness of the members AB and AC was increased by bending in opposite senses, and the frame reloaded. Measured strains are plotted in Fig. 114 and the corresponding Southwell Plots in Fig. 115. Parallel straight lines of slope (1/72) lb.$^{-1}$ are obtained.

The calculated critical load is

$$W_{cr} = \sqrt{3}\, P_{cr} = \sqrt{3} \times (3.16)^2 \times 4640/(32.7)^2 = 75 \text{ lbs.}$$

Mode B. Angle-section members.

The members AB and AC of a triangular frame having member length ℓ = 16.75 in. were bent in the same sense, and the frame loaded as before. The measured longitudinal strains are plotted in Fig. 116 and the Southwell Plots in Fig. 117. The plots have slope 1/290 lb.$^{-1}$, while the theoretical buckling load is

$$W_{cr} = \sqrt{3} \times (3.15)^2 \times 4640/(16.75)^2 = 284 \text{ lb.}$$ (See equation 109b).

PLATE 4

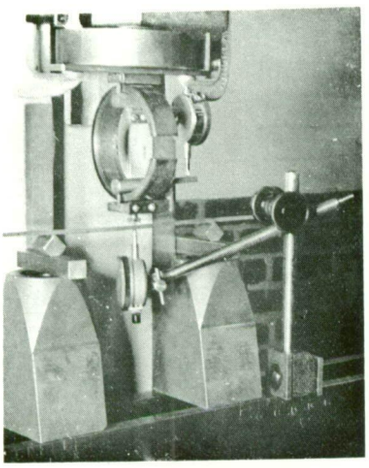

Measurement of flexural rigidity of rectangular strip material.

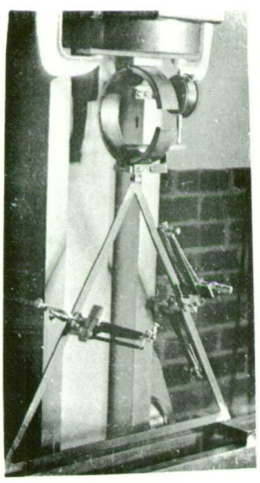

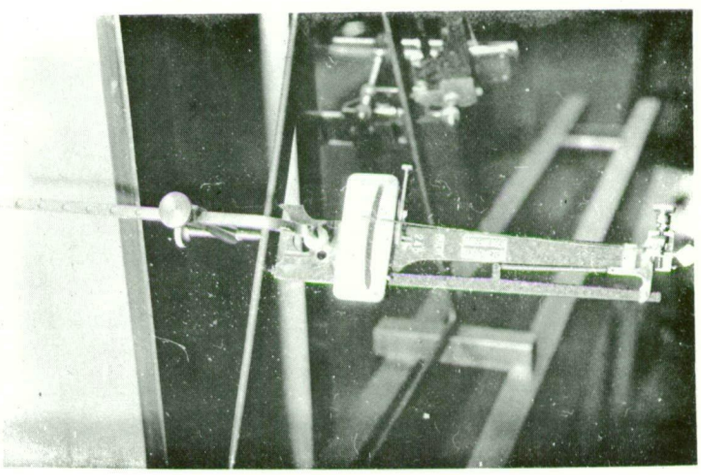

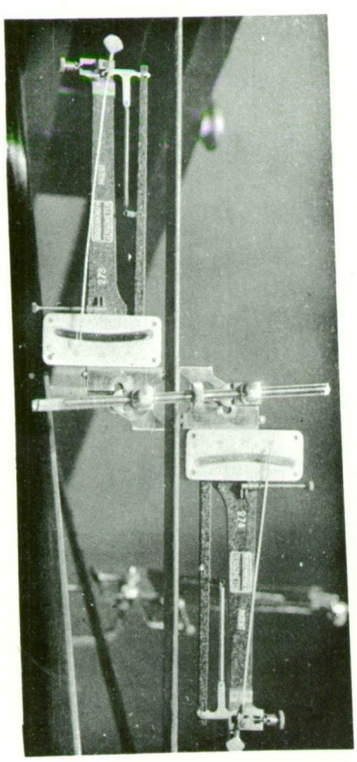

One of the buckling modes.

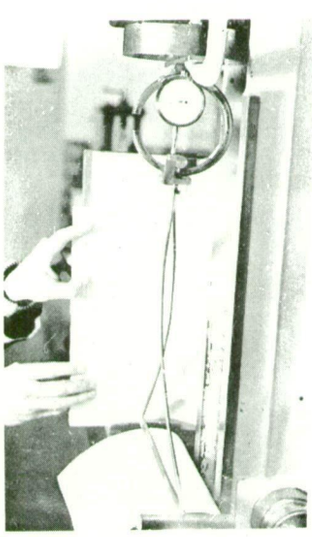

Measurement of strains in a triangular frame made of rectangular strip material buckling out of its plane.

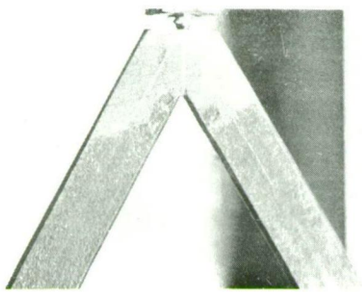

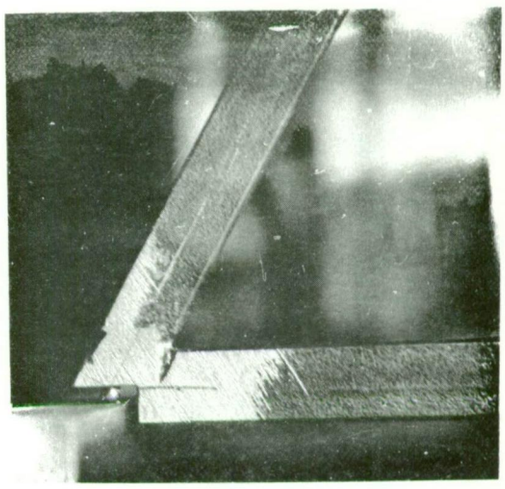

Method of loading frame made of rectangular strip.

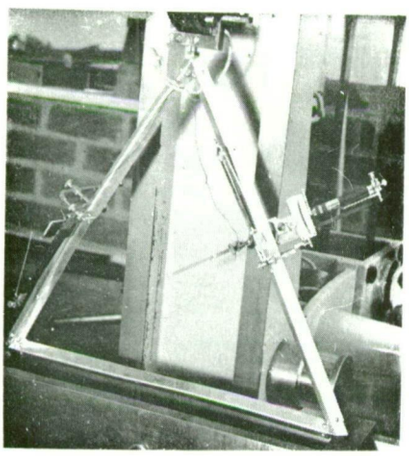

Frame made from angle-section members buckling out of its plane.

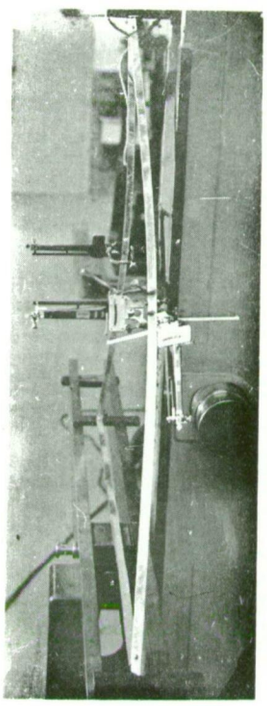

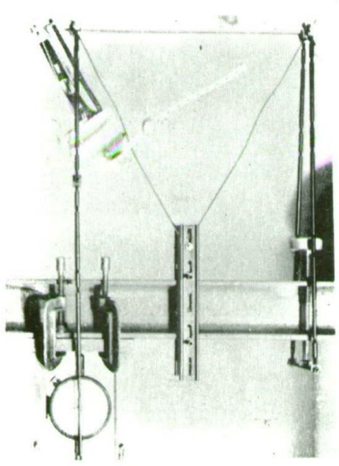

Test on a triangular frame made of flexible strip, buckling in its plane.

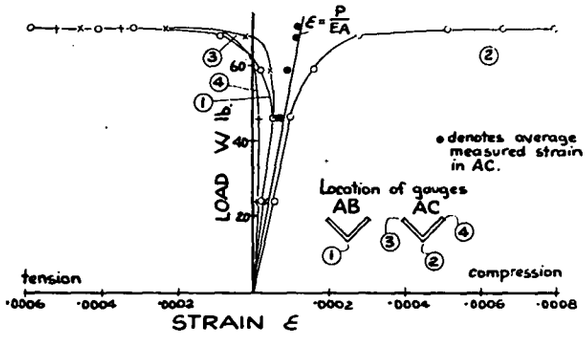

Fig. 112.

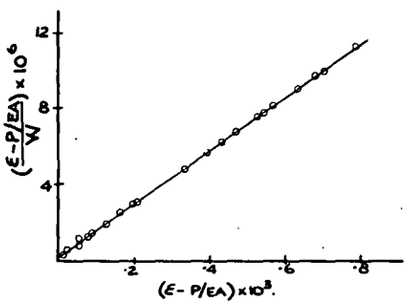

Fig. 113.

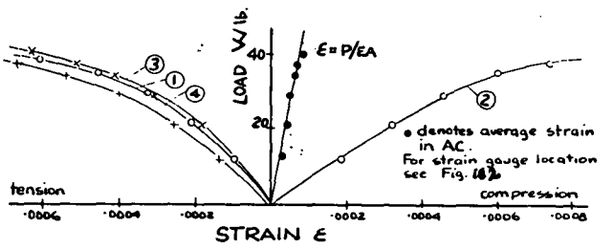

Fig. 114.

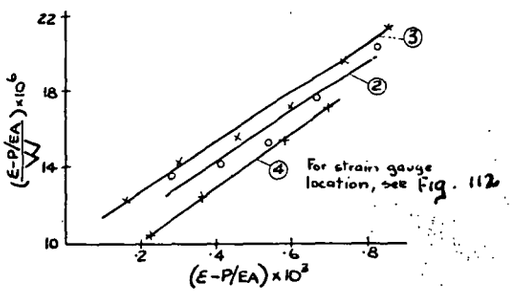

Fig. 115.

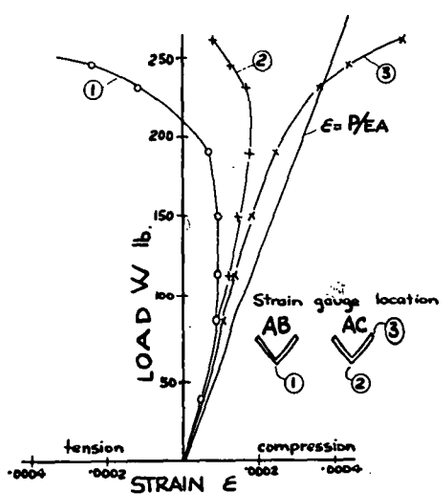

Fig. 116.

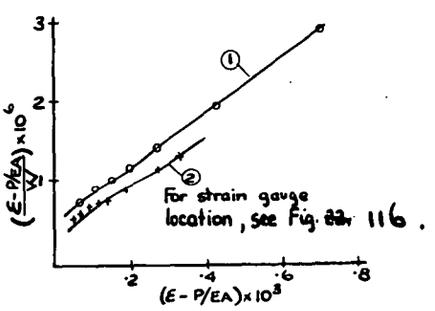

Fig. 117.

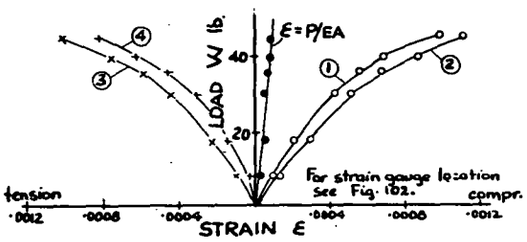

Fig. 118.

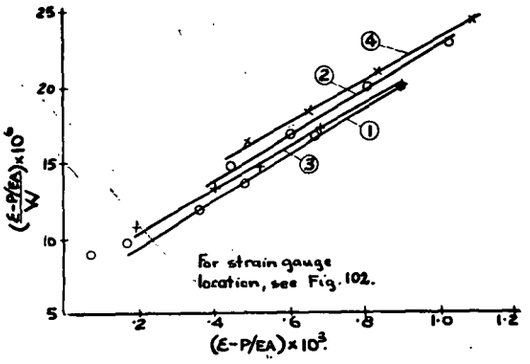

Fig. 119.

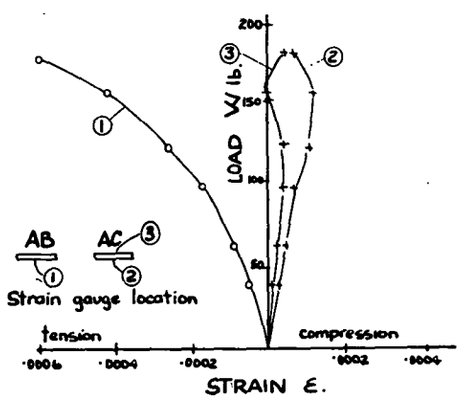

Fig. 120.

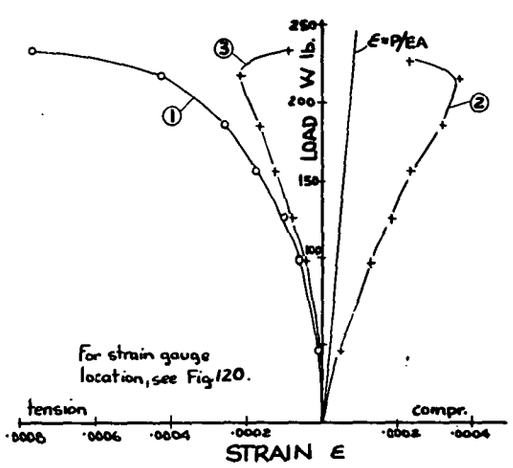

Fig. 121.

Using members of length 32.7 in., the strain against load graphs and Southwell plots are given in Figs. 118, and 119. Parallel linear Southwell Plots of slope (1/72) lb.$^{-1}$ are obtained. The theoretical buckling load is

$$W_{cr} = \sqrt{3} \times (3.15)^2 \times 4640/(32.7)^2 = 74.5 \text{ lb.}$$

In the case of angle-section members, the critical loads for the two different modes are themselves not very different. This is due to the low torsional rigidity of the members. However, when buckling occurs in either mode, the Southwell Plot on longitudinal strains gives a close approximation to the theoretical buckling load.

The Application of the Strain Plot to Torsional Flexural Buckling Problems

It is seen that though the relative torsional and bending stiffnesses of the members markedly influences the critical load of the triangular frame when buckling out of the plane of the frame occurs (see equations 100 and 109), the Southwell Plots on longitudinal strains are linear, and give a good approximation to the critical load of the frame. Hence, though this method has so far been mathematically justified only for flexural buckling, it appears from the foregoing experimental results that its use can be extended to problems of buckling in torsion and flexure. The method, and in particular the equation of the linear Southwell Plot, can thus be used with some confidence for such problems, as it appears to have reasonable justification.

It may be mentioned that the buckling mode of the frame used is dependent to a large extent on the initial imperfections of the frame. The effect of the magnitude and the sense of the initial crookedness of the members has been shown. In the case of the frame made of rectangular strip material, it was found that for small initial crookedness values of opposite sense in AB and AC, deformations in the anti-symmetrical mode A occurred at early stages of the loading. As loading progressed, however, the strains in one member reversed, and the symmetrical mode B became the governing mode. Typical strain plots are shown in Figs. 120 and 121. In this case, of course, linear Southwell Plots are not obtained, though if strain measurements were continued until large deformations in Mode B occurred, it might be expected that the latter part of the Southwell Plot would be linear, provided the material remained elastic. It appears therefore that, as is to be expected, the Southwell Plot on strains is linear only if buckling in one given mode governs the strain measurements taken. The Southwell Plot on deflections is of course similarly limited.

When testing structures, the author has usually found, however, that when the buckling of some members participates first in one mode and then in another mode, resulting in a non-linear Southwell Plot, some other member of the structure buckles throughout in one mode and thus determines failure. The Southwell Plot for this member is usually approximately linear, and its equation can be used to define the failure load.

80. The Lateral Buckling of a Model Lattice Girder.

Tests have been carried out on a model lattice girder. The equation of the Southwell Plot on longitudinal strains in the compression chord is similar in form to the usual column formula. Further tests on model and full size structures should establish the necessary empirical information for this equation to be useful in design. Good agreement was reached between the critical load obtained from the Southwell Plot and the value calculated using the theory of a beam with a continuous web.

Notation.

ϵ	strain
M	bending moment
I_{XX} and I_{YY}	major and minor moments of inertia of the girder (see Fig. 122)
v	co-ordinate measured from XX of a point where strains are measured (see Fig. 122)

Experimental work

A model lattice girder made of $\frac{1}{8}$ in. dia. brass rod with silver-soldered joints, and having the dimensions shown in Fig. 122 was set up and loaded in its plane as in Fig. 123 in order to set up a uniform bending moment in its central portion. Loads were measured with a proving "C". The top and bottom chords were supported laterally at points 7.5 in. apart. (Fig. 124) The elastic properties of the brass were:

Young's Modulus	$E = 15.3 \times 10^6$ p.s.i. (from tension test)
Shear Modulus	$G = 5.92 \times 10^6$ p.s.i. (from torsion test)
Yield Stress	$f_{YP} = 45{,}000$ p.s.i. in tension.

During the test, longitudinal strains were measured on the sides of the compression chord in two places, as shown in Figs. 122 and 124, using Huggenberger mechanical strain gauges. Graphs of strain ϵ, against moment M, are shown in Fig. 125. On this graph, the line $\epsilon = Mv/I_{XX}E$ is drawn. This represents the strain which would occur due to the action of the bending moment alone, if no lateral deformation took place. Graphs of $(\epsilon - Mv/I_{XX}E)/M$ against $(\epsilon - Mv/I_{XX}E)$ are plotted in Fig. 126. This is a type of Southwell Plot, and $(\epsilon - Mv/I_{XX}E)$ represents the strain due to the lateral deformation, since ϵ is the total strain measured. It should be noted that $(\epsilon - Mv/I)$ is analagous to the value $(\epsilon - P/EA)$ for a single column. It is the part of the strain that depends on bending effects, and is therefore expected to run away as buckling develops. These plots are found to be parallel straight lines, whose equations can be written in the form

$$\frac{(\epsilon - Mv/EI_{XX})}{M} = \frac{(\epsilon - Mv/EI_{XX})}{M_{cr}} + C_2 \qquad \ldots (110)$$

PLATE 6

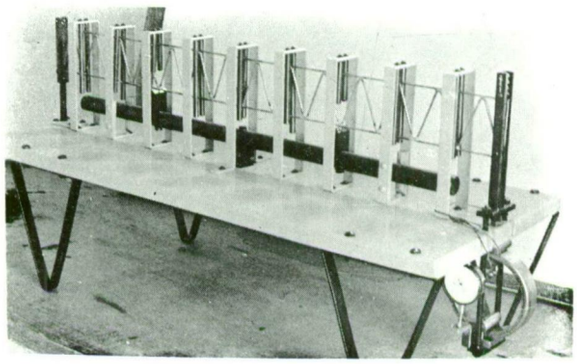

Test set-up for lateral buckling of a model lattice girder made from $\frac{1}{8}$ inch dia. brass rod.

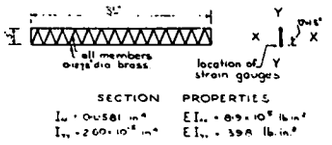

Fig. 122.

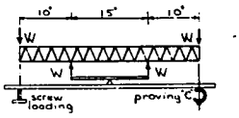

Fig. 123.

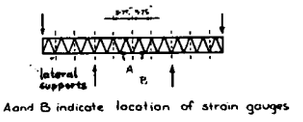

Fig. 124.

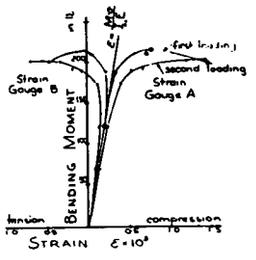

Fig. 125.

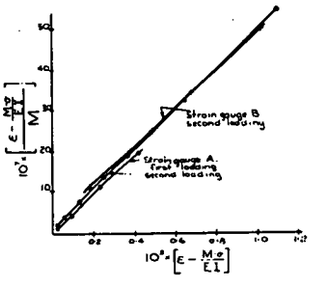

Fig. 126.

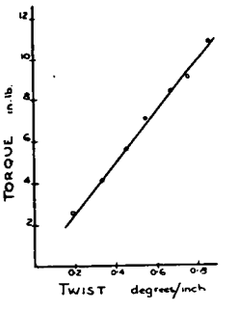

Fig. 127.

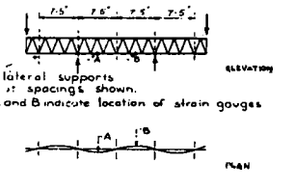

Fig. 128.

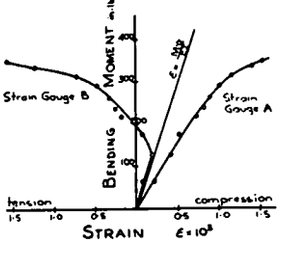

Fig. 129.

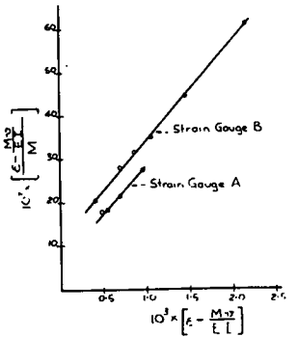

Fig. 130.

where M_{cr} is the reciprocal of the slope of the graph, and C_2 its intercept on the strain/moment axis. In this case, $M_{cr}^2 = 215$ in. lb. M_{cr} represents the critical moment which would cause elastic buckling of the structure possessing no initial imperfections.

The torsional rigidity of the girder was also measured under pinned-end conditions and the torque-twist curve is shown in Fig. 127. At the angles of twist involved, the curve is linear, and the torsional rigidity is C = 705 in. lb. per radian per in. The torsional rigidity can also be calculated as the sum of the torsional rigidities of the two chords and that of the lattice, assuming the joints between the chords and the lattice are rigid. The lattice members are both bent and twisted by the torsion of the girder. Using the measured elastic properties of the brass, this calculation gave the value C = 750, which is 6% greater than that measured. It is thought that the difference may be due to the softness of the solder at the joints of the lattice, or to the fact that the centre lines of the lattice members do not intersect at a point. Strains were measured in the lattice members during twisting, and were found to be 5% less than those calculated.

The lateral buckling of beams is discussed by S. Timoshenko in "Theory of Elastic Stability" (1936), McGraw Hill, p. 239. The theoretical lateral buckling moment of the girder treated as a beam with continuous web is

$$M_{th} = (\pi/\ell)\sqrt{EI_{YY}C}$$

$$= (\pi/7.5)\sqrt{398 \times 705}$$

$$= 222 \text{ in. lb.}$$

where ℓ is the length of the half-wave of the buckled shape. In calculating M_{th} the actual measured value of C has been used. Thus M_{th} is the theoretical lateral buckling moment of a girder having the torsional rigidity measured.

This is in very close agreement with the value obtained from the Southwell Plot on strains. The agreement is to be expected, but it gives confidence in the use of the method, which, it must be remembered, has as yet incomplete analytical justification and is defensible only from a general physical standpoint.

The model was set up again with lateral supports spaced 3.75 in. apart (Fig. 128). Strains were measured and plotted as before. (Figs. 129 and 130). The graphs are similar to those obtained in the first test. The value of M_{cr} the reciprocal of the slope of the Southwell Plot, is now 432 in. lb. The calculated value is

$$M_{th} = (\pi/3.75)\sqrt{398 \times 705}$$

$$= 444 \text{ in. lb.}$$

This is again in close agreement with the value obtained from the Southwell Plot.

The equation of the Southwell Plot on strains can be used as a design formula. Equation (110) reduces to

$$E\varepsilon = (Mv/I_{XX}) \left[1 + \phi/(1 - M/M_{cr})\right] \quad .. \quad (111)$$

where $\phi = C_2 E I_{XX}/v$.

Given the value of the yield stress f_{YP}, we can put $E\varepsilon = f_{YP}$, and solve for M. This gives the moment which will cause the compression chord to yield as it buckles laterally. The application of a load factor enables the safe working moment to be calculated. It is necessary to know M_{cr} and ϕ. Both are obtainable from the Southwell Plot, though in certain cases M_{cr} can be calculated as above, provided the torsional rigidity of the lattice is known. ϕ is a crookedness-eccentricity function, and the carrying out of the Southwell Plot on many types of structures should establish empirical information. Equation (111) has the same form as the usual column formula, and its solution is familiar to engineers.

81. The Lateral Buckling of 30 ft. and 28 ft. span Lightweight Roof Trusses.

Development of lightweight trusses has been carried out by the author at the University of Tasmania for Messrs. Charles Davis Ltd., Elizabeth Street, Hobart. The details of the trusses are as follows (see Fig. 131):

Flanges - Continuous, roll-formed from mild steel strip (patent held by Chas. Davis Ltd.) Up to the present time, 8" wide by 14 gauge mild steel strip having a yield point of 35,000 lb./sq. in. has been used.

Lattice members - The web members consist of continuous tubing which is bent to the required zig-zag, flattened, fed endways into the flanges, and spot-welded. Up to the present time, $\frac{7}{8}$" dia. or 1" dia. electric resistance welded semi-bright steel tubing having a yield and ultimate strength of 69,000 lb./sq. in. has been used, though in the early stage of the development of these trusses, 1½ in. x 3/16 in. mild steel flat was used.

With the use of lightweight structures and high working stresses, there arise buckling problems not usually met in standard practice. Failure at low loads can occur if such structures are used indiscriminately without the provision of proper restraint to compression members. The development of these trusses has afforded an excellent opportunity for research on buckling problems.

About twenty full-size girders and trusses have been tested. In many cases a great deal of information was available in the elastic range without causing permanent deformation, and the same truss was tested many times under different loading conditions. The results reported in this thesis are representative only.

Short trusses have been loaded so that they failed by buckling of web compression members rather than by yielding or buckling of the flanges. These experiments are reported in Art. 82. Other trusses have been tested full-size by loading at about the quarter points by jacking against a rolled steel joist fixed to the concrete floor. (Fig. 132). Various spacings and types of lateral restraint to the compression flange have been used, and some of the work is reported here. All testing set-ups

PLATE 7

LIGHTWEIGHT TRUSSES

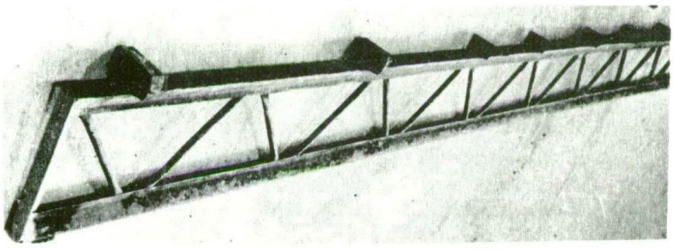

Portion of a typical 30 ft. span roof truss. Plates have been welded to the compression chord and wooden blocks attached. Under test, the compression chord was restrained by preventing later movement of these simulated purlins.

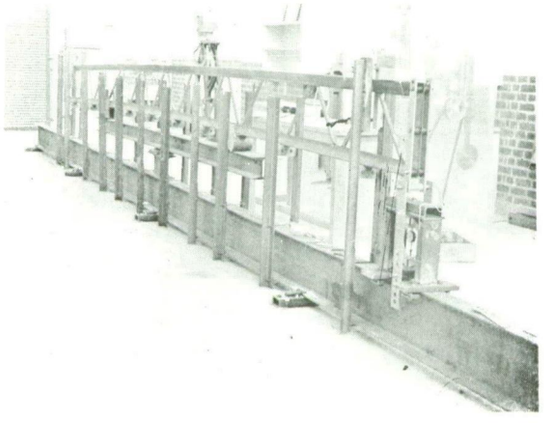

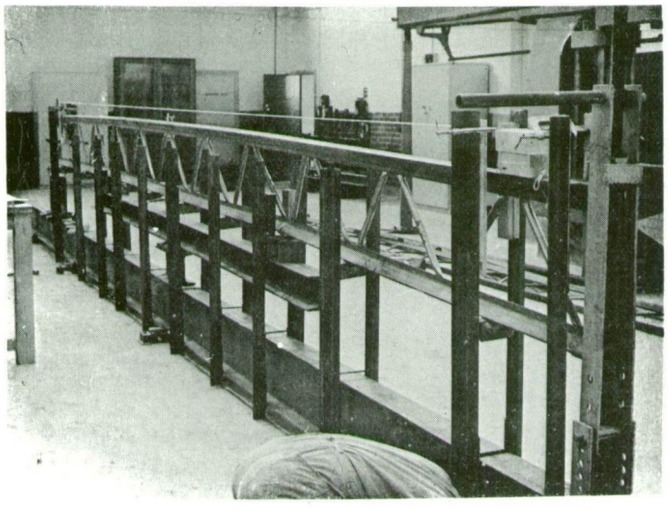

Set up for testing 28 ft. span truss.

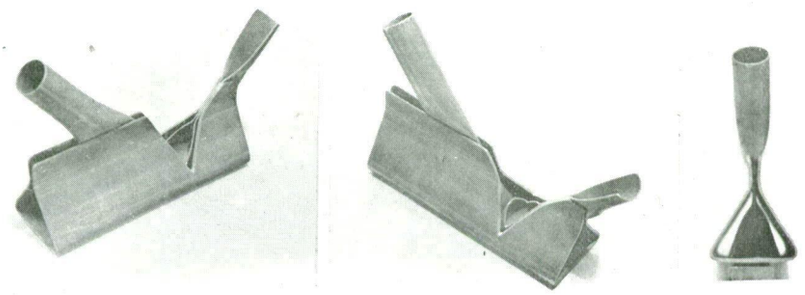

Cut away portions of lightweight trusses showing details of the roll-formed flanges and continuous tubular web-members.

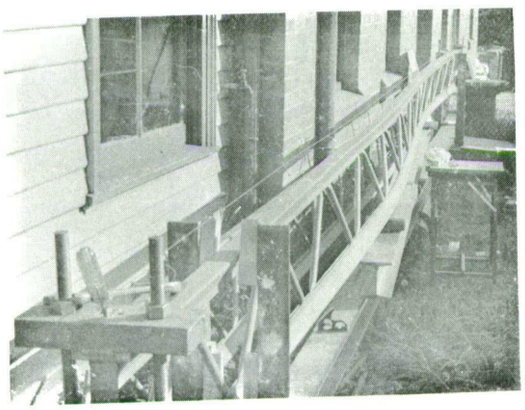

Lateral buckling of 30 ft. span truss in two half waves.

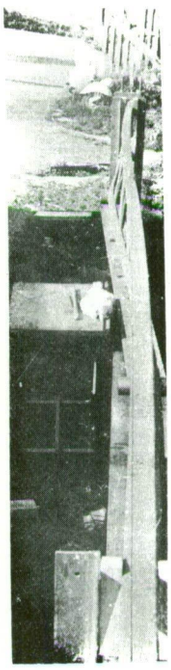

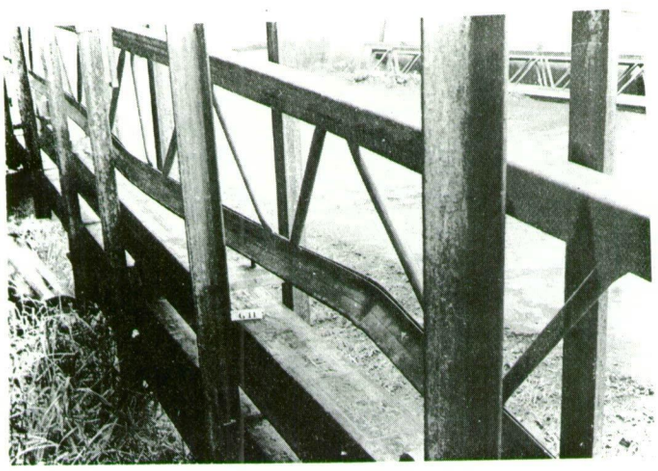

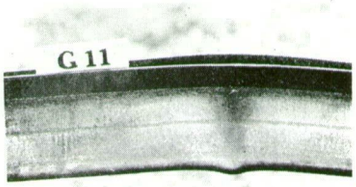

Well-developed buckle in compression chord of truss.

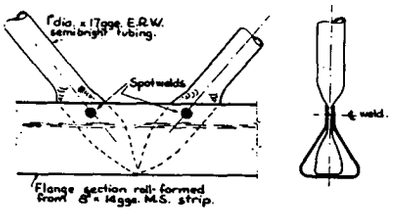

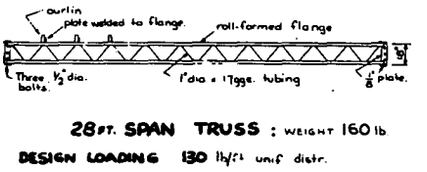

Fig. 131.

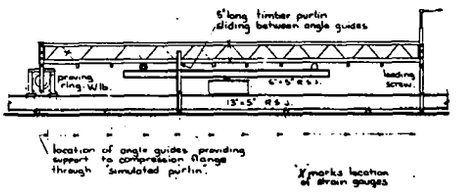

Fig. 132.

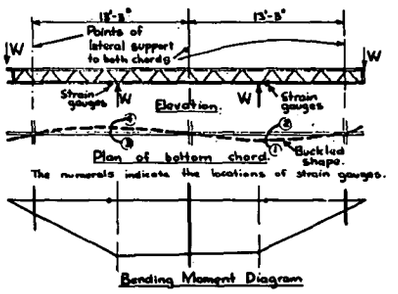

Fig. 133.

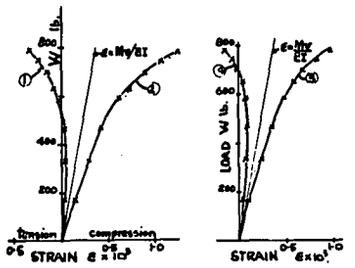

Fig. 134.

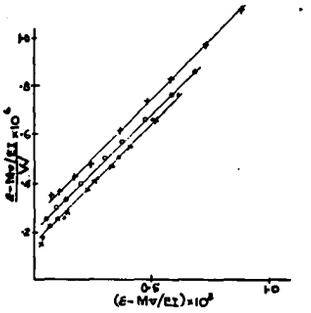

Fig. 135.

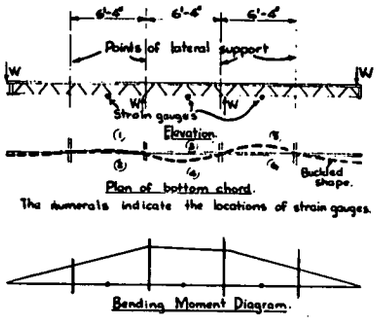

Fig. 136.

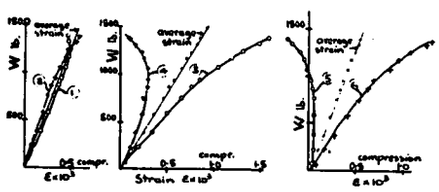

Fig. 137.

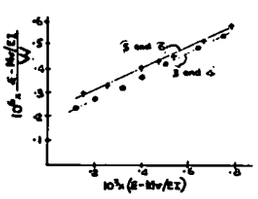

Fig. 138.

Fig. 139.

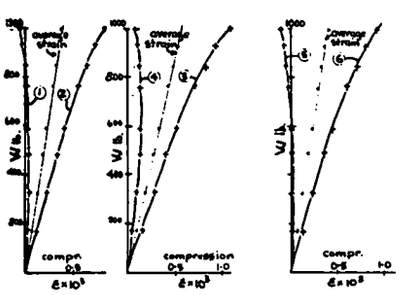

Fig. 140.

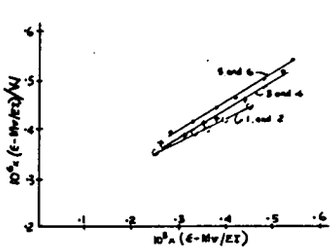

Fig. 141.

have been designed not only to give the failure load of trusses, but also to furnish information on their behaviour under load, with a view to obtaining as far as possible a fundamental understanding of the buckling effects. In particular, strains in critical members have been measured and Southwell Plots drawn. The work described in Art. 80 was in fact a preliminary investigation before carrying out research on the lateral buckling of the full size trusses.

A truss similar to that shown in Fig. 131 was 30 ft. long and 16" deep overall. The flanges were rolled from 8" x 14 gge. mild steel strip, and the web members were $\frac{7}{8}$" dia. steel tubing. The torsional rigidity of the truss was measured and found to be C = 1,800,000 lb. in.^{2} The lateral bending rigidity was found to be $B_1 = EI_{xx} = 19,500,000$ lb. in.^{2} The truss was loaded as in Fig. 133, the compression and tension flanges being laterally supported at points 13' - 3" apart. Midway between the supports, strains were measured on each side of the compression flange in order to pick up the lateral buckling effects. Strains are plotted against load in Fig. 134 and the corresponding Southwell Plots in Fig. 135. The slopes of the plots give W_{cr} = 1040 lb. or M_{cr} = 115,000 in. lb. for the critical bending moment. The truss was not under uniform bending moment (see Fig. 133) but the departure from uniformity is not great. If the bending moment were uniform and the truss had a continuous web, the theoretical critical moment is

$$M_{cr} = \pi\sqrt{B_1 C}/\ell = 117,000 \text{ in. lb.}$$

The value obtained from the Southwell Plot is in good agreement, showing that when buckling occurs between nodes about thirteen feet apart the critical load is controlled by the torsional and flexural stiffnesses in the same way as a beam with a continuous web.

The same truss was then set up and loaded as in Fig. 136 with lateral supports 6' - 4" apart. Strain and Southwell Plots are shown in Figs. 137 and 138. It should be noted that the strains denoted by 1 and 2 are almost entirely axial, following the line $\varepsilon = Mv/EI$, whereas the other sets show large buckling strains. This can be attributed to the initial crookedness pattern in the compression flange. It is not until a fairly late stage in the loading that the strains at the point 1, 2 are forced to reverse by the developing buckle in the remainder of the flange. The flange then begins to deform in a wave having nodes at the points of restraint. However, until this time the point 1, 2 is itself a node. The slope of the plot gives W_{cr} = 2,130 lb. or M_{cr} = 290,000 in. lb. The calculated value is

$$M_{cr} = \pi\sqrt{B_1 C}/\ell = 245,000 \text{ in. lb.}$$

The fact that the measured critical moment is higher than the calculated value can be attributed to the fact that the buckling mode is not the simple sine wave form assumed, but one possessing a higher critical load.

In order to check this, an initial crookedness pattern as shown in Fig. 139 was artificially introduced into the compression flange. The resulting strain readings and Southwell Plots are given in Figs. 140 and 141. From Fig. 141 we have W_{cr} = 1,800 lb. and hence M_{cr} = 250,000 in. lb.

The accuracy of calculation here is not good, but this value is in good agreement with the calculated value of 245,000 in. lb. given above. It is clear, however, that the artificial crookedness pattern imposed on the truss has induced early buckling in the fundamental mode and lowered the critical load.

The same truss was then given the artificial crookedness pattern shown in Fig. 142, set up, and loaded, with lateral supports only 3' - 6" apart. Strain and Southwell Plots are shown in Figs. 143 and 144. From Fig. 144 we have $W_{cr} = 2,500$ and hence $M_{cr} = 330.000$ in. lb. The theoretical elastic buckling load for a member with a continuous web is

$$M_{cr} = \pi\sqrt{B_1 C}/\ell = 442,000 \text{ in. lb.}$$

The value obtained from the Southwell Plot is a good deal lower than this. Several reasons may be advanced. Firstly, measurements were not taken to very high strains, the maximum load reached being not a very high proportion of W_{cr}. Hence the Southwell Plot does not furnish an accurate estimate of W_{cr}. Secondly, some yield occurred, and this lowers W_{cr}. Thirdly, it is likely that the theory of a beam with a continuous web is breaking down at such close spacings of the lateral supports, particularly in view of the inherent local instability of the open type of flange section.

The foregoing experiments were devoted to the elastic buckling of the lightweight truss, with a view to determining the load carrying capacity of the truss for various spacings of lateral restraints. It has been established that the theory of lateral buckling of a beam with a continuous web is adequate down to quite low support spacings, and the Southwell Plots on strains which participate in the buckling mode have also been shown to be linear. If the occurrence of yielding at these locations is accepted as a sufficient definition of failure, then the method of substituting the yield strain in the equation of the Southwell Plot on strains enables the failure load to be calculated. This has been given in Art. 80. In fact the reserve of strength of these trusses in the plastic range is quite low. The susceptibility of the flange section to local buckling causes quick failure once yielding of any magnitude occurs. Of course, many tests are required before the empirical information necessary for engineering design can be furnished.

The use of the equation of the Southwell Plot as a design formula is also limited to cases where considerable elastic buckling effects occur before failure. By reference to equation (110) it can be seen that if $(\epsilon - Mv/EI)$ is small up to the stage when ϵ reaches the yield strain, then the Southwell Plot is not well defined. For structures which have very small initial crookedness or imperfections, this may well be the case. This behaviour will be illustrated by tests on a 28 ft. span lightweight truss.

The truss was loaded as shown in Fig. 132, the compression flange being laterally restrained at each panel point. The compression flange was initially straight and remained straight during loading until the strains approached the yield strain. On further loading, slight deflections were immediately followed by local buckling of the compression flange, and failure. Sets of strain readings, taken on the tension flange and on the bottom and sides of the compression flange are shown in Fig. 145. It can be seen that the strains closely

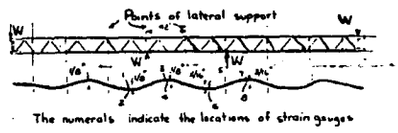

Fig. 142.

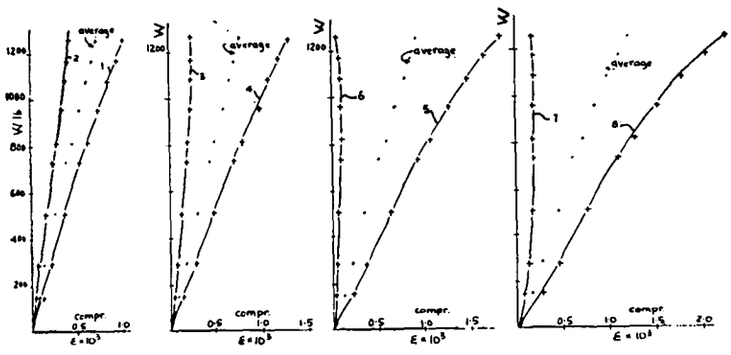

Fig. 143.

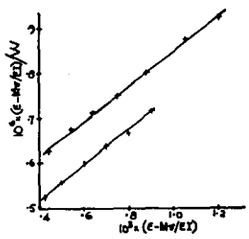

Fig. 144.

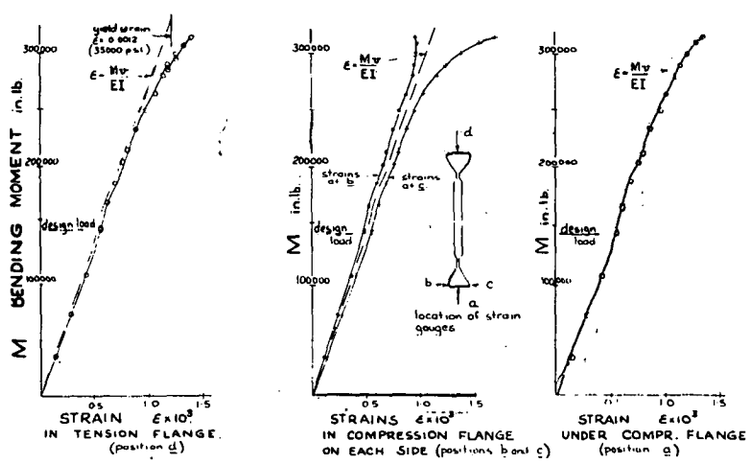

Fig. 145.

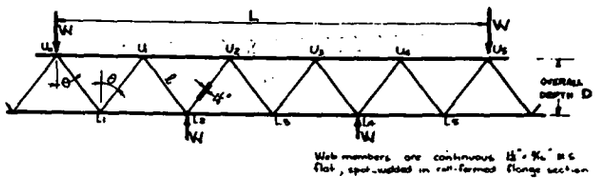

Fig. 146.

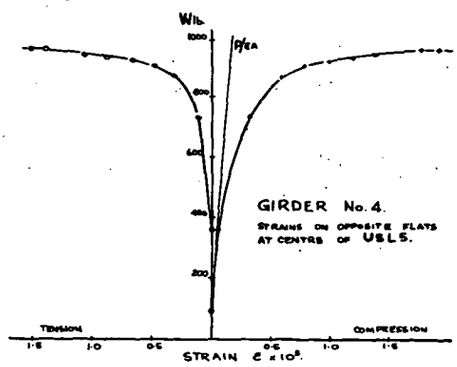

Fig. 147.

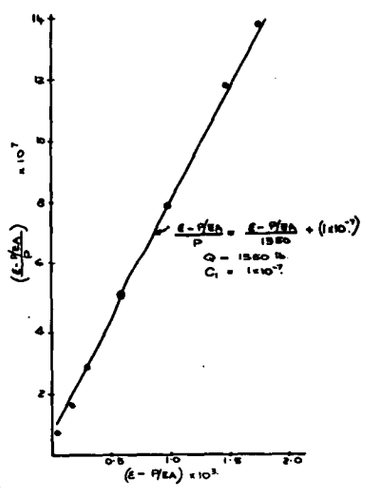

Fig. 148.

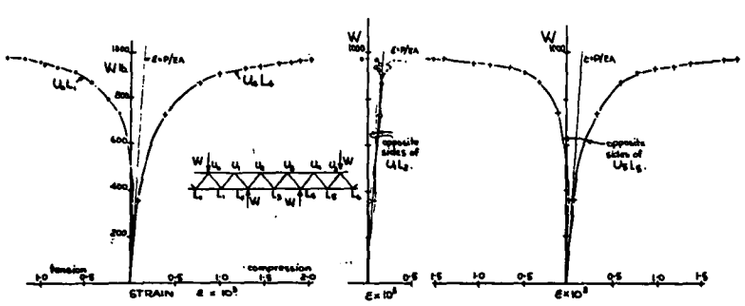

Fig. 149.

PLATE 9

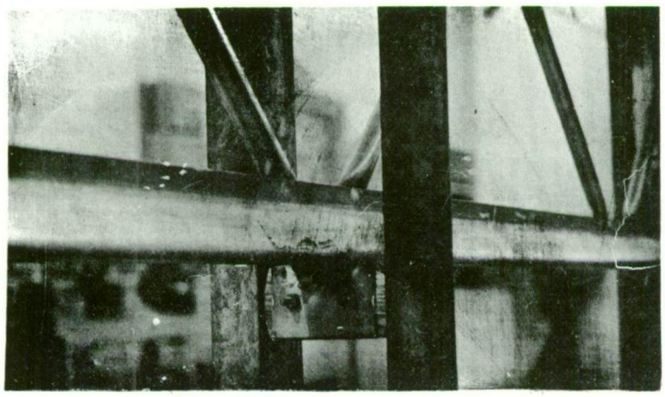

Simulated purlin used to restrain compression chord in some tests.

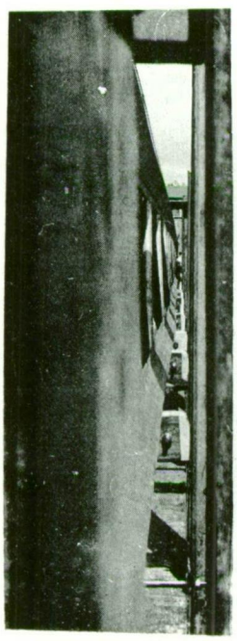

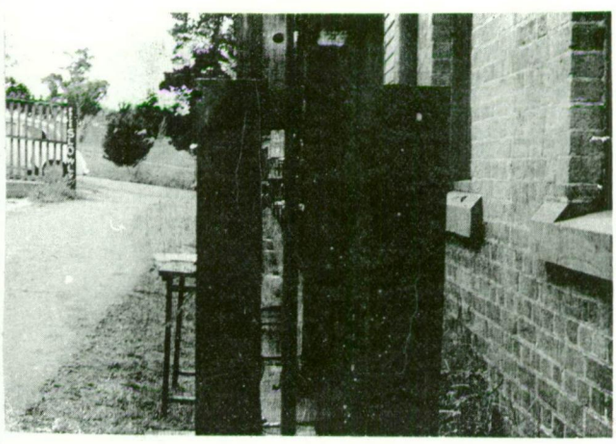

Developing plastic buckling of compression chord of truss. Note the waving of the lower chord between each restraining purlin.

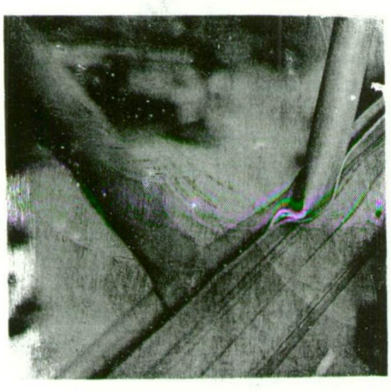

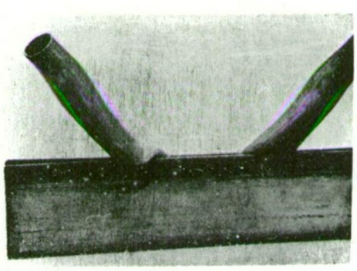

Local buckling of flattened ends of tubular web members.

follow the line $\varepsilon = Mv/EI$ until failure is approached. Up until ε approaches the yield strain, buckling effects as given by $(\varepsilon - Mv/EI)$ remain quite small. The difference in behaviour between Fig. 145 and Fig. 143 is of course due to the difference in the initial crookedness pattern of the compression flange. In Fig. 143 an artificial unfavourable crookedness pattern was impressed on the flange.

It appears then that the use of the Southwell Plot on strains is essentially a technique for tackling elastic buckling problems. Buckling effects in the elastic range must be considerable before the application of the method is useful. This will also be illustrated by the study of the buckling of the web members of the lightweight trusses.

82. <u>The Buckling of the Web Members of the Lightweight Trusses</u>:

In the early stages of development of the lightweight trusses, the web members were continuous 1¼ in. x 3/16 in. mild steel flat bent about the major axis and spot-welded to the patented roll-formed steel section flanges. Five trusses of this type were tested. The trusses were loaded as in Fig. 146 so that failure occurred by buckling of the web compression members, rather than by yielding or buckling of the flanges, or weld failure. Since the minor axes of the web members lay in the plane of the truss, they buckled out of that plane. During the progress of the test, strains were measured using Huggenberger mechanical strain gauges on opposite flats at the centres of the web members. Typical plots of strain ε against load P are shown in Fig. 147. The steel used in the web members had a yield point of 45,000 lb./sq. in., corresponding to a strain of 1.5×10^{-3}. It is seen from the graphs that the reserve of strength beyond the yield is only about 6%.

In Fig. 147 the strain P/EA (where $P = W/\cos\theta$, and A is the area of the member) is also plotted. The measured strains on opposite sides of the member are symmetrical about this line. Similar results were obtained from many strain plots. In Fig. 148 values of $(\varepsilon - P/EA)/P$, the strain due to buckling effects divided by the load in the member, are plotted against $(\varepsilon - P/EA)$. In every case where failure occurred by buckling, (and this was always in single curvature, the fundamental mode), this plot gave a straight line. Fig. 148 is typical of many such plots. The equations of these straight lines are of the form

$$\frac{\varepsilon - P/EA}{P} = \frac{\varepsilon - P/EA}{Q_{cr}} + C_1 \qquad .. \quad (112)$$

where Q_{cr} is the reciprocal of the slope of the plot, and C_1 the intercept. Q_{cr} can be regarded as the critical load corresponding to the Euler load of some reduced length, and C_1 as a crookedness-eccentricity parameter.

Values of Q_{cr} and C_1 are given in the following table.

Girder No.	Test No.	Euler load of struts (Calculated on full length) Q lb.	Experimental values		Effective Length / Total Length = Q/Q_{cr}.
			Q_{cr} lb.	$C_1 \times 10^7$ $lb.^{-1}$	
1	1	925	2300	1.0	0.63
	2		3000	1.85	0.55
	3		3200	2.5	0.54
			3000	1.0	0.55
			3000	0.5	0.55
	4		3600	0.6	0.60
			2900	1.0	0.57
2	1	1360	4100	0.8	0.55
			3800	0.15	0.60
	2		4300	0.7	0.57
			4300	0.5	0.57
			3600	0.15	0.61
3	1	1420	4000	1.7	0.60
			4000	1.1	0.60
4	1	510	1350	1.0	0.62
			1350	1.0	0.62
5	1	670	1820	1.3	0.61
			1820	1.9	0.61

Equation (112) represents the behaviour of these struts in an actual structure. Minimum values of Q_{cr} and maximum values of C_1 obtained in such a way, represent (when properly substantiated by a sufficient number of tests) valuable empirical information for the design of similar compression members. To define failure, it is safe to put ε equal to the yield strain. There is, of course, some reserve of strength beyond the yield, and for shorter struts it may pay to find a better failure criterion.

Thus for design purposes, we put Q_{cr} equal to its minimum likely value, C_1 equal to its maximum likely value, and ε equal to f_y/E where f_y is the yield stress. Equation (112) can then be solved for the failure load P. Use of a suitable load factor gives the working load.

In fact, this method of design is very similar to the Perry Robertson formula (see equation 57, Article 64), except that the relevant empirical factors have been obtained from tests on actual structures and not merely assumed with little rational justification. Putting $E\varepsilon$ equal to f_y, equation (112) reduces to

$$\frac{f_y - P/A}{P/A} = \frac{f_y - P/A}{Q_{cr}/A} + EAC_1 \quad .. \quad (113)$$

where P is the applied load to cause failure, Q_{cr} is the critical load obtained from the Southwell Plot on strains, E is Young's modulus, A is the area of the member, f_y is the yield stress, and C_1 is an imperfections parameter obtained from the Southwell Plot. The Perry Robertson formula is obtained by solving

$$f_y = P/A \left[1 + \eta\, Q_1/(Q_1 - P) \right]$$

where f_y is the yield stress, $\eta = 0.003\, \ell/r$, a crookedness function, and Q_1 is the Euler load of an assumed effective length. This formula reduces to

$$\frac{f_y - P/A}{P/A} = \frac{f_y - P/A}{Q_1/A} + \eta$$

which has exactly the same form as equation (113) obtained from the Southwell Plot. In applying the code formula to continuous or restrained columns, Q_1 is the Euler load of an arbitarily assumed effective length, and η is a crookedness parameter for pin-ended columns. In applying the results of the Southwell Plot, both C_1 and Q_{cr} are obtained from actual tests on similar columns. For any particular member, equation (113) can be solved in exactly the same way as the code formula. A sufficient number of tests would give C_1 as a function of ℓ/r, for example. It is therefore possible by means of the Southwell Plot on strains to assess the effects of initial crookedness eccentricity of loading and restraint at the ends of columns built into structures, and thus obtain design formulae which are related to the performance of struts in actual structures. It is unnecessary to rely on vague and tenuous extensions to pin-ended column theory.

Not every strut in every truss tested buckled in single curvature. The mode of deformation of any structure is a complex function of the whole initial crookedness and loading pattern. Fig. 149 shows typical sets of strain readings for one truss. Some members deformed in single curvature right from the start. In other members the initial deformation was forced to reverse by strongly developing deformations in adjacent members. However, in all trusses tested there were always some members which buckled largely in single curvature giving linear Southwell Plots on strains measured at their centres. The plots for these members can be used to define failure of the whole frame.

83. The Southwell Plot on Strains applied to the Buckling of Structures.

Methods exist for determining critical loadings for the mathematically perfect structure for simple buckling modes. The critical loading is analogous to the calculated Euler load of an initially perfect pin-ended strut. However, all structures have imperfections, such as crooked members or eccentric joints, and some method of relating the behaviour of the practical structure to the critical loading for the perfect structure is required. What is needed is something analogous to the Perry formula, which, by the use of a crookedness-eccentricity factor, takes care of the practical imperfections of the pin-ended Euler strut.

In his 1932 article when advancing the linear deflection plot, Southwell emphasized the generality of his method, though he did not specifically mention strains. Experimenters have used the generality in the direction of more difficult structures, but have not generally used other measures of the distorted configuration than deflections to define the buckling mode. Rayleigh has stated that the assumption that any distorted configuration in any eigenvalue problem can be expresses as a synthesis of normal modes "exaggerated" by the loading is defensible from a physical standpoint for any elastic system, though it may require much elaborate analysis to justify it from the standpoint of a mathematician.

It has previously been shown mathematically in this thesis that, with certain restrictions, if $\mathcal{E}$ is the strain measured at the centre of a pin-ended column under load P, then the graph of $\mathcal{E}/P$ against $\mathcal{E}$ is a straight line of slope $1/Q$, where Q is the Euler load. Good experimental agreement was obtained.

Experimental work carried out on more difficult problems such as triangular frames, web members of lattice girders, bolted angle members in frames, and the compression chord of a lattice girder as it buckles laterally has also resulted in linear Southwell Plots on strains. The mathematical analysis of a triangular frame having a simple crookedness pattern has been carried out and it has been shown that strain at the centres of the compression members (and also other distorted configurations such as the rotation of the corners) all give linear plots. The method therefore appears to be fundamentally sound.

The value of the linear plot on strains is that it gives an equation of the form

$$(\mathcal{E} - \mathcal{E}_1)/A = (\mathcal{E} - \mathcal{E}_1)/A_{cr} + C_1 \quad .. \quad (114)$$

where $\mathcal{E}$ = the total measured strain
$\mathcal{E}_1$ = the calculated strain if no buckling occurs
A = some action, whether force or bending moment.
A_{cr} = the reciprocal of the slope of the plot, and equals the critical action causing elastic buckling for the mode which governs the strain measurements taken. This is determined by the location of the strain gauge. In many cases it is obvious where to locate the gauge to measure the gravest mode. Otherwise the gravest mode must be found by trial and error.

C_1 = the intercept of the plot on the strain/load axis.

Equations (110) and (112) are particular examples of equation (114). Equation (114) reduces to

$$\mathcal{E} = \mathcal{E}_1 + AC_1/(1 - A/A_{cr})$$

Now $\mathcal{E}_1$ is usually of the form $\mathcal{E}_1 = kA$ (e.g. $\mathcal{E}_1 = P/EA$ for a strut whose axial load P is known, or $\mathcal{E}_1 = Mv/EI$ for the compressive strain in a structure subject to a bending moment M.)

This gives $\mathcal{E} = kA + AC_1/(1 - A/A_{cr})$

$$= \mathcal{E}_1 \left[1 + \phi/(1 - A/A_{cr})\right] \quad .. \quad (115)$$

where $\phi = C_1/k$.

A_{cr} is the reciprocal of the slope of the Southwell Plot on strains and C_1 its intercept. Given sufficient experimental work to obtain A_{cr} and C_1 for many types of structures, equation (115) can be used as a design formula by putting ε equal to the yield strain. The solution of equation (115) is familiar to engineers, being similar to the Perry formula.

84. Limitations of the Strain Plot.

The use of the plot is limited to elastic theory. By defining failure of a strut as the attainment of the yield stress in some part, reserve of strength in the plastic range is neglected. For short struts, this may be important. In this event, the result of the plot is still useful in determining when first yield occurs.

A great deal of experimental work is required to determine, systematize, and tabulate the variation of ϕ and A_{cr} for many types of structures. A_{cr} can be calculated in some cases, but usually it will be necessary to determine both ϕ and A_{cr} from measurements on actual structures.

The gravest buckling mode must also be determined in order that strain gauges are suitably located and this may not always be obvious, especially in cases of combined torsional flexural buckling. In general it may be stated that the measured strains must participate in the buckling mode that governs and immediately precedes failure. It has been shown that at low loads a structure may deform in one mode but at higher loads a change to a different mode may take place. For no portion of the structure is the Southwell Plot then inherently linear. However, when this behaviour occurs, the author has found that if strains are measured at the correct locations on members which govern the final deformation pattern, then approximately linear plots are obtained.

If the buckling effects ($\varepsilon - \varepsilon_1$) of Equation (114) are small compared with the non-buckling effects ε_1 up until yield occurs, then the equation of the plot is inaccurate. However, if this occurs, a method of design is usually available by putting the linear part of the strain, namely ε_1, equal to some limiting strain equal to or slightly less than the yield strain. In such a case, the measurement of strains at suitable locations gives the required information on the magnitude of buckling effects.

Particular care in the application of the method is required where local buckling is liable to occur.

BIBLIOGRAPHY AND NOTES FOR CHAPTER THREE

The numerals refer to the Articles in the Text.

64, 65. The discussion is partly drawn from Bleich "Buckling Strength of Metal Structures", pp.1, 3, 196, 222, 224 and 225, but has been considerably modified. See also Biezeno and Grammel "Engineering Dynamics" Vol. II, p. 369, where various load deformation diagrams involving instability are discussed.

67. See Bleich "Buckling Strength of Metal Structures", p.225.

69. See W. Merchant "The Failure Load of Rigidly Jointed Frameworks as Influenced by Stability". The Struct. Engnr. Vol. 32, No. 7, July 1954, p. 185. The suggestion for applying these ideas to all problems of instability however, seems to have originated with Lord Rayleigh. (The author has a quotation in a letter from Sir Richard Southwell but has been unable to locate the reference).

See also:

N.W. Murray "The determination of the collapse loads of rigidly jointed frameworks with members in which the axial forces are large", Proc. I.C.E. London, Vol. 5, April 1956, No. 1, p. 213; also, the discussion on this paper, Proc. I.C.E., December, 1956, p.876,

N. W. Murray "A method of determining an approximate value of the critical loads at which lateral buckling occurs in rigidly jointed trusses", Proc. I.C.E. London, Vol. 7, p. 387, June 1957.

N. W. Murray "Further tests on braced frameworks", Proc. I.C.E. London, Vol. 10, p. 503, August, 1958.

W. G. Godden "The lateral buckling of tied arches," Proc. I.C.E. London, Vol. 10, p.503, August, 1958.

Chin Fung Kee "The design of the unbraced Stabbogen Arch", Struct. Engnr. September 1959, Vol. 37, No. 9, p. 265.

J.G. Nutt "The Collapse of triangulated trusses by buckling within the plane of the truss", The Struct. Engnr., May 1959.

L. K. Stevens, "Ultimate load capacity of steel trusses", A.N.Z.A.A.S. Adelaide Congress, August 1958.

--------000--------

BOLTED ANGLE STRUTS

(With particular reference to the design of transmission towers)

85. Part of this thesis is concerned with the buckling of structures containing bolted angle-section members, and the strength of bolted angle struts. Such members are used in many structures due to their ease of erection with comparatively unskilled labour: an important example is the electricity transmission tower which is often designed entirely of angle-section members, with heavy main legs and lighter cross-bracing. Connections are made by drilling-holes on the centre line of the leg of the angle, and single or double bolting. At present, the design of bolted angle members is very empirical and presumably over-conservative. This is the case partly because so many highly variable factors, such as the variability of the end connection, are involved.

86. The usual mode of failure of a bolted angle strut in a structure is for the central part to buckle about its minor axis of inertia. If each end of the members is held by one leg, the strut twists near its ends. This twisting may be accommodated by the opening out of the angle, yield or large movement in the connection, local buckling of the outstanding leg of the angle near the connection, or merely twisting of the member. There may also be local buckling of the member near its centre. Mild steel struts of slenderness ratio (the ratio of length to the smallest radius of gyration, ℓ/r) less than 180 have passed well into the plastic region at failure. For ℓ/r between 180 and 250, failure may be elasto-plastic or entirely elastic.

In must non-redundant structures, if the loads are known, axial forces can be determined with sufficient accuracy by considering the members pin-ended. There is never enough distortion of the geometry of the structure for the actual forces to depart far from the pin-ended values, even if the members are rigidly connected. The load-carrying capacity of the strut is, however, entirely dependent on the restraint at its ends.

87. Existing Design Methods for Bolted Angle Struts.

The British Standard for the Use of Structural Steel in Building, B.S. 449:1948, lists permissible working stresses for discontinuous angle struts with double-bolted, welded, or single-bolted connections. In this code, the design of all columns is based on the Perry formula as recommended by Robertson in the First Report of the Steel Structures Research Committee, 1931. The derivation of this formula is discussed in Arts. 64 and 82. Difficulty arises in the application of the Perry formula to the design of columns in structures. Practical columns are not pin-ended but continuous, or restrained at their ends by other members. In "The First Report of the Steel Structures Research Committee", 1931, Robertson says: "The central problem in strut work can be stated as the determination of the strength of a free-ended eccentrically loaded bent strut. The strength of any strut in a given structure then depends on the length of a free-ended strut equivalent to it, and it is also assumed that the determination of this free length is a problem of stress analysis." He considers that the solution of cases of continuity,

restraint, or fixity of the ends merely lies in estimating the probable free length. Criticising this approach, J. F. Baker (The Steel Skeleton Vol. 1., p. 15) says: "In putting forward this formula it was assumed that the main problem had been solved. The strength of a strut in any given structure then depended only on the length of a free-ended strut equivalent to it, the determination of the free length then being merely a problem of stress analysis. No guidance to the solution of this very difficult problem was offered to the designer."

However, most civil engineering codes list values of the ratio of effective length to actual length to be used in design, for varying conditions of end restraint and also values of eccentricities to be used. But the provisions are vague, not supported by measurement, and a great deal is left to the discretion of the designer, though the work of J. F. Baker and others has given partial solutions for the case of structural steel building frames. In this chapter it will be shown that the necessary information for insertion in a Perry type formula for the strength of bolted angle struts can be obtained from the Southwell Plot on strains. It is not necessary to rely on vague extensions of pin-ended column theory. However, the designer of bolted angle struts must distinguish between the failure of the structure as a whole when the joints are rigid, and the separate failure of a strut if the end connection is loose enough for the member to be almost pin-ended. It must also be remembered that some modes of failure such as local buckling may produce more disastrous effects than others, and it is necessary to apply variable factors of safety.

88. Loading tests carried out by Mackey on lattice girders at the University of Leeds (British Constructional Steelwork Association, Publication No. 7, "Report on Experimental Investigation into the Behaviour of Angle Purlins, Ties and Struts" (1953) p. 19) have shown that the B.S. 449 code gives a safe design method in all cases tested, but is over-conservative. Complete girders were tested because the buckling of a compression member is dependent on its end conditions and the restraint afforded by adjacent members, and strain measurements were taken on the truss members during loading. In the tests, actual load factors of 2.4, 2.7 and 3.0 were obtained for the critical compression members, ie. those which failed first. The load factors for other members were, of course, even higher, and it was suggested that the effective length of angle struts can be taken as considerably less than the value of 0.8 times the actual length, as laid down by the code. Incorporating the eccentricity of loading assumed in B.S.449 (i.e. adding the assumed eccentricity to the crookedness term) in the Perry formula, some agreement was established with experimental measurements. In fact, a similar procedure was advocated for design purposes by Robertson in the First Report of the Steel Structures Research Committee, p. 228, in which he puts forward the Perry formula for centrally loaded columns, but for columns having a definite eccentricity, he proposes that the relevant term be added.

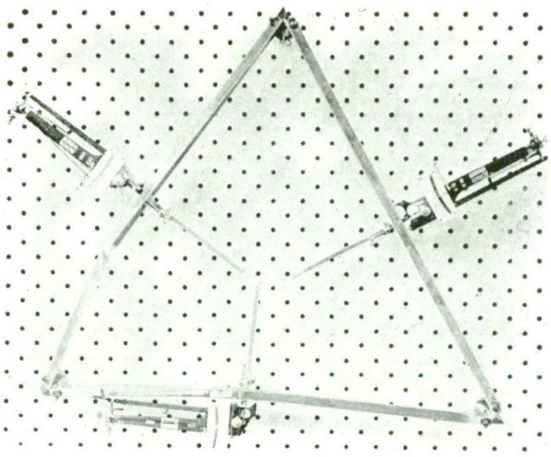

Measurement of strains in a triangular frame made of bolted angle-section members, buckling in its plane.

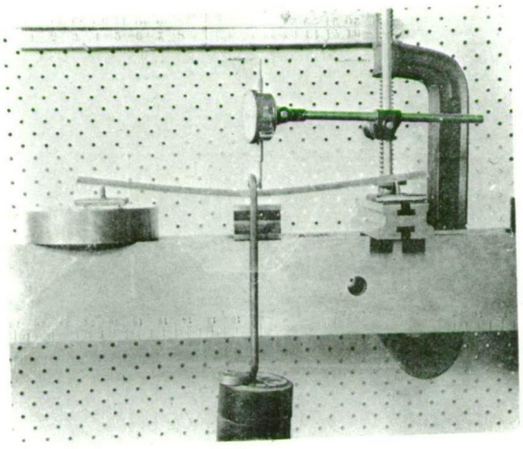

Angle section member being loaded as a simple beam.

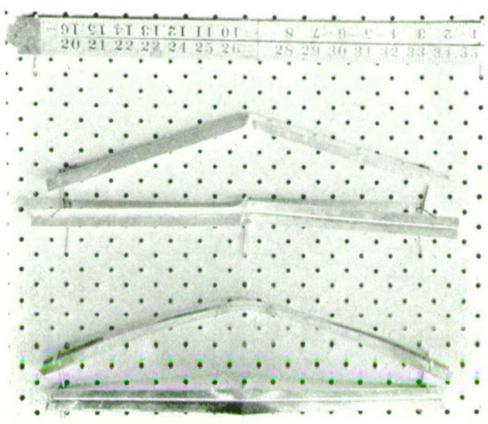

Failure of angle-section member loaded as a simple beam. For these members, b/t = 15. Top member was loaded with outstanding legs in compression, and local buckling occurred. Bottom member was loaded with corner of angle in compression.

89. The third method of design is almost purely empirical, using tables of allowable stresses against the ℓ/r ratio, with little or no theoretical justification (e.g. the Johnston parabola formula, with coefficients adjusted to fit tests on single columns, and some assumed ratio between effective and actual length). This procedure is justifiable providing it is safe, and not too conservative.

In the case of an electricity transmission tower, we have a structure which can be tested full-scale under simulated service conditions, and, because of the number of structures involved, this is often done. It is a pity that, apparently because of the large number of members involved, strains or even deflections are very seldom measured. Tests are usually designed to establish the safety of the structure under perhaps 10% overload for a number of loading arrangements, and to determine its overall load factor for one loading arrangement, but apart from giving such qualitative information as the number and position of the members which fail, tests as conducted provide little information which can be used in future design.

90. Because a full-size test can be carried out, the transmission tower is probably one of the most economical structures designed. Most designers work on permissible axial stresses much higher than the standard civil-engineering codes allow. However, it is felt that there is still room for valuable economy. It is a step in the dark to proceed further along an already dim path even by judicious pruning of the empirical factors involved. The possibility of economy certainly exists; to achieve it safely a better fundamental understanding of the structure is required, and this can be obtained only by detailed measurements on actual structures, conclusions being supported analytically, where possible. Research by tests on models and actual structures, and concerning both the elastic and plastic regions, should be fruitful.

91. Preliminary experimental work on angle-section members:

Prior to testing model trusses containing bolted angle members, single members have been subjected to simple loading systems with a view to obtaining an understanding of their elastic and plastic properties. An angle-section member is an example of a thin-walled open section member, and as such, is liable to various instability effects such as torsional buckling or local buckling. Single members have been subjected to bending, twisting, or axial thrust. Some of the work has been reported in Chapter Two, Articles 58-62, and the remainder is given here.

92. The behaviour of angle-section members in simple bending:

Angle section members measuring 0.590 in. x 0.590 in. x 0.036 in. were bent from 20 gauge sheet aluminium. The stress-strain curve for the material is shown in Fig. 150. When loaded as simple beams, deflection measurements gave values for the flexural rigidity EI very close to those calculated from the value of Young's modulus and the section dimensions. The members were bent about their minor axes in both senses, and in the elastic range there appeared to be no opening out of the

angle and consequent reduction in stiffness. Fig. 151 shows typical results. Similar experiments were carried out with 1 in. x 1 in. x $\frac{1}{8}$ in. mild steel angle section members. The stress strain curve is shown in Fig. 152, and typical deflection measurements in Fig. 153.

However, when the experiments were carried into the plastic range, considerable difference in behaviour was observed when the corner of the angle was in compression from when the outstanding legs were in compression. See Fig. 154. These tests were carried out for varying values of b/t where b = width of leg and t = thickness. Up to the value b/t = 16, the maximum moment carried was independent of the sense of the bending. Above b/t = 16, local buckling of the outstanding legs, if these were in compression, considerably reduced the bending strength. Where the corner of the angle was in compression and local buckling did not occur till large deflections were reached, the observed maximum moment was in good agreement with the calculated fully plastic moment using a uniform stress of 14,500 lb./sq. in (See Fig. 150). Increase in the length of the member subjected to the maximum moment also resulted in a reduction in strength where local buckling occurred.

Figs. 155 and 156 show load deflection curves for 0.59 in. x 0.59 in. x 0.036 in. aluminium angle-section members bent in opposite senses. The sudden drop in load and the lack of power to absorb energy when buckling occurs is apparent.

It appears from the above that the usually accepted figure of b/t <16 (B.S.449:1948) is sufficient to minimize local buckling effects, and to ensure that local buckling does not precede yielding under conditions of simple bending.

93. <u>The behaviour of angle-section members under pure torque</u>:

Bolted angle struts are observed to twist markedly at failure and some understanding of the behaviour of a member in torsion is required. During a preliminary investigation a peculiar bending under the action of a pure torque was observed. This effect, while similar in origin to the non-linear shortening effect examined by Weber, has apparently not been previously noticed. (For discussions of the shortening effect of pure torsion see S. Timoshenko "Strength of Materials" p.87; Cullimore, M.S.G. (1949) Research, Engineering Structures Supplement, p.153; Cullimore, M.S.G. & Pugsley A.G. (1952) A.D.A. Research Report No. 9; and Weber, C. (1921) Forschungsarbeiten No. 249.) Other possible sources of the bending might be the yielding of a small portion near the root of the angle, or the effect of buckling under pure torque. These are later discussed but rejected. A satisfactory explanation can be found by considering elastic effects only. The theory of non-linear shortening due to the simplest stress system which will satisfy statics is developed in this article, and it is shown that all structural sections with a certain lack of symmetry are subject to this behaviour. The magnitude of the bending under pure torsion is calculated for an angle section. Some experimental measurements subsequently carried out on a brass member to determine the validity of the analysis are reported, and good agreement is obtained.

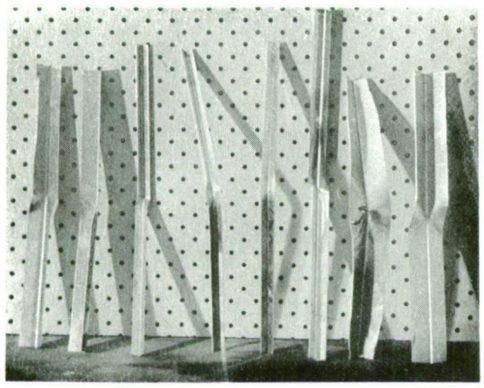

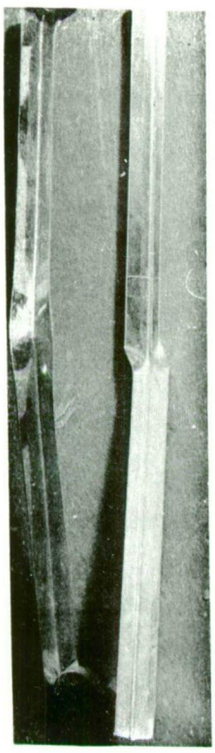

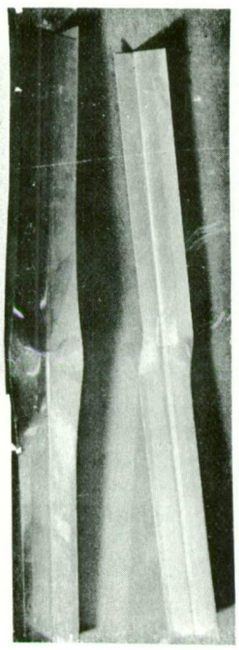

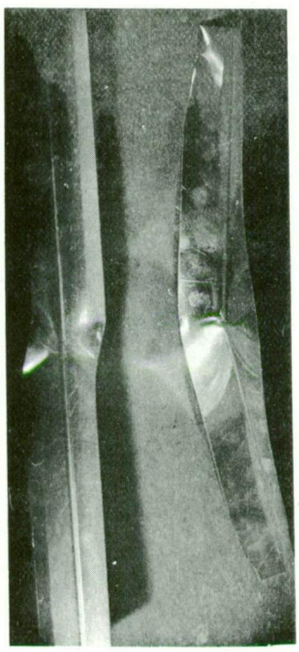

Note the developing local buckle at the corner of the angle for large b/t.

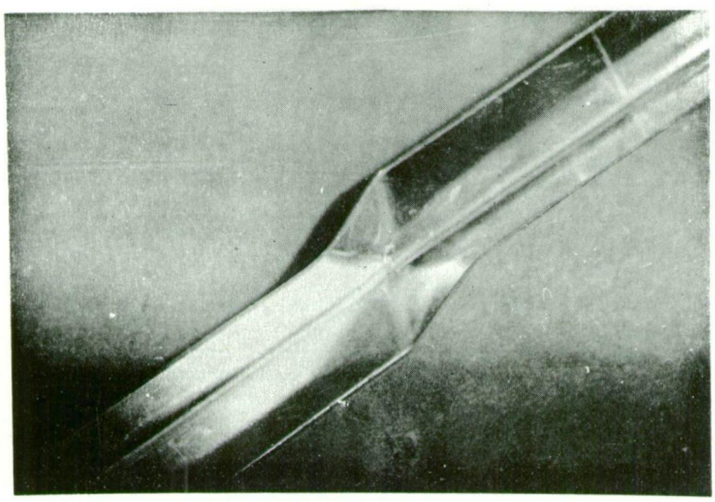

Failure of pairs of angle-section members with varying b/t loaded as beams. The direction of bending was opposite for each member of each pair.

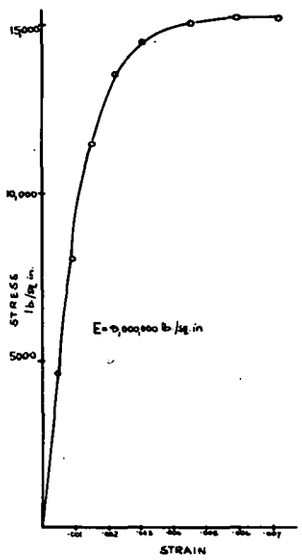

Fig. 150.

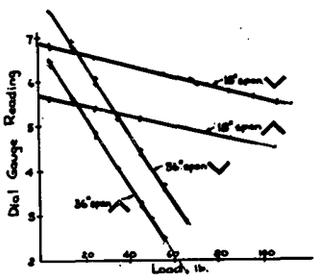

Fig. 151

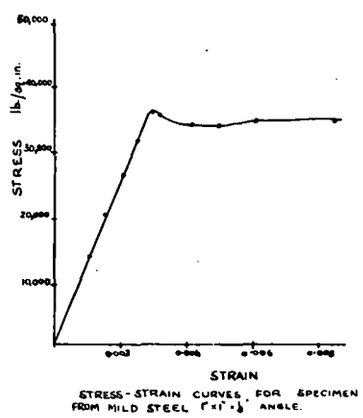

Fig. 152.

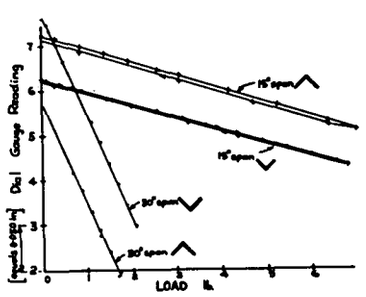

Fig. 153.

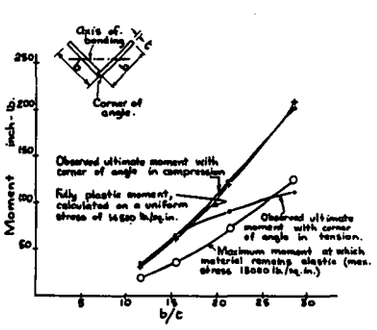

Fig. 154.

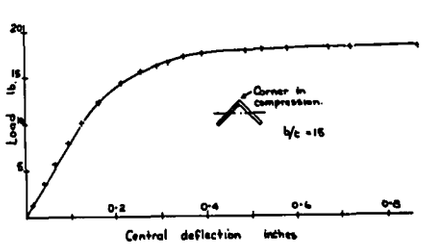

Fig. 155.

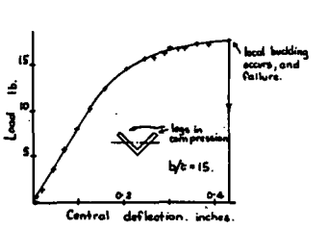

Fig. 156.

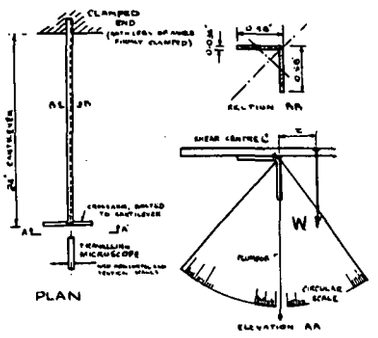

Fig. 157.

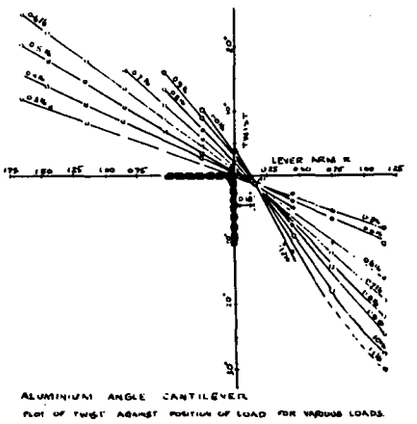

Fig. 158.

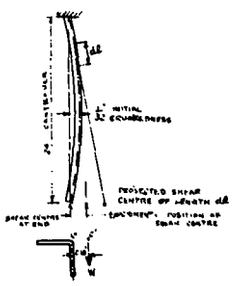

Fig. 159.

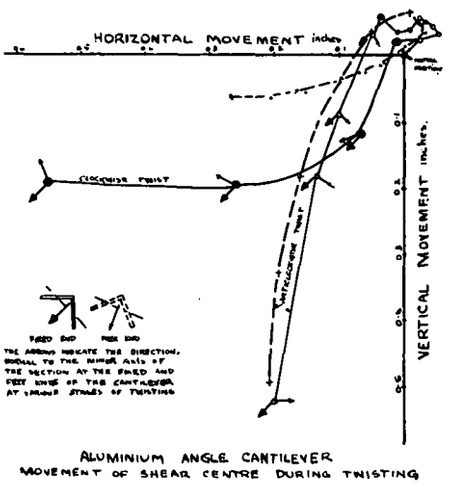

Fig. 160.

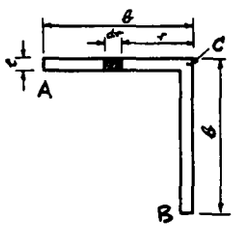

Fig. 161.

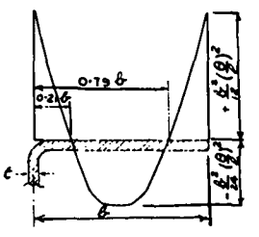

Fig. 162.

The analysis and its experimental verification indicate that Weber's theory can be extended satisfactorily to thin-walled members, provided that the extension is properly done and the bending of certain unsymmetrical sections is taken into account.

The secondary effect of this phenomenon on the buckling of angle struts is discussed later.

Notation:

ℓ, L	length of bar
θ	angle of twist
ω	angle of twist per unit length (specific twist)
f	longitudinal stress
ϵ	longitudinal strain
E	modulus of elasticity
τ	torque
a	radius of a circular bar
b	leg width of an angle-section member
t	thickness of an angle-section member.

Preliminary Experimental Work

A cantilever of angle section was twisted and bent by loading it at its free end as in Fig. 157 and the shear centre determined experimentally.. (Fig. 158). The small discrepancy between the observed position of the shear centre C' and the theoretical position C was attributed to the slight initial crookedness of the member. (See Fig. 159).

A pure torque was then applied at the free end of the cantilever, and horizontal and vertical deflections and twist observed. By Maxwell's reciprocal theorem, if the behaviour of the member is linear, the centre of twist is expected to coincide with the shear centre C at the end of the cantilever. The point C was, however, observed to move, and its deflection is plotted in Fig. 160.

Measurements were taken on two members. The direction of the deflection was different for twists of opposite hand. In order to show this graphically, the directions perpendicular to the minor axes of inertia of the angle at the fixed and free ends of the cantilever have been plotted in Fig. 160 at various stages of twisting. The translational movement at every stage of the twisting, whether the twisting is clockwise or anti-clockwise, lies on a path whose direction is somewhere between the normals to the minor axes of the section at its fixed and free ends. The section seems to be bending about its minor axis. These deflections are largely recovered on removing the torque, so the effect is elastic.

The Shortening Effect of a Member under Pure Torque

Weber has shown that when a bar of solid circular or rectangular section is subjected to pure torque, the longitudinal strain system which arises causes the bar to shorten. The argument has been recapitulated by Cullimore. When a prismatic bar is twisted by couples, the usual assumption is that the generators remain straight, and although the cross-sections are distorted by warping, they remain parallel in the sense that corresponding elements remain the same distance apart. Strictly, however, the generators become helices. If the axis of the centre of twist of the bar remains the same length, the lengths of all the generators of the bar become greater. A tensile stress suitably varying over the cross-section must be applied, and the whole bar is in tension. Alternatively, if there is no external tension the bar must shorten. The argument may be summarized as follows: the stress distribution due to the assumed strain distribution must satisfy the boundary conditions of the problem as given by the equations of statics; under pure torque of a symmetrical section, the central axis must shorten. Under pure torque, warping is the same for all cross-sections, and the shortening effect is superimposed on the warping.

In this article, it will be shown that the "shortening" is uniform over the cross-section of the bar only if the section is symmetrical or anti-symmetrical about the shear centre, and that pure torsion of other sections is accompanied by bending. Before proceeding to the analysis of the torsion of unsymmetrical sections, the shortening effect when a solid circular bar is twisted will first be discussed.

Longitudinal Strains in a Solid Circular Elastic Bar under Pure Torque

Consider a bar of length ℓ and diameter 2a, twisted by pure couples through an angle θ. Tension is considered positive. At radius r, the new length of an axial fibre (which was originally straight but becomes helical as the bar is twisted is

$$\sqrt{\ell^2 + r^2\theta^2}$$

assuming the central axis of the bar remains straight and at length ℓ. The elongation of the fibre is therefore

$\sqrt{\ell^2 + r^2\theta^2} - \ell$ or approximately $r^2\theta^2/2\ell$. The resulting tensile strain is $\varepsilon = r^2\theta^2/2\ell^2$ and the tensile stress is $f = E\varepsilon = Er^2\theta^2/2\ell^2$ which is positive for all r.

This stress system does not satisfy statics as no normal force is applied. The simplest condition which satisfies statics is an additional uniform tensile strain ε_1.

Hence $\varepsilon = r^2\theta^2/2\ell^2 + \varepsilon_1$

and $f = E\, r^2\theta^2/2\ell^2 + E\varepsilon_1$

For no normal force $\int f\, dA = 0$ where dA is an element of the area of the bar.

Therefore $\int_0^a 2\pi r \, dr \, E (r^2\theta^2/2\ell^2 + \varepsilon_1) = 0.$

This gives $\varepsilon_1 = -a^2\theta^2/4\ell^2.$

Putting $r = a$, the longitudinal strain at the circumference is $\varepsilon = a^2\theta^2/2\ell^2 + \varepsilon_1 = a^2(\theta/\ell)^2/4$

At $r = 0$, the strain is $-a^2(\theta/\ell)^2/4$. That is, the central axis of the bar shortens.

There is, of course, no warping of the cross-sections of a circular bar under pure torsion. In the case of symmetrical sections where warping does occur, a strain distribution similar to that discussed above is superimposed on the warping.

The stress system f, above, does not act in the direction of the axis of the bar, but in the direction of the longitudinal fibres, which lie on a helical path inclined to the axis of the bar at a small angle. The torque component of this system can be calculated, and results in a departure from linear of the torque-twist diagram according to the relation

$$T = A_1 (\theta/\ell) + A_2 (\theta/\ell)^3$$

where A_1 and A_2 are constants. The second term has the same appearance as Timoshenko's correction for the case of the twisting of a bar when cross-sections are not free to warp or if the torque varies along a bar, and should not be confused with this.

Longitudinal Strains in an Angle Section under Pure Torsion

Consider an angle section of length ℓ, leg width b, and thickness t. (Fig. 161). Assume t/b is small, and the material is elastic. Tension is considered positive.

Under conditions of pure torsion, to a first approximation, no warping of the mid-line of the cross-section occurs, as both legs diverge from the shear centre C, assuming that the bar twists about C. Then the tensile strain at a point given by r due to the difference in length between the helix and the original straight length is, as before,

$\varepsilon = r^2\theta^2/2\ell^2$. This is everywhere positive, and does not satisfy statics, as no normal tension is applied. Therefore put

$$\varepsilon = r^2\theta^2/2\ell^2 + \varepsilon_1 \qquad \ldots (118)$$

where ε_1 is an assumed additional strain necessary to satisfy statics. We can assume ε_1 to be uniform over the cross-section of the bar only if the strain distribution ε then satisfies the conditions of zero normal force and zero applied bending moment. It will be shown that ε_1 cannot be uniform for an unsymmetrical section such as an angle.

Assume $\varepsilon_1 = g + hr$ .. (119)

where g and h are constants. This is the simplest expression for ε_1 which will satisfy statics.

Therefore $f = E\varepsilon = E\,(r^2\theta^2/2\ell^2 + g + hr)$ (120)

For zero normal force

$$\int f\ dA = 0$$

and therefore $2\int_0^b f\ t\ dr = 0$

which gives $G + hb/2 = -b^2(\theta/\ell)^2/6$. .. (121)

For zero bending moment, taking moments about an axis through C perpendicular to the bisector of the angle, we have

$$2\int_0^b f\ t\ dr\ \ r/\sqrt{2} = 0$$

which gives $g/2 + hb/3 = -b^2\,(\theta/\ell)^2/8$ .. (122)

Equations (121) and (122) can be solved for g and h.

They give $h = -\frac{1}{2}\,b\,(\theta/\ell)^2$

and $g = b^2\,(\theta/\ell)^2/12$.

The required strain distribution is then

$$\varepsilon = (\theta/\ell)^2\left[r^2/2 + b^2/12 - br/2\right]. \qquad (123)$$

At the point C, r = 0

and $\varepsilon = b^2\,(\theta/\ell)^2/12.$

At A and B r = b

and $\varepsilon = b^2\,(\theta/\ell)^2/12.$ That is, the corner and the edges of the legs are in tension. At the centre of the leg r = b/2,

and $\varepsilon = -b^2(\theta/\ell)^2/24.$ Putting $\varepsilon = 0$ in Equation (123), zero strain occurs at r = 0.21 b and 0.79 b. The strain distribution over the section is as shown in Fig. 162.

It can be seen that the non-uniform strain distribution causes the bar to bend. We have $\varepsilon_1 = g + hr$, (Equation 119), where $h = -b\,(\theta/\ell)^2/2$. The term hr in ε_1 causes the bar to bend about its minor axis uu, (Fig. 163), so that it is concave towards the edges of the legs, A and B. The curvature is

$$1/R = d\phi/d\ell = \frac{b^2\,(\theta/\ell)^2/2}{b/\sqrt{2}}$$

$$= b\,(\theta/\ell)^2/\sqrt{2} \qquad .. \qquad (124)$$

Cullimore (see page 94 for reference) establishes equation (118), but following Weber's analysis for a rectangular or circular section, he assumes $\mathcal{E}_1$ is uniform over the cross-section in every case, thus unfortunately making the elementary mistake of neglecting to satisfy statics in the case of an angle-section. The longitudinal stress distribution based on his derivation is as shown in Fig. 164, and does not satisfy statics, as an external bending moment must be applied to give this distribution. More unfortunately still, the error was not noticed in the course of the discussion. The assumption $\mathcal{E}_1$ = constant is satisfactory for symmetrical sections, or for a section which is anti-symmetric about the centre of twist such as a Z - section but not for other unsymmetrical sections.

The foregoing treatment of the bending effect of pure torque is due to the author, and is believed to be original. The analysis has been extended to any thin walled member of open cross-section. (See Appendix A, No. 15).

The Deflection of the End of a Cantilever of Angle-section when Subjected to a Pure Torque

Consider a cantilever of length L, (Fig. 165), clamped at the end $\ell = 0$. A pure torque is applied at the end $\ell = L$, and the angle of twist there is θ. Put $\theta = \omega L$, where ω is the twist per unit length or specific twist. Assume only the small element $d\ell$ of the bar is elastic as far as the bending given by Equation 124 is concerned, and neglect the fact that $d\omega/d\ell = 0$ at the clamped end. Then the curvature due to bending about the minor axis of the section within the length $d\ell$ is, from equation (124)

$$d\phi/d\ell = b(\theta/L)^2/\sqrt{2}$$

There is a resulting deflection at the end of the bar in the direction perpendicular to the minor axis of the section at ℓ, of

$$dv_\ell = (L - \ell)(d\phi/d\ell)\, d\ell.$$

Resolving parallel and perpendicular to the axes of u and v at $\ell = 0$, the components of the deflection at the end $\ell = L$ are:

$$du = dv_\ell \sin \omega\ell = (b/\sqrt{2})(\theta/L)^2 (L - \ell) \sin \omega\ell \, d\ell$$

and

$$dv = dv_\ell \cos \omega\ell = (b/\sqrt{2})(\theta/L)^2 (L - \ell) \cos \omega\ell \, d\ell$$

Integrating along the bar with respect to $d\ell$, from 0 to L, the components of the displacement of the end of the bar parallel to the u and v axes at $\ell = 0$ are:

$$\left.\begin{aligned} u &= b(\theta - \sin\theta)/\sqrt{2} \\ \text{and} \qquad v &= b(1 - \cos\theta)/\sqrt{2} \end{aligned}\right\} \quad .. \quad (125)$$

The path of the end of the bar is shown in Fig. 166. It is to be noted that the deflection depends only on the width of the leg of the angle and the total angle of twist θ.

Experimental Verification Using a Short Angle-section Member Bent from Sheet Brass

An angle section member 0.575 in. x 0.575 in. x 0.0378 in. x 7 in. long was bent from sheet brass. The tensile stress-strain curve for the material is shown in Fig. 167. The Young's Modulus is 13,000,000 lb./sq. in., and the material is elastic up to a tensile stress of 55,000 lb./sq. in., or a shear stress of about 27,000 lb./sq. in.

The member was loosely held at one end, and a pure torque applied at the other. The torque-twist curve is shown in Fig. 168. Longitudinal strains were measured at various points around the angle members using light Huggenberger strain gauges, and are shown plotted in Fig. 169. The measured strain distribution at the maximum torque applied is shown in Fig. 15, on which the theoretical distribution as given by Equation (123) is also shown. The agreement is quite close. The parabolic distribution of strain is evident, and it is quite clear that the corners of the angle are in tension and the centres of the legs in compression. The measured strains are also quantitatively in close agreement with the calculated values.

The member was then clamped at one end and a pure torque applied at the other end. The deflections of the end of the cantilever were measured, and are shown plotted in Fig. 171 for increasing and decreasing torque. It is seen that the deflections are recovered as the torque is removed. The calculated deflections according to Equation (125) are also plotted, and the agreement is quite close.

Discussion of the Assumptions

In writing down Equation (118) it has been assumed that under pure torque each element of length of the bar twists about its axis of shear centres, and that the warped cross-sections remain the same axial distance apart, though the distance along each helical path taken up by individual longitudinal fibres varies. That is, warping has been taken as unaffected by the presence of longitudinal stresses in the bar. That this is not strictly true can be seen from the fact that the longitudinal stress system sets up shear stresses which in turn affect the warping of the cross-sections. However, this affect seems to be small, and the experimental work has verified the analysis based on Equation (118).

Lateral buckling under pure torque has also been neglected. (This effect is discussed by Greenhill, A.J. (1883) Proc. Inst. Mech. Engineers (1883) p. 182; Timoshenko, S. (1936) Theory of Elastic Stability, p. 167; and Biezeno and Grammel (1956) Engineering Dynamics Vol. (ii) p. 411 and p. 413 (Blackie).) Biezeno and Grammel show that a shaft of length ℓ between supports buckles at a twist per unit length ω given by

$$\left.\begin{aligned} \tan \omega\ell/2 &= e \tan \rho\omega\ell/2 \\ \tan \rho\omega\ell/2 &= e \tan \omega\ell/2 \end{aligned}\right\} \quad .. \quad (126)$$

or by

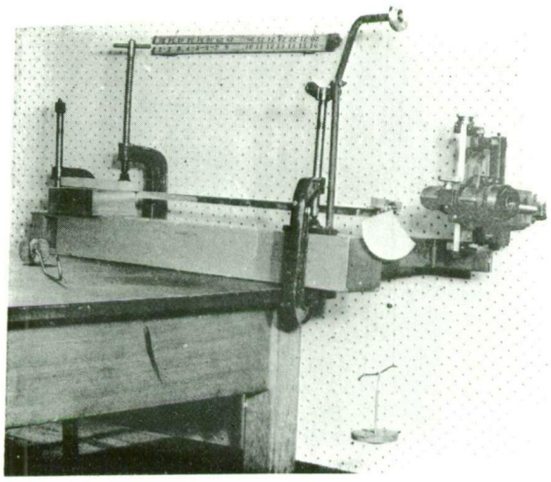

Preliminary experiments on twisting an aluminium angle-section cantilever. Deflections were measured with a travelling microscope, and longitudinal strains with Huggenberger mechanical strain gauges.

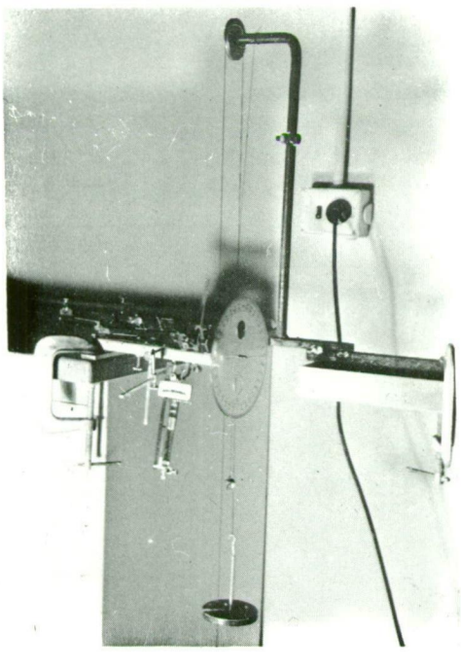

Twisting a short brass angle-section cantilever, longitudinal strains being measured.

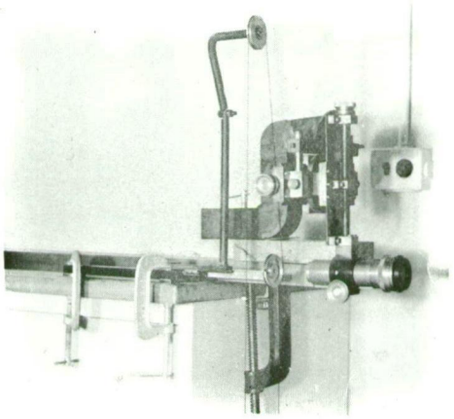

Measurement of deflection of end of brass angle-section cantilever with travelling microscope.

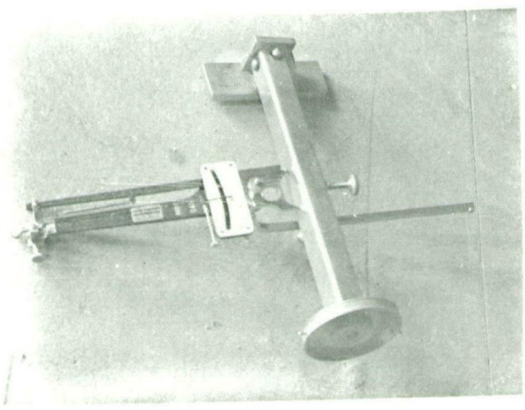

Method of measurement of longitudinal strains.

PLATE 13

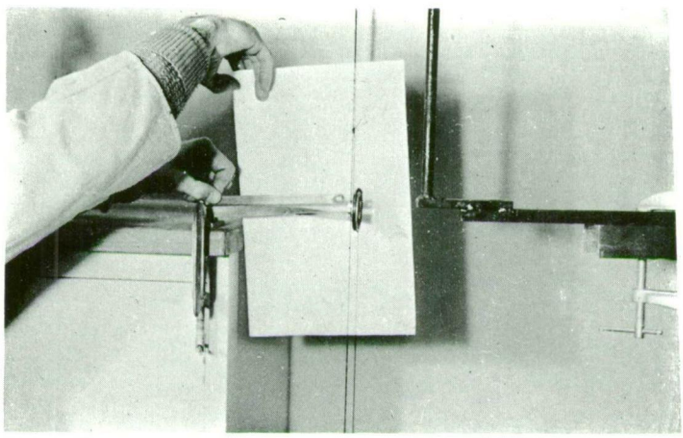

Lateral bending of angle-section member
under pure torque.

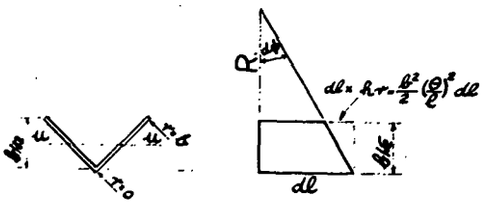

Fig. 163.

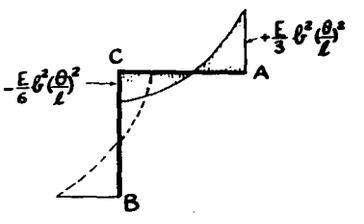

Fig. 164.

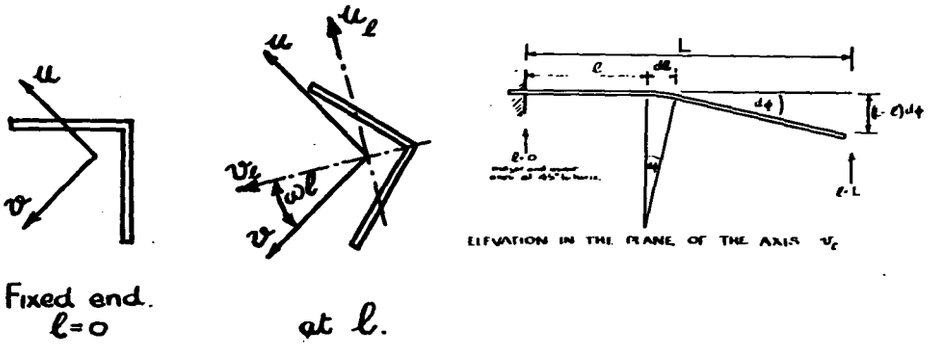

Fig. 165.

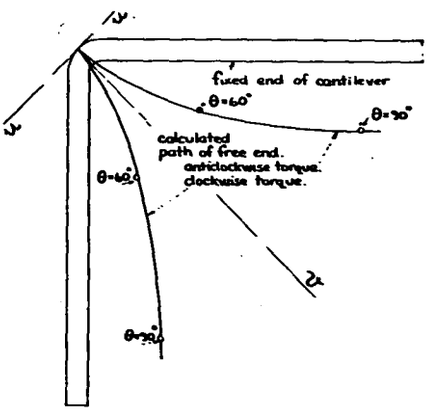

Fig. 166.

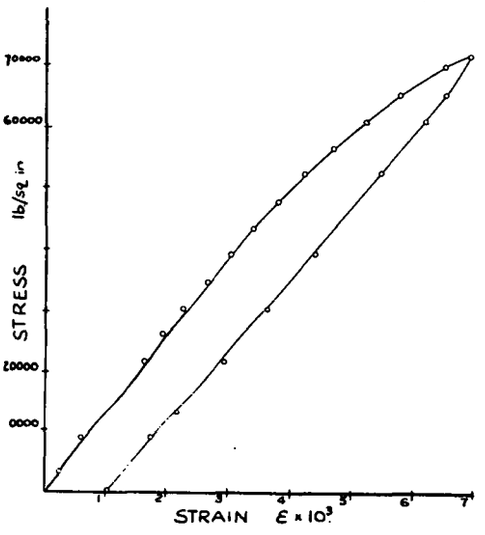

Fig. 167.

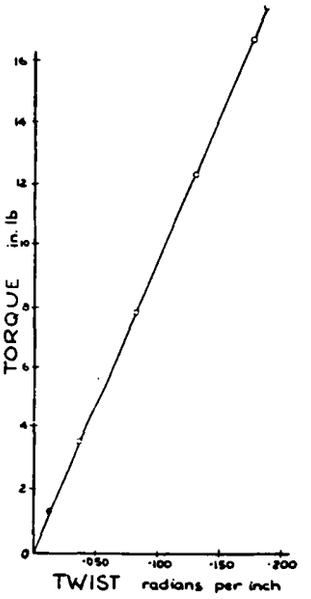

Fig. 168.

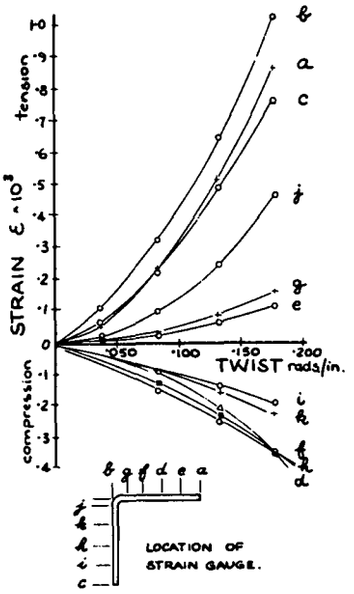

Fig. 169.

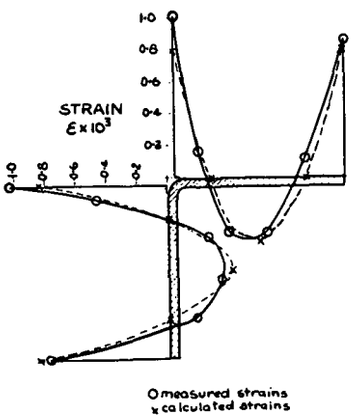

Fig. 170.

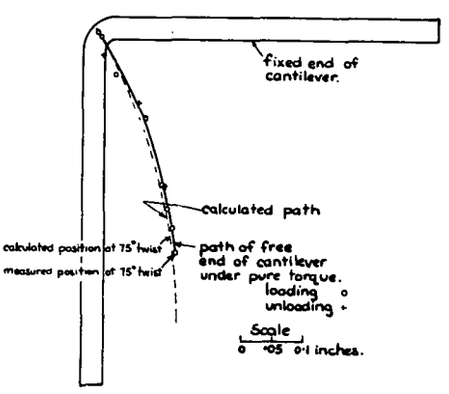

Fig. 171.

where
$$e = \frac{2\alpha_2 - \alpha_t}{2\alpha_1 - \alpha_t} \cdot \sqrt{\frac{\alpha_1}{\alpha_2} \cdot \frac{\alpha_1 - \alpha_t}{\alpha_2 - \alpha_t}}$$
$$\rho = \sqrt{(\alpha_1 - \alpha_t)(\alpha_2 - \alpha_t)/\alpha_1 \alpha_2} \quad \Bigg\} \ldots (127)$$

and α_1 and α_2 are the maximum and minimum flexural rigidities of the shaft, and α_t its torsional rigidity.

The brass member tested had the computed values $\alpha_1 = 7{,}800$ lb. in.^{2}, $\alpha_2 = 31{,}100$ lb. in.^{2} and $\alpha_t = 92$ lb. in.^{2} Substitution in Equations (127) yields $e = 1.000024$ and $\rho = 0.99300$. Equation (126) then reduces to:

$$\tan \omega \ell/2 = 1.000024 \tan (0.993000\, \omega \ell/2).$$

The first solution of this equation occurs at a very large value of $\omega \ell/2$, (approximately $\omega \ell/2 = 140\pi$, or $\omega = 20\pi$, for $\ell = 14$ in., twice the length of the cantilever used), whereas the member was twisted through only 0.2 radians per inch. Actually the theoretical twist at which the cantilever buckles must be rather greater than the value calculated here, as the cantilever is rather stiffer than a simply-supported beam of twice the length, since the specific twist at the clamped end is zero.

Of course, as soon as the member is bent, whether due to initial crookedness or to the bending effect of pure torsion, the applied torque has a resolved bending moment component. This however appears to be small, as neglecting it has caused little error.

The bending effect of pure torque has been calculated for a member made of material having a linearly elastic stress-strain curve, and all measurements have been carried out in the elastic range. The effect of yielding at the root of the angle-section member is probably very marked, but it has not been investigated.

Longitudinal strains of the order of 0.001 at angles of twist of about 0.2 radians per inch were measured in angle-section members due to the bending effect of pure torque. Quite high longitudinal stresses are involved. Bolted angle struts are observed to twist markedly as failure is approached, the magnitude of the twist being of the same order as measured above. The bending effect of torsion on the buckling of an angle strut is probably considerable. In particular, measured longitudinal strains will be affected as twisting develops.

94. <u>The Behaviour of Bolted Angle-section Members in Compression</u>:

Tests on angle-section members as single pin-ended struts have been reported in Art. 58 of Chapter Two, where the Southwell Plot on measured strains in the elastic range was shown to be linear, the slope of the plot giving the Euler load of the strut. The tests were extended into the plastic range in Arts. 60 and 61. As these struts were bent about their minor axes, twisting did not occur until very large deflections were reached and local buckling took place.

In Art. 75 the elastic buckling of a triangular frame made from angle-section members is reported. The major axes of the members lay in the plane of the frame and buckling took place in that plane. The members were again bent about

their minor axes without twisting. The Southwell Plot on strains again resulted in good agreement with the calculated critical load.

In Art. 79, the buckling of a triangular frame out of its plane is discussed. In this case both bending and twisting of the members was involved. Two buckling modes were treated, and it was shown that the critical load is markedly dependent on the torsional and bending stiffnesses of the members. Because of the low torsional stiffness of angle-section members, the struts in these frames acted almost as if pin-ended. The Southwell Plot on strains again gave a close estimate of the critical load.

In the above tests on frames, the angle-section members were firmly bolted by both legs to brass end pieces. A bolted angle strut is in practice less firmly held. The end fixing consists usually of one or two bolts in one leg only. Some triangular frames have been made up using angle-section members singly bolted through one leg to brass corner pieces. In all cases the Southwell Plots on measured strains were linear, but gave critical loads much less than those calculated in the articles mentioned above. This is undoubtedly due to the less rigid end fixing. Where a member is very firmly held at its ends, the relations between end moment and end slope are entirely dependent on the torsional and bending stiffnesses of the member as a whole. However, where a single bolt is used as an end fixing, the local strength of the leg of the member, the placing of the bolt in the leg, the size of the washer, and the tension in the bolt all assume vital importance. No matter what the details of the fixing are, single bolting results in a reduction in stiffness of the member, and critical loads are therefore reduced also.

95. Tests on a Model Lattice Girder.

A model lattice girder was made to simulate several bays of a plane frame near the base of a transmission tower, as shown in Fig. 172, the main chords of the model being made parallel. The bracing of the model was made up of aluminium angles bent from 20 gauge sheet, and the legs were mild-steel rolled angles. Aluminium was chosen as the material for the bracing members as the low Young's Modulus gives greater strains which are easier to measure. A comparison of the model and prototype is given in Table 1.

Table 1. - Dimensions of Angle Members

		Length between bolt centres	Cross Section A	Least rad. of gyration. r	Length/ rad. of gyration. ℓ/r	Leg width/ leg thickness b/t
	Transmission tower	in.	sq. in.	in.		
Legs	5 x 5 x $\frac{5}{8}$ in. ..	72	5.86	0.97	80	8
	$3\frac{1}{2}$ x $3\frac{1}{2}$ x 5/16 in...	72	2.09	0.68	100	11
Bracing	$2\frac{1}{4}$ x $2\frac{1}{4}$ x 3/16 in...	84	0.81	0.44	190	12
	or					
	2 x 2 x 3/16 in. ..	84	0.71	0.39	210	11
	Model					
Legs	(i.e. main chords of girder) 1 x 1 x $\frac{1}{8}$ in. mild steel ..	15	0.23	0.19	79	8
Bracing	0.58 x 0.58 x 0.036 in. aluminium ..	15.75	0.040	0.12	130	16

The model is similar to the prototype. The ℓ/r ratio of the main legs is about the same for each. Since buckling is controlled by the Young's modulus of the material, the ℓ/r of 130 for the aluminium bracing of the model is equivalent, if the members were steel, to an ℓ/r of 390, since E for steel/E for aluminium = 30/10. The equivalent figure for the prototype is about 200. The bracing of the model has been deliberately lightened in order that it may be the controlling factor. In most towers as at present designed, the leg members fail in load tests, and it is felt that the bracing is rather heavy. In the actual tower, the ratio of area of leg member to area of bracing member is 5.86/0.81 = 7.2, or 2.09/0.71 = 3.0. For the model, if we allow for the difference in strength of the aluminium and steel by multiplying in proportion to their yield strengths the ratio is (0.23/0.040) x (35,000/15,000) = 12.8. The bracing is again shown to be relatively light.

The above figures are intended merely as a guide to the relation between the model and prototype.

The connections in the actual tower consisted of $\frac{5}{8}$ in. or $\frac{3}{4}$ in. diameter black bolts in the main leg members, and $\frac{1}{2}$ in. diameter bolts at the intersection points of the bracing. The model thus calls for an $\frac{1}{8}$ in. diameter bolt. The strength of a strut is almost completely determined by the torsional and bending restraints at its ends, and these are dependent on the torsional and bending stiffnesses of adjacent members and on the connections between them. It is important in model studies to reduce to a minimum the variability of the connection. (This would also be an advantage in actual structures.) The bolts used in the model were $\frac{1}{8}$ in. diameter metal threads, bolts having a rolled thread of 40 threads per inch. These bolts have been subjected to a great deal of work hardening during manufacture. In a pure tension test, bolts failed at loads of 600 to 660 lb. With a root area of 0.0064 sq. in., this corresponds to a stress of 100,000 lb. per sq. in. Screwing tests on these bolts gave consistent tensions of about 200 lb. at a torque of 12 in. lb. At higher torques, the thread strips.

Strength of the Bolted Connections

Tearing-out tests were carried out. Typical results are given in Table II.

Table II. - Tearing-out Tests on Bolted Connections

Type of test	Edge clearance (centre of hole to end of member)	Tearing-out loads
	in.	lb.
Aluminium bolted to aluminium	$\frac{1}{8}$	105, 105, 110
	3/16	140, 130, 130
	$\frac{1}{4}$	165, 170, 160
Aluminium bolted to steel	$\frac{1}{4}$	210, 225

Dry bolts and nuts were used. Greased bolts gave higher tensions at the same torque, and therefore higher tearing-out loads, but the results showed higher scatter. A distance of $\frac{1}{4}$ in. from centre of hole to end of member was adopted.

Stress-strain curves for the aluminium and steel are shown in Fig. 173.

First Loading Test

The model truss was set up as a lattice girder and loaded as in Fig. 174, using dead weights. Load-deflection curves are shown in Fig. 175. At the loads used, the curves are linear and there is no permanent distortion, indicating complete absence of bolt slip.

The truss was set up again as in Fig. 176, and strains were measured on the members shown, using light Huggenberger mechanical strain gauges. A plot of strains was taken around the cross-section of the angle member near its centre. Load-deflection curves are shown in Fig. 177 and the measured strains in Fig. 178. All the graphs are linear, showing that the elastic limit has not been reached.

There is considerable variation in the stress across the section (as shown by the measured strains), giving evidence of high bending moments in the members. Fig. 179 is a section through the members concerned, just above the leg angle. By integrating the stresses across the section, the forces in the members can be calculated. In Table III the forces in the members (per 100 lb. applied load) are obtained. A comparison with the force calculated from statics if the joints are assumed pinned, shows reasonable agreement. In each case the measured forces are rather less, as some of the load is taken by bending of the main leg. This is in agreement with the usual design assumptions: the bending due to the rigidity of the joints is never sufficient greatly to alter the total forces in the members, but a comparison of the average stress and the measured stresses (Table III) shows that bending can increase the stresses by up to 90% in the elastic range. "Experimental load" was obtained by integrating measured strains, taken at the positions shown in Fig. 179, over the area. The "calculated load" was obtained from statics, assuming pinned joints.

Table III. - Strains, Stresses and Forces in Members

Member	Position	Strain	Stress $E = 9 \times 10^6$ lb./sq. in.	Average stress	Experimental load	Calculated load
		x 10^3	lb./sq. in.	lb./sq. in	lb.	lb.
L1 U2	1	0.177	1590 compr.	1073	42.8	57
	2	0.214	1930 compr.			
	3	0.150	1350 compr.			
	4	0.065	590 tension			
L3 U2	1	0	0	1246	49.9	57
	2	0.127	1145 tension			
	3	0.206	1860 tension			
	4	0.220	1980 tension			
L3 U4	1	0.134	1210 tension	1358	54.3	57
	2	0.120	1180 tension			
	3	0.138	1250 tension			
	4	0.198	1790 tension			

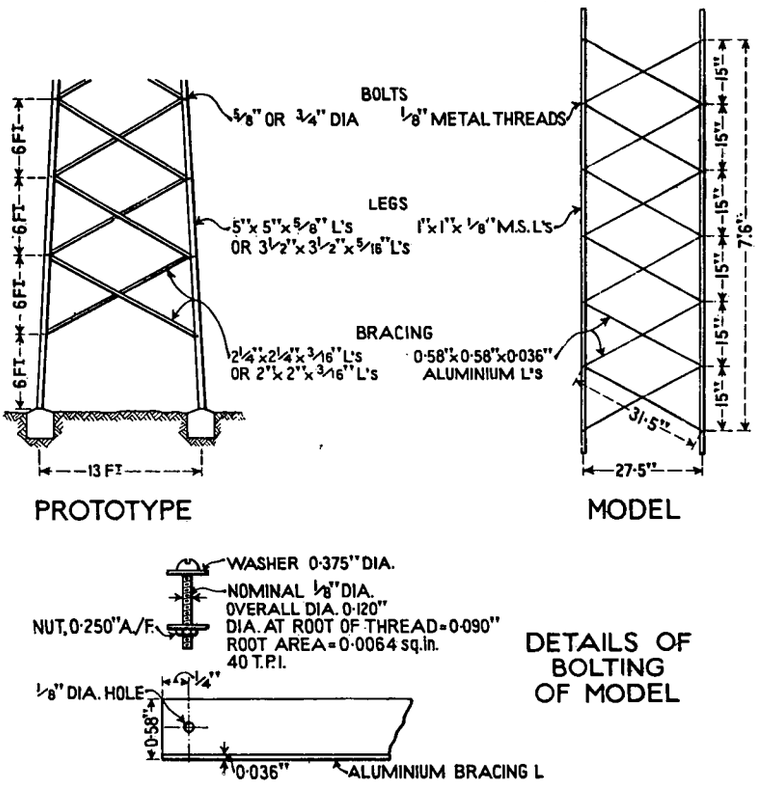

Fig. 172.

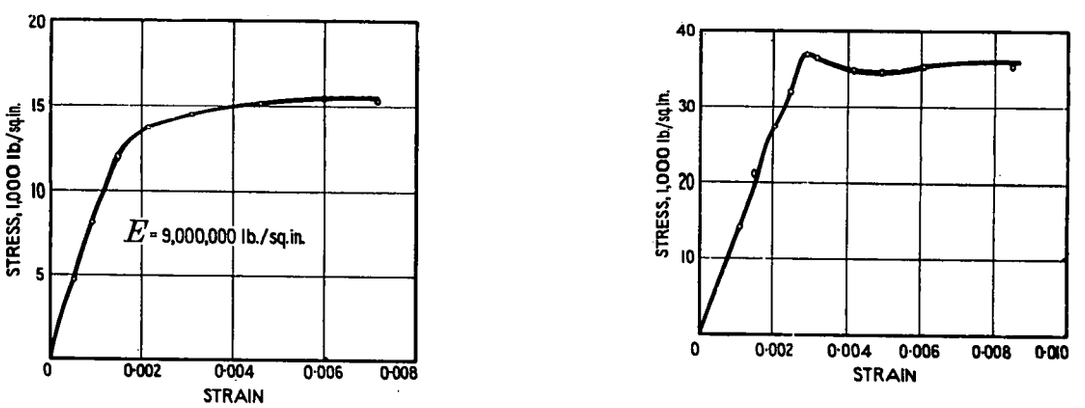

Fig. 173.

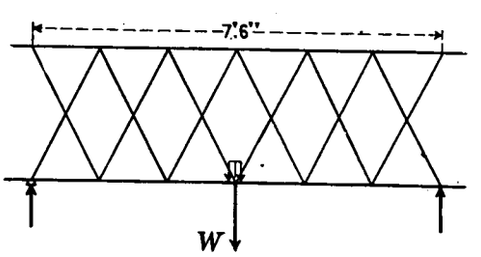

Fig. 174.

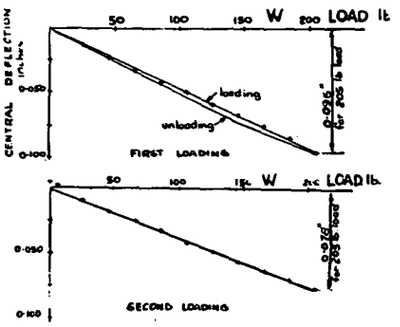

Fig. 175.

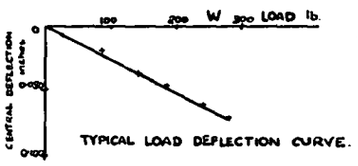

Fig. 176.

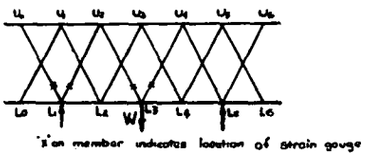

Fig. 177.

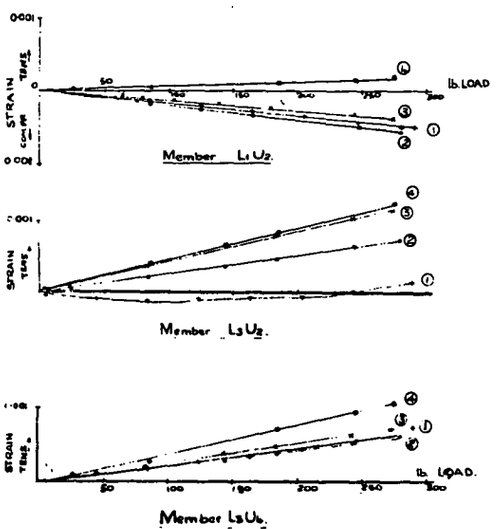

Fig. 178.

Second Loading Test

The truss was set up again as in Fig. 180 and loaded to failure, using a screw jack and proving ring. At 320 lb. load, the lower half of member L3 U2 began to fail by twisting just away from the bolts, and buckling about its minor axis in the central portion. The upper half of U1 L2 behaved in a similar way. The members which failed showed considerable deflection at constant load due to creep in the aluminium. There was some spring in the loading system, and these members were permanently deformed. It is interesting to note the members which failed, thus determining the load capacity of the truss. They are shown dotted in Fig. 180.

It was found previously that the forces in the lower sections of L3 U2 and L3 U4 were the same, but the stress distribution was considerably different, L3 U2 being the more highly stressed. L3 U2 is the member which is bolted to the outside of the main angle; L3 U4 is bolted inside. In the truss as loaded, L3 U2 and U1 L2, the two members bolted on the outside of the main legs, buckled in compression, whereas the corresponding equally loaded compression members L3 U4 and L4 U5, bolted inside, did not fail and in fact remained elastic. The load-carrying capacity of these struts has been determined by the restraining moments and torsions at their ends.

With the loading system used, the transverse location of the point of application of the load on the main leg is important. It is apparent that the bending of L3 U4 and L3 U2 (favourable to L3 U4 and unfavourable to L3 U2) can be caused only by twisting of the leg angle, and this will be influenced by the location of the load point(Fig. 181).

The Southwell Plot on Strains

Strains measured on the corners of the angles L3 U2 and L3 U4 are plotted in Fig. 182, and prove to be rectangular hyperbolae. The plot of ε/P against ε is shown in Fig. 183, where ε = measured strain, and P = calculated axial force in the member, assuming the joints pinned. These graphs are straight lines in each case. The lines lie fairly close together and are parallel. It has been shown that the inverse slopes of these lines represent a critical load for the members concerned. In the case of L3 U2, the inverse slope is 230 lb.; for L3 U4, it is 240 lb. It is important to note that this critical load is the same for each member L3 U2 and L3 U4, even though one failed and the other remained nearly elastic.

For the 0.58 x 0.58 x 0.036 in aluminium angle members concerned,

$$I_{min.} = 5.6 \times 10^4 \text{ in.}^4$$

Length between bolts = 15.75 in.

$$\text{Euler load} = \pi^2 EI/\ell^2 = 200 \text{ lb.}$$

The critical load for L3 U2 and L3 U4 is about 235 lb. This may be interpreted as meaning that they have an effective pin-ended length of $\sqrt{(200/235)} = 0.9$ of their actual full length, if they are considered as buckling about their minor axes. This is reasonable, in that the bracing angles are firmly bolted to the leg angle at one end, but only bolted to each other at their intersections.

The tests carried out on this model have served to emphasise the factors which control the load-carrying capacity of bolted angle struts, in particular, the end torsional and bending restraints. It is not claimed that model tests will give results of immediate practical utility. In fact, though it simulated the lower frames of a transmission tower, the model was loaded as a lattice girder. Bending and torsional restraints will also be different in the space frame. There are however many difficulties associated with full-size testing. One is the question of accurate, controllable loading. It may be possible to overcome this by building two adjacent towers, and jacking one against the other. With a model, certain difficulties associated with strain and deflection measurement are reduced, but greater accuracy is needed because of the small size. It is felt that model tests are a useful preliminary to the testing of a larger structure.

96. Further Tests on Bolted Angle Structures:

A number of simple frames made of bolted angles has been made and tested. Strains in the members were measured, and in each case, the Southwell Plot on strains has proved to be a straight line. The equation of this linear plot defines the behaviour of the strut in the elastic range, and can be used as a criterion of the load carrying capacity.

Five trusses (L2 to L6) were made up and tested as in Fig. 184. The flange members U_0U_5 and L_1L_6 were single 1 x 1 x $\frac{1}{8}$ in. M.S. angles. The web members U_0L_1, U_5L_5, etc. were 0.58 x 0.58 x 0.036 in. aluminium angles. The members were bolted together with single $\frac{1}{8}$ in. metal threads, through holes drilled in the centre of the angle leg; the bolts were tightened to a predetermined torque, in an attempt to get a constant fixing.

During loading, longitudinal strains were measured in the web compression members at the corners of the angles (see Fig. 185). It was found that this corner was always the most highly stressed point in the angle under the loading conditions adopted.

Fig. 186 shows a typical set of graphs of strain ε, against applied load W, or the load in the struts P. Similar graphs were obtained in each case. On these graphs, the calculated average axial strain P/EA is also shown, where

P = the axial load in the member = W/cos θ.
E = Young's modulus = 9,000,000 lb. per sq. in.
A = cross-sectional area of the member = 0.0403 sq. in.

Fig. 187 shows the corresponding Southwell Plots on the strains. It was found that the graphs of $(\varepsilon - P/EA)/P$ against $(\varepsilon - P/EA)$ consistently gave straight lines. Again, the plots in Fig. 187 are typical of sets of straight lines obtained for every compression member in every truss tested.

The equations of these lines may be written:

$$\frac{\varepsilon - P/EA}{P} = \frac{\varepsilon - P/EA}{Q_1} + C_1 \qquad .. \quad (128)$$

where ε = the measured maximum strain at the centre of the member.
Q_1 = the inverse slope of the Southwell Plot.
C_1 = the intercept of the Plot on the strain/load axis.

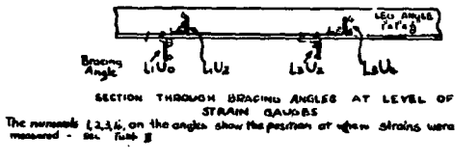

Fig. 179.

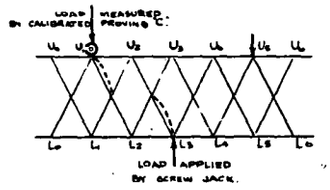

The members which failed are shown dotted.

Fig. 180.

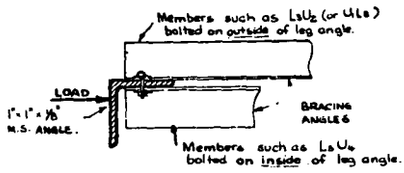

THE INFLUENCE OF BOLTING POSITION ON MEMBERS WHICH FAIL IN COMPRESSION

Fig. 181.

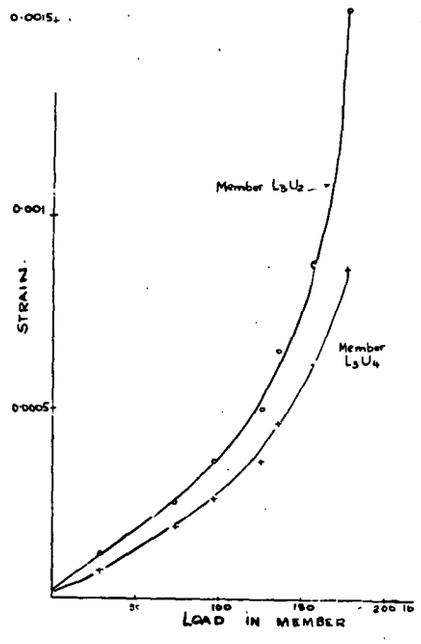

Fig. 182

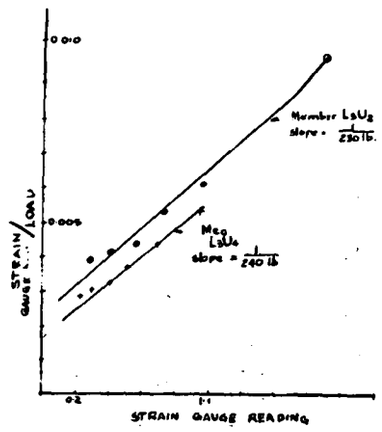

Fig. 183.

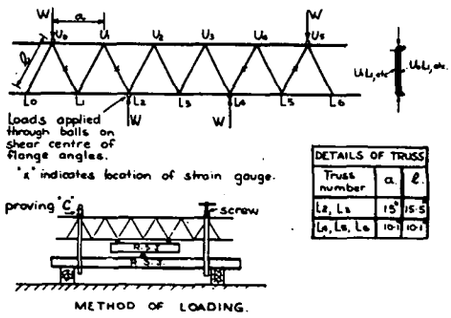

DETAILS OF TRUSS		
Truss number	α.	ℓ.
L2, L3	15°	15·5
L4, L5, L6	10·1°	10·1

Fig. 184.

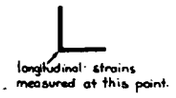

Fig. 185.

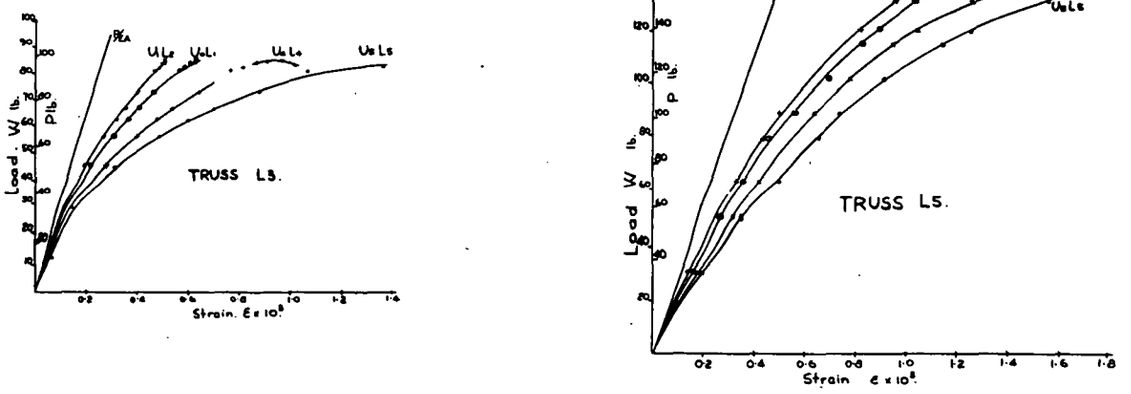

Fig. 186.

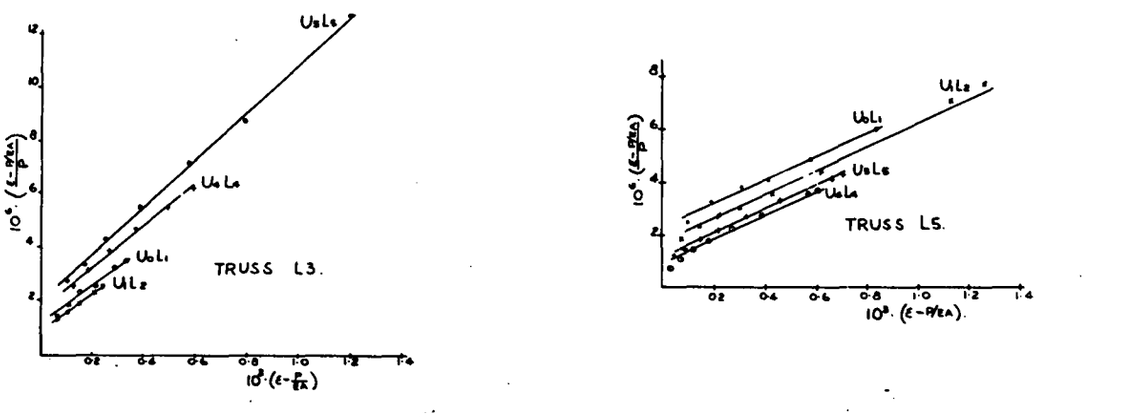

Fig. 187

Equation (128) reduces to:

$$E\varepsilon = P/A \left[1 + \eta_1 Q_1/(Q_1 - P)\right] \quad .. \quad (129)$$

where $\eta_1 = EAC_1$.

A sufficient number of tests on many types of structures should give values of Q_1 and η_1 likely to be met with in practice. These values obtained from the Southwell Plot on strains can be used to give a design formula similar to the Perry formula but based on actual tests, not on arbitrarily assumed factors. This is the procedure advocated in Arts. 64 and 82. It should be noted, however, that the variability of the effects of single bolting of angle members will necessitate a great deal of testing, supported by statistical analysis, before results can be used.

The test results are summarised in Table 4.

Table 4.

Truss	Web Member			Q_1 (lb.)	$C_1 \times 10^{-6}$ (lb.$^{-1}$)	$\eta_1 = EAC_1$	Member	L/ℓ
	Length (in.)	ℓ/r	Failure load P (lb.)					
L_1	15.45	130		230	1.8	0.65	L3U2(i)	
			180	240	2.3	0.84	L3U4(o)*	0.93
L_2	15.45	130		280	2.7	0.98	UoL1(i)	
				200	1.2	0.44	U1L2(i)	
				174	3.0	1.09	U4L4(o)	
			103	174	4.1	1.49	U5L5(o)*	1.10
L_3	15.45	130		140	1.1	0.40	UoL1(i)	
				140	0.8	0.29	U1L2(i)	
				124	1.6	0.58	U4L4(o)	
			100	112	1.9	0.69	U5L5(o) *	1.37
L_4	10.13	85		320	1.4	0.51	UoL1(i)	
				320	0.8	0.29	U1L2(i)	
				320	2.5	0.91	U4L4(o)	
			160	320	2.9	1.06	U5L5(o)*	1.22
L_5	10.13	85		220	1.0	0.36	UoL1(i)	
				220	1.3	0.47	U1L2(i)	
				220	1.7	0.61	U4L4(o)	
			155	220	2.3	0.82	U5L5(o) *	1.48
L_6	10.13	85		360	1.4	0.51	UoL1(i)	
				360	1.1	0.40	U1L2(i)	
				260	1.9	0.69	U4L4(o)	
			180	260	1.9	0.69	U5L5(o) *	1.36

NOTE:
(1) * indicates member that failed
(2) Truss L1 is reported in Article 95.
(3) "o" indicates that member was bolted on outside of flange member; "i", on inside.
(4) Effective length ratio $= L/\ell = \sqrt{Q/Q_1}$.
where Q = Euler load of member considered as pin-ended between bolts.

It is seen that there is quite a wide variation in values of Q_1 and η_1, even under apparently similar conditions. It is suggested that this may be due to the varying torsional stiffness of the flange angles. The restraint which the flange angle affords a web angle depends a good deal on the location of the latter. Also, new bolts were used in some trusses and not in others, and the fixing may have varied.

In spite of this variation, the following important conclusions can be drawn:

1. The behaviour of each compression member can be defined by Q_1 and η_1. These factors may vary somewhat, but it is important to carry out sufficient tests to determine the maximum value of η_1 and the minimum value of Q_1 for each type of fixing in each type of structure.

2. Maximum load carrying capacity for this material occurs at a strain of 0.0013. The Southwell Plot is linear up to this strain, and there is very little reserve of strength beyond this point. For the aluminium members concerned, equation (129) reduces to

$$(P/A)\left[1 + \eta_1 Q_1/(Q_1 - P)\right] = E\varepsilon = 12{,}700 \text{ lb. per sq. in.}$$

In the case of mild-steel members, the yield stress is substituted for $E\varepsilon$, and P becomes the load to cause first yield. Due to the high value of η_1, this is for all practical purposes the failure load for bolted angles struts.

It has been shown that the axial loads P in rigidly jointed trusses can be calculated with sufficient accuracy by assuming pin-joints. The above method thus furnishes a direct design method for statically determinate braced frameworks.

97. The Collapse of Triangulated Frames Containing Bolted Angle Struts:

Tests on bolted angle struts in some simple frames which have resulted in linear Southwell Plots on strains have been described in Art. 96. Further experimental work is reported here, and a proposed method of rationalization of the design of such members is presented. The tests indicate that, because of the eccentric connection, the reserve of strength of a bolted angle strut beyond the point at which yielding first occurs is not very great. Further tests may make it possible to obtain the statistical distribution of this reserve of strength as a function of the ℓ/r ratio for the strut. This means that the collapse load can be obtained in terms of the load to cause first yield, and a difficult elasto-plastic analysis of the behaviour of the strut is avoided.

Experimental Work

In all, ten plane frames (L_1 to L_{10}) having the form of six-bay lattice girders, and one space frame (S1) have been tested to failure. Flange members were single or double 1" x 1" x $\frac{1}{8}$" M.S. angles. (Fig. 188). The frames were proportioned so that failure occurred by buckling of the lattice members rather than by yielding or buckling of the flange angles. During loading, strains were measured in lattice compression members. Previous experience that the highest stress occurred at the corner of the angle rather

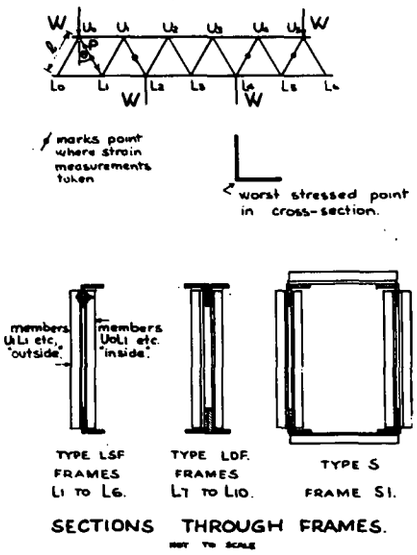

Fig. 188.

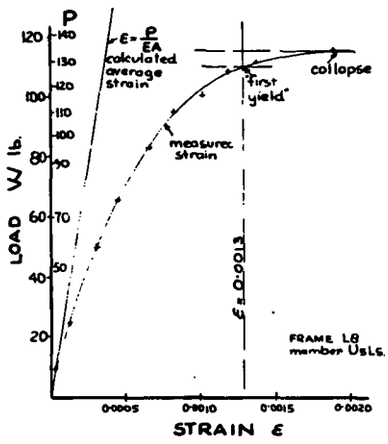

Fig. 189.

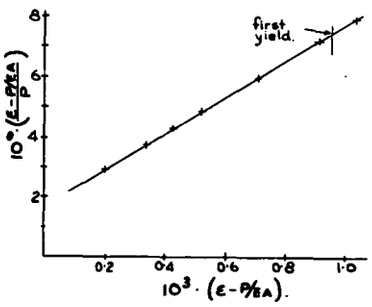

Fig. 190.

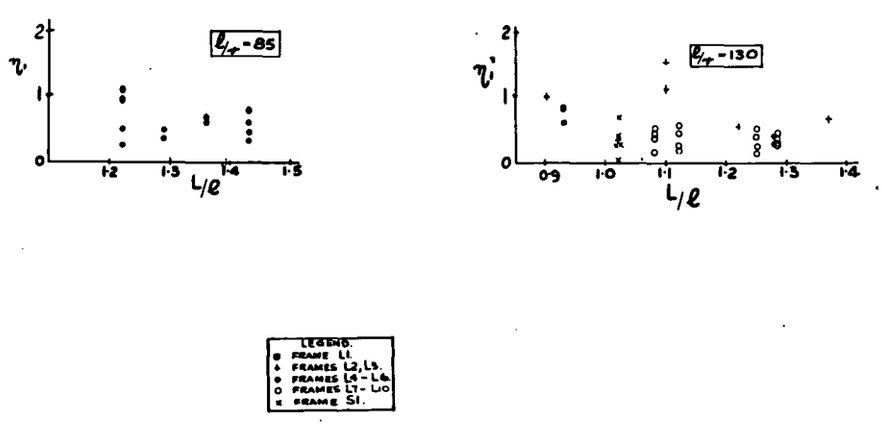

Fig. 191.

than at the edge of the leg was confirmed. (Fig. 188) Where single flange angles were used, a lattice member bolted to the outside of the flange angle was always the first to fail. It appears that the torsion of the flange angle is always such as to make the end restraint of such a member quite low, and thus to cause its early failure. A lattice member bolted on the inside of the flange angle seems to be less eccentrically loaded.

A typical plot of maximum strain against load is shown in Fig. 189. It is seen that the measured strain increases steadily and diverges quite quickly from the calculated average strain P/EA. This is due to the quite large eccentricity of the bolted connection.

In Table 5 details of the frames are given and collapse loads are listed. The collapse load is larger for smaller ℓ/r ratios. Also, for the same ℓ/r ratio, the collapse load is larger where double flange angles were used. This is to be expected, as the stiffer flange offers more restraint to the lattice member as it deflects. Besides this fact, there are no lattice members bolted on the "outside", as with the single flange angle. The effect of the increased end restraint on the collapse load is markedly demonstrated by these tests. Table 5 also lists the load to cause first yield. This is taken at a strain of 0.0013 (or a stress of 12,000 lb./sq. in.), which corresponds to the point on the stress-strain curve for the aluminium at which the strains increase very rapidly.

Table 5

Failure of Lattice Compression Members

Frame	Type (See Fig.188)	ℓ in.	ℓ/r	Collapse Load lb.	Load at First Yield lb.	(Collapse Load)/(First Yield Load)	Reserve Beyond First Yield %
L1	LSFX	15.5	130	180	175	1.03	3
L2	LSF	15.5	130	103	103	1.00	0
L3	LSF	15.5	130	100	95	1.05	5
L4	LSF	10.1	85	160	152	1.05	5
L5	LSF	10.1	85	165	155	1.06	6
L6	LSF	10.1	85	185	169	1.09	9
L7	LDF	15.5	130	125	115	1.08	8
L8	LDF	15.5	130	139	129	1.08	8
L9	LDF	15.5	130	150	146	1.03	3
L10	LDF	15.5	130	143	139	1.03	3
S1	S	15.5	130	130	128	1.01	1

Frame L1 is reported in Art. 95 and frames L2 to L6 in Art. 96.

If the behaviour of the members can be defined in the elastic range, the load to cause first yield can be calculated. For the frames tested, the collapse load is not more than 9% greater than the load to cause first yield, and for practical purposes it may conservatively be taken as the first yield load. The reserve of strength in the plastic range can then be regarded as a small extra safety margin. Calculation of the collapse load then reduces to the problem of determining the behaviour of the frame in the elastic range.

Fig. 190, which is typical of forty-two such plots on bolted angle struts, shows the Southwell Plot on strains for one of the lattice members which failed. Similar plots were obtained for every compression member in every frame tested. The graph is linear, and is defined by equation (128), which reduces to Equation (129). (See Art. 96)

This equation defines the behaviour of all struts in all the frames tested to date.

The behaviour of the strut as bolted in the structure is thus defined by two parameters, η_1 and Q_1. It is convenient to consider an effective length ratio $L/\ell = \sqrt{Q/Q_1}$ instead of Q_1. (Q is the Euler load of the strut considered as pin-ended at the bolt). Fig. 191 shows values of η_1 and L/ℓ obtained for forty-two compression members in the eleven frames tested. The distribution is somewhat random, as is to be expected. For practical design purposes, it is required to know the maximum value of η_1 and the maximum value of L/ℓ to be expected in the structure concerned. That is, some envelope above and to the right of all the plotted points is needed. Given sufficient tests, such an envelope can be drawn. A functional relation between η_1, L/ℓ and ℓ/r can then be written. Substitution of this relation in Equation (129), putting $E\epsilon$ equal to the yield stress, then enables solution for the value of P/A to cause first yield. A suitable load factor can be applied to give working loads. In the long run, of course, permissible stresses can be tabulated as in present codes.

98. Reserve of Strength in the Plastic Range:

For shorter stiffer struts, the reserve of strength beyond first yield may be considerable. Tests on other structures indicate that the collapse load may exceed first yield load by up to 30% for centrally loaded struts, but the reserve is much less in the case of eccentric loading. Further tests should make it possible to systematize this reserve as a function of ℓ/r. The results of experimental work by Mackey are of value here. (See S. Mackey "An Experimental Investigation of the Behaviour of Mild Steel Compression Members in Light Lattice Frameworks". The Struct. Engnr. Vol. 32, July, 1954. No. 7, p. 190.) Two girders and fifteen triangular frames made of mild steel angle-section members were tested, strains being measured at five positions along each member, taking plots around the angles. Fig. 192 shows a plot of (maximum load/load to cause first yield) against ℓ/r for the struts, taken from Mackey's paper. ℓ is the length of the strut between bolts. These results indicate that for $\ell/r > 140$ the reserve of strength in the plastic range is not greater than about 10%. For practical design purposes this may be neglected. For stiffer struts the reserve may be taken as varying linearly from 0% at $\ell/r = 140$ to 20% at $\ell/r = 80$.

Some indication of the reserve of strength of I section members in the plastic range can be obtained by studying the figures in a paper by J. C. Nutt - "The Collapse of Triangulated Trusses by Buckling within the Plane of the Truss" The Struct. Engnr. May, 1959.

Of course the reserve of strength beyond first yield is a function not only of ℓ/r but of many other factors, but the above values appear reasonable until more extensive test results are available.

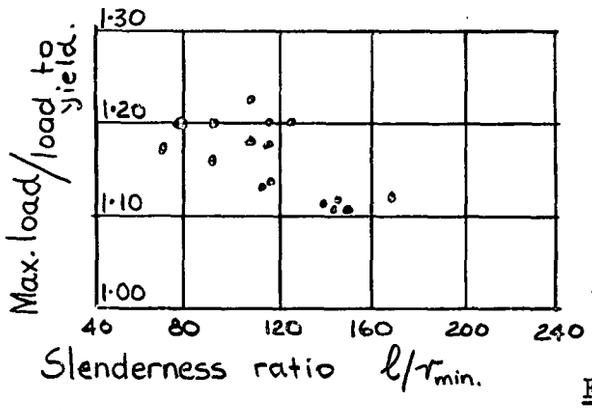

Fig. 192

99. The Design of Bolted Angle Struts:

It appears possible therefore, in view of the foregoing results, to systematise the design of bolted angle struts in the following manner. The required empirical information is presumed known in each case.

(i) Short Stiff Struts: (e.g. slenderness ratio ℓ/r less than 140, for mild steel rolled sections.)
The load to cause first yield can be calculated from the equation of the Southwell Plot on strains. The collapse load can then be estimated, the reserve of strength in the plastic range being known from Mackey's tests or other empirical work.

(ii) Intermediate stiffness struts (e.g. slenderness ratio ℓ/r ranging from 140 upwards, for mild steel rolled sections.)
The maximum load can be obtained directly from the equation of Southwell Plot on strains, the reserve of strength in the plastic range being negligible.

(iii) Very Slender Struts:
It is convenient to be able to limit the deflections of very slender struts in practice. There is no difficulty in doing this using the equation of the Southwell Plot on deflections. If a pin-ended column has initial central crookedness a_1, then the central deflection under load P is $y = a_1/(1 - P/Q)$, (See Art. 18), and the equation of the Southwell Plot on strains is

$$(\varepsilon - P/EA)/P = (\varepsilon - P/EA)/Q + C_1 \text{ where}$$

$a_1 = EIC_1/v$, (see Art. 56). The values of a_1 and Q can be obtained from the Southwell Plot on strains. Substitution in the deflection equation enables the load P for some limiting deflection to be calculated.

The method can be extended to struts which are not pin-ended. Equation (128) is the equation of the Southwell Plot on strains. The plot furnishes values of Q_1 and C_1. Since a bolted angle strut buckles with large central deflection, we may assume that the central deflection is given by:

$$y = (EIC_1/v)/(1 - P/Q_1)$$

This gives

$$P = Q_1 (1 - EIC_1/vy) \quad .. \quad .. \quad (130)$$

Empirical values of Q_1 and C_1 obtained from equation (128) can be substituted in equation (130) and the load P for some limiting value of y can be calculated.

The method given above is also valid for structures other than those containing bolted angle struts. However, it is of particular practical value for bolted angle struts because of the relatively large values of γ_1 which obtain for these members. Because of the eccentric connection, bolted angle struts fail by large central deflection. There is generally no doubt about the buckling mode, and the required location of strain gauges to pick up the longitudinal strains due to the buckling is obvious. Buckling effects $(\varepsilon - P/EA)$ are large compared with non-buckling effects (P/EA). Hence the Southwell Plot on strains can be accurately drawn from experimental measurements, and as a design formula, it can be relied on.

Also, because of the eccentric connection, failure of a bolted angle strut follows very quickly after the occurrence of first yield. The reserve of strength in the plastic range is considerable only for short stiff struts. This serves to widen the range in which the design criterion is merely the simple substitution of a limiting strain in the equation of the Southwell Plot on strains.

101. The Southwell Plot on strains can thus be used as a convenient experimental technique for determining the conditions which bring about the collapse of structures liable to instability or compression members built into structures. The method is based on elastic theory, but the principal difficulties associated with elastic analysis are avoided. It is realised that all structures in the elastic range are very sensitive to imperfections, that yielding under working loads at highly stressed locations can be tolerated, and that it is impossible to carry out an exact elastic stress analysis of any structure. However, using the method given, attention is concentrated on strains due to the buckling mode which causes failure, and the load-carrying capacity is related to the failure pattern.

In practice it is found that the failure loads of framed structures are extremely sensitive to the imperfections (such as initial crookedness of members, etc.) of the structure. The simplifications used when plastic theory is applied to bending of mild steel beams are therefore not available, and it is unlikely that elastic analysis of struts in framed structures will ever be entirely discarded.

PLATE 14

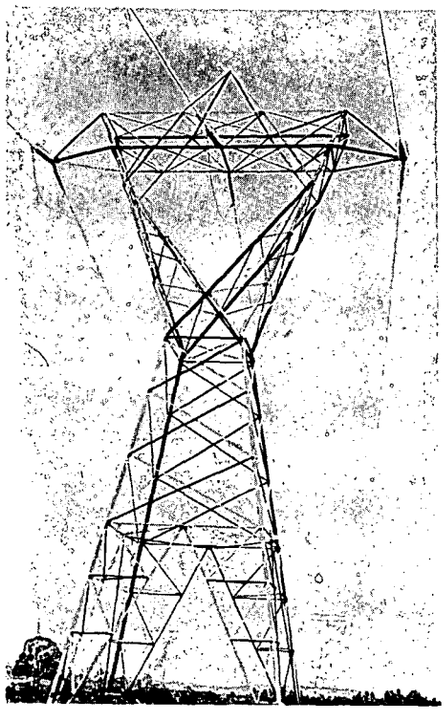

A transmission tower made of bolted angle members.

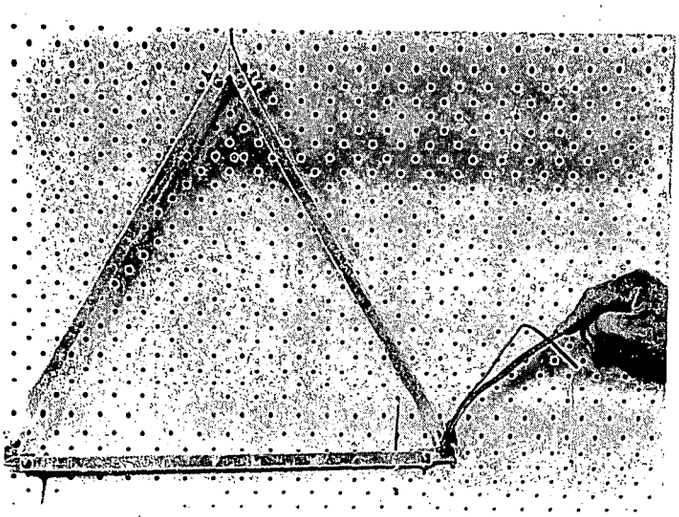

Triangular frame made from aluminium angle-section members.

Small torque spanner for tightening bolts in frames used in model experiments.

PLATE 15

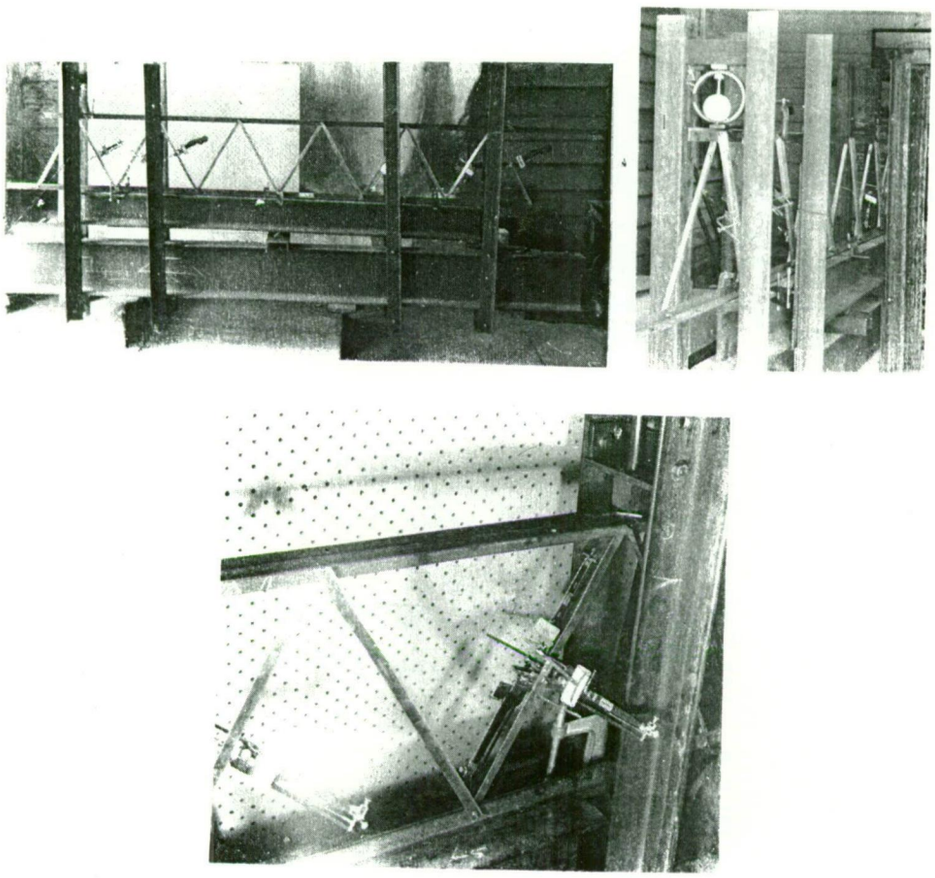

Test on model frames containing bolted angle members.

PLATE 16

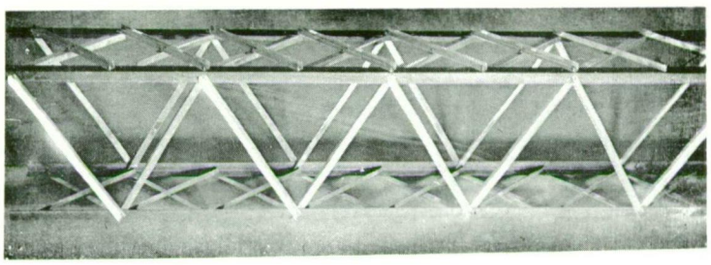

Space frame made from bolted angle members.

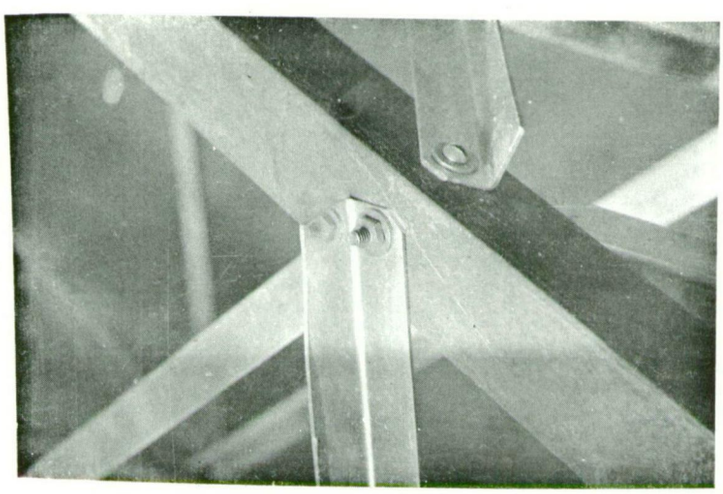

Detail of bolting of frame.

Framed structures which are redundant even if the joints are considered pin-ended - those frames in which the forces in the members cannot be calculated from statics - present special problems. The method of the Southwell Plot is still available, but it must be related to the overall loading, rather than to the forces in individual members, as these are difficult to determine in even the simplest redundant frames once buckling effects become important, and difficulty is experienced here in systematising the empirical information required for design purposes.

---- oOo ----

BIBLIOGRAPHY AND NOTES ON CHAPTER FOUR

The numerals refer to the articles in the text.

91. See S. Timoshenko "Theory of Bending Torsion and Buckling of thin-walled members of open cross-section." Collected Papers of Stephen P. Timoshenko, McGraw Hill (1953), p. 559.

F. Bleich "Buckling Strength of Metal Structures", Chapters 3 and 9.

---- oOo ----

REDUNDANT STRUCTURES

102. Many framed structures are redundant in the sense that they are statically indeterminate even when the joints are considered pinned. Various inter-related methods of analysis of redundant structures are available, of which energy methods are important examples. In this chapter, energy methods are discussed and some simple illustrative problems worked. Complementary energy is applied to a pin-jointed redundant braced frame in order to define the behaviour of compression members as they buckle or tension members as they yield. The extension to the study of rigid jointed redundant frames is discussed. The energy principles outlined are valid for all structures, but the argument is restricted to general types of framed structures. To discuss problems involving bending of beams, for example, ability to handle general non-linear load deformation relationships is required.

103. Notation:

General:

C	Complementary energy
U	Strain energy
P	Generalized force in an element or member of a structure.
W	Generalized external load applied to a structure, or a non-redundant reaction.
X	Generalized force applied across a cut in a redundant member (internal redundancy) or a redundant reaction (external redundancy).
δ	Generalized deformation corresponding to any P, W, or X.

Note: P, W, X may be forces or moments etc., and δ may be a displacement or rotation, etc. For a definition of a generalized force and its corresponding displacement see Timoshenko and Young, "Theory of Structures", McGraw Hill (1945), p.226. In general, there is a certain arbitrariness of grouping as to whether a given force is considered as an internal force, an external force, or a reaction, ie. whether the force is considered as an independent or dependent variable.

Members of Braced Frameworks:

F	Force in a member (compression taken positive)
ℓ	Length of a member
A	Cross-sectional area
E	Modulus of elasticity
$I = Ar^2$	Second moment of area
a	Initial crookedness of a strut
Q	First Euler load: $\pi^2 EI/\ell^2$

Other symbols are defined in the text.

104. The Analysis of Redundant Structures:

The equilibrium state of a redundant structure is dependent on the load-deformation relation for at least some of the elements of which it is made. Such a structure can be analysed by ensuring that the deformations of the elements considered are consistent with one another, that is that compatibility is satisfied. Three different types of equation are thus necessary and sufficient for the analysis of statically indeterminate structures:

(a) the equations of statics
(b) load-deformation relations for the members of the structure
(c) compatibility equations.

In general, the compatibility equations are the most difficult to handle, as they often result in very complicated expressions. Various techniques have been devised to reduce the labour involved. For instance, the method of moment distribution used on building type frames involves writing down a preliminary solution which satisfies the conditions (b) and (c) but not (a). Corrections or adjustments which continue to satisfy (b) and (c) are then applied until (a) is satisfied.

However, in this chapter attention will be drawn to the types of technique similar to that known as angle balancing, as they appear to be the most powerful in non-linear problems. The general procedure is to place sufficient imaginary cuts in the structure so that it is statically determinate if all the generalized forces X across the cuts are known. These forces are then taken as the unknowns. All the forces P in the structure are written down in terms of the forces X and the external loads W. The load-deformation relations for all the elements of the structure must be known, and hence the generalized deformations δ of the structure can be written as functions of X and W. For convenient application, deformations δ must be explicitly expressed as functions of forces P. For compatibility to be satisfied, the forces X across the cuts must be such that continuity exists, and the cut is closed. δ across a cut is zero. To summarize, a set of internal forces satisfying the equations of statics is chosen, the corresponding deformations are written down using the load-deformation relations for the members of the structure, and it is then ensured that these deformations are geometrically compatible.

The iterative method of angle balancing applied to the rigid joints of building type frames, and familiar to engineers, is an example of the above technique. Using this method, a first solution satisfying conditions (a) and (b) but not (c) is chosen. The discrepancy in satisfying the equations (c) of compatibility is calculated and expressed in terms of the dislocation at certain points. Corrections which continue to satisfy (a) and (b) are applied until the errors in equations (c) are negligible, and compatibility is satisfied. The iterative technique is usually convenient only in linear problems, as in such a case the closing of the dislocation or cut is linearly related to the action X across the cut.

105. The Energy Theorems.

The value of energy methods lies in the fact that they may afford a convenient means of writing down the compatibility equations or the equations of statics, (see (a) and (c), Art. 104); also a convenient grouping of variables is obtained.

The strain energy of a structure is defined as

$$U = \Sigma \int_0^{\delta_1} P \, d\delta \qquad .. \quad (131)$$

where P is the load (force or moment) in some element of the structure, and δ its corresponding deformation (see Fig. 193) and U is summed over all the elements of the structure. It is implied that P is given or can be expressed as a function of δ, so that the integration can be performed.

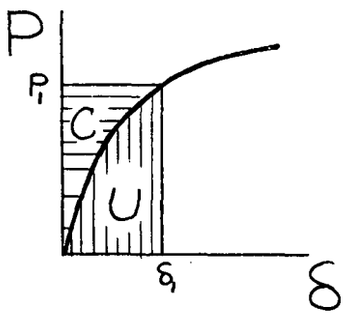

Fig. 193.

Suppose that for some element, $\delta = \delta_1$, when $P = P_1$. Then partial differentiation of U with respect to δ_1, gives

$$\partial U/\partial \delta_1 = P_1 \qquad .. \quad (132)$$

This equation is valid for non-linear as well as linear structures.

The complementary energy of a structure is defined as

$$C = \Sigma \int_0^{P_1} \delta \, dP.$$

It is implied that δ can be expressed as a function of P so that the integration can be carried out. Therefore

$$\partial C/\partial P_1 = \delta_1 \qquad .. \quad (133)$$

This holds whether the relation between δ and P is linear or non-linear.

Across a cut, where the displacement corresponding to any X is zero, we have

$$\partial C/\partial X = 0 \qquad .. \quad (134)$$

As stated in Art. 104, redundant structures can be analysed by making use of the equations of statics, the load deformation relations for the members, and equations of compatibility. The value of strain energy lies in the fact that, given a set of geometrically compatible deformations, the corresponding loads in the members being obtained from the load deformation relations, equation (132) can be used to replace the equations of statics. Alternatively, when complementary energy is used, if a set of internal forces satisfying

statics is chosen, the corresponding deformations are available from the load deformation relations, and equation (133) or equation (134) can be used to ensure compatibility of deformations. The duality of approach discussed in Art. (104) is thus directly extendable to the application of energy methods. This duality can be exploited to obtain a solution in the most convenient way. For example, it is evident that it is more convenient to use complementary energy when δ is given explicitly as a function of P, since in this case we begin with a set of forces P satisfying statics and solve for the corresponding deformations δ ; this mode of expression is also convenient when using equation (133). Strain energy is conveniently used when P is given explicitly as a function of δ , since it is then necessary to solve for the loads resulting from the initially chosen set of compatible deformations; this mode of expression is also convenient when using equation (132). The choice of method depends on the way in which the relevant information is expressed, and the information which is required. In general, compatibility equations are difficult to handle; this is the reason for the wide applicability of complementary energy methods, since equation (133) or (134) furnishes a means of handling the compatibility conditions.

The above treatment is valid for linear or non-linear structures. In the case of a linear structure, we have

$C = U$, and equations (132) or (133) reduce to

$$\partial U/\partial P_1 = \delta_1 \qquad .. \qquad (135)$$

Across a closed cut, we have

$$\partial U/\partial X = 0 \qquad .. \qquad (136)$$

Equations (135) and (136) are widely used strain energy equations, but it is seen that their use is an example of the approach which has been discussed above under complementary energy.

An interesting integrated treatment of the analysis of structures is given by F. Baron, "Successive Corrections: A Pattern of Thought" in "Numerical Methods of Analysis in Engineering" ed. Grinter, p.122, (Macmillan, 1949), though some of the statements concerning energy methods now need revision. For a treatment of strain energy, see R. V. Southwell, "Theory of Elasticity" 2nd ed. O.U.P. (1941). Complementary energy is discussed by H. M. Westergaard in the following references: "On the method of Complementary Energy". Proc. A.S.C.E. Feb. 1941, Vol. 67, No. 2, p. 199, and Trans. A.S.C.E. Vol. 107 (1942) p. 765.

The treatment of energy methods given in this thesis is rather short. For a fuller more rigorous treatment in which the basic theorems are worked out and the duality of approach is emphasized, see "Energy Methods of Solving Structures", a thesis presented for the degree of B.E. (Hons.) by S. Guidici, University of Tasmania, Feb. 1960. This work was carried out partly under the author's direction.

106. The Development of Complementary Energy Methods:

The originator of the conception of complementary energy was Engesser, and the method of application has since been developed by Westergaard, Charlton, and Brown. In a series of papers, Brown has systematically analysed the strain and complementary energy theorems and shown their inter-relation. In practice, complementary energy methods are as easily handled as strain energy methods, and the purely mathematical definition appears to be an advantage. No physical "feel" is needed. Complementary energy opens up a wide field which cannot be handled by strain energy methods.

Undue emphasis has been placed on elastic structures, that is, structures from which all the strain energy can be regained, and all the deflections reduced to zero, by the removal of the loads. As early as 1956, Hoff applied complementary energy to solve a redundant truss beyond the elastic limit. However, many authors still unnecessarily restrict themselves to load-deformation relations which are the same for decreasing as for increasing loads. This restriction is not needed so long as the load-deformation path is known, and the complementary energy is known at all stages of the loading of a structure.

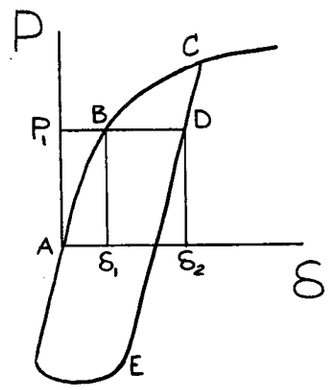

Fig. 194.

For example, the load-deformation curve for a member may have the form shown in Fig. 194. It is possible to arrive at the load P_1 by following the path AB, or the path ABCD, or the path ABCDEAB, resulting in deformations δ_1, δ_2, or δ_1, respectively. The complementary energy is thus not uniquely defined in terms of the load, but it is defined if the load-deformation path is determined. This restriction is important, and the restriction to elasticity may be discarded. It will also be shown later that in order to apply the complementary energy method, $\partial C/\partial P$ must be defined at the point under consideration.

Complementary energy is treated by the following: N. J. Hoff: "The Analysis of Structures" Wiley (1956) p. 346; T. M. Charlton: Engineering vol. 174 (1952) p. 389; E.H. Brown: Engineering vol. 179 (1955) p. 305, p. 339, p. 400; J.A.L. Matheson: Engineering vol. 180 (1955) p. 828; and T.M. Charlton "Energy Principles in Applied Status " (Blackie, 1959). Other papers having a bearing on the use of complementary energy in structural analysis are: J.W.H. King: "Some Notes on Plane Frames not Obeying Hooke's Law", The Engineer, Vol. 196 (1953), p. 4; T.M. Charlton: "Statically Indeterminate Frames: The Two Basic Approaches to Analysis." Engineering Vol. 182, p. 822 (1956); Symonds and Prager "Elastic Plastic Analysis

of Structures subjected to Loads varying arbitrarily between prescribed Limits" Jnl. Applied Mechanics Vol. 72, p. 315, Sept., 1950; (See also discussion by Charlton on this paper); H. L. Langhaar "The Principle of Complementary Energy in Non-Linear Elastic Theory", Jnl. Franklin Inst. Vol. 256 (1953) p. 255; T.M. Charlton "Some Notes on the Analysis of Redundant Systems by means of the Conception of Conservation of Energy" Jnl. Franklin Inst. Vol. 250, P. 543 (1950); and T. M. Charlton "The Analysis of Structures with Particular Reference to the Prediction of Deflexions". N.E. Coast Inst. of Engineers and Shipbuilders, Vol. 74, p. 163 (1957-8).

In this chapter, complementary energy is used to solve for the forces in pin-jointed redundant braced frameworks. The buckling of compression members and the yielding of tension members will be considered, and a number of simple examples worked.

107. The Complementary Energy of a Linear Member:

Consider the linear load-deformation relation

$$\delta = P/k \quad \text{(Fig. 195)} \qquad \ldots \qquad \ldots \qquad (137)$$

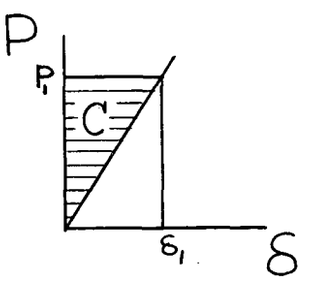

Fig. 195.

Then at any load P_1, the complementary energy is

$$C = \int_0^{P_1} \delta \, dP = P_1^2/2k \qquad \ldots \qquad \ldots \qquad (138)$$

Also $\partial C / \partial P_1 = P_1/k$. (In the usual notation, $k = EA/\ell$, where E = Young's modulus, A = area of member, ℓ = length of member.)

The Complementary Energy of a Yielding Tension Member:

Consider a tension member whose load-extension relation consists of two straight lines of slope $k = AE/\ell$ in the region $0 > F > -F_1$ and slope k_1 in the region $F < -F_1$, as shown in Fig. (196). Compression is taken as positive.

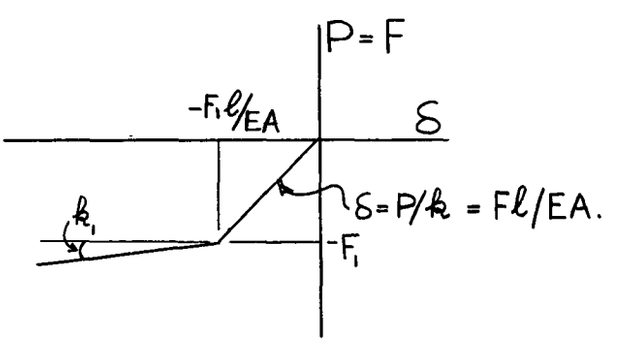

Fig. 196.

Then, for $0 > F > -F_1$, we have

$$\delta = F\ell/AE \text{ and } C = F^2\ell/2EA$$

and for $F < -F_1$, we have

$$\delta = F_1/k_1 + F/k_1 - F_1\ell/EA$$

and $$C = F_1^2\ell/2EA + \int_{-F_1}^{F} (F_1/k_1 + F/k_1 - F_1\ell/EA)\, dF$$

$$= F_1^2\ell/2EA + F_1 (1/k_1 - \ell/EA)(F + F_1) + (F^2 - F_1^2)/2k_1$$

therefore $$\partial C/\partial F = F_1 (1/k_1 - \ell/EA) + F/k_1 \quad .. (138)$$

The Complementary Energy of a Member Having a Curved Load-deformation Diagram:

Consider a member for which

$$\delta = aF + bF^3$$

In practice, any easily integrable function can be fitted to the load-deformation diagram. If the behaviour is the same in tension as in compression, it is necessary to use an odd function.

Now $$C = \int_0^F \delta\, dF$$

$$= aF^2/2 + bF^4/4.$$

108. As a simple example of the use of complementary energy, consider the rigid bar ABC supported by three rods and loaded as shown in Fig. 197.

This problem is worked by J. A. L. Matheson in Engineering: 187, 581, (1959). Using a series of straight lines to represent the stress strain curve, solution is achieved by means of the equation of virtual work. However, in this article the problem is used to illustrate how complementary energy can be applied.

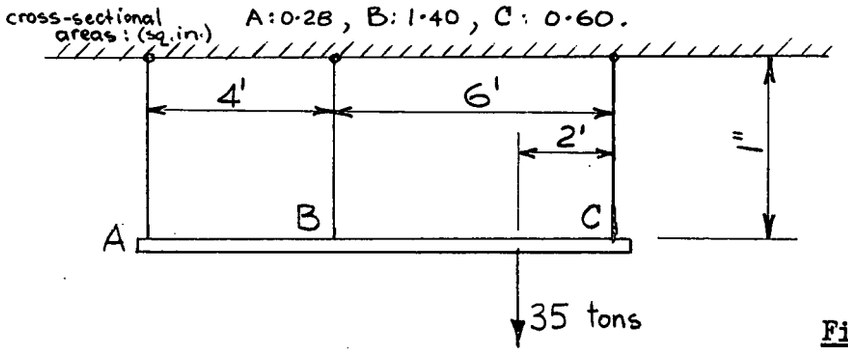

Fig. 197

We have two equations of statics:

$$F_A + F_B + F_C = 35 \text{ (vertical equilibrium)} \quad .. (139)$$

and $$8F_A + 4F_B - 2F_C = 0 \text{ (moments about the point of application of the applied load)} \quad .. (140)$$

where F_A, F_B, and F_C are the forces in tons in the rods A, B and C, tension being considered positive.

Suppose the stress strain curve for each of the rods is given by

$$\varepsilon = 1.125\, f + 4.76 \times 10^{-4} f^3$$

Then the load deformation relation is

$$\delta = 1.125\, F/A + 4.76 \times 10^{-5}\, F^3/A^3 \qquad .. (141)$$

the equation being assumed valid in both tension and compression.

Imagine rod A cut, and a force F_A applied across the cut to close it. Then $\partial C/\partial F_A = 0$, from equation (134). Using equations (139) to (141), the complementary energy C of the whole structure can be expressed in terms of the force F_A in the redundant member at A and the external load.

8 We have

$$\left.\begin{aligned} F_B &= 35/3 - 5F_A/3, & \partial F_B/\partial F_A &= -5/3 \\ F_C &= 70/3 + 2F_A/3, & \partial F_C/\partial F_A &= 2/3 \end{aligned}\right\} .. (142)$$

Hence the total complementary energy of the system is

$$C = \int_0^{F_A} \delta_A\, dF_A + \int_0^{F_B} \delta_B\, dF_B + \int_0^{F_C} \delta_C\, dF_C$$

since the complementary energy of the rigid beam is zero.

The use of equations (142), putting $\partial C/\partial F_A$ equal to zero, results in a third degree equation in F_A, and the solution is

$$F_A = -3.5, \quad F_B = 17.5, \quad F_C = 21.0,$$
$$\delta_A = -15, \quad \delta_B = 15, \quad \delta_C = 60.$$

These values of δ satisfy the equation of the rigid beam which is

$$(\delta_C - \delta_B)/6 = (\delta_B - \delta_A)/4 \qquad .. (143)$$

In fact, the complementary energy method has merely furnished a convenient method of writing down equation (143), the equation of geometrical compatibility, which must hold when the cut is closed.

This problem can also be solved by replacing the curved stress-strain diagram by a series of straights. It is then required to solve linear equations only, but it is necessary to guess and check in order that the solution may not lie on an extension of a straight line which is not applicable.

109. <u>The Complementary Energy of an Initially Crooked Pin-ended Strut</u>:

Consider the elastic strut whose unloaded shape is

$$y_o = \sum_1^\infty a_n \sin n\pi x/\ell \quad . \quad \text{(Fig. 198)}$$

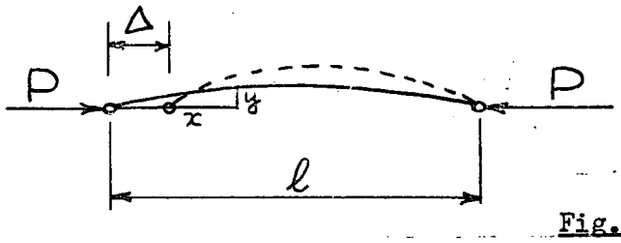

Fig. 198

Under axial load P, the shape changes to

$$y = \sum_1^\infty \left[a_n/(1 - P/n^2Q)\right] \sin n\pi x/\ell$$

where $Q = \pi^2 EI/\ell^2$ (See Art. 18)

The deformation Δ corresponding to P is given by the shortening. Therefore

$$\Delta = \int_o^\ell \tfrac{1}{2}(dy/dx)^2\,dx + P\ell/EA - \int_o^\ell \tfrac{1}{2}(dy_o/dx)^2 dx$$

$$= \sum_1^\infty n^2\pi^2 a_n^2 /4\ell(1-P/n^2Q)^2 + P\ell/EA - \sum_1^\infty n^2\pi^2 a_n^2/4\ell .$$

For values of P up to the first Euler load Q, provided a_2/a_1 etc. are small, the n = 1 term governs and we obtain

$$\Delta = \pi^2 a_1^2 /4\ell(1 - P/Q)^2 + P\ell/EA - \pi^2 a_1^2/4\ell \quad ..(144)$$

It is interesting to note that similar expressions, governed by n = 1 and involving the factor $1/(1 - P/Q)$, are obtained for the maximum deflection of the strut (see equation 20) and also the maximum strain (see equation 50). Empirically this furnishes a method of determining suitable values of the parameter a_1 for various types of struts. Strains are measured during a loading test, and by comparing the equation of the Southwell Plot on the measured strains with equation (51), the value of a_1 can be calculated. This has been carried out for a particular strut in Art. 59. The method also gives the value of P at which equation (144) is no longer valid due to yielding.

A graph relating P to Δ is shown in Fig. 199. The complementary energy of the strut is

$$C = \int_o^P \Delta\,dP$$

$$= (\pi^2 a^2/4\ell) \int_o^P dP/(1 - P/Q)^2 + P^2\ell/2EA - \pi^2 a^2 P/4\ell$$

$$= P^2\ell/2EA + (a^2\ell/4EI)\left[P^2/(1 - P/Q)\right] \quad ..(145)$$

if the subscript of a_1 is dropped.

Differentiating, we have

$$\partial C/\partial P = P\ell/EA + (a^2\ell/4EI)P\lambda \quad ..(146)$$

Where $\lambda = (2 - P/Q)/(1 - P/Q)^2$ ..(147)

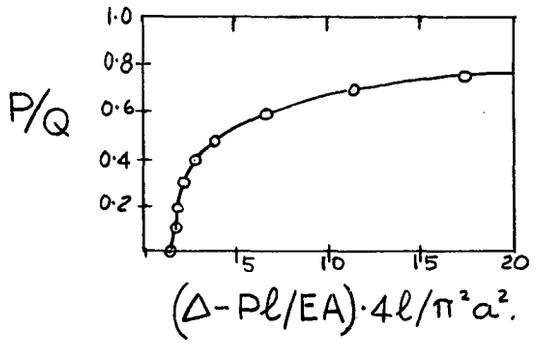

Fig. 199

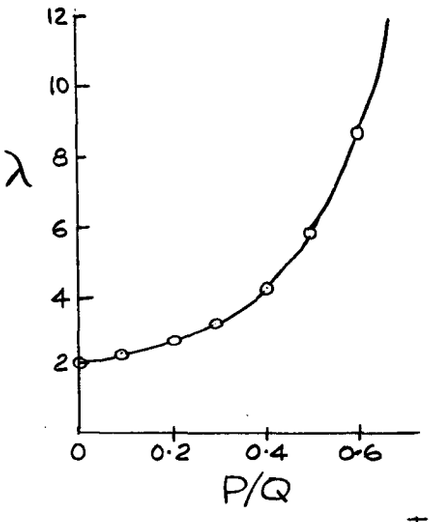

Fig. 200

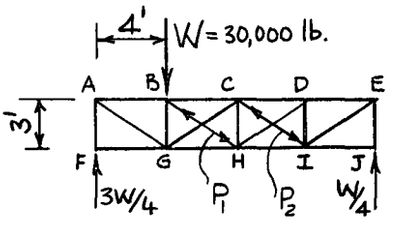

Fig. 201

TABLE I.

Member	1 Length in.	2 FORCE F compr. pos.	3 COMPLEMENTARY ENERGY C.	4 EA ∂C/∂P1	5 EA ∂C/∂P2	6 FORCES W=30 P1=P2=0	7 Eqns F
AB	48	W	$\frac{48}{2EA}W^2$	0	0	30	30
BC	"	$W-\frac{4}{5}P_1$	$\frac{48}{2EA}(W-\frac{4}{5}P_1)^2$	$2(W-\frac{4}{5}P_1)(-\frac{4}{5})\times 24 = -38.4W+30.7P_1$	0	30	23.6
CD	"	$\frac{2}{3}W-\frac{4}{5}P_2$	$\frac{48}{2EA}(\frac{2}{3}W-\frac{4}{5}P_2)^2$	0	$-25.6W+30.7P_2$	20	15.1
DE	"	$\frac{1}{3}W$	$\frac{48}{2EA}(\frac{W}{3})^2$	0	0	10	10
FG	48	0	0	0	0	0	0
GH	"	$-\frac{2}{3}W-\frac{4}{5}P_1$	$\frac{48}{2EA}(-\frac{2}{3}W-\frac{4}{5}P_1)^2$	$2(-\frac{2}{3}W-\frac{4}{5}P_1)(-\frac{4}{5})\times 24 = 25.6W+30.7P_1$	0	-20	-26.4
HI	"	$-\frac{1}{3}W-\frac{4}{5}P_2$	$\frac{48}{2EA}(-\frac{1}{3}W-\frac{4}{5}P_2)^2$	0	$12.8W+30.7P_2$	-10	-14.9
IJ	"	0		0	0	0	0
AG	60	$-\frac{5}{4}W$	$\frac{60}{2EA}(-\frac{5}{4}W)^2$	0	0	-37.5	-37.5
BH	"	$+P_1$	$\frac{60}{2EA}P_1^2+\frac{60a^2}{4EI}\cdot\frac{P_1^2}{1-P_1/Q}$	$(60+3.75\lambda_1)P_1$	0	0	8
CI	"	$+P_2$	$\frac{60}{2EA}P_2^2+\frac{60a^2}{4EI}\cdot\frac{P_2^2}{1-P_2/Q}$	0	$(60+3.75\lambda_2)P_2$	0	6.2
CG	60	$\frac{5}{12}W+P_1$	$\frac{60}{2EA}(\frac{5}{12}W+P_1)^2$	$2(\frac{5}{12}W+P_1)\times 30 = -25W+60P_1$	0	-12.5	-4.5
DH	"	$-\frac{5}{12}W+P_2$	$\frac{60}{2EA}(-\frac{5}{12}W+P_2)^2$	0	$-25W+60P_2$	-12.5	-6.3
EI	"	$-\frac{5}{12}W$	$\frac{60}{2EA}(-\frac{5}{12}W)^2$	0	0	-12.5	-12.5
AF	36	$\frac{3}{4}W$	$\frac{36}{2EA}(\frac{3}{4}W)^2$	0	0	22.5	22.5
BG	"	$W-\frac{3}{5}P_1$	$\frac{36}{2EA}(W-\frac{3}{5}P_1)^2$	$2(W-\frac{3}{5}P_1)(-\frac{3}{5})\times 18 = -21.6W+12.9P_1$	0	30	25.2
CH	"	$\frac{W}{4}-\frac{3}{5}P_1-\frac{3}{5}P_2$	$\frac{36}{2EA}(\frac{W}{4}-\frac{3}{5}P_1-\frac{3}{5}P_2)^2$	$2(\frac{W}{4}-\frac{3}{5}P_1-\frac{3}{5}P_2)(\frac{-3}{5})\times 18 = -5.4W+12.9P_1+12.9P_2$	$-5.4W+12.9P_1+12.9P_2$	7.5	-1.0
DI	"	$\frac{W}{4}-\frac{3}{5}P_2$	$\frac{36}{2EA}(\frac{W}{4}-\frac{3}{5}P_2)^2$	0	$-5.4W+12.9P_2$	7.5	3.8
EJ	"	$\frac{W}{4}$	$\frac{36}{2EA}(\frac{W}{4})^2$	0	0	7.5	7.5

Note: The complementary energy (column 3) is tabulated here merely to indicate the effect of initial crookedness on the complementary energy of the members BH and CI. In practice the differential is obtained directly.

The plot of λ against P/Q is shown in Fig. 200. The fact that Δ and hence C can be expressed explicitly as functions of P enables complementary energy to be conveniently applied.

110. The Solution of a Pin-Jointed Redundant Truss using Complementary Energy:

The braced frame shown in Fig. 201 is doubly internally redundant. All members are taken as having cross-sectional area A = 0.80 sq. in., minimum moment of inertia I = 0.20 $in.^4$, Young's modulus E = 30,000,000 lb./sq. in., and minimum radius of gyration r = 0.50 in. Also the applied load W equals 30,000 lb. All members are considered linear except the compression members BH and CI, whose initial crookedness is taken as a = 0.25 in. (A method of obtaining practical values of initial crookedness has been outlined in Art. 109. This is further elaborated and supported by experimental evidence in Art. 111, where the results of Southwell Plots on measured strains and shortening of a pin-ended column are compared.) For these members, $Q = \pi^2 EI/\ell^2 = 16{,}700$ lb. Compression is taken as positive.

Table I gives the forces and complementary energy for the various members if the forces in the redundant members BH and CY are taken as P_1 and P_2. See columns 2 and 3 of the Table. In columns 4 and 5, the complementary energy of each member is differentiated with respect to P_1 and P_2 respectively. The constant factor EA is taken out for convenience.

From equation 136, we have

$$\partial C/\partial P_1 = \partial C/\partial P_2 = 0.$$

Summation of columns 4 and 5 gives the two equations,

$$(207{,}2 + 3.75\,\lambda_1)P_1 + 12.9\,P_2 = 64.8W = 1944 \text{ kips} \quad .. \quad (148)$$

$$(207.2 + 3.75\lambda_2)P_2 + 12.9\,P_1 = 48.6W = 1458 \text{ kips} \quad .. \quad (149)$$

These are non-linear equations, as the factors λ_1, λ_2 involve P_1, P_2: (Equation 147). Solution is facilitated by putting, provisionally, $\lambda_1 = \lambda_2 = 2$, the value of λ at P/Q = 0. The resulting linear equations give

$$P_2 = 6.27 \text{ kips}, \; P_2/Q = 0.38, \; \lambda_2 = 4.2$$

$$P_1 = 8.70 \text{ kips}, \; P_1/Q = 0.52, \; \lambda_1 = 6.3.$$

Substitution of these more accurate values of λ in the original equations (148) and (149) gives

$$P_2 = 6.16 \text{ kips}, \; P_2/Q = 0.38, \; \lambda_2 = 4.1$$

$$P_1 = 8.00 \text{ kips}, \; P_1/Q = 0.48, \; \lambda_1 = 5.6 .$$

The corrected values of P_1 and P_2 satisfy the original equations closely enough for practical purposes. One adjustment to the approximate solution obtained by putting $\lambda = 2$ has been found to give a sufficiently accurate answer in problems which have been worked.

Values of the forces in the members are given in columns 6 and 7 of Table I.

Suppose the area of the tension member DH is reduced to some value A_{DH} so that it yields at a load of $F_1 = 4$ kips. See Fig. 196. It is apparent from Table 1 that this will affect the solution. It is necessary to alter the differential of the complementary energy of the member DH to the value given by equation (138). This gives

$$\partial C/\partial F = F_1 (1/k_1 - \ell/EA_{DH}) + F/k_1.$$

Substituting $F_{DH} = -5W/12 + P_2$, $\partial F/\partial P_2 = 1$,

$F_1 = 4$, and $\ell = 60$,

we have

$$EA_{DH}\, \partial C/\partial P_2$$
$$= EA_{DH} (\partial C/\partial F)(\partial F/\partial P_2)$$
$$= (EA_{DH}/k_1)(4 - 5W/12) - 240 + EA_{DH} P_2/k_1.$$

Equation (149) is now altered to

$$(147.2 + 3.75\lambda_2 + EA/k_1) P_2 + 12.9 P_1$$
$$= 23.6W + (EA/k_1)(5W/12 - 4) + 240 A/A_{DH} \quad .. (150)$$

Equation (148) is unaltered. Putting $W = 30{,}000$ lb., P_2 can be obtained for any value of k_1. In particular for the purely plastic case ($k_1 = 0$), equation (150) can be multiplied throughout by k_1, and k_1 then allowed to tend to zero. This gives

$$P_2 = 5W/12 - 4 = 8.5 \text{ kips}$$

$$F_{DH} = -5W/12 + P_2 = -4.0 \text{ kips}.$$

This is the value to be expected, as for $k_1 = 0$, F_{DH} is limited to 4 kips tension.

Care must be exercised in dealing with tension members which yield plastically. Too early substitution of $k_1 = 0$ leads to $\partial C/\partial F$ becoming undefined, and no solution is possible.

Throughout the analysis, the joints in the frame have been assumed pinned. Tests show that this assumption allows a reasonably close estimate of the forces when the joints are rigid. The use of the complementary energy of the pin-ended strut is considered to give a conservative estimate of the contribution of the redundant compression members to the strength of the frame, because end-fixing has been neglected.

111. Experimental Work on Column Shortening:

Some experimental work has been carried out to determine the validity of equation (144) and also to investigate the behaviour of a column in the plastic range beyond the stage where maximum load is reached.

In the elastic range we have the measured shortening of a pin-ended column given by

$$\Delta = \pi^2 a^2/4\ell(1 - P/Q)^2 + P\ell/EA \quad \text{(See equation 144)}$$

where a is the initial central crookedness.

This reduces to

$$\sqrt{\Delta - P\ell/EA} = (P/Q)\sqrt{\Delta - P\ell/EA} + \pi a/2\sqrt{\ell} \quad ..(151)$$

This is the equation of a type of Southwell Plot on the portion of the shortening due to buckling effects, namely $(\Delta - P\ell/EA)$.

A rectangular section steel member was loaded as a column between balls. This was the same member for which deflection readings are given in Art. 57, and strain readings in Art. 59. Load is plotted against shortening in Fig. 202 and the Southwell Plot in Fig. 203. The Southwell Plot is linear, and of slope 1/190 lb.$^{-1}$ which agrees well with the Euler load of 188 lb. This demonstrates the validity of equations (144) and (151). Similar experiments were carried out on $\frac{5}{8}$" x $\frac{1}{8}$" steel members, good agreement being obtained as before.

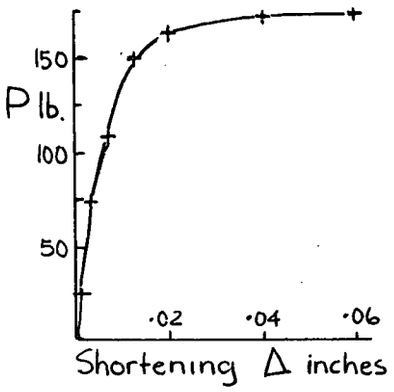

Fig. 202

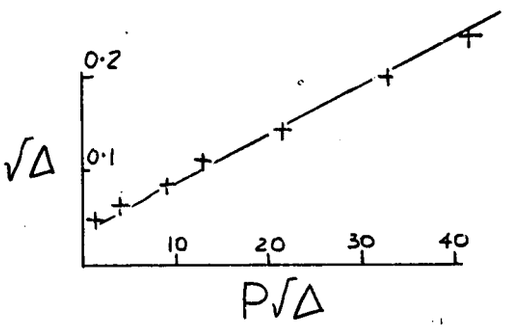

Fig. 203

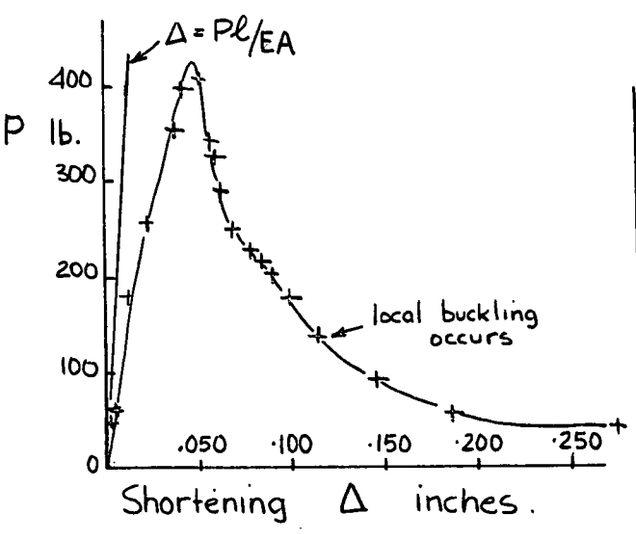

Fig. 204

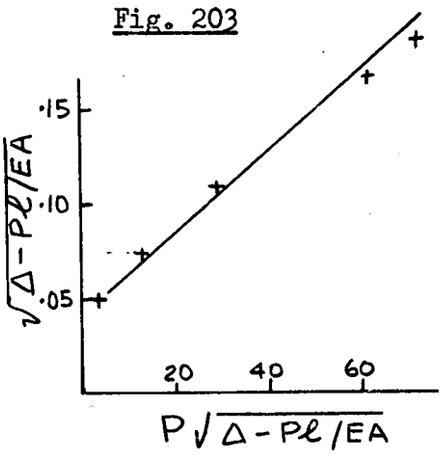

Fig. 205

The shortening of the steel angle-section member discussed in Art. 61 was also measured. The results are plotted in Figs. 204 and 205. The slope of the Southwell Plot is 1/470 lb.$^{-1}$ which compares well with the Euler load of 467 lbs. In Fig. 204, the graph of P against Δ is continued into the plastic range.

112. In view of the foregoing experimental work it appears that equation (144) satisfactorily defines the shortening of a pin-ended strut in the elastic range. Therefore, the derived expression for the complementary energy (equation 145) may be used with confidence to analyse the behaviour of a pin-jointed redundant frame in the elastic range. To study the strength of such a frame it is necessary to be able to calculate the complementary energy of the members in the elasto-plastic range, that is to obtain some practical definition of the whole of the relation between P and Δ. The difficulties involved in this programme, even for pin-jointed trusses, are large; but the task becomes even more formidable for rigid-jointed frames where the members are subjected to end moments (and, in general, torsions) as well as axial loads.

However, the Southwell Plot on strains as developed by the author is a powerful tool particularly when used in conjunction with complementary energy methods. Assuming the complementary energy of the member of an initially perfect rigid-jointed redundant plane frame is equal to $P^2\ell/2EA$, that is that all the members are initially straight, and no bending moments arise until buckling occurs, the load distribution among the members of the frame can be calculated, and the forces in individual members are linearly related to the applied loading. This enables an estimate to be made of a first elastic critical load, either by the method of moment distribution, or in simple cases by writing down all the equations of equilibrium at the joints and setting the determinant equal to zero. However, due to the redistribution of the forces in the members, there may be one or more modes of deformation into which the frame can deflect successively, and failure may not occur until the load reaches a value greatly in excess of the first critical load as calculated above. For any distribution of forces in the members of a redundant frame, there can be calculated a corresponding critical loading on the frame. There is therefore a critical load which may be considered as governing at failure.

In practice, the initial behaviour of a redundant frame with fairly straight members is related to the first critical load. This holds so long as the complementary energy of the members approximates to the value $P^2\ell/2EA$. For this to be true, the deformations of the members must be predominantly axial, and bending effects must be small. It is therefore necessary that members should have small initial crookedness, and also that secondary bending effects due to the geometrical distortion of the frame should be small. However, as distinct from the behaviour of a non-redundant frame, this first critical load does not necessarily set an upper limit to the load-carrying capacity of a redundant-frame. The forces in the members redistribute once bending effects become important, and failure may not occur until the load reaches a value greatly in excess of the first critical load.

Experimental work has been carried out at the University of Tasmania, under the author's direction, on a rigid-jointed flexible frame of the forms shown in Fig. 206. (The work referred to is incorporated in a thesis for the degree of B.E. (Hons.) in the University of Tasmania by G. Peck, Feb. 1960).

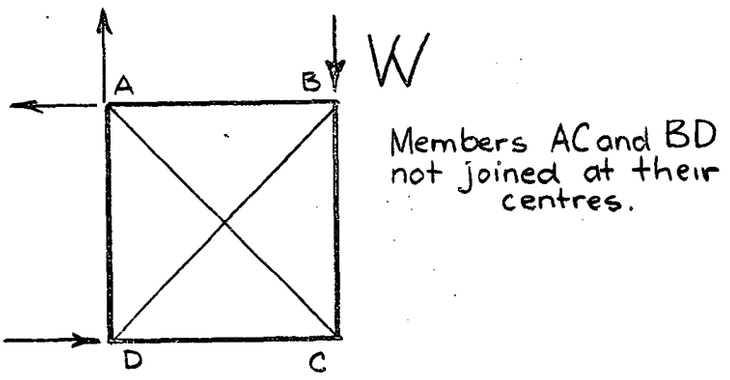

Fig. 206

On loading the frame, it was found that strains increased rather quickly as the first critical load (as calculated above) was approached. The member BD buckled, in the sense that it became very flexible and could be moved about easily when a force was applied at its centre. However, the load W could still be increased, with BD continuing to deflect rapidly. Failure as given by very large deformation of BC, did not occur till more than double the first critical load was obtained.

Strain measurements were made at different points in the members of the frame and Southwell Plots drawn. The latter gave two approximately linear portions, the inverse slope of the first linear part being equal to the first elastic critical load as calculated above, and the inverse slope of the second linear part indicating a critical load somewhat higher than the failure load. It appears therefore that the members of the frame were initially straight enough, and the deformations and secondary bending effects in the frame small enough, for bending effects to be small up to nearly the first critical load. This critical load thus governs the initial behaviour. If the loads in the members could not redistribute, this first critical load would govern right up to failure, but as the load is increased, deflections increase, bending effects become important and the loads in the members redistribute; BD continues to deflect while its load falls off, and the load in BC increases until failure occurs.

The forces in the members BD and BC were calculated from the measured strain readings around their cross-sections and their variation with the applied load W was qualitatively in agreement with the foregoing argument. An analysis of the complementary energy terms for the members of the frame was carried out in order to obtain some quantitative measure of the complementary energy of bending, and thus to analyse the behaviour of the frame as it approached the failure condition. The total complementary energy of a member is the sum of the energies of the axial load in it and of the bending moments acting as its ends. These bending moments are unknown, but in an attempt to take some account of them, the complementary energy of a bent strut in a rigid-jointed frame was taken as

$$C = P^2\ell/2EA + (a^2\ell/4EI)\left[P^2/(1-P/Pcr)\right] \quad .. (152)$$

This equation is taken by analogy from equation (145)., the value of Pcr., the relevant critical load for the frame, being substituted for Q, the Euler load of the pin-ended strut. The analogy has reasonable justification: it has been shown previously that the deflections and strains of a member in a frame increase or are magnified in the ratio $1/(1-P/Pcr)$, and the corresponding assumption applied to the complementary energy

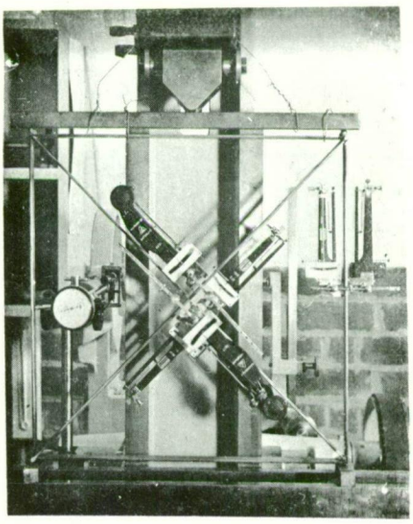

Experiment with model redundant frame.

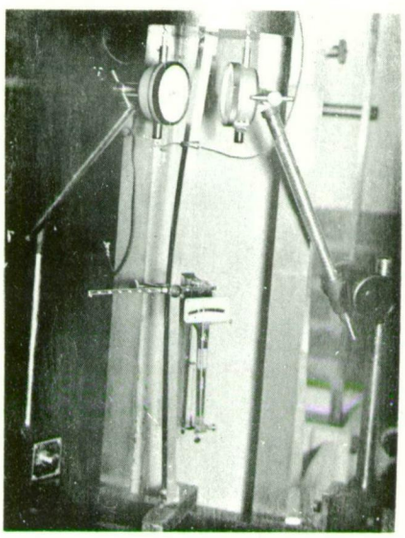

Measurement of shortening of a pin-ended strut.

of bending should be reasonably accurate. Values of Pcr. and also of the crookedness, a, were taken from the Southwell Plots on measured strains and substituted in equation (152). By this means the Southwell Plot on measured strains was used to obtain an estimate of the complementary energy of the members of the frame. It was therefore possible to calculate the forces in the members with increasing W. A reasonable quantitative substantiation of the measured variation of the axial forces in the members was achieved.

113. Summary:

The experimental and analytical work so far carried out on redundant frames has been devoted to analysis of the elastic behaviour of flexible frames; a reasonably successful attempt has been made to analyse the redistribution of loads in members as loading proceeds by obtaining an estimate of their complementary energy, this estimate being based entirely on imformation obtained from Southwell Plots on measured strains. It is felt that further investigation will necessarily be limited to elastic behaviour for some time. The author is confident that the use of energy methods supported by empirical information obtained from strain measurements, particularly such information as is available from Southwell type plots, will ultimately yield a method of analysis. However, the determination of the strength of a practical redundant frame will certainly involve an elasto-plastic analysis.

-------- o 0 o --------

APPENDIX A

The following is a list of papers published by the author in connection with this research. Most of this published work is embodied in this thesis.

1. "Bolted Angle Struts: A Review of Existing Design Methods with Particular Reference to Transmission Towers." Water Power. Jan. 1959, 25 - 27.
2. "Model Investigations on Bolted Angle Structures." Water Power, May 1959, 178 - 182.
3. "Further Research on Bolted Angle Structures." Water Power, Aug. 1959, 308 - 310.
4. "The Collapse of Triangulated Frames Containing Bolted Angle Struts". Water Power. Oct. 1959, 390 - 392.
5. "The Use of Measured Strains to obtain Critical Loads". Civ. Engng. Lond. Vol. 55, No. 642: 80-82.
6. "The Elastic Buckling of Columns in Structures: The Use of the Southwell Plot on Strains to Obtain Design Criteria." Civ. Engng. Lond. (in press).
7. "The Buckling of Structures." Civ. Engng. Lond. (in press).
8. "The Use of Complementary Energy in Non-linear Redundant Braced Frames". Civ. Engng. Lond. (in press).
9. "The Development of Lightweight Trusses at the University of Tasmania." Aust. Civ. Engng. & Construction (in press).
10. "The Use of the Southwell Plot on Strains to Determine the Failure Load of a Lattice Girder when Lateral Buckling Occurs." Aust. J. Appl. Sci.10: 371-376.
11. "The Buckling of an Equilateral Triangular Frame in its Plane". Aust. J. Appl. Sci. 10: 377 - 387.
12. "A Non-linear Bending Effect when Certain Unsymmetrical Sections are Subjected to a Pure Torque". Aust. J. Appl. Sci. 11: 33-48.
13. "The Application of the Southwell Plot on Strains to Problems of Instability of Framed Structures when Buckling of Members in Torsion and Flexure is Involved." Aust. J. Appl. Sci. 11: 49-64.
14. "The Use of Complementary Energy in Structural Analysis." Civil Eng. Trans. I.E. Aust. Vol. CE2 . No. 1. Mar.1960, 9-13.
15. "The Bending and Shortening Effect of Pure Torque". Aust. J. Appl. Sci. Vol. 11, No. 3 (1960). (Not incorporated in this thesis.)

The following letters or discussions of papers are also relevant:

on "The Buckling of Struts with varying Cross-Sections". J.I.E. Aust. 31, 9:231.

on "Virtual Work and Complementary Energy Applied to Non-linear Braced Frameworks". Engineering 188:19.

——— o 0 o ———